The role of SecA2 in targeting substrates to the Sec-dependent protein translocase

Krzysztof Gizynski

Thesis submitted to the

University of Newcastle upon Tyne for

the degree of Doctor of Philosophy

November 2012

Acknowledgements

I would like to expresses special thanks to my supervisor, Prof. Colin Harwood, through whose support the completion of my postgraduate studies was possible.

I also wish to thank all members of the Harwood lab Group as well in CBCB for their help, advice and assistance.

Especially, I would like to acknowledge the input and express my thanks to:

Dr. Susanne Pohl for collaboration in many experiments and enduring support.

Dr. Lorraine Hewitt for help with the protein work.

Dr. Gouqing Wang for collaboration on work in *B. subtilis*. He is behind most of the work presented in Section 5.2.

Dr. Patricia Dominguez-Cuevas for help with fluorescent microscopy and qPCR experiments.

This work was funded by a BBSRC-CASE studentship between the University of Newcastle upon Tyne and Novozymes, Denmark.

Krzysztof Gizynski (November 2012)

Programme of related studies

5th International Conference on Gram-Positive Microorganisms, 15th International Conference on Bacilli, 14-18 June, 2009. Catamaran Hotel, San Diego, California, USA.

Poster presentation: 'Substrate specificity of the *Bacillus anthracis* accessory protein translocase.'

Susanne Pohl, Krzysztof Gizynski, Stephen G. Addinall, Georg Homuth, Ulrike Mäder, Pijug Summpunn, Rachel C. Williams and Colin R. Harwood.

Society for General Microbiology, Autumn Meeting, 6-9 September, 2010. University of Nottingham, UK.

Poster presentation: 'The major surface antigens of *Bacillus anthracis* are secreted *via* an accessory SecA2-mediated pathway.'

Krzysztof Gizynski, Susanne Pohl, Stephen G. Addinall, Georg Homuth, Ulrike Mäder, Pijug Summpunn, Rachel C. Williams and Colin R. Harwood.

6th International Conference on Gram-Positive Microorganisms, 16th International Conference on Bacilli, 14-18 June, 2011.

Poster presentation: 'The insights into *Bacillus anthracis* secondary translocase.'

Krzysztof Gizynski, Susanne Pohl, Stephen and Colin R. Harwood.

BACELL meeting. 2011. 14th March, 2011. Georg-August-University of Göttingen, Germany.

Oral presentation: 'The secondary protein secretion translocase of *Bacillus anthracis.'*

Krzysztof Gizynski, Susanne Pohl and Colin R. Harwood.

Postgraduate Research Symposium Final Year Postgraduate Research Presentations. 6th April 2011. Newcastle University, Faculty of Medicine, UK.

Oral presentation: 'The role of SecA2 in targeting substrates to the Sec-dependent protein translocase.'

Krzysztof Gizynski, Susanne Pohl and Colin R. Harwood.

Contents

List of Figures

List of Tables

Abbreviations

2DE	Two-dimensional electrophoresis
aa	Amino acid
Amp	Ampicillin
ATP	Adenosine triphosphate
Ban	*Bacillus anthracis*
Bp	Base pair
Bsu	*Bacillus subtilis*
ca.	Approximately
cAMP	Cyclic adenosine monophosphate
°C	Degree Celsius
Cm	Chloramphenicol
C-terminus	Carboxy terminus
DNA	Deoxyribonucleic acid
Da	Dalton
DMSO	Dimethyl sulfoxide
DNA	Desoxyribonucleic acid
dATP	Desoxyadenosine-5`-triphosphate
EDTA	Ethylendiamine tetra acetic acid
E. coli	*Escherichia coli*
Ffh	Fifty four homologoue
h	Hour
GTP	Guanosine triphosphate
g	Gram
g	Gravitational force
GRAS	Generally recognized as safe
IPTG	Isopropyl-b-D-thiogalactoside
k	Kilo
kb	Kilobases
knt	kilonulceotides
kDa	Kilodalton
Km	Kanamycin
L	Litre
LB	Luria-Bertani
LC/MS/MS	Liquid chromatography tandem mass spectrometry
M	Molarity (mol/L)
m	Mili
µ	Micro
MALDI-TOF-MS	Matrix-assisted laser desorption-ionisation time-of-flight mass spetrometry
MCS	Multiple cloning site
Min	Minutes
MLST	Multilocus sequence typing
mRNA	Messenger ribonucleic acid
MS	Mass spectrometry
n	Nano
nt	Nucleotide
N-terminus	Amino terminus
NCBI	National Center for Biotechnology Information

OD	Optical density
RNA	Ribonucleic acid
SRP	Signal recognition particle
TAT	Twin-arginine protein transport
TF	Trigger factor
TM	Transmembrane
ori	Origin of replication
PAGE	Polyacrylamid gel electrophoresis
PCR	Polymerase chain reaction
rbs	Ribosome binding site
s	Second
v/v	volume/volume
w/v	weight/volume
wt	Wild type

Abstract

The Sec pathway is the major route for secretion of proteins by bacteria. Its major components are: (i) the translocation channel comprising the SecYEG proteins; (ii) SecA: a chaperone/targeting/molecular motor that drives the movement of proteins across the membrane with participation of SecB or SRP (signal recognition particle) chaperones. Following translocation, proteins are folded to their mature conformation by folding factors such as PrsA. When compared with *B. subtilis*, the secretory translocase of *B. anthracis* contains homologues of several Sec pathway components: (i) two homologues of SecA (SecA1 and SecA2), (ii) two homologues of SecY (SecY1 and SecY2), (iii) three homologues of the PrsA foldase (PrsAA, PrsAB and PrsAC). In previous studies, SecA2 was shown to be specific for secretion of S-layer proteins: Sap and EA1, while SecY2 has not been shown to have any substrate specificity. Instead, it seems to ensure high levels of protein secretion in later phases of the growth cycle.

A combination of approaches was used to continue the analysis of functioning of the SecA2 secretion pathway. They involved analysis of deletion mutants of *B. anthracis*, complementation studies, gene expression analysis, protein interaction investigation.

We found that a novel protein BA0881 facilitates secretion of Sap and EA1, but is not essential for the processes, and was renamed SecH. Moreover, protein interaction and complementation studies revealed putative interactions between (i) SecA2 and EA1, (ii) SecA2 and SecH, (iii) EA1 and SecH, (iv) SecA1 and SecA2, raising the possibility that SecA2 and SecA1 form a dimer, which might be a functional entity for the secretion of Sap and EA1, with SecH having a role in enhancing interaction between SecA1/SecA2 dimer and its substrates.

The role of PrsA-like foldases on secretion was also investigated. PrsAB was found to show substrate specificity for Sap and EA1, while PrsAA showed substrate specificity for penicillin binding proteins.

Analysis of cell morphology suggests that PrsAB and SecA2 may also have substrates other than those of Sap and EA1 as their null-mutants show changes in cell length and shape.

Lastly, analysis of gene expression showed that the deletion of genes encoding elements of the translocation sytem: SecA2, SecH, PrsAA, PrsAB, PrsAC, SecY2 leads to changes in the level of expression of *sap* and *eag*.

Chapter 1: General introduction

1.1 Genus Bacillus

Bacillus is a bacterial genus which comprises spore-forming, Gram-positive rods which are aerobic or facultatively anaerobic. The members of this genus are widely distributed in the environment. Although most members of the genus are non-pathogenic, a few species are responsible for well-known diseases. The best known disease-causing member of the genus is *Bacillus anthracis*, the causative agent of anthrax. On the other hand, *B. subtilis* is generally recognised as safe (GRAS), and is used for the production of a wide range of bioproducts. Taxonomically, based on 16S rRNA/DNA sequence similarities, the genus *Bacillus* can be divided into six RNA groups (Ash *et al.*, 1991; Nielsen, *et al.*, 1994, Fritze, 2004). The species included in this research are *B. subtilis* and *B. anthracis*. They belong to the RNA group 1 and within it, they are categorised to the *Bacillus subtilis* and *Bacillus cereus* groups, respectively.

1.2 *Bacillus cereus* group

The *B. cereus* group comprises six members: *B. anthracis, B. cereus, B. mycoides, B. pseudomycoides, B. thuringiensis, B. weihenstephanensis*. *B. mycoides, B. pseudomycoides, B. weihenstephanensis* are non-pathogenic, while *B. thuringiensis* may cause disease in insects, and *B. anthracis* as well as *B. cereus* in mammals. *B. anthracis, B. cereus* and *B. thuringiensis* are phylogenetically closely related and have very similar genomes. In the study by Ash et al. (1991), the 16S rRNA sequences of *B. thuringiensis, B. cereus* and *B. anthracis* differed less than 1%. Other studies confirmed very close relationship between those species. MLST (multilocus sequence typing) studies, which compare the sequences of specific housekeeping genes, showed that some of the strains of *B. cereus* and *B. thuringiensis* analysed in that study were more closely related to some strains of *B. anthracis* than to other strains within their own species (Halgeson, 2004). Comparison of the genomic sequences of *B. anthracis, B. cereus* and *B. thuringiensis* showed a high degree of similarity, with conserved gene order and only a small subset of genes that were unique to any of those species (Rasko *et al.*, 2005). Thus, as *B. thuringiensis* and *B. cereus sensu stricto* and *B. anthracis* are genetically very closely related, they might be re-classified as a single species: *B. cereus sensu lato* (Helgason et *al.*, 2000, Bavykin *et al.*, 2004). The most striking difference between the chromosome of *B. anthracis* as compared with those of *B. thuringiensis* and *B. cereus* is a point mutation in the *plcR* gene of the former (Agaisse *et al.*, 1991).

The product of the *plcR* gene is a pleiotropic regulator controlling most of the secreted virulence factors in *B. cereus* and *B. thuringiensis*. The *plcR* gene is non-functional in *B. anthracis*. The lack of PlcR in *B. anthracis* renders this bacterium non-haemolytic and sensitive to γ phage. These features distinguish *B. anthracis* from *B. cereus* and *B. thuringiensis* on the phenotypic level (Drobniewski, 1993). The other distinguishing features of *B. anthracis* are the presence of plasmids and the products of genes encoded by them. *B. anthracis* carries plasmids pXO1 and pXO2 encoding key virulence factors and their regulators (Koehler, 2009), while the distinguishable feature of *B. thuringiensis* is the possession of crystals formed by Cry proteins, which are usually plasmid encoded (Konstad *et al.*, 1983, Gonzales *et al.*, 1984).

1.3 *B. anthracis* is the causative agent of anthrax

B. anthracis is the etiological agent of anthrax (Spencer, 2003). Anthrax is a disease that affects mainly herbivores, but humans can also be infected. The infection occurs via spores, which enter the host through skin lesions, consumption of contaminated food or inhalation of contaminated air. Depending on the point of entry, cutaneous, gastrointestinal and pulmonary anthrax can develop (Spencer, 2003). Spores are ingested by macrophages local to the point entry. Spores germinate inside macrophages to the vegetative bacillus and produce capsule and toxins. The vegetative cells get released from macrophages and continue multiply and produce the edema and lethal toxins at the site of entry. Their action impairs functioning of the immune system and triggers development of anthrax-related pathological changes: edema, vascular damage, hemorrhage, tissue necrosis (Tournier *et al.*, 2007). Bacteria may also get into the bloodstream, disseminate to other parts of the body and cause septicaemia, which if untreated promptly leads ultimately to death. The cutaneous form is most common, accounting for about 95% of cases (Tutrone *et al.*, 2002). The characteristic symptom of cutaneous anthrax is a raised bump that develops into a black necrotic ulceration, which may be surrounded by edema (Meade, 2004). If untreated, approximately 20% of patients will develop septic shock and die. However with the appropriate antibiotic treatment the mortality is below 1% (Carucci *et al.*, 2002). In gastrointestinal anthrax the necrotic ulcerations, edema and hemorrhages are formed in the intestines leading to the development of symptoms which include nausea, loss of appetite, fever, abdominal cramps, vomiting of blood and severe diarrhoea. The gastrointestinal form of anthrax is often undiagnosed which leads to high mortality due to septicaemia (Sirisanthanta and Brown, 2002). Pulmonary anthrax is the most severe form (Shafazand *et al.*, 1999**)**.

Anthrax toxins cause development of edema, hemorrhages and necrosis in the pulmonary tracts. Cells of *B. anthracis* disseminate to other parts of the body causing similar pathological changes as in the pulmonary tract. At first symptoms resemble those of flu but the patient's condition rapidly deteriorates usually leading to death (>95% of untreated cases), which is the result of respiratory failure due to pulmonary edema and of septicaemia. When appropriate treatment is applied, the mortality can drop to 45% (Jernigan *et al.*, 2002).

Treatment of anthrax

In vitro B. anthracis exhibits sensitivity to penicillins, fluoroquinolones, tetracycline, chloramphenicol, aminoglycosides, macrolides, imipenem/meropenem, rifampicin, and vancomycin. According to the recommendations of the Health Protection Agency (2010) the use of penicillins alone is not recommended due to the occurrence of β-lactamase encoding strains. Instead, ciprofloxacin or doxycycline are used in combination with one of the following antibiotics: rifampin, vancomycin, imipenem, chloramphenicol, penicillin, ampicillin, clindamycin and clarithromycin. The use of the combination of antibiotics gives firstly synergistic effect against *B. anthracis* and secondly it is effective against *B. anthracis* strains being resistant to one of the antibiotics used.

Prevention of anthrax

The veterinary anthrax vaccine employs the toxigenic, non-encapsulated, attenuated *B. anthracis* strain, Sterne $34F_2$ strain (Turnbull *et al.*, 1989). Human vaccines usually are also based on *B. anthracis* Sterne $34F_2$ and can use either live spores (of attenuated non capsulated strain) or cell-free culture filtrates. In the USA the non-encapsulated, non-proteolytic derivative of bovine isolate V770-NP1-R is used (Turnbull *et al.*, 1989).

The pathogenicity factors of *B. anthracis*

Pathogenicity of *B. anthracis* is due to its two toxins: lethal toxin and edema toxin as well as its capsule. Each of the toxins is formed by two proteins: lethal toxin by protective antigen and lethal factor, and edema toxin by protective antigen and edema factor. The protective antigen, lethal and edema factors are encoded by the *pagA*, *lef* and *cya* genes, respectively (Bhatnagar and Batra, 2001). Those genes, together with genes encoding regulatory elements AtxA and PagR, are located on the pXO1 virulence plasmid. *B. anthracis* also harbours a second pathogenicity plasmid, pXO2, encoding

the *cap* operon responsible for the production of the poly-γ-D-glutamate capsule, which inhibits the phagocytosis of vegetative cells of *B. anthracis* by the immune system (Makins *et al.*, 1989).

While the role of the capsule is to protect, against host's immune system, lethal and edema toxins are involved in both: modulation of the immune responses and the development of the specific symptoms of anthrax. Individually, none of the toxin components: protective antigen, lethal factor, edema factor is toxic. The protective antigen is necessary to deliver the toxic components: lethal and edema factor to the interior of the cell, where those factors exert their toxic action. And only when lethal or edema factors are in the presence of the protective antigen, then their toxicity can be observed. Initial research in regard to the effects exhibited by the those toxins showed that a combination of the protective antigen and the lethal toxin induces lethal shock in experimental animals, while a combination of the protective antigen and edema factor induces edema at the site of infection (Smith and Stoner, 1967).

Protective antigen, a component of both *B. anthracis* toxins, is a receptor binding protein responsible for delivering the enzymatic components of the toxins (lethal and edema factors) into the interior of the host cell, where they perform their toxic action. Upon binding to the cell surface, protective antigen (PA 83; 83 kDa) undergoes cleavage by a furin-like protease at an RKKR site, leading to removal of its 20 kDa N-terminal fragment (PA20). The 63 kDa fragment (PA63) remains bound to the receptor and undergoes a structural rearrangement to form a pre-pore, which binds lethal and edema factors. The complexes of the protective antigen with lethal and edema factor are internalised by endocytosis, followed by the release of lethal and edema factor from the resulting endosome into the cytosol via a channel formed by protective antigen (Young and Collier, 2007). Once in the cytosol, the enzymatic sub-units (lethal and edema factors) of the toxins exhibit their cytotoxic effects. The lethal factor inhibits mitogen-activated protein kinase kinases (MAPKK) (Duesbery *et al.*, 1999; Vitale *et al.*, 1998) (model of action of the anthrax toxins is presented on the Figure 1.1).

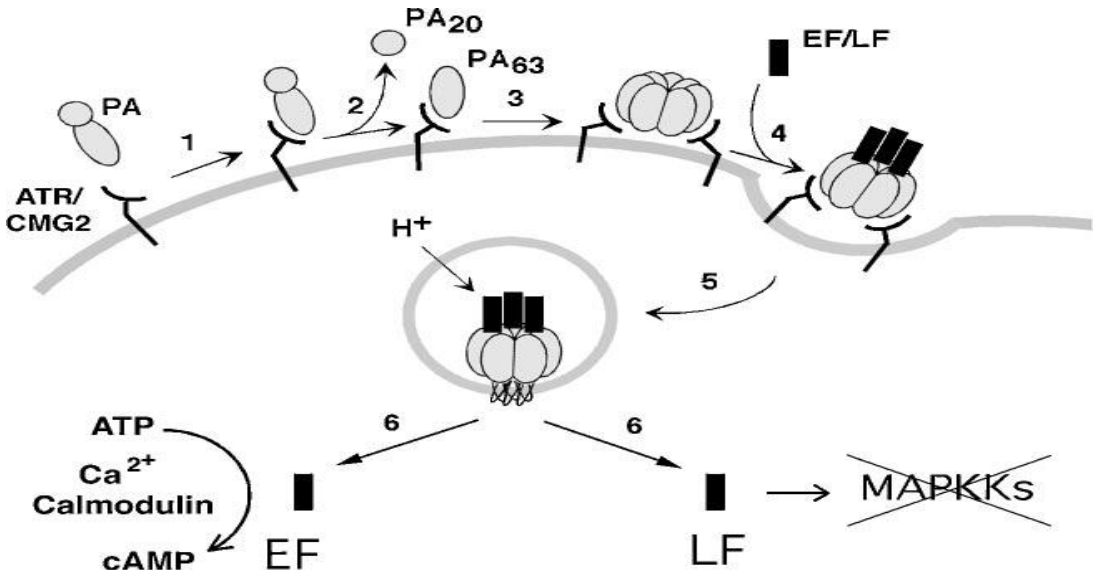

Figure 1.1: Action of anthrax toxin at the molecular level. (1) The protective antigen (PA) binds to a receptor, ATR or CMG2; (2) cleavage by a furin protease removes 20 kDa fragment (PA20); (3) 63 kDa (PA63) self-associates to form the heptameric prepore; (4) up to three molecules of EF and/or LF bind to the prepore; (5) the complex is endocytosed and trafficked to an acidic intracellular compartment; (6) under the influence of low pH the prepore converts to a pore, and EF and LF are translocated to the cytosol. There, EF catalyzes the formation of cAMP, and LF proteolytically inactivates MAPKKs (Collier and Young, 2003).

The main effect associated with the lethal toxin is cell death and resulting necrosis, vascular damage and haemorrhages, which belong to the main symptoms of anthrax. The effects of the action of the lethal toxin are mediated by the disruption of cell's signalling pathways due to cleavage of MAPKKs, but it is not completely clear how the lethal toxin-induced cell death is achieved. However, the research that has been done offers some clues to how that death occurs. The detrimental effect of the lethal toxin, that have been observed, include: (1) changes in the membrane permeability, triggering colloid-osmotic lysis (Hanna *et al.*, 1992); (2) toxic effects exerted by reactive oxygen intermediates (Hanna *et al.*, 1994); (3) inhibition of certain NF-B target gens leads to the apoptosis of activated macrophages (Park *et al.*, 2002). Lethal toxin is also implicated in development of toxic shock, but the mechanism in not yet known. It was postulated that the septic shock could develop due to macrophage lysis and cytokine (TNF-α/IL-1β) induction by lethal toxin (Hanna *et al.*, 1993). However, it was shown that the septic shock induced by the lethal toxin does to require cytokine shock or macrophage sensitivity to toxin (Moayeri *et al*., 2003). Additionally, the lethal toxin is able to supress functioning of the immune system by a number of means which include: (1) inhibition of neutrophil's mobility (During *et al.*, 2005); (2) inhibition of proliferation and differentiation of monocytes (Kassam *et al.*, 2005), (3) suppression of

cytokine production of macrophages (Erwin *et al.*, 2005); (4) activation of cell death of macrophages (Kassam *et al.*, 2005); (5) cell death of immature dendritic cells (Alileche *et al.*, 2005), (6) Inhibition of activation, proliferation, surface-molecule expression and cytokine expression in T cells (Paccani *et al.*, 2005; Comer *et al.*, 2005).

The effect of the increased concentrations of edema toxin-induced levels of cAMP in the cell is the disruption of water homeostasis and cellular signalling pathways leading to edema, one of the symptoms of anthrax (Leppla, 1982**,** Dixon *et al.*, 1999). Other major effect of the edema toxin is impairment of function of the immune system as edema toxin-induced levels of cAMP cause: (1) inhibition of phagocytosis (O'Brien *et al.*, 1985); (2) cell death of macrophages (Voth *et al.*, 2005); (3) suppression of cytokine production in the dendritic cells (Tournier *et al.*, 2005); (4) Inhibition of activation, proliferation, surface-molecule expression and cytokine expression in T cells (Paccani *et al.*, 2005; Comer *et al.*, 2005).

Regulation of pathogenicity of *B. anthracis*

AtxA is the master regulator of the expression of the genes involved in the pathogenicity of *B. anthracis*. It was shown to mediate activation or repression of genes located on pXO1 and pXO2 plasmids, as well as on the chromosome (Mignot *et al.*, 2003; Bourgogne *et al.*, 2003). It can directly induce the expression of pathogenicity factors genes such as *pagA*, *lef* and *cya* (Uchida *et al.*, 1993; Koehler *et al.*, 1994), as well as regulators (e.g. *pagR*, *acpA*, *acpB*) whose products in turn affect the expression of genes further down the regulatory cascade. *pagR* is part of the *pag* operon which also contains the *pagA* gene. PagR autogenously controls the *pag* operon by inhibition (Hoffmaster and Koehler, 1999) and also regulates two chromosomal genes, *sap* and *eag*, that are key elements of this project. PagR up-regulates *eag* and down-regulates *sap*. As the expression of *sap* and *eag* is part of the regulation mediated by toxigenicity regulatory factors and as it is highly energy-consuming process it has been postulated that products of those genes, namely Sap and EA1 are pathogenicity factors, but this hypothesis has not been proved.

AtxA and CO_2 both induce *acpA* and *acpB*. Their products, AcpA and AcpB are required for the activation of the capsule-encoding *cap* operons (Drysdale *et al.*, 2004; Vietri *et al.*, 1995). The AtxA-mediated regulation is depicted on the Figure 1.2.

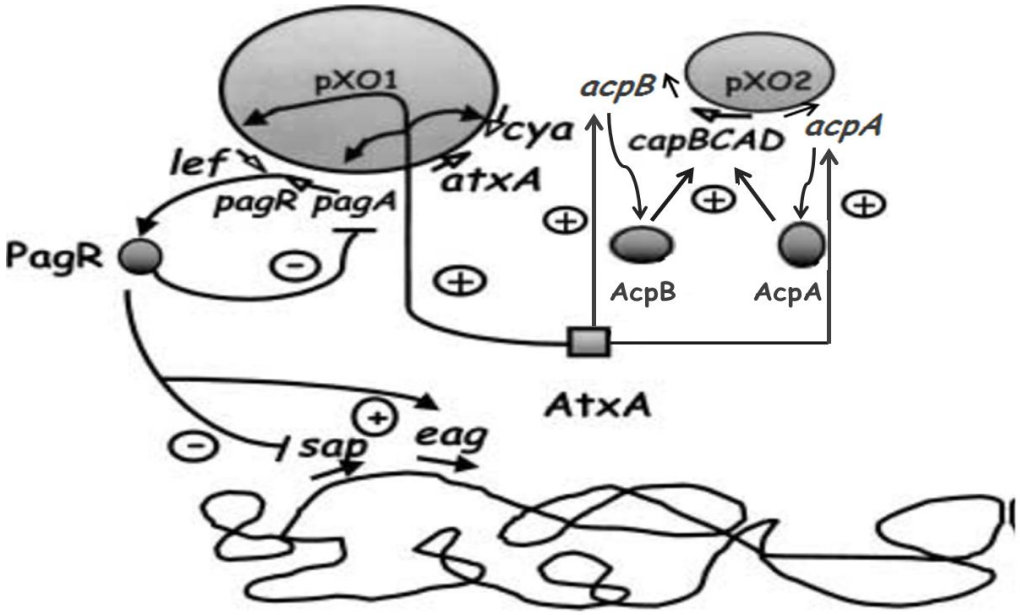

Figure 1.2: AtxA-mediated regulation of genes encoding virulence factors and *sap* and *eag* (modified from Mignot *et al*., 2004). Plasmids pXO1 and pXO2 are shown as two grey ovals, while the chromosome is showed as a big, closed, entangled circle at the bottom of the diagram. pXO1 plasmid harbours genes of the regulatory molecules (*atxA* and *pagR*) and of toxin components (*cya*, *lef*, *pagA*). pXO2 harbours *capBCAD* operon responsible for the capsule production, as well as *acpA* and *acpB* genes encoding regulators of *capBCAD* operon. '+' means stimulatory effect, while '-' means inhibitory effect on the gene expression. AtxA is the master regulator and induces expression of genes of the regulators *pagR*, *acpA*, *acpB* as well as of the toxin components: *lef*, *cya* and *pagA*. *pagR* and *pagA* constitute a single operon. When PagR is produced it autoinhibit its own operon, as well in up-regulates *eag* and down-regulates *sap* expression. Induction of *acpA* and *acpB* leads to the production of AcpA and AcpB, which in turn induce expression of *capBCAD* operon.

1.4 Bacterial protein secretion

The analysis of completed genome sequencing projects reveals that 15-25% of the genome encodes proteins that are destined for secretion in most bacteria (identified by the presence of the N-terminal signal peptide) (Liu and Rost, 2001). Their secretion is mediated primarily via the Sec-dependent secretion (Sec) pathway (Tjalsma *et al.*, 2000; Bendtsen *et al*., 2005). The Sec pathway is described in detail in the **Section 1.5.1**. Gram-negative bacteria additionally possess specialized secretion pathways for the secretion of a sub-set of proteins across the outer membrane. In both Gram-negative and Gram-positive bacteria a small subset of proteins are translocated across the cytoplasmic membrane via the twin-arginine translocation (Tat) pathway. The Tat pathway serves to secrete fully-folded proteins (Figure 1.3c) that mostly contain metal cofactors, which must be bound to the folded protein in the cytoplasm. Thus folding

must occur before the translocation of these proteins to *trans* side of the cytoplasmic membrane.

The secreted proteins can be integrated into the cytoplasmic membrane (membrane proteins) or secreted across it (extracellular proteins). Subsets of extracellular proteins become bound to the cell wall. The subsequent fates of the rest of remaining extracellular proteins depend on the type of bacterium. In Gram-negative bacteria these proteins are either compartmentalised in the periplasm or are integrated into the outer membrane. Gram-positive bacteria lack an outer membrane and, as a result, a conventional periplasm. In consequence, in Gram-positive bacteria, the proteins that fulfil the variety of functions in the periplasm of Gram-negative bacteria, are usually tethered to the cell membrane by virtue of an acyl modification at their N-terminus (*i.e.* lipoproteins) or attached to the cell wall or they are secreted to the surrounding medium. In case of cell surface proteins, they can be attached to the cell wall via covalent or non-covalent (ionic) interactions. Covalent linkage is carried out by enzymes, called sortases, which link the C-terminus of their target proteins to the peptidoglycan. Sortases recognise their substrates by the virtue of the presence of a sortase recognition sequence (typically LPXTG), a stretch of hydrophobic amino acids and a positively charged C-terminal tail (Fischetti *et al.*, 1990; Mazmanian *et al.*, 1999**)**. Non-covalent linkage of surface proteins includes predominately interactions with anionic wall polymers (reviewed in Navarre and Schneewind, 1999). Some proteins are attached to the cell wall by electrostatic interaction between their SLH (S-layer homology) domains and negatively-charged polymers attached to the cell wall (more extensively described in the **Section 1.8**).

1.5 Sec pathway

The main components of the bacterial Sec translocation system are: (1) the cytoplasmic chaperones: SecB and SRP; (2) the SecA ATPase, which serves as a piloting protein and the molecular motor driving movement of preproteins through the translocation channel; (3) a membrane-spanning translocation channel formed by a heterotrimeric SecYEG complex; (4) accessory proteins (**Section 1.5.4**).

The secretion of proteins by the Sec pathway takes place while they are in an unfolded conformation (secretion competent state) as they must pass through the narrow channel of the SecYEG translocase on their way to the *trans* side of the cytoplasmic membrane or to be integrated into the membrane itself. The competent state of the secretory proteins is maintained by the cellular chaperones SecB (found only in Gram-

negative bacteria) (**Section 1.5.3a**) and Signal Recognition Particle (SRP) (found in both Gram-positive and negative bacteria) (**Section 1.5.3b**). The SecB chaperone mediates translocation post-translationally by recognising the signal peptide and binding along the full length of the preprotein. The resulting binary complex then interacts with SecA, which drives the translocation of the preprotein through SecYEG translocation channel (Randall and Hardy, 2002; Zhou and Xu, 2005). In Gram-positive bacteria the CsaA chaperone is a putative functional (but not structural) homologue of SecB (**Section 1.5.3a**). In contrast, SRP drives co-translational protein translocation (Luirnik and Sinning, 2004; Shan and Walter, 2005). SRP binds the signal peptide of the nascent protein during its synthesis on the ribosome, arrests translation and delivers the preprotein-ribosome complex to the membrane-bound docking protein FtsY. The preprotein is then passed to SecA which drives translocation through the translocation channel (Figure 1.3).

1.5.1 Signal peptides and targeting cytosolic factors

The common feature of all secretory proteins targeted to the Sec or Tat pathways is their N-terminal signal peptide (Tjalsma *et al.*, 2004; Harwood and Cranenburgh, 2008). The structure features of the signal peptides of both the Sec and Tat pathways substrates exhibit the same pattern: (i) an N-terminus consisting of positively charged amino acids (N region); (ii) a hydrophobic core (H region); (iii) a C-terminal cleavage region (C-region) (Figure 1.3). Signal peptides are recognized by membrane targeting cytosolic factors, *e.g.* SRP or SecB that compete with each other and other cytosolic factors for binding to polypeptides emerging from the ribosome. In the case of polypeptides lacking signal sequences, the competition is won by factors other than SRP or SecB and the polypeptides are generally folded and are retained in the cytoplasm. If the N-terminal end of the protein is strongly hydrophobic and helical, then SRP binds and targets it for the secretion in a co-translational way (Bruch *et al.*, 1989; Valent *et al.*, 1998). In contrast, SecB binds the mature regions of the preprotein after it has been synthesized (post-translational mode of secretion). The SecB binding sites are located in the unfolded parts of the preprotein, thus proteins with a lower rates of folding are preferential targets for SecB (Topping and Randall, 1997). The signal peptides of the SecB-mediated secretory pathway may serve to delay protein folding so that SecB binding can maintain their substrates in a secretion competent state (Beena *et al.*, 2004).

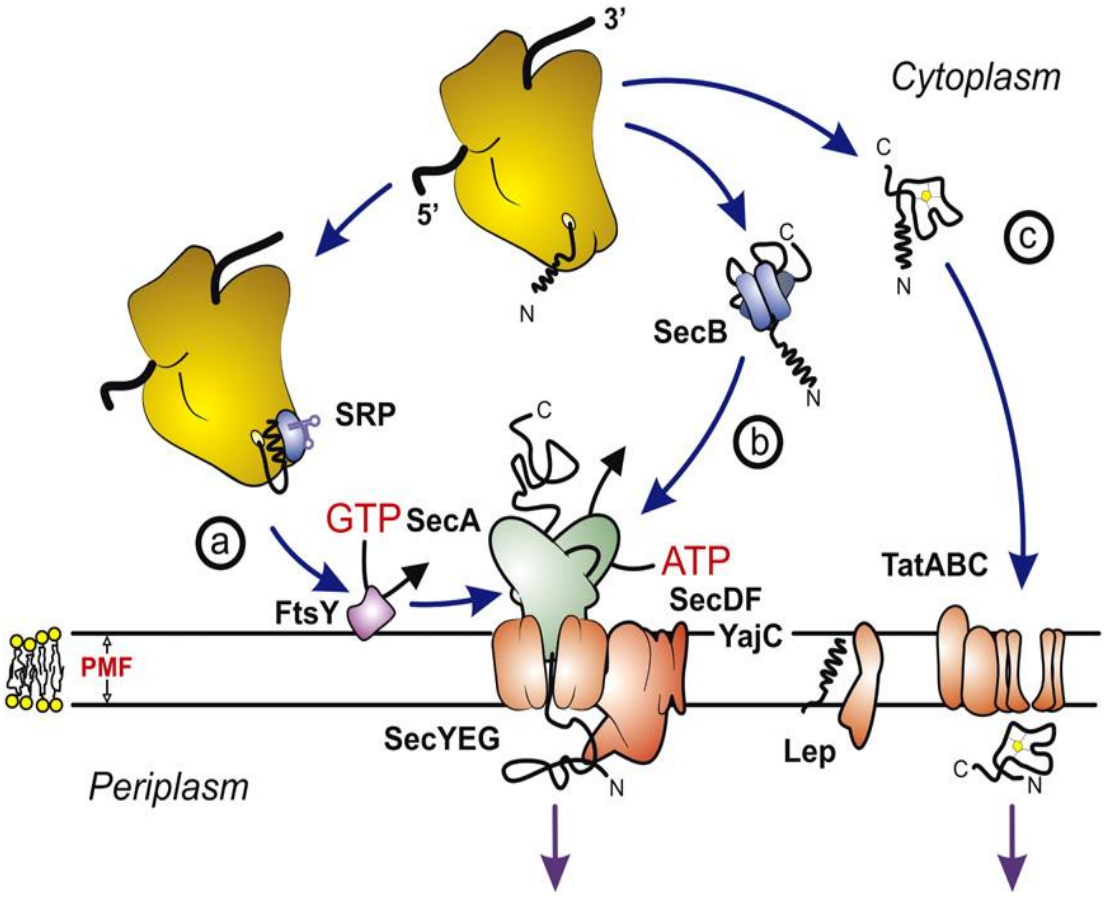

Figure 1.3: Schematic overview of the *Escherichia coli* Sec and Tat translocases. (a) Co-translational and (b) post-translational targeting routes, of translocation of unfolded proteins by the Sec translocase. (c) Translocation of folded precursor proteins by the Tat translocase (Natale *et al.*, 2008). Proteins are secreted by the means of the N-terminal signal peptide (helical structure). Co-translational mode of translocation (a) is mediated by the Signal Recognition Particle (SRP), which binds to the signal peptide of the nascent protein and delivers the ribosome with the protein being synthesized to the docking protein FtsY which provides energy (from GTP hydrolysis) for passing the ribosome/nascent protein to the SecA molecular motor. The SecA drives protein translocation through the translocation channel (SecYEG) with energy for the processes obtained through the hydrolysis of ATP. The auxiliary complex (SecDFYajC) facilitates the process. While the protein has been translocated the signal peptidase (Lep) cleaves the signal peptide. The co-translational mode of translocation (b) is mediated by the SecB chaperone. SecB binds fully synthesised protein and delivers it to the SecA, which drives its translocation. Substrates of the Tat pathway (c) are secreted by the TatABC transporter. N-terminal and C-terminal ends of proteins are annotated as 'N' and 'C', respectively.

The fate of proteins piloted by SRP is predominately membrane integration, while the fate of those piloted by SecB is secretion across the cytoplasmic membrane. In the above model the main function of the signal peptide is targeting. However, recently a new model was proposed by Gouridis et al. (2009), in which the signal peptide is not indispensable for targeting, but has other important functions. The model assumes that the signal peptides of the Sec pathway drive three successive states: first, "triggering"

that drives the translocase to a lower activation energy state; then "trapping" that engages the mature part of the preprotein with translocase and, finally, "secretion" during which the preprotein is secreted by the action of SecA. This model is based on studies in *E.coli* on the secretion of proPhoA (periplasmic alkaline phosphatase), which is SecB independent. It was observed that proPhoA binds with high affinity to SecYEG-bound SecA but not to SecYEG alone. When the signal peptide becomes impaired, the binding affinity is reduced only slightly (Gouridis *et al.*, 2009 and references within). In contrast, truncation of the carboxy terminal part of proPhoA reduced the SecA binding affinity seven-fold (Gouridis *et al.*, 2009), indicating that the mature part of the protein is also important to binding with SecA, and hence important for targeting. The study also indicated that the signal peptide is not necessary for targeting, but is necessary for translocation since it drastically lowers the ATPase activation energy. The initiation of protein secretion induced by lowering the activation energy by the signal peptide was termed "triggering". The next step, which is also signal peptide-dependent is called "trapping" where the mature part of the protein becomes bound in the translocase. Lastly, the preprotein is translocated by SecA driven by rounds of ATP hydrolysis. The findings based on experiments with proPhoA which gave rise to the above model were validated using other combinations of signal peptides and PhoA as well the signal peptide of PhoA and mature domains of other proteins (Gouridis *et al.*, 2009).

Types of signal peptides

Within the Sec pathway substrates, two classes of protein can be differentiated on the basis of their signal peptides: types I and II (Figure 1.3) (Tjalsma *et al.*, 2004; Harwood and Cranenburgh, 2008). Proteins with Type I signal peptides are targeted to the periplasm (Gram-negative bacteria), cell wall or to the external medium, while proteins with type II peptides are acyl modified and directed to the cytoplasmic membrane and, in the case of Gram-negative bacteria, also to the outer membrane.

In spite of their common overall structural patterns, there are differences in the signal peptides of Gram-positive and Gram-negative bacteria. Type I signal peptides of Gram-negative bacteria are on average less hydrophobic and shorter (ca. 25 amino acids) than those of those Gram-positive bacteria (ca. 30 amino acids). After the protein has been translocated, the signal peptide is removed by cleavage by a signal peptidase at a target site in the C-terminal region. In Gram-negative bacteria, signal peptides are usually cleaved 3-7 residues downstream of the C-terminal part of the H region. In

Gram-positive bacteria, the signal peptides are preferentially cleaved 7-9 residues downstream of the C-terminal part of the H region (Dalbey *et al.*, 1997).

Gram-negative bacteria encode only a single type I signal peptidase (Lep), while Gram-positive bacteria can encode more that one of those proteins. *Bacillus subtilis* for example encodes 5 type I signal peptidases: SipS, SipT, SipU, SipV and SipW. SipS and SipT are the major signal peptidases and at least one of those proteins must be present for *B. subtilis* to maintain viability (Tjalsma *et al.*, 1997). Some *Bacillus* strains contain additional plasmid-encoded signal peptidases (e.g. SipP), which in some cases can complement the lethality of the SipS and SipT double deletion (Tjalsma *et al.*, 1999).

Type II signal peptides are found at the N-terminus of lipoproteins and are cleaved by a type II signal peptidase (LspA) (Tjalsma *et al.*, 2001). In comparison to the type I signal peptides, the type II signal peptides possess shorter N and H regions as well rather different signal peptidase recognition site (consensus LAG-Cys), called the Lipobox (Figure 1.4).

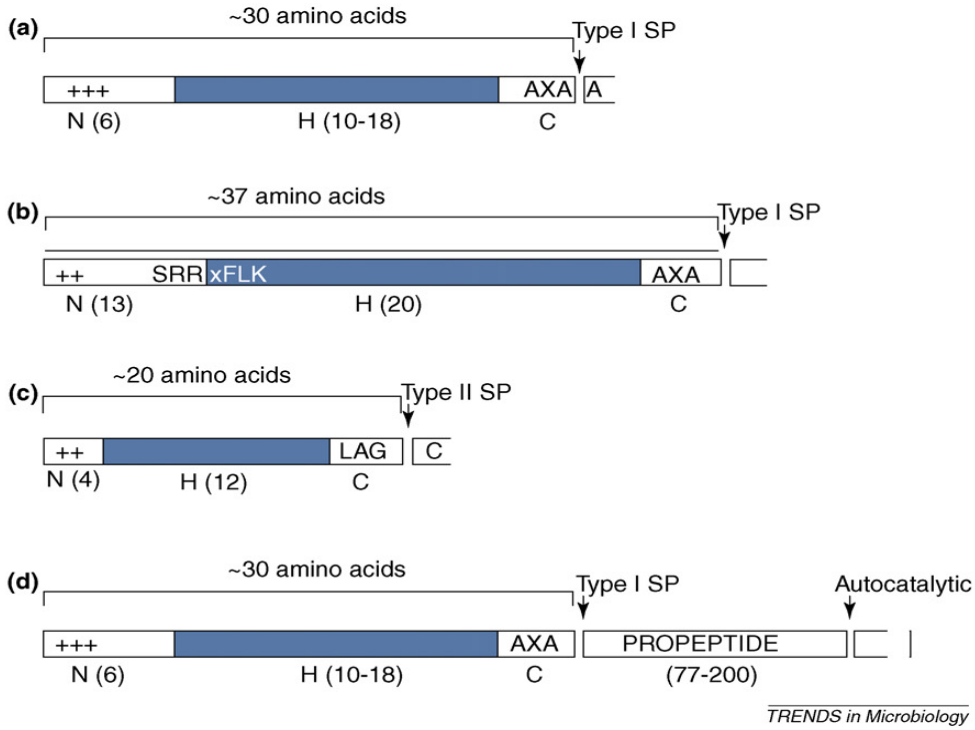

Figure 1.4: General features of the signal peptides and propeptides of *Bacillus* secretory proteins. The N-terminal (N), hydrophobic (H) and cleavage (C) regions are identified by contrasting shading and their lengths (amino acyl residues) are indicated in brackets. Cleavage sites are indicated by arrows. (a) Sec-dependent signal peptide cleaved by a type I signal peptidase (SP) at the AXA cleavage site. (b) Tat-dependent signal peptide with twin arginine motif (SRRxFLK), also cleaved by a type I SP. (c) Lipoprotein signal peptide cleaved by the type II SP. (d) The signal peptide and propeptide (prepropeptide) at the N-terminal end of a secretory protein requiring the propeptide for folding on the trans side of the cytoplasmic membrane (Harwood and Cranenburgh, 2008).

The signal peptides of proteins secreted by the Tat pathway include the so-called twin arginine motif (SRRxFLK) at the junction between the N and H regions. Overall, they are longer (ca. 37 amino acids) and exhibit lower hydrophobicity in comparison to the signal peptides of the Sec pathway substrates (Figure 1.3). Moreover, they have basic residues in the C-region. This latter characteristic is likely to play a role in preventing Tat substrates from being secreted via the Sec pathway (Cristobal *et al.*, 1999).

1.5.2 Structure and mode of action of SecA

SecA has been found to exist in a monomer-dimer equilibrium, but with the balance shifted towards the dimeric form (Woodbury *et al.*, 2002; Vassylyev *et al.*, 2006; Papanikolau *et al.*, 2007). Based on crystallographic studies (Hunt *et al.*, 2002; Sharma *et al.*, 2003; Osborne *et al.*, 2004; Mitra *et al.*, 2006; Vassylyev *et al.*, 2006; Zimmer *et al.*, 2006; Papanikolau *et al.*, 2007), SecA can be divided into the following regions/domains (Figure 1.5): (1) the DEAD motor domain; (2) helical scaffold domain (HSD); (3) substrate specificity domain (SSD); (4) C- terminal domain. The C- terminal domain can be further divided into additional sub-structures: (i) the helical Wing domain (HWD); (ii) IRA1 (intermolecular motor of ATPase activity) and (iii) the C-terminal region (CTD) containing a SecB-binding site. The DEAD domain is composed of nucleotide-binding domains (NBD1 and NBD2). The cleft formed at their interference is the site of ATP binding and its entrance is covered by ATP flap, which has a role in regulating ATP binding (Karamanou *et al.*, 1999). The SSD is the site of the preprotein binding (Musial-Siwek *et al.*, 2007; Papanikou *et al.*, 2005). The helical scaffolding domain (HSD) spans the SecA molecule serving as a scaffold for the other domains. The C-terminal domain is thought to have a role in the translocation process itself.

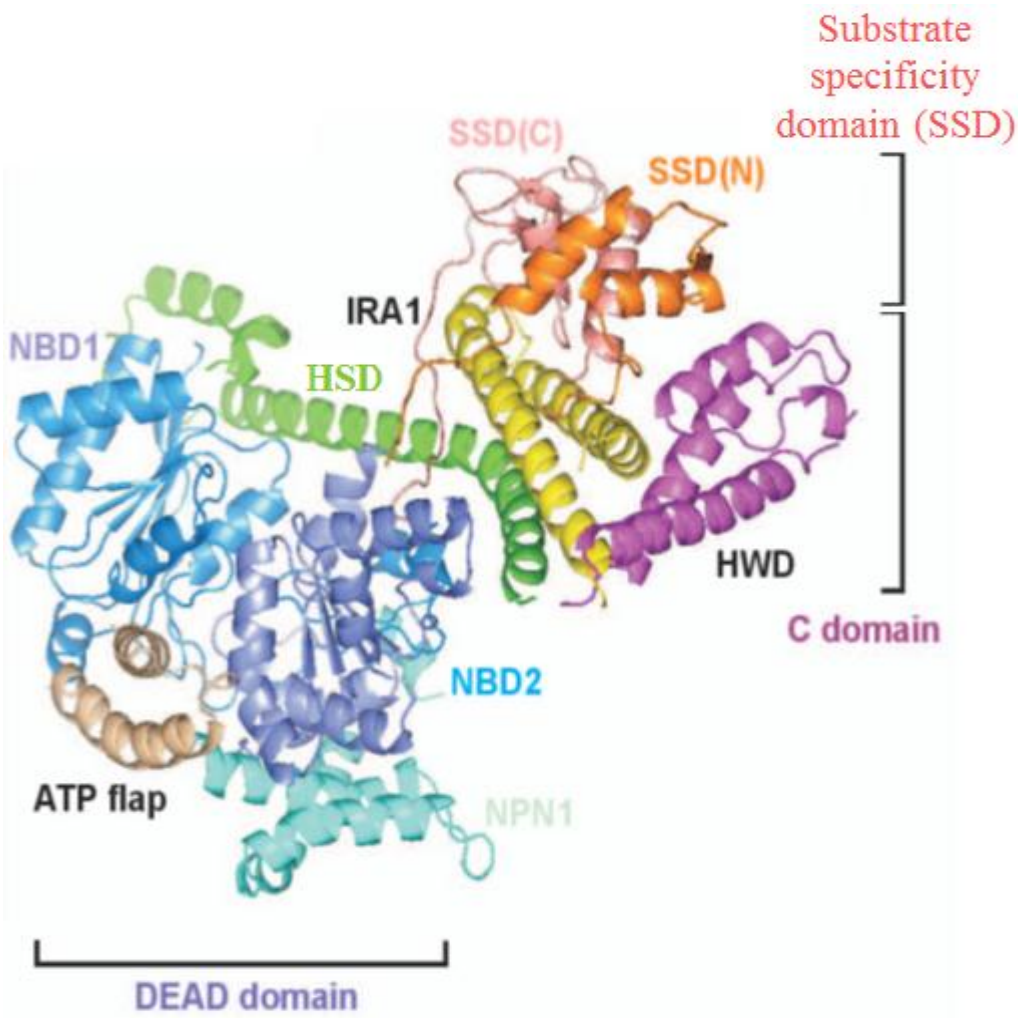

Figure 1.5: Structure of SecA. SecA consist of four main domains: (1) DEAD domain; (2) C domain and (3) substrate specificity domain (SSD), which can be divided into N-terminal subdomain (SSD(N)) (orange ribbons) and C-terminal subdomain (SSD(C)) (pink ribbons); (4) helical scaffolding domain (HSD) (green ribbons). C-domain can be further divided into: (i) intermolecular motor of ATPase activity (IRA1) (yellow ribbons); (ii) wing domain (HSD) (purple ribbons) and the C-terminal region (CTD) (not shown). DEAD domain is composed of: (i) nucleotide binding domain 1 (NBD1) (dark blue ribbons), its N-terminal part is shown in light blue (NPN1); (ii) nucleotide binding domain 2 (NBD2) (violet ribbons). The cleft between NBD1 and NBD2 is covered by ATP flap (brown ribbon) (from Mitra *et al.*, 2006).

SecA drives translocation by pushing the secretory protein through the translocation channel by repeated cycles of insertion and deinsertion. ATP and preprotein-bound SecA interacts with the SecYEG translocon and, as it inserts, pushes 20-30 amino acids of the preprotein through the channel (Schiebel *et al.*, 1991; Joly *et al.*, 1993; Economou *et al.*, 1994; Wolk *et al.*, 1997). ATP hydrolysis triggers the release of the preprotein from SecA results in the deinsertion of the latter. Repeated cycles of insertion and deinsertion lead to preprotein integration into the membrane or secretion (the model is presented on the Figure 1.6). When the translocation is well advanced, the proton motive force can continue to drive translocation (Schiebel *et al.*, 1991; Driessen, 1992).

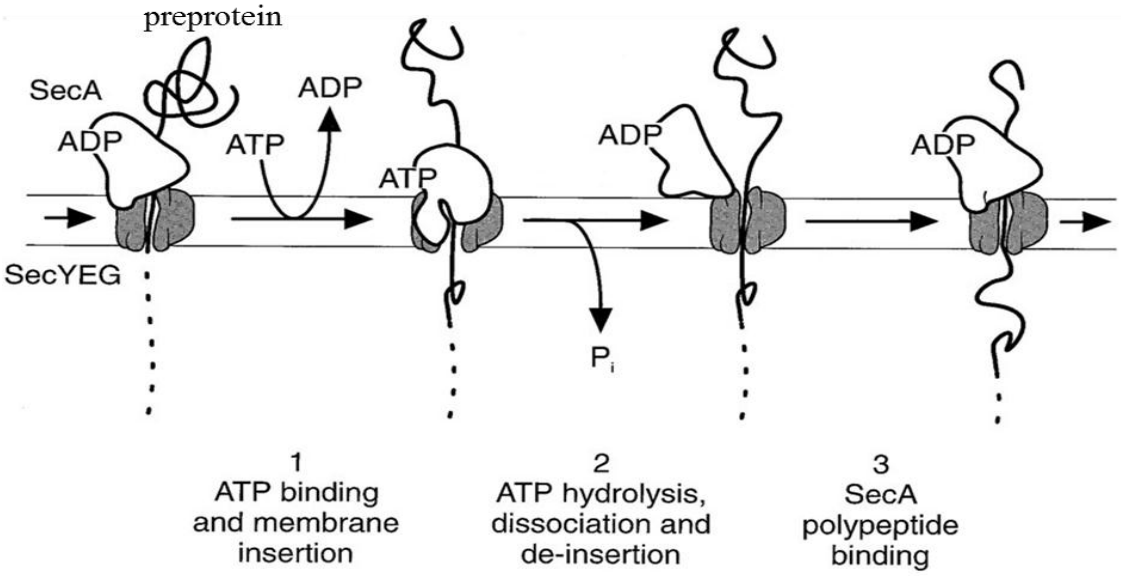

Figure 1.6: Model for ATP-driven preprotein translocation. At the start of translocation: ADP-bound SecA – preprotein complex is docked onto the SecYEG channel. The three steps of translocation can be distinguished: (Step 1): ADP dissociates and is replaced by ATP, which triggers insertion of SecA into the translocation channel pushing around 30 amino acids of the pre-protein into it, (Step 2): Hydrolysis of ATP causes dissociation of SecA from the pre-protein and de-insertion from the translocation channel; (Step 3): De-inserted SecA binds to the exposed portion of the partially-translocated preprotein. The cycles of the insertion and de-insertion continue pushing the whole preprotein is pushed through the channel (Figure modified from Wolk *at al.*, 1997).

Interaction between signal peptide and SecA

The signal peptide binds to a groove in SecA located at the interface of the substrate specificity domain and IRA1. The groove is mostly hydrophobic, but is surrounded by a number of polar and charged residues (Gelis *et al.*, 2007). Firstly, the positively charged amino acids located at the N-terminus of the signal peptide form electrostatic interactions with acidic residues of SecA found around this hydrophobic groove. Next, hydrophobic interactions are formed between the signal peptide and the groove. However, part of the signal peptide binding grove is occluded by the C-terminal domain of SecA, preventing the binding of the signal peptides of SecB-dependent proteins. This auto-inhibition can be overcome by the action of SecB in displacing the C-terminal domain of SecA. In the case of SecB-independent substrates such as PhoA, the inhibition of signal peptide binding by the C-terminal domain is low, and consequently the signal peptide binds without the need for additional factors (Gelis *et al.*, 2007).

1.5.3 Intracellular pathways

1.5.3a Post-translational mode of translocation

The key component of the post-translational mode of translocation is SecB, which is a molecular chaperone responsible for keeping a subset of secretory proteins of the Sec pathway in a secretion competent state, *i.e.* in an essentially unfolded conformation. This chaperone has been found only in the Gram-negative bacteria (Fekkes *et al.*, 1999; Muren *et al.*, 1999). Unlike SecA, SecB is not essential for viability (Kumamoto *et al.*, 1983). When the *secB* gene is disrupted, leading to the lack of a functional SecB protein, the secretion of SecB-dependent proteins is prevented. Such a mutant is unable to grow in rich media, but is viable in minimal media. The first protein to be shown to be SecB dependent was the maltose binding protein, MBP (Gannon *et al.*, 1993). It was observed that in the absence of a functional SecB, the preMBP folds in the cytoplasm and is retained within this compartment. Subsequently, SecB was shown to be involved in the secretion of a variety of proteins including: GBP, PhoE, LamB, OmpF, OmpA, DegP, FhuA, FkpA, OmpT, OmpX, OppA, TolB, TolC, YbgF, YgiW and YncE (Baars *et al.*, 1996). The predominant model for the chaperoning action of SecB is called the ‘’kinetic partitioning model’’ (Hardy and Randall, 1991). It assumes that the signal peptides of SecB targeted proteins, slow down their folding. In the environment of the cytoplasm, there is competition between chaperones. If a molecular chaperone, such as DnaK or the trigger factor outcompete SecB, the protein will be retained in the cytoplasm. If SecB wins, the protein is destined for secretion. The resulting SecB/preprotein binary complex interacts with SecA, to form a ternary complex (Hartl *et al.*, 1990). The affinity of the SecB/preprotein complex to SecA depends on the association of the later with the SecYEG translocation channel. When SecA is bound to the translocation channel, then its affinity for SecB increases greatly. The interaction becomes even stronger when SecB is present as a binary complex with preprotein substrate (Fekkes *et al.*, 1998; Hartl *et al.*, 1990). So the model that emerges from these data is that SecB binds to its preprotein substrate and the binary complex binds dimeric SecA already docked on the SecYEG channel. The preprotein is transferred to the SecA molecular motor, triggering the displacement of ADP and its replacement by ATP. This in turn induces the dissociation of SecB. Finally SecA drives protein translocation (Fekkes *et al.*, 1997).

Although a SecB homologue has not been found in Gram-positive bacteria, the CsaA protein of *Bacillus subtilis* has been proposed to possess chaperone-like activity. Moreover, CsaA stimulates the secretion of SecB-dependent proteins in SecB-negative

mutants of *E. coli* (Müller *et al.*, 2000). Bioinformatic analysis revealed that CsaA is also present in other bacteria (both Gram-positive and Gram-negative) including: *Bacillus anthracis, Bordetella bronchiseptica*; *Bacillus haloduran, Legionella pneumophila*; *Pseudomonas aeruginosa*; *Rhodobacter sphaeroides*; *Thermus thermophile* (Kawaguchi *et al.*, 2001).

The structure of SecB has been shown to be tetrameric, consisting of a dimer of dimers (Muren *et al.*, 1991; Topping *et al.*, 2001, Dekker *et al.*, 2003). Each monomer is comprised of four stranded β-sheets in an anti-parallel arrangement. The cores of each monomer, built by β-sheets, are linked by α-helices and the subunits of each dimer are rotated with respect to each other at 180^{o} (Figure 1.7) (Dekker *et al.*, 2003).

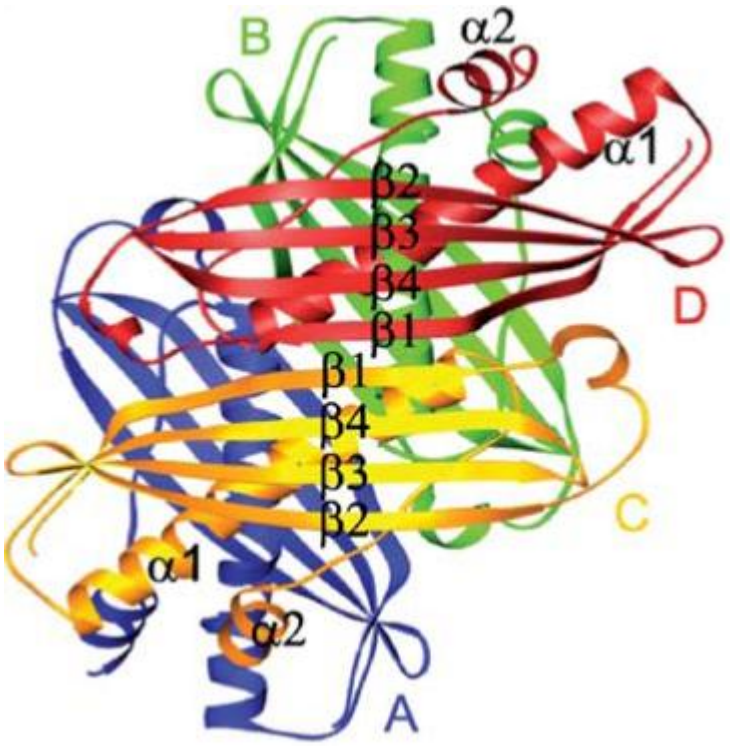

Figure 1.7: View of SecB, showing its tetrameric structure (subunits A-D). Each subunit consists of four β-sheets strands linked by α-helices (*Dekker et al.*, 2003).

Each side of the tetramer possesses two channels (called also grooves), harbouring two putative substrate binding sites with leucine at the position 42 being crucial for substrate binding (Figure 1.8) (Bechtluft *et al.*, 2010). Preprotein substrates are probably wrapped around the tetramer in such a way to access these binding sites and in such a way as to be maintained in an essentially unfolded state (Peltier *et al.*, 2002; Mogk *et al.*, 2003).

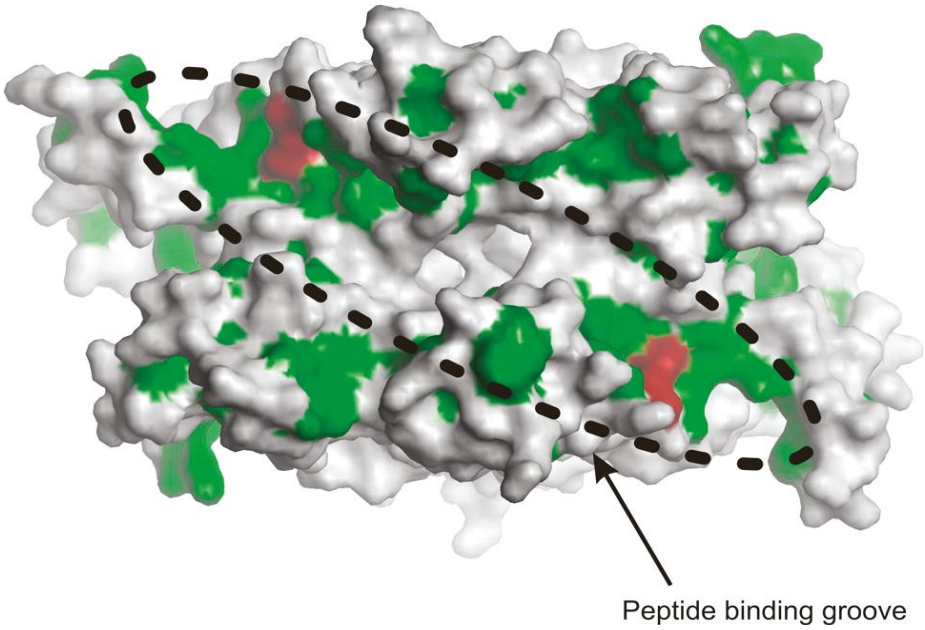

Figure 1.8: Solvent-accessible surface of the SecB tetramer (Protein Data Bank entry 1QYN) with the hydrophobic surface colored green and the position of leucine 42 colored dark red. The proposed peptide binding groove is encircled (Bechtluft *et al.*, 2010).

1.5.3b Co-translational mode of translocation

The signal recognition particle (SRP) is involved in the co-translational mode of translocation (Figure 1.3). It has been found in both Prokaryotes and Eukaryotes (Keenan *et al.*, 2001). The SRP of *E. coli* is a ribonucleoprotein comprising the Ffh (fifty-four kDa protein homologue) protein and 4.5S RNA. In *B. subtilis* the SRP is additionally comprised of the histone-like HBsu protein (Nakamura *et al.*, 1999). Ffh has a flexible, hydrophobic groove which can accommodate a wide range of peptides (Luirink *et al.*, 2004). The 4.5S RNA probably aids the processes by interacting with the positively-charged amino acids of the N-terminus of the signal peptide (Luirink *et al.*, 2004). The current model assumes that SRP binds to the signal peptide of the nascent protein, which in Eukaryotes halts translocation (Walter and Blobel, 1981). This translation arrest has not been shown to occur in bacteria. Consistent with this observation, the SRP of Gram-negative bacteria lacks the domains (5' and 3' RNA domains) responsible for translational arrest (Nakamura *et al.*, 1999; Siegel and Walter, 1988). Gram-positive bacteria do, however, contain those domains, although it remains to be established whether SRP-mediated translational arrest occurs in these bacteria (Siegel and Walter, 1988). Next, the ribosome/nascent protein complex is delivered to the docking protein FtsY and then passed to the SecA/SecYEG translocase, where SecA drives translocation of the preprotein through the channel. The intracellular process leading to transferring the preprotein to SecA is driven by the energy released from the

hydrolysis of GTP, as SRP and FtsY have GTPase activity (Shan and Walter, 2005). Both key components specific to this pathway, SRP and FtsY, are essential for viability in *E. coli* (Phillips *et al.*, 1992; Luirnik *et al.*, 1994) and in *B. subtilis* (Kobayashi *et al.*, 2003). However, in streptococci, the SRP pathway was shown not to be essential under non-stressfull growth conditions (Crowley *et al.*, 2004).

1.5.4 SecYEG translocation channel

The SecYEG translocation channel is composed of three proteins, SecY, SecE and SecG (Brundage *et al.*, 1990; Akimaru *et al.*, 1991), which form a pore in the cytoplasmic membrane through which secretory proteins pass across or into the membrane (Figure 1.9). SecY and SecE are closely associated and form the core of the translocation channel. The largest subunit of the translocation channel is SecY. In *E. coli* SecY is 443 amino acid long (Cerretti *et al.*, 1983), while In *Bacillus subtilis* SecY is 423 amino acids in length. In *B. subtilis,* like in *E. coli*, SecY and possesses ten transmembrane domains (TMDs) with the N- and C-termini residing in the cytoplasm (Akiyama and Ito, 1987). SecY is essential for protein translocation and therefore viability (Ito *et al*., 1984; Kobayashi *et al.*, 2003). The transmembrane segments are organized into two domains: N-terminal (with TMD 1-5) and C-terminal (with TMD 6-10). This dimeric-like arrangement is referred to as a clamshell-like structure, in which the domains are joined by a hinge-like loop. SecY is the main component of the translocation pore and is opened and closed by a structure called the plug, which was studied in *E. coli*. The equilibrium between the open and closed states moves towards the open state when a signal peptide becomes bound to the side of the translocation channel (between TMD 2 and 7) (Plath *et al.*, 1998). This triggers a shift of the equilibrium towards the open state by the formation of a disulphide bond between the plug and the SecE protein, while the closed state is triggered by the reduction of that bond (Harris and Silhavy, 1999). At its narrowest point, a ring of hydrophobic amino acids lines the pore, forming a gasket-like structure around the protein being translocated. This presumably prevents the passage of small molecules during translocation (Berg *et al.*, 2004). After the movement of the plug out of the channel, the ring of hydrophobic amino acids opens slightly, allowing for the insertion of the mature region of the secretory substrate into the pore of the channel in the form of the loop. Membrane proteins move to the membrane via a lateral gate formed by the open face of the clamshell.

SecY may exist in dimeric (Sluis *et al.*, 2002; Duong *et al.*, 2003; Tziatzios *et al.*, 2004) and oligomeric (Beckmann *et al.*, 1996; Beckman *et al.*, 2001; Menetret *et al.*, 2005; Mitra *et al.*, 2005; Scheuring *et al.*, 2005) arrangements, with the dimer probably being the minimal functional entity. Observations suggest that the dimeric arrangement of SecY may exist in two forms: (i) back-to-back (Veenendaal *et al.*, 2002) and (ii) "front-to-front" (Mitra *et al.*, 2006). In case of the "front-to-front" arrangement, SecYEG might fuse to form a single large channel.

SecE is the second component of the translocation channel and, like SecY, is essential for viability and protein secretion. *E. coli* SecE is 127 amino acids in length and encompasses three transmembrane domains. In Gram-positive bacteria, SecE is smaller consisting of approximately 60 amino acids and encompasses only one transmembrane domain, which corresponds to cytoplasmic loop 2 and the third TMD of *E. coli* SecE (Murphy *et al.*, 1994). In *E. coli* the first two transmembrane domains are not necessary for viability and protein secretion (Schatz *et al.*, 1991; Nishiyama *et al.*, 1992). SecE is closely associated with and forms a clamp across SecY, probably holding two SecY subunits together. It participates in the opening of the translocation channel upon its bind the signal peptide of the the substrate protein, by binding the plug by means of the disulphide bond (Harris and Silhavy, 1999).

SecG is loosely associated with the translocation channel and consists of 110 amino acids and forms two transmembrane domains in *E. coli* (Kontinen *et al.*, 1996). *B. subtilis* was found to possess *yvl* gene encoding functional homologue of SecG of *E. coli* (van Wely *et al.*, 1999). In both, *E. coli* and *B. subtilis*, they are predicted two posses two transmembrane domains linked through a glycin-rich loop, but *B. subtilis* SecG is shorter as its lacks carboxy-terminal extension. It is not essential for viability or protein translocation, but its deletion leads to a cold-sensitive phenotype (Flower *et al.*, 2000). However, SecG has an enhancing effect on translocation at least in an *in vitro* translocation assay (Douville *et al.*, 1994; Nishiyama *et al.*, 1993). In the *secG*-negative strain of *B. subtilis*, the cold-sensitive phenotype was only observed under conditions of α-amylase overproduction (van Wely *et al.*, 1999).

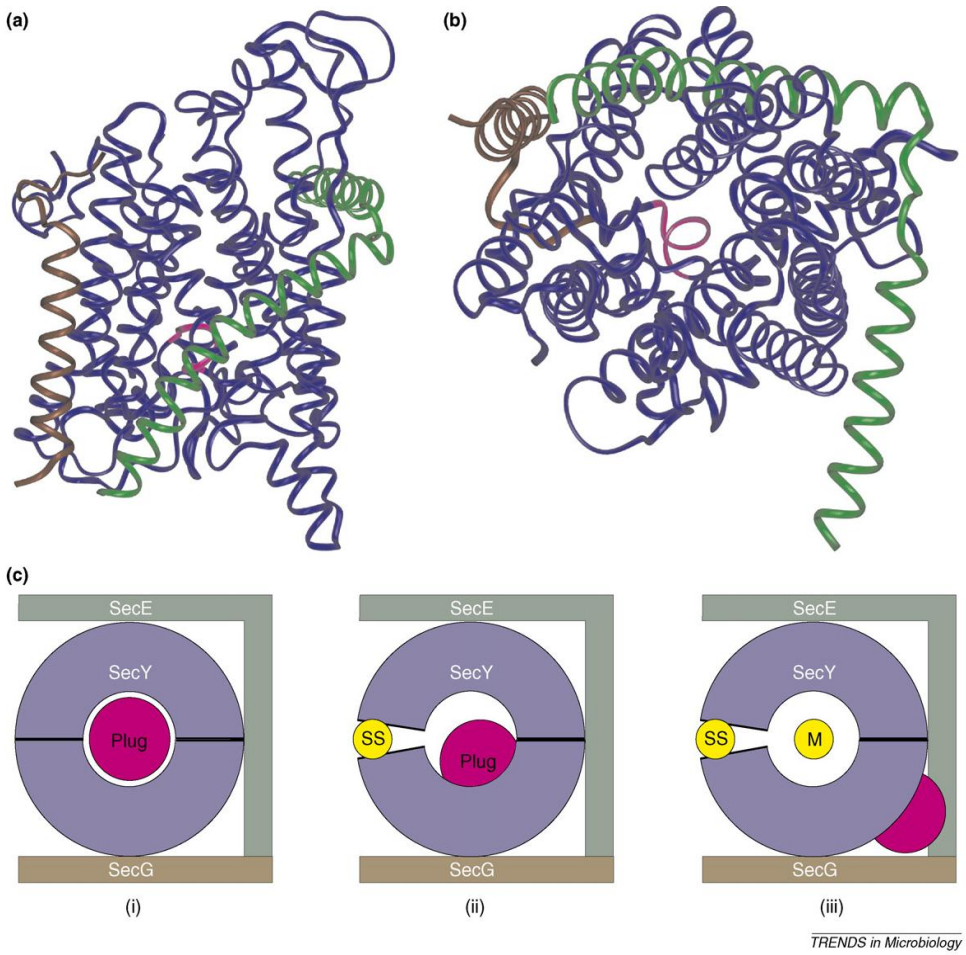

Figure 1.9: Structure of the SecYEG translocation complex from *Methanococcus jannaschii*. (a) The SecY structure as seen from the plane of the membrane. SecY is coloured blue, SecE is green and SecG is brown. The cytoplasm is to the top and the periplasm to the bottom. (b) The complex viewed from the periplasmic side. The three chains are the same colours as in part (a) but the plug is highlighted in pink. The complex forms a channel with the plug blocking translocation in the inactive state. SecE and SecG are located on three sides of the complex, leaving the fourth side open to accept signal sequence binding and to enable lateral exit of membrane domains. (c) The diagrams illustrate the export pathway: (i) The SecY complex is in the inactive state. The plug prevents passage of molecules and the ring is closed. (ii) Binding of a signal sequence (SS) to SecY TM7 and TM2 triggers movement of the plug out of the channel and opening of the hydrophobic ring. (iii) The fully active state is depicted. The plug has moved to interact with the periplasmic portion of SecE and the ring has widened to enable movement of the mature secretory protein (M) through the channel (Flower *et al.*, 2007).

The SecD, SecF proteins form an auxiliary translocation complex, which associates with SecYEG to facilitate protein translocation. In *E. coli* SecD and SecF are two separate proteins to form a complex with YajC protein (Duong and Wickner, 1997). In contrast, *B. subtilis* SecD and SecF are fused into a single membrane protein of 571 amino acids that is predicted to span the membrane 12 times and form complex with YrbF, which is a homologue of *E. coli* YajC (Bolhius *et al.*, 1998). However, in

B. halodurans, SecD and SecF are two seprate proteins (Takami *et al.*, 2000). In other Gram-positive bacterium *Lactococcus lactis* a homolog of SecDF has not been found (Bolotin *et al.*, 1999). When the SecD and SecF proteins are depleted, cell viability and protein secretion were observed to be severely compromised in *E. coli* (Duong *et al.*, 1997). In *B. subtilis*, depletion of SecDF results in a weak cold sensitivity of growth and a reduced efciency of the secretion of neutral protease (Bolhuis *et al.*, 1998). It is has been proposed that the SecD, SecF, YajC complex participates in the release of translocated proteins from the membrane or the regulation of SecA cycling (Economou *et al.*, 1995).

YidC, that has been found in *E. coli*, participates in the insertion of proteins into the cytoplasmic membrane and is essential for viability (Dalbey and Kuhn, 2004). It accomplishes its action on its own or in co-operation with the SecYEG complex. YidC is also required for the correct folding of transmembrane proteins and depletion of YidC leads to the induction of membrane stress (Shimohata *et al.*, 2007). In *B. subtilis* two homologs of YidC are found: SpoIIIJ and YqjG. Both: SpoIIIJ and YqjG are able to complement *E. coli* YidC-deficiency in the respect to SecYEG-dependent membrane proteins, but not to SecYEG-independent proteins (Saller *et al.*, 2009). Either SpoIIIJ or YqjG must be present in *B. subtilis* so that bacterium remains viable (Murakami *et al.*, 2002, Tjalsma *et al.*, 2003).

Summery comparison of the components of the translocation channel and the associated proteins in Gram-negative and Gram-positive bacteria is presented in the Table 1.1.

Table 1.1: Summery comparison of the components of the translocation channel and the associated proteins in Gram-negative and Gram-positive bacteria.

Component	Gram-negative (*E. coli*)	Gram-positive (*B. subtilis* if not mentioned otherwise)
SecY	Common features	
	• Essential for protein secretion and viability • 10 transmembrane segments are organized into two domains with dimeric-like arrangement which is referred to as a clamshell-like structure. • Main component the of the translocation channel, where the pore is located.	
	Differences	
	• Size: 443-amino acid polypeptide	• Size: 423-amino acid polypeptide
SecE	Common features	
	• Essential for protein secretion and viability. • forms a clamp across SecY probably stabilising it.	
	Differences	
	• Size: 127 amino acids in length • Three transmembrane domains	• Size: approximately 60 amino acids • One transmembrane domain
SecG	Common features	
	• Not essential for protein secretion and viability, but cold-sensitive phenotype observed. • Composed of two transmembrane domains.	
	Differences	
	• *B. subtilis* SecG is shorter then SecG of *E. coli* as in comparison, it lacks carboxy-terminal extension.	
SecDF/ YajC/YrbF	Common features	
	• Not essential for protein secretion and viability, but enhance secretion	
	Differences	
	• SecD and SecF are two separate proteins to form a complex with YajC. • Deletion of SecDF has strong negative effect on cell viability and protein secretion.	• SecD and SecF are fused into a single membrane protein that forms a complex with YrbF. In *B. halodurans* SecD and SecF are two separate proteins. • *Lactococcus lactis* lacks a clear SecDF homolog. • In *B. subtilis*, depletion of SecDF results in a weak cold sensitivity of growth and a reduced efficiency of the secretion of neutral protease.
YidC /its homologs	Common features	
	• Involved in the biogenesis of membrane proteins.	
	Differences	
	• YidC has been found in *E. coli* • involved in the insertion of hydrophobic sequences into the membrane in the SecYEG-dependent and in the SecYEG-independent manner. • essential for viability.	• In *B. subtilis* two homologs of YidC are found: SpoIIIJ and YqjG. • SpoIIIJ and YqjG are able to complement *E. coli* YidC-deficiency in the respect to SecYEG-dependent membrane proteins, but not to SecYEG-independent proteins. • Either SpoIIIJ or YqjG must be present in *B. subtilis* so that bacterium remains viable.

1.5.5 Extracellular pathways

After their translocation across the cytoplasmic membrane in an essentially unfolded state, proteins must be properly folded so that they are functional; misfolded proteins are removed by 'quality control' extracellular proteases (Miot and Betton, 2004). The rapid folding of secreted proteins is critical since it avoids the formation of protein aggregates and inappropriate interactions with the cell wall, potentially blocking cell wall growth sites. A number of factors (called foldases) are employed to ensure the correct and rapid folding of secretory substrate proteins. Those include: (i) peptidyl-prolyl *cis-trans* isomerases; (ii) thiol-disulphide oxidoreductases; (iii) propetides; (iv) certain metal cations.

Peptidyl-prolyl *cis/trans* isomerases (PPIases) are important folding factors of a subset of secretory proteins containing proline residues, which can exist in either the *cis* or the *trans* isomeric form. Since peptide bonds require the *trans* isomer of proline, *cis-trans* isomerisation is required to ensure the *cis* isomers are converted to the *trans* form (Schmid, 2001). In Gram-negative bacteria, the PPIases involved in secretion are found in the periplasm. However, in Gram-positive bacteria the PPIases involved in secretion are lipoproteins attached to the outer interface of the cytoplasmic membrane so that they are active at the membrane-cell wall interface. In terms of structure and function, PPIases can be grouped into three families: cyclophilins, FK506-binding proteins (FKBP) and parvulins (Gothel *et al.*, 1999). *B. subtilis* PrsA belongs to the a parvulin family with parvulin-like domain surrounded by N- and C-terminal regions that share homology only to PrsA-like proteins encoded by species related to *B. subtilis* (Rahfeld *et al.*, 1994). Its PrsA is essential for both protein secretion and cell viability (Kontinen and Sarvas, 1993; Kontinen *et al.*, 1991). Interestingly, one of *B. subtilis* PrsA substrates, AmyQ does not possess proline residues, suggesting that the PPIase activity of PrsA may not be involved in processing this protein. This was confirmed by the ability of a derivative of PrsA with mutations in the putative active centre of its PPIase domain to be active for the folding of AmyQ. This suggests that in addition to its PPIase activity, PrsA, has a second, but as yet unknown, chaperone-like activity (Vitikainen *et al.*, 2001). In comparison, *B. anthracis* encodes three PrsA-like proteins, PrsAA, PrsAB, PrsAC, all three are able to complement a *prsA*-null mutant of *B. subtilis* (Williams *et al.*, 2003).

Some secretory proteins contain disulphide bonds that are necessary for their stability and activity. Formation of these bonds takes place following translocation. The reaction is catalysed by thiol-disulphide oxidoreductases. Four of these enzymes have

been described in *B. subtilis:* BdbA, BdbB, BdbC, BdbD (Bolhuis *et al.*, 1999; Meima *et al*., 2001).

Propeptides are a common feature of *Bacillus* secretory proteins, particularly proteases and are located between the signal peptide and the mature protein (Figure 1.4d). When present in proteases, they inhibit their proteolytic activity prior to translocation (Wanderman, 1989) but, once translocated, the propepides catalyse their folding (Gallagher *et al.*, 1995; Wang *et al.*, 1998) and activation (Yabuta *et al.*, 2001).

Finally, most *Bacillus* secretary proteins are metalloproteins and metal cations are important for their folding, stability and activity. Metal ions are adsorbed to the anionic cell wall and are readily available for proteins as they emerge from the translocation channel.

1.6 Additional SecA and SecY systems (secondary translocases)

Multiply homologues of SecY (SecY1 and SecY2) and SecA (SecA1 and SecA2) have been found in some Gram-positive bacteria such as: *Streptococcus gordonii, S. parasanguinis, S. pneumoniae, Staphylococcus aureus, Mycobacterium tuberculosis, Listeria monocytogenes*, *Bacillus anthracis Mycobacterium smegmatis*, *Listeria innocua*, and *Corynebacterium glutamicum* (Rigel and Braunstein, 2008). SecA1 and SecY1 are so named because their sequences are more similar to the canonical SecA and SecY, respectively, and they have 'house-keeping' roles. SecA2 and SecY2 share less homology with canonical SecA and SecY, respectively, and are always (in the case of SecA2), or in many cases (in the case of SecY2), involved in export of a subset of proteins, especially virulence factors (Bensing and Sullam, 2002; Bessing *et al.*, 2005; Braunstain *et al.*, 2003; Chen *et al.*, 2004; Lenz and Portnoy, 2002, Lenz *et al.*, 2003; Machata *et al.*, 2005). The last observation may indicate that secondary translocases have evolved to facilitate pathogenesis of certain pathogenic bacteria. Secretion pathways comprising additional types of SecA-like and SecY-like proteins can be split into two categories: (i) those containing both SecA2 and SecY2, and (ii) those containing SecA2 only.

SecA2 only systems have been found in *Mycobacterium tuberculosis, M. smegmatis* and *Listeria monocytogenes*. In these bacteria, SecA2 drives the secretion of a subset of proteins some of which possess clearly identifiable signal peptides, (*e.g.* p60 autolysin of *L. monocytogenes*, Lenz *et al.*, 2003), and others that do not (*e.g.* superoxide dismutase of *L. monocytogenes*, Archambaud *et al.*, 2006). The failure to delete SecA1, while overexpressing SecA2 in mycobacteria showed the SecA1 is

essential for viability in this group of bacteria and SecA2 cannot complement its function. Similarly, SecA1 cannot replace SecA2 in the secretion of SecA2-dependant proteins (Braunstain *et al.*, 2001).

Systems comprising both SecA2 and SecY2 have been found in many species of the *Streptococcus* group as well in *S. aureus* and *B. anthracis*. Here, two types of systems are postulated to exist (Rigel and Braunstein, 2008): (i) SecA2 and SecY2 co-operate with SecA1 and SecY1 to form a canonical translocon; (2) SecA2 and SecY2 form a novel translocon without the participation of SecA1 and SecY1 (Figure 1.10).

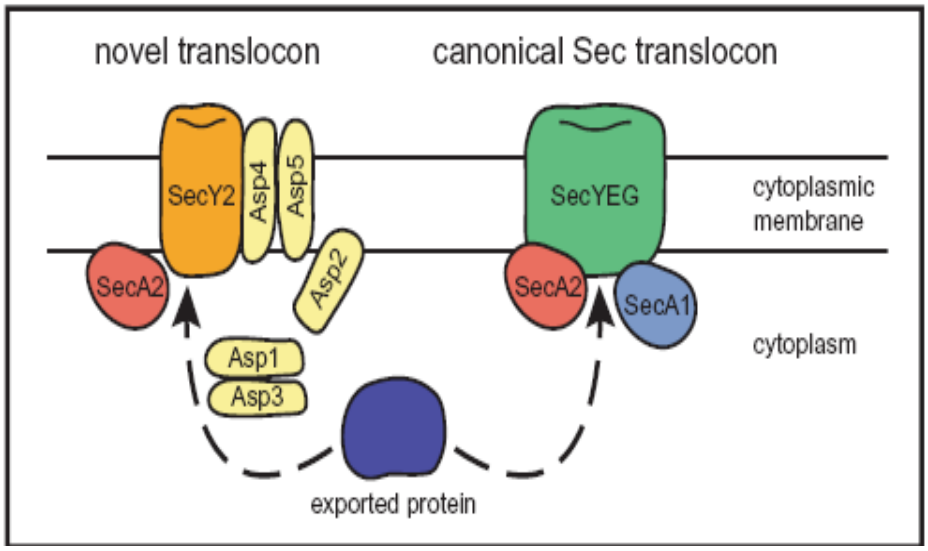

Figure 1.10: Models for SecA2-dependent export. In the various accessory Sec systems, a SecA2-exported protein (shown in blue) might be exported either through a novel translocon or the canonical SecA1/SecYEG translocon with the assistance of SecA2. The example of a novel translocon is modelled on the SecA2/SecY2 system of *S. gordonii*, which is a candidate for this type of pathway (Rigel and Braunstein, 2008).

An example of a species encoding a novel translocon is *Streptococcus gordonii* (Figure 1.10). This accessory translocon is thought to consist of SecA2, SecY2 and five accessory proteins, Asp1 to Asp5 (Bensing and Sullam, 2002; Takamatsu *et al.*, 2004; Takamatsu *et al.*, 2005). The secretory preprotein substrate of this system, GspB, is a virulence factor responsible for the binding of *S. gordonii* to platelets (Bensing and Sullam, 2002). SecA2 and SecY2 are thought to act together in the secretion of this protein as the deletion of either prevents GspB secretion (Bensing and Sullam, 2002). Asp1-3 are predicted to be intracellular proteins, while Asp4 and Asp5 are homologues of SecE and SecG, respectively. They appear to interact with SecY2 to form a translocation channel, which interacts specifically with SecA2 to transport GspB (Takamatsu *et al.*, 2005). GspB and all of the other components of this accessory translocon are encoded in a common locus. Similar loci are found in related pathogenic bacteria e.g. *S. parasanguinis* (Rigel and Braunstein, 2008) (Figure 1.11), suggesting

that the putative substrate proteins encoded within those loci are also pathogenicity factors.

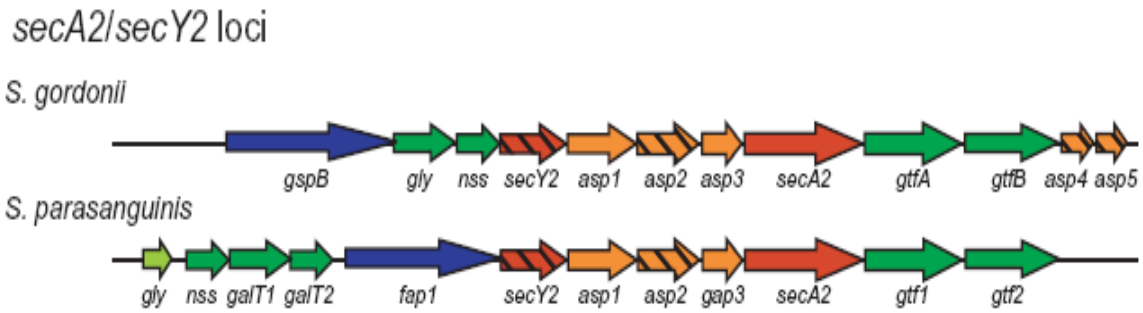

Figure 1.11: Organization of accessory *sec* loci. Genes with similar colouring encoded proteins with homology or similar properties. Genes encoding SecA2-dependent substrates are in blue, glycosyl transferases in green, accessory Sec proteins in red, accessory SecA2-dependent secretion factors in orange. Genes encoding proteins with predicted transmembrane domains are hatched (Rigel and Braunstein, 2008).

1.7 Secondary translocase of *B. anthracis*

B. anthracis contains homologues of many elements of the *B. subtilis* secretion pathway. Apart from two homologues of SecA (SecA1 and SecA2) and two homologues of SecY (SecY1 and SecY2) mentioned before, it also contains: three homologues of the PrsA foldase (PrsAA, PrsAB and PrsAC), and 7 homologues of signal peptidase, called Sip; in comparison five homologues of Sips are found in *B. subtilis* (Figure 1.12).

The role of SecA2 and SecY2 in *B. anthracis* was investigated by Pohl and colleagues (unpublished). The supernatant fractions of the extracellular proteins isolated from the wild type and Δ*secA2* and Δ*secY2* mutants of *B. anthracis* were analysed by two-dimensional gel electrophoresis (Figure 1.13). Comparison of the protein profiles of the wild type and the mutants showed that SecA2 is necessary for the secretion of two prominent proteins, identified by mass spectrometry as Sap and EA1. In contrast, the pattern of proteins secreted by the Δ*secY2* was identical to that of the wild type, indicating that under these conditions SecY2 is not required for the exclusive secretion of any protein, including Sap and EA1.

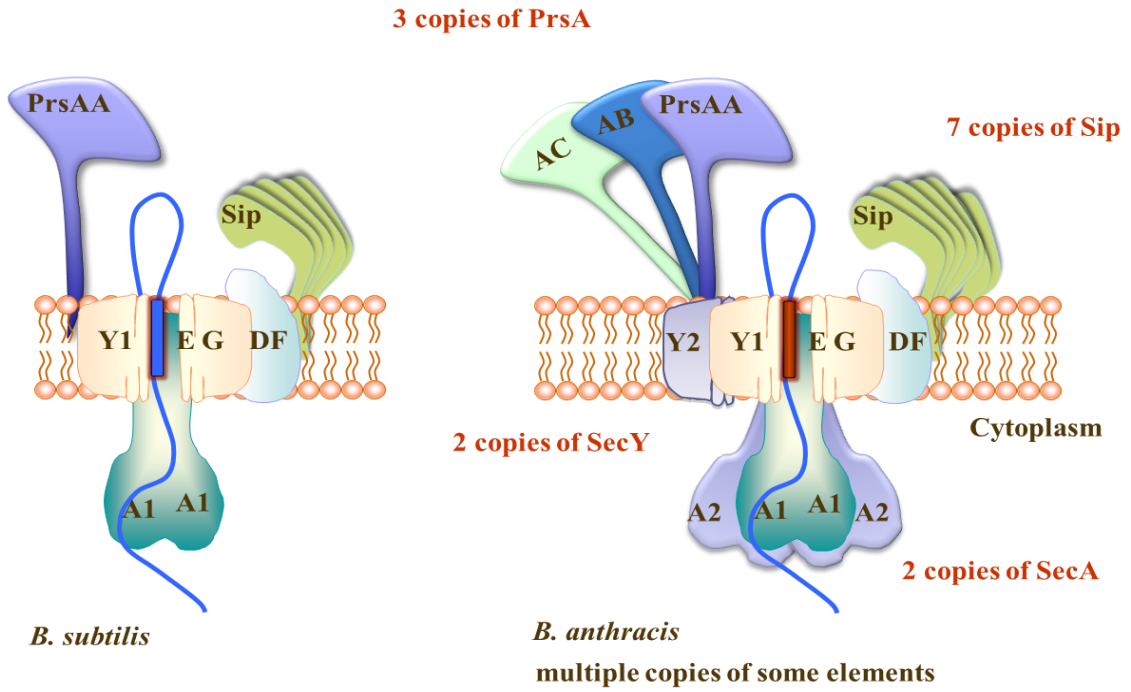

Figure 1.12: Sec translocation systems of *B. anthracis* and *B. subtilis*. The translocase of *B. subtilis* encompasses one type type of SecY and SecA molecular motor. SecY together with SecE and SecG forms the translocation channel. SecDF is an auxiliary translocation complex which facilitates secretion, but is not essential for the processes. Five homologues of the Sip signal peptidase are present in *B. subtilis* with the role of removing the signal peptide after a secretory protein has been translocated. PrsA foldase (also only one type of PrsA is present in *B. subtilis*) folds its substrate proteins into the mature conformation on the outer surface of cytoplasmic membrane. In comparison, in *B. anthracis*, there are two homologues of SecA (SecA1 and SecA2) and two homologues of SecY (SecY1 and SecY2) as well as three homologues of PrsA (PrsAA, PrsAB, PrsAC) and seven homologues of signal peptidase Sip.

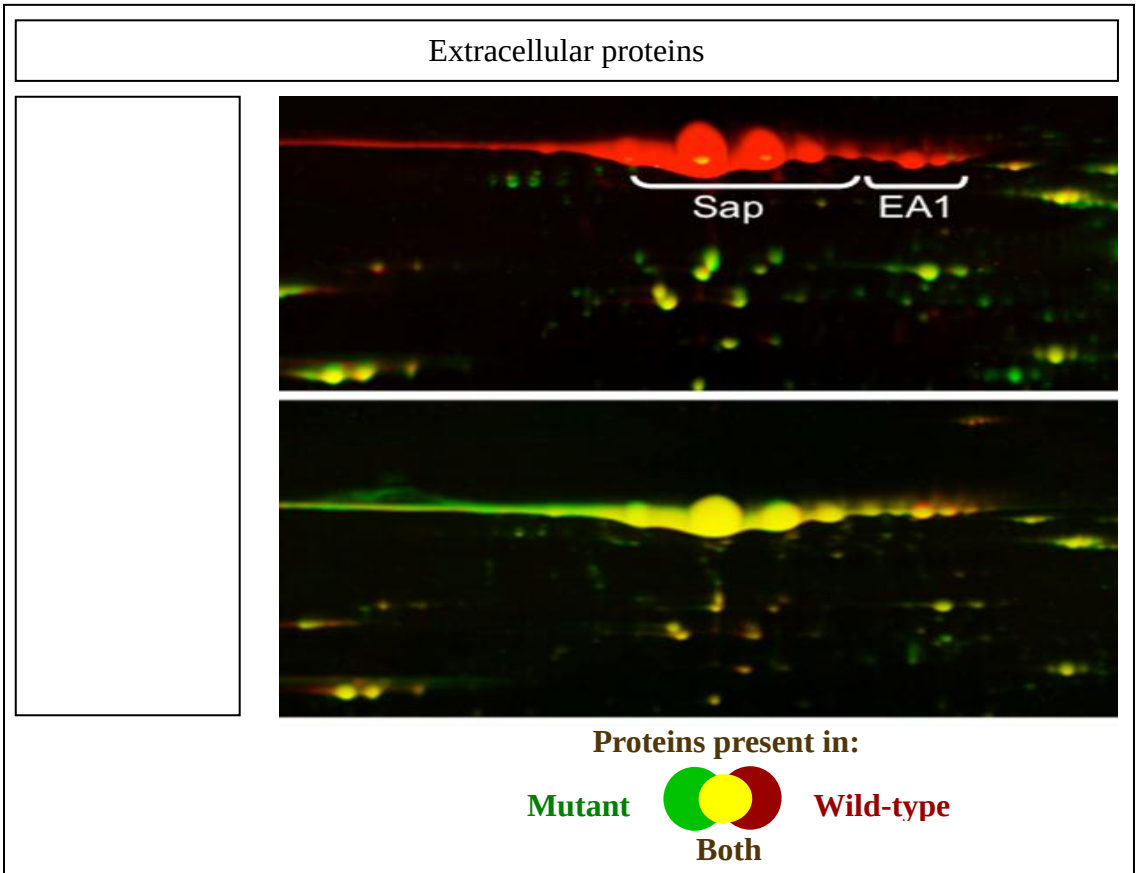

Figure 1.13: False-coloured 2D gel overlays of *B. anthracis* extracellular proteins isolated from the wild-type, Δ*secA2* and Δ*secY2*. Extracellular proteome of the Δ*secA2* mutant showed a dramatic reduction in the secretion of two of the major surface-associated antigens, namely Sap and EA1 (red spots). In contrast, the extracellular proteome of the Δ*secY2* mutant gave an identical profile to that of the wild-type (yellow spots) (Pohl *et al.*, unpublished).

Analysis of the intracellular proteins of Δ*secA2* and Δ*secY2* mutants by 2D PAGE gels (Figure 1.14) (Pohl *et al.*, unpublished) showed that when *secA2* was not expressed, the precursors of Sap and EA1 (preSap and preEA1) were no longer found in the cytoplasm. One interpretation of this observation is that SecA2 not only functions in the secretion of Sap and EA1 but also as a cytoplasmic chaperone preventing the degradation of these proteins.

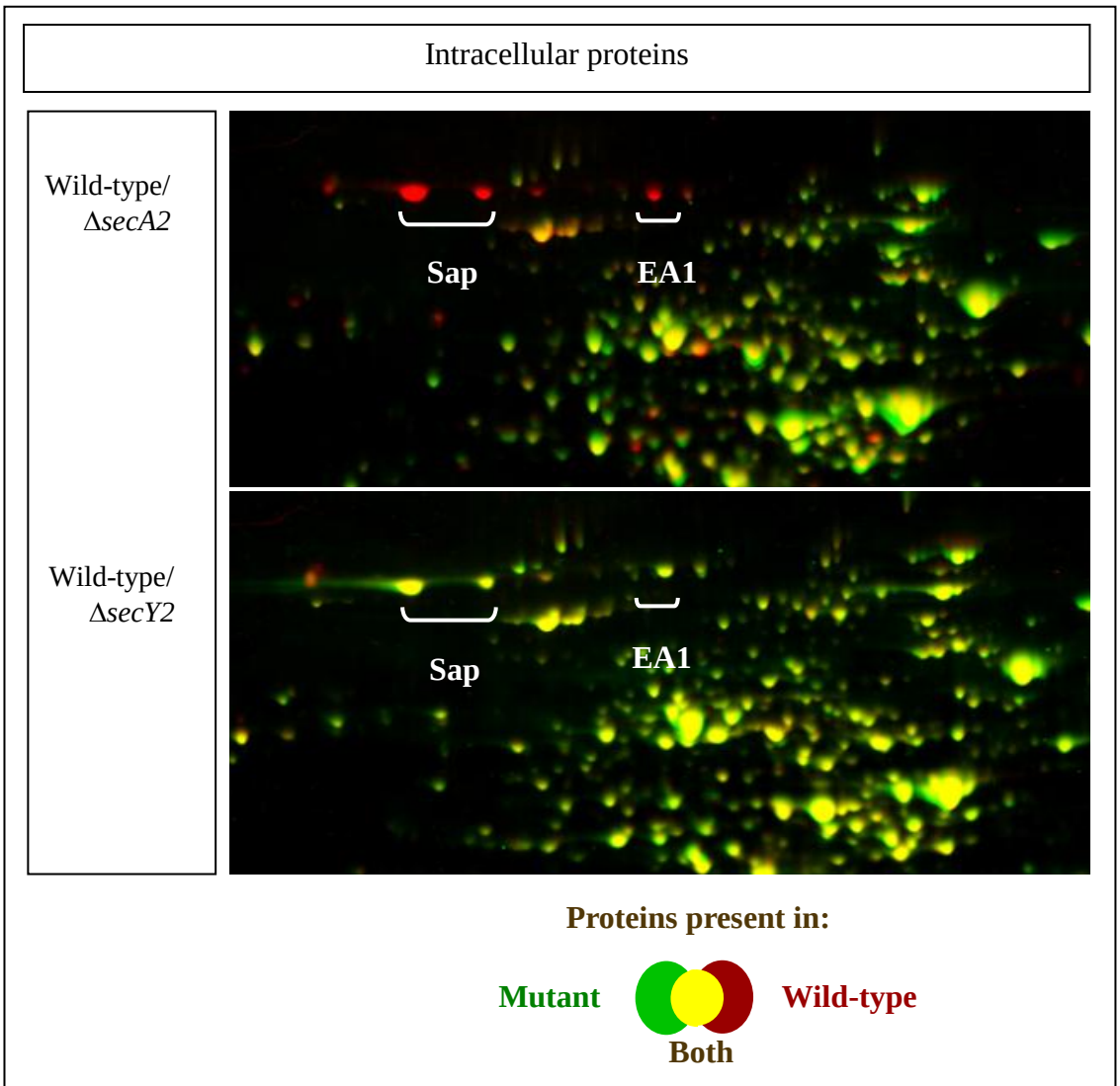

Figure 1.14: False-coloured 2D gel overlays of *B. anthracis* intracellular proteins isolated from the wild-type, Δ*secA2*, Δ*secY2*. Intracellular proteome of the Δ*secA2* mutant showed an absence of the major surface-associated antigens, namely Sap and EA1 (red spots). In contrast, the extracellular proteome of the Δ*secY2* mutant gave an identical profile to that of the wild-type (yellow spots) (Pohl *et al.*, unpublished).

To investigate the role of SecY2, the expression profiles of the *B. anthracis secY1* and *secY2* genes were analysed in the wild-type strain (Figure 1.15) (Pohl *et al.*, unpublished). RNA purified from cultures harvested at different phases of growth cycle (exponential, transitional, early stationary and late stationary phases) was analysed by Northern blotting. Hybridization with a *secY1*-specific probe showed that *secY1* expression was highest during the exponential phase and decreased progressively towards late stationary phase. *secY1* is located within the extensively processed 13.5 kb S10-*spc*-α ribosomal operon that gives rise to transcripts of various sizes. Hybridization with a *secY2*-specific probe showed that *secY2* expression peaked in the transitional

phase but remained high throughout stationary phase. These results suggest that SecY2 serves to maintain high levels of protein secretion throughout the entire growth cycle.

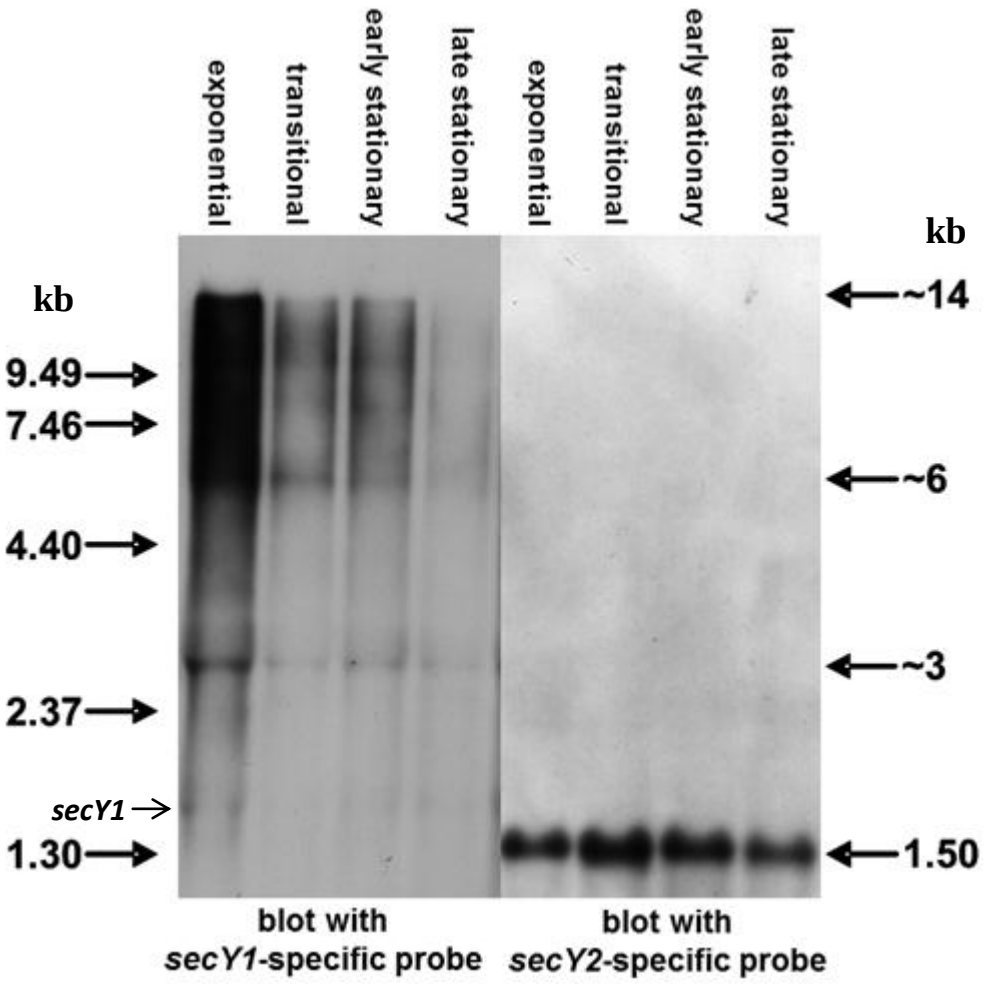

Figure 1.15: Expression profiles of *secY1* and *secY2* in *B. anthracis* wild type strain at various stages of the growth cycle (*Pohl et al*., unpublished).

The above experimental data suggest that SecA2 and SecY2 do not form a novel translocon in *B. anthracis,* but instead interact with or form components of the canonical translocase. This is consistent with the observation that *B. anthracis secA2* and *secY2* genes are located at well-separated chromosomal locations (Read *et al.*, 2003). Additionally, there is a question of the roles of the multiply homologues of PrsA foldase and Sip signal peptidase. The *B. anthracis* PrsA-like foldases PrsAA, PrsAB and PrsAC are all able to complement the *B. subtilis* native PrsA foldase although, the PrsAC complementation mutant exhibits a different colony morphology (Williams *et al.*, 2003). The last observation suggests that the PrsA-like proteins show at least some substrate specificity. This leads to the question as to whether one or more of the PrsA and Sip homologues are specifically involved in secretion of SecA2-dependent substrates.

1.8 S-layer proteins as markers for the analysis of secretory machinery of *B. anthracis*

1.8.1 General features of S-layers

As S-layer proteins were found to be substrates for SecA2, they were subsequently used as marker proteins allowing evaluation of participation of other components in the formation of secondary translocase. This section gives an overview of S-layer proteins, with a focus on the S-layer proteins of *B. anthracis*.

S-layers can be found in some species of bacteria and archea on their surfaces and are defined as crystalline arrays (lattices) of proteins. They can be aligned in oblique (p2), trimeric (p3), tetragonal (p4), hexagonal (p6) symmetries (images and schematic illustrations of oblique, tetragonal and hexagonal arrangements are shown on the Figure 1.16).

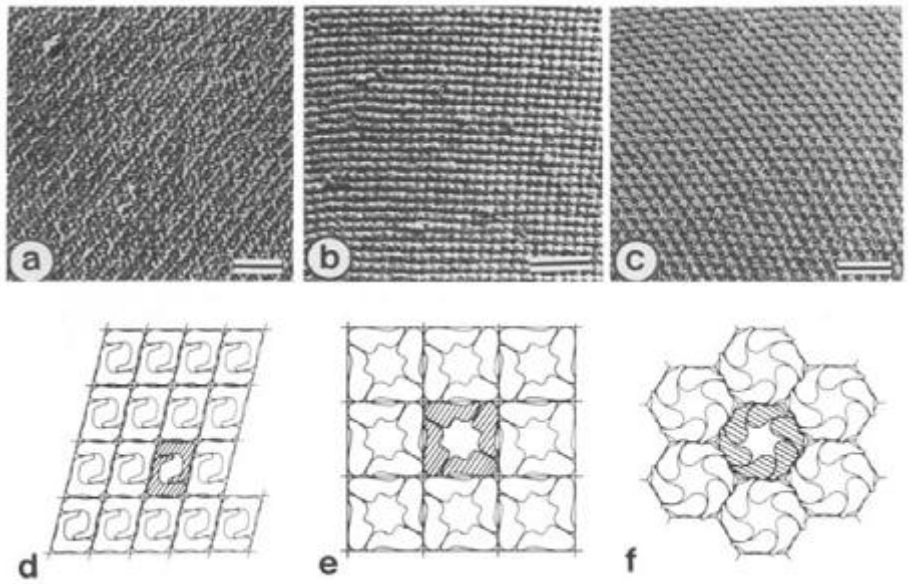

Figure 1.16: (a-c) Freeze-etching images of S-layers on intact cells showing the three different lattice types schematically illustrated in (d-f). (a,d) oblique (~2) lattice; (b,e) square (~4) lattice; (c,f) hexagonal (~6) lattice. The bars represent 50 nm (Holt and Leadbetter).

With few exceptions S-layers consist of a single type of protein or glycoprotein. However, S-layers of *Clostridium difficile*, *Bacillus anthracis*, *Brevibacterium brevis* and *Aquaspirillum serpens* consist of two types of proteins. In the case of *Clostridium difficile* both constituent subunits of the S-layer combine to form a single lattice (Takeoka *et al.*, 1991). In *B. anthracis* each protein-type forms separate lattices, each existing at different phases of the cell growth cycle (Mignot *et al.*, 2002). *Brevibacterium brevis* and *Aquaspirillum serpens* possesses superimposed S-layer lattices, each composed of distinct proteins (Yamada *et al.*, 1981, Kist *et al.*, 1984). S-

layer proteins are very abundant, covering the entire surface of the bacterium. Pores occupy up to 70% of the S-layer surface. Bacteria exhibiting a generation time of 20 minutes must synthesize and extend the existing S-layer at the rate of at least 500 S-layer proteins per second in order to maintain the complete coverage of the cell surface (Sletyr *et al.*, 1983). S-layer proteins are attached to the cell wall (Gram-positive bacteria, cell wall possessing archea) or outer membrane (Gram-negative bacteria and cell wall – deprived archea) and to each other via non-covalent bonds.

Functions of S-layers

Many functions have been identified or proposed for S-layers. S-layers are often the outermost component of the cell-envelope and are thought to be involved in the regulation of macromolecule exchange with the environment, by acting as a molecular sieve (Sára and Sleytr, 1987; Sára *et al*., 1992). They may also have a role in cell integrity and shape maintenance in archaea, in which it is often the only cell-envelope component (Baumeister *et al.*, 1992; Hovmöller *et al.*, 1998; Peters *et al.*, 1995; Mescher and Strominger, 1976; Wildhaber and Baumeister, 1987). They may also serve as an attachment site for cell-associated exoenzymes (Egelseer *et al.*, 1995; Matuschek *et al.*, 1996).

The S-layers of some bacteria (*e.g. A. salmonicida*, *C. fetus*, *A. serpens*, *C. crescentus*) protect them from attack by the bacterial parasite *Bdellovibrio bacteriovorus* (Koval 1997).

S-layers are also implicated in the interaction with host by mediating binding and adhesion with various cell types and tissues. S-layer-mediated interaction with host includes both normal human microflora, e.g. lactobacilli as well as pathogens. S-layers can mediate adhesion of microbial flora to the walls of the intestine by interaction with various components of the intestinal tissue, like laminin and collagens. It was shown that S-layer protein CbsA of *Lactobacillus crispatus* is involved in adherence to the collagen and laminin, while SlpA of *Lactobacillus brevis* has the affinity towards epithelial cells and fibronectin (Sillanpää *et al.*, 2000, Antikainen *et al.*, 2002, Hynönen *et al.*, 2002). In the case of S-layer mediated interactions between host and pathogen, S-layers are classified as the virulence factors. For example S-layers of *Bacillus cereus* strains, isolated from periodontal and endodontic infections, were shown to mediate interaction with laminin, as well as they are the site of attachment of protease which mediates interaction with fibronectin (Kotiranta *et al.*, 1998). S-layer protein of *Bacteroides forsythus*, BspA, another periodontal pathogen was shown to adhere to KB

cells (subline of the keratin-forming tumor cell line HeLa), which implies the ability to adhere to the epithelium. After, the stage of adherence, *Bacteroides forsythus* invades the cells, which is also thought to be mediated by BspA. That S-layer protein also mediates haemagglutination. The role of BspA as a virulence factor was confirmed by the ability of *B. forsythus* S-layer to cause the formation of abscesses in mice which were not immunised against BspA, but not in the immunised mice (Sabet *et al.*, 2003).

In some pathogenic bacteria, S-layers endow them with protection against the immune system through various mechanisms. In *Campylobacter fetus, Campylobacter rectus,* S-layer protects them against complement-mediated cell lysis by preventing binding complement factors (Blaser *et al.*, 1988; Okuda *et al.*, 1997). Additionally, S-layer of *C. fetus* was observed to provide protection against antibody opsonisation by the antigenic variance of S-layer proteins (Garcia *et al.*, 1995, Grogono-Thomas *et al.*, 2000), while in *C. rectus* S-layer was shown to down-regulate proinflammatory cytokines (IL-6, IL-8, and TNFα) which may favour *C. rectus* survival (Wang *et al.*, 2000).

In *Aeromonas salmonicida* S-layer is called A-layer and is a virulence factor with both adhesive and immune-protective functions, mediated by various mechanisms. Those mechanisms include: (1) protection against the complement-mediated killing (Munn *et al.*, 1982); (2) adhesion to the extracellular matrix through the interaction with fibronectin, laminin and collagen (Doig *et al.*, 1992; Trust *et al.*, 1993); (3) adhesion to macrophages (Garduño and Kay 1992*a*; Garduño *et al.*, 1992*a*; Trust *et al.*, 1983) and survival inside them (Garduño *et al.*, 1993*a*; Graham *et al.*, 1988; Olivier *et al.*, 1986).

The role of S-layer in the virulence of *B. anthracis* hasn't till now been elucidated. As the expression of *eag* and *sap* genes, encoding, Sap and EA1 S-layer proteins are subject to the regulation mediated by AtxA and PagR pathogenicity regulatory molecules, it might indicate that S-layer in *B. anthracis* is also involved in virulence. Consistently with that assumption, the S-layer was shown to protect against binding of C3 component of the complement system, in the strain deprived of the capsule (Ray *et al.*, 1998). However, during infection the capsule but not the S-layer is the outermost surface layer. In accordance with this, no difference in virulence was observed in the mouse model upon infection with the S-layer-deprived mutant in the $pXO1^{+}$ $pXO2^{-}$ or $pXO1^{-}pXO2^{+}$ backgrounds (Mesnage *et al.*,1998, Fuet, 2009). Other potential role of Sap and EA1 proteins lies in the cell wall metabolism, as they both were found to possess some murein hyrolytic activity (Ahn *et al.*, 2006). When strains lacking Sap only or both Sap and EA1 were grown in the liquid medium, then they

flocculated and sedimented abnormally upon stopping of shaking (*Bahl et al.*, 1997). This could be caused by alterations in cell surface properties, and implying that *B. anthracis* S-layer might be involved in adhesion within the host.

Applications of S-layers in biotechnology and medicine

S-layers can be extracted from cell surfaces using various methods using agents that disrupt hydrogen bonds, by metal-chelating agents or by cation substitution (Sletyr *et al.*, 1986; Sletyr *et al.*, 1988; Beveridge *et al.*, 1976; Beveridge 1994; Koval *et al.*, 1984). As, they re-assemble spontaneously in the liquid suspension or on the solid surfaces or interfaces (e.g. lipid films, liposomes), the S-layer containing structures are easy to produce. S-layers exhibit uniform physico-chemical properties as they are composed of identical protein or glycoprotein species. That's why S-layers have been found to be suitable for production of isoporous filtration membranes (Sára and Sleytr, 1987).

They also found application as matrices for immobilisation of molecules (e.g. enzymes, antibodies). The immobilization can be directly to the S-layer due to the high density and defined position of carboxyl groups. For example *Staphylococcus* protein A, and some enzymes (glucose oxidases, galactosidases, invertases) were experimentally immobilized on such matrices forming an approximation of a monolayer on the S-layer matrices (Küpcü *et al.*, 1995). Alternatively, hybrid molecules of a protein of interest and a S-layer protein can be generated. A typical chimeric protein comprises (1) an accessible N-terminal SCWP (secondary cell wall polymer)-binding domain, which could be exploited for oriented binding and recrystallization on artificial solid supports precoated with SCWP, (2) the self-assembly domain and (3) a functional sequence fused to the C-terminal end of the S-layer protein (Sára *et al.*, 2005). Various ligands were can be part of such chimeric proteins, for example biotin, antigens, antibodies and specific affinity domains. Affinity matrices composed of S-layer proteins (rSbsB or rSbpA) with the streptavidin fused to them was demonstrated to effective in capturing any biotinylated molecules (Moll *et al.*, 2002; Huber *et al.*, 2006a, b). Chimeric protein of the ZZ domain (a synthetic analogue of the B-domain of Protein A, capable of binding the Fc-part of IgGs) and rSbpA S-layer protein were coated on microbeads; and they can find application detoxification of the extracorporeal blood (Völlenkle *et al.*, 2004). The camel antibody against the prostate specific antigen was coated on gold chips precoated with thiolated cell wall secondary polymers, containing S-layer proteins and those chips were used in the surface plasmon resonance technique for sensing

prostate specific antigen (Pleschberger *et al.*, 2003, 2004). S-layers can also be used as surfaces for assembly of inorganic superlatices. This process has been observed in Cynaobacteria, on which S-layers calcium sulfate and calcium carbonate get crystallised (Schultze-Lam *et al.*, 1992). Under laboratory conditions other compounds like for example can be crystallised on the S-layer surfaces and such nano-technological constructs could be used in electronic and non-linear optics (Pum and Sleytr, 1999; Bohr, 2002).

S-layer can also be used for stabilization of liposomes, which are used for targeted drug delivery or immunodiagnostic assays. The drawback of liposomes is their instability. S-layers re-crystallise readily between two phases, including lipid bi-layers. When they crystallise in the liposomal bi-layer, they stabilise liposomes (Mader *et al.*, 1999). When S-layers have recrystallized on the liposomal surface, functional molecules for specific therapeutic or diagnostic applications can be covalently attached (Küpcü *et al.*, 1995, Mader *et al.*, 2000).

S-layer can also be used as vaccines. S-layer protein of *Campylobacter fetus* was employed to construct vaccine against abortion in chickens, caused by this pathogen (Grogono-Thomas *et al.*, 1997). S-layers can also serve as carriers for haptens and as adjuvants (Smith *et al.*, 1993). The experiments of have also been done with the chimeric S-layer proteins as a part of live vaccines. Epitopes of oncoprotein c-Myc and poliovirus were expressed in Lactobacillus brevis as chimeric proteins of SlpA S-layer protein (Avall-Jaaskelainen *et al.*, 2002). S-layer proteins are also tested as a component in the vaccines for immunotherapy of type 1 allergy as S-layer proteins immunomodulating properties (Breitwieser *et al.*, 2002; Ilk *et al.*, 2002; Bohle *et al.*, 2004).

1.8.2 S-layer of *B. anthracis*

Molecular structure

In *B. anthracis* there are two S-layer proteins: Sap (surface array protein) and EA1 (extractable antigen1), encoded by the *sap* and *eag* genes, respectively (Mesnage *et al.*, 1997, Mesnage *et al.*, 1998, Fouet *et al.*, 1999). The molecular size of Sap and EA1 determined by mass spectroscopy is 86.6 kDa and 91.3 kDa, respectively (Walz *et al.*, 2007). The S-layer formed by them has the hexagonal arrangement (Gerhardt, 1967). In *B. anthracis*, as is the case with the S-layer proteins of other Gram-positive bacteria, Sap and EA1 proteins consist of N-terminal domains that facilitate interaction with the cell wall and C-terminal crystallisation domains that are responsible for interacting with

other S-layer proteins to form a crystalline array (Mesnage *et al*., 1999). The N-terminus of pre-S-layer proteins typically consists of a cleavable signal peptide that is responsible for targeting the protein for secretion. The signal peptide is followed by three positively charged SLH (S-layer homology) domains (Mesnage *et al.*, 2000) that interact electrostatically with the negatively charged polymers of the cell wall. In *B. anthracis* both Sap and EA1 were shown to interact with pyruvate substituents of the cell wall (Chauvaux *et al.*, 1999, Mesnage *et al.*, 2000). Sap was also demonstrated to interact with acetyl groups (Laaberki *et al.*, 2010).

Genomic context of *sap* and *eag* genes

It is noteworthy to see that *sap* and *eag* genes are located in the proximity of *secA2* (Figure 1.17). Located between *secA2* and *sap* are two genes, *csaA (BA0883)* and *csaB*, which encode the proteins (CsaA and CsaB) responsible for the pyruvyl modification of the cell wall.

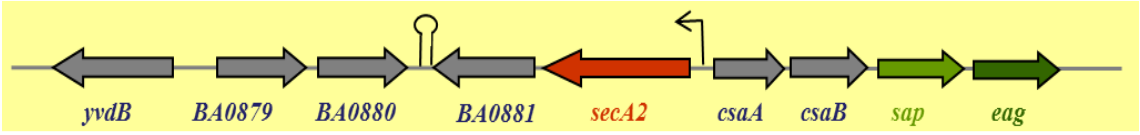

Figure 1.17: Genomic context of *sap* and *eag* genes.

The nomenclature of CsaA is somewhat confusing since, in *B. anthracis*, two different proteins have been ascribed this name. One CsaA is a molecular chaperone described in the **Section 1.5.3a** and it is encoded by the *csaA* gene (*BA2064*). The other CsaA is an oligosaccharide transporter encoded by *BA0883* gene that, together with CsaB (polysaccharide pyruvyl transferase) is involved in the attachment of Sap and EA1 to the cell wall (Mesnage *et al.*, 2000). However, only CsaB was shown to be essential for the attachment of Sap and EA1 as well as all other SLH domain-containing proteins (Mesnage *et al.*, 2000; Kern *et al.*, 2010). CsaB is responsible for adding pyruvate groups to the secondary cell wall polymer (SCWP), called neutral polysaccharide of *B. anthracis* and pyruvylation is necessary for the interaction between SLH domains and SCWP to take place. Thus, in a *csaB*-null mutant, the attachment of SLH domain-containing proteins is abolished (Mesnage *et al.*, 2000; Kern *et al.*, 2010).

Regulation of *eag* and *sap* expression

In rich media, Sap and EA1 are synthesized sequentially in a growth phase-dependent manner (Mignot *et al.*, 2002) (Figure 1.18). Sap is predominantly synthesized in the

exponential phase and EA1 in the stationary phase, during which Sap production is inhibited. When EA1 emerges onto the cell surface, it displaces Sap releasing it to the growing medium. This leads to the sequential occurrence of two (Sap and EA1) S-layers in the exponential and stationary phases, respectively. The growth phase-dependent expression of *sap* and *eag* partly relies on their transcription being driven by different sigma factors – *sap* expression is driven by σ^A (the predominant σ factor of the exponential phase) and while that of *eag* is predominately by σ^H (the predominant σ factor of the stationary phase). Moreover, Sap and EA1 were shown to possess DNA-binding activity and to repress *eag* expression (Mignot *et al.*, 2002). In the synthetic medium, which is thought to best resemble the conditions encountered by *B. anthracis* during infection, the expression of *sap* and *eag* is dependent on the presence or absence of the pXO1 plasmid. The plasmidless strain grown in the synthetic medium losses its growth phase-dependent manner of *sap* and *eag* expression, with high level of *sap* and low level of *eag* expression regardless of the growth phase. However, when *sap* is disrupted *eag* transcription increases indicating that *eag* is constantly suppressed by Sap when the plasmidless strain is grown in synthetic medium (Mignot *et al.*, 2002). When the $pXO1^+$ strain is grown in synthetic medium, the expression pattern of *sap* and *eag* becomes altered – *eag* is expressed at the expense of *sap* irrespective of the growth phase (Mignot *et al.*, 2003). This is due to regulation mediated by the regulatory molecules encoded on the pXO1 plasmid, namely AtxA and PagR. AtxA induces expression of PagR, which in turn induces the expression of *eag* and the repression of *sap*. *In vivo*, the EA1 S-layer predominates when the toxins and capsule are produced, while the Sap S-layer predominates in non-capsulated bacteria (Mignot *et al.*, 2004). This may indicate that Sap and EA1 play distinct roles *in vivo*. Sap, as the outermost layer, may participate in interaction with the environment, while EA1 might play role inside the host.

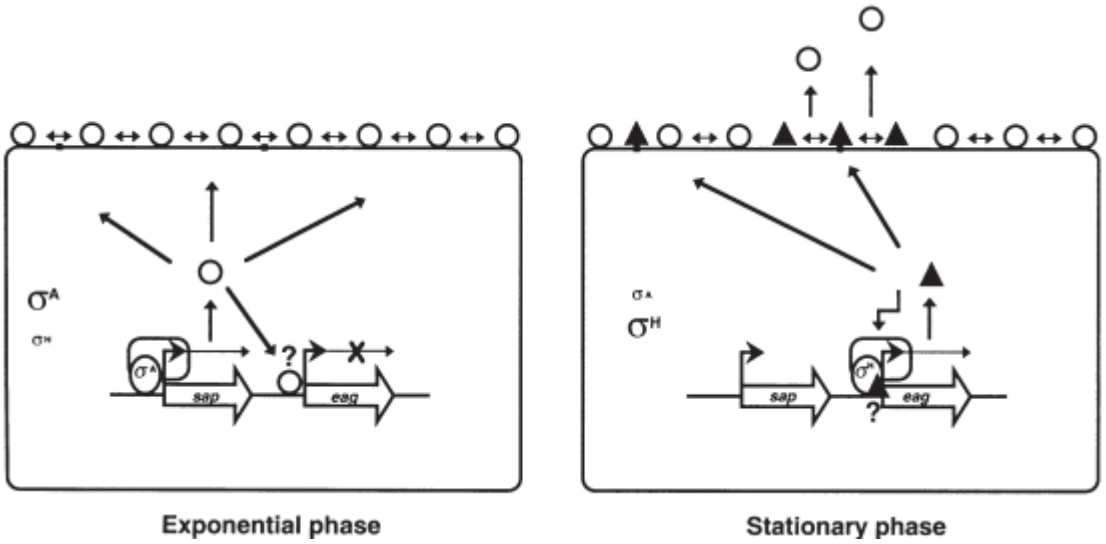

Figure 1.18: Proposed model for developmental control of the S-layer switch in *B. anthracis*. In the exponential growth phase, transcription of *sap* is actively driven by σ^A. Sap (open circles) is exported to the surface, where it forms an S-layer lattice by homologous interactions. The synthesis of EA1 is completely inhibited, possibly because Sap directly represses the transcription of *eag* by binding to the *eag* promoter. The transcription of *sap* is turned off during stationary phase, possibly because the availability of σ^A is limited. This results in the release of the *eag* promoter from Sap repression and full transcription of *eag* is driven by σ^H. EA1 (closed triangles) binds available sites at the cell surface and establishes homologous interactions that destabilize the Sap lattice and facilitate propagation of the EA1 lattice. The strict co-ordination of EA1 synthesis according to surface requirements is a consequence of the feedback control of *eag*, presumably because EA1 reduces the transcription of *eag* directly or indirectly. (Closed squares) SLH-anchoring sites not occupied by Sap. The S-layer proteins are shown at one surface of the cell for reasons of clarity only; the assembly process is not polarized (Mignot *et al.*, 2002).

1.9 The objectives of the project

B. anthracis contains homologues of several Sec pathway components: (i) two homologues of SecA (SecA1 and SecA2), (ii) two homologues of SecY (SecY1 and SecY2), (iii) three homologues of the PrsA foldase (PrsAA, PrsAB and PrsAC). In previous studies, SecA2 was shown to be specific for secretion of S-layer proteins: Sap and EA1, while SecY2 has not been shown to have any substrate specificity. Instead, it seems to ensure high levels of protein secretion in later phases of the growth cycle. The objective of this project was to get new insights into the functioning of the *B. anthracis* secondary translocase. More specifically the project aimed to:

1. Identify components of the SecA2-dependent secretion pathway.
2. Elucidate interactions of SecA2, its substrates and the other elements of the SecA2-dependent pathway.
3. Elucidate the role of PrsA-like foldases in secretion of substrates of the SecA2-dependent pathway.

Chapter 2: Materials and Methods

The general methods applied in this study are described in this chapter. Growth media and buffers are presented in **Appendix A**.

2.1 Bacterial strains, plasmids and oligodeoxyribonucleotides

A list of oligodeoxyribonucleotides is given in **Appendix B**. The bacterial strains and plasmids used in the study are described in the tables of **Appendix C**.

2.2 Growth and storage of bacterial strains

Cultures of *E. coli*, *B. subtilis* and *B. anthracis* were grown on solid and in liquid cultures in Luria-Bertani (LB) medium (unless stated otherwise) at 37°C. Liquid cultures were incubated with shaking at 200 rpm. When required, antibiotics and/or growth supplements were added as shown in the Tables 2.1 and 2.2. Strains were stored as 10% glycerol stocks.

Table 2.1: Antibiotic stock and working concentrations

Antibiotic (abbreviation)	Solvent	Stock concentration ($mg.ml^{-1}$)	Working concentration ($\mu g.ml^{-1}$)
Ampicillin (Amp)	dH_2O	100	100
Chloramphenicol (Cm)	50% ethanol (v/v)	5	5
Erythromycin (Em)	100% ethanol (v/v)	0.3	0.3 (*B. subtilis*)
		5	5 (*B. anthracis*)
Kanamycin (Km)	dH_2O	10	10 (*B. subtilis*)
			50 (*E. coli*)
			20 (*B. anthracis*)
Lincomycin (Lm)	50% ethanol (v/v)	25	25

Table 2.2: Growth supplements

Supplement	Solute	Stock concentration	working concentration
IPTG	dH_2O	1 M or 0.1 M	1 mM or 0.1 mM or 0.5 M
X-Gal	DMF	40 $mg.ml^{-1}$	40 $\mu g.ml^{-1}$
Xylose	dH_2O	20% (w/v)	1% (w/v)

2.3 DNA isolation, purification and analysis

2.3.1 Isolation of genomic DNA from *B. subtilis* and *B. anthracis*

B. subtilis colonies from streak plates were picked and inoculated into 5 ml of LB broth, then incubated at 37°C overnight with shaking at 180 rpm. Overnight cultures were centrifuged at 2,665 *g* for 5 minutes and the supernatant was removed. The chromosomal DNA was purified from the pelleted cells using the DNeasy Blood & Tissue Kit (Qiagen) according to the manufacturer's instructions. The isolation of genomic DNA of *B. anthracis* was carried out in similar way with some modifications.

The cell pellet obtained from centrifugation of the overnight culture was resuspended in 550 µl of the Enzymatic Lysis Buffer (20 mM TrisCl, pH 8.0, 2 mM EDTA, 1.2% Triton X-100) and then added to a 2 ml tube with the amount of glass beads corresponding to 500 µl H_2O. The cells were subjected to the disruption in the Mikro-Dismembrator S (Braun, Germany) at 2,600 rpm for five minutes in the presence of glass beads. Next, supernatant was transferred to fresh 2 ml Eppendorf tube and was processed using the DNeasy Blood & Tissue Kit (Qiagen) according to the manufacturer's instructions. The resulting purified chromosomal DNA was stored at -20^{o}C.

2.3.2 Purification of PCR products

PCR products from the amplification reaction and after restriction digest were purified using QIAquick^{TM} PCR purification kit (Qiagen, Crawley, West Sussex, UK) according to the manufacturer's instructions.

2.3.3 Isolation of plasmid DNA from *E. coli*

E. coli colonies from streak plates were picked and inoculated into 5 ml of LB broth with appropriate antibiotic, then incubated at 37^{o}C overnight with shaking at 180 rpm. Overnight cultures were centrifuged at 2,665 *g* for 5 minutes and the supernatant was removed. The plasmid was purified from the pelleted cells using the GeneJET™ Plasmid Miniprep Kit (Fermentas) according to the manufacturer's instructions. The resulting purified plasmid was stored at 4^{o}C.

2.3.4 Isolation of plasmid DNA from *B. anthracis*

B. anthracis colonies from streak plates were picked and inoculated into 5 ml of LB broth with appropriate antibiotic, then incubated at 37^{o}C overnight with shaking at 180 rpm. Overnight cultures were centrifuged at 16,060 *g* for 5 minutes and the supernatant was removed. The plasmid was purified from the pelleted cells using the GeneJET™ Plasmid Miniprep Kit (Fermentas) according to the following, modified protocol: the pellet was resuspended in 300 µl resuspension buffer. 300 µl lysis buffer (20 mM TrisCl, pH8.0, 2 mM EDTA, 1.2% Triton X-100) was added and the sample was mixed by inverting, followed by its transfer to a 2 ml tube with the amount of glass beads corresponding to 200 µl H_2O. The cells were disrupted by using a Micro Dismembrator S (Braun Biotech International, Melsungen, Germany) for 5 minutes at 2,600 rpm. The sample was centrifuged (16,060 *g*, 10 minutes). The resulting supernatant was transferred into 1.5 ml Eppendorf. 300 µl neutralization buffer was added and the

sample was mixed and centrifuged (16,060 *g*, 10 minutes). The supernatant was transferred onto the spin column and the standard protocol for GeneJET™ Plasmid Miniprep Kit (Fermentas) was followed. The resulting purified plasmid was stored at 4^{o}C.

2.3.5 Recovery of DNA fragments from agarose gels

Following gel electrophoresis, the DNA bands were visualised using a UV light transilluminator and the appropriate DNA band of interest was excised and transferred into a 1.5 ml Eppendorf tube. The DNA was purified with the GeneJet^{TM} Gel Extraction Kit (Fermentas), according to the manufacturer's instructions.

2.3.6 DNA quantification

The DNA concentration and purity was determined using the Nanodrop spectrophotometer ND-1000 (LabTech) following the manufacturer's protocol. Both the concentrations and the purity of samples were determined from A_{260}/A_{280} ratio. A ratio value of between 1.8 and 2 indicates good DNA purity; lower values indicate contamination with protein.

2.3.7 Agarose gel electrophoresis of DNA

DNA size and integrity was analysed by agarose gel electrophoresis using 1 x TAE or TBE buffer (**Appendix A**). The gels were made with ethidium bromide or SafeView (final concentration 0.5 µg/ml for both dyes). 0.8% gels were prepared for the separation of DNA fragments bigger than 1 kb in size; 1.3 or 1.6% gels were prepared for the separation of DNA fragments smaller than 1 kb. The DNA samples were prepared in an appropriate volume of 6 x loading dye and loaded into the gel. The electrophoresis was run at 2 V/cm. Following electrophoresis, DNA was visualised using a UV light transilluminator (GelDoc1000, Bio-Rad Laboratories Ltd. Hempel, Herts, UK) and the gel was photographed. DNA size was determined in relationship to molecular size markers, 100 bp and 1 kb molecular ladders (Promega & Fermentas) and 2-log ladder (NEB) as appropriate.

2.3.8 PCR

PCR primers were designed using Primer3 software, which is available on-line: http://frodo.wi.mit.edu/), or were designed manually. Sequences containing appropriate restriction sites and 5' overhangs were introduced into the 5' end of primers when needed. PCR amplification of DNA fragments was performed with Taq polymerase (NEB) for diagnostic PCR or Phusion polymerase (Finnenzymes) for cloning purposes.

The components of the PCR reaction were added according to the manufacturer's instructions. The standard conditions for PCR with Taq polymerase were: 1 x (2 min 95°C); 35 x (30 s 95°C; 30 s 5-10°C below melting temperature of the primers; 30 s up to 3 min 68°C, depending on the length of target gene – 1 min per 1 kb), 1 x (10 min 72°C). Conditions for PCR with Phusion polymerase were: 1 x (2 min 98°C); 35 x (30 s 98°C; 30 s 5°C above melting temperature of the primer with the lower melting temperature; 15 s up to 3 min 72°C, depending on the length of target gene – 30 s per 1 kb), 1 x (10 min 72°C). For cloning purposes, PCR products were purified using the QIAquick™ PCR purification kit (Qiagen) according to the manufacturer's instructions.

2.3.9 Sequencing

DNA sequencing was used to verify the correct construction of the recombinant plasmids. Plasmid DNA was purified by GeneJET™ Plasmid Miniprep Kit (Fermentas). The appropriate concentration of primers and plasmids for sequencing were prepared: for plasmid 50-100 ng/µl, minimum 1 µg per reaction, for primer 2 pmol/µl in a minimum volume of 15 µl. The sequencing of DNA fragments was performed by MWG Biotech AG (Germany). The DNA sequence of the sequenced DNA was compared with the template using the on-line software ClustalW2 (http://www.ebi.ac.uk/Tools/msa/clustalw2/).

2.3.10 Restriction digest

Plasmid DNA and amplified fragments were treated with appropriate restriction enzymes (FastDigest, Fermentas), according to the manufacturer's instruction. The digestion reaction was run for 1 hour at 37°C. Additionally, alkaline phosphatase (Fermentas) was added to the plasmid digestion mixes (according to the manufacturer's instructions) to dephosphorylate the sticky ends to prevent vector re-ligation.

2.3.11 Ligation

Plasmid and insert DNA concentrations were mixed in a ratio of 1:3 or 1:6. The amount of plasmid added was 50 ng or 100 ng and the amount of the insert to be added was calculated according to the formula: ((50 or 100 x MWi)/MWp)) x 3 (or 6), where MWi is the molecular size of the insert and MWp is the molecular size of the plasmid. Volumes of plasmid and insert to be added were calculated by dividing the amount to be added by the concentration of each DNA solution. 1 µl of T4 DNA ligase (1 unit/µl) and 2 µl of the appropriate buffer (Fermentas) were added per reaction mix. ddH2O was

added to give a total volume of 20 µl. The ligation mix was incubated overnight at 4°C or for 2h at room temperature.

2.4 Standard procedure for preparation of chemically-competent cells of *E. coli*

The preparation of chemically-competent cells of *E. coli* was based on Inoue et al. (1990) with modifications. The strain of *E. coli TOP10* or *E. coli XL-I blue* were grown in 5 ml LB overnight. 25 ml of fresh LB was inoculated with the overnight culture. The volume of overnight culture for inoculation was calculated using formula: $(0.05/OD_{600})$ x 25 ml. The culture was incubated to an optical density of 0.5 to 0.6 at 600 nm. The culture was placed on ice for 10 minutes and cells were pelleted by centrifugation at 2,665 *g* for 10 minutes at 4°C. Cells were resuspended in 8 ml ice-cold Transformation Buffer (**Appendix A**), kept on ice for 10 minutes, then centrifuged at 2,665 *g* for 10 minutes at 4°C. The pellet was resuspended in 2 ml ice-cold Transformation Buffer containing 140 µl DMSO. Subsequently, the competent cells were used immediately and a drop of 80% glycerol was added to the remaining suspension which was then divided into 200-400 µl aliquots using pre-cooled 1.5 ml Eppendorf tubes. The aliquots were snap-freezed in liquid nitrogen and stored at -80°C.

2.5 Transformation of *E. coli*

10 µl of the ligation mix was added to 100 µl of competent cells. A positive control was prepared by the addition of 1 µl of uncut vector and the negative control consisted of 100 µl of competent cells without any DNA additions. The transformation reactions were incubated for 10 minutes on ice. Subsequently, cells were heat shocked for 45-50 s at 42°C and incubated for 2 minutes on ice afterwards. 900 µl of SOC broth (**Appendix A**) was added to each reaction and the mixture incubated for 1.5 hour at 37°C with shaking. The transformants were then plated on the LB agar. IPTG, X-gal and ampicillin were added when appropriate to the LB agar for the selection and identification of the transformants.

2.6 Bacterial Two Hybrid assay (B2H)

To test protein-protein interactions by Bacterial Two-Hybrid assay, the BACTH System Kit (Euromedex) was used. The genes encoding the target proteins were cloned into plasmids pUT18, pUT18C, pKT25, pKT25N. The cloning was done using *E.coli XL-I blue* host strain. All pairwise combinations of T25- and T18-based clones were tested by co-transforming them into *E.coli BTH101*. Co-transformants were grown on the LB plates with ampicillin (100 µg/ml), kanamycin (25 µg/ml), IPTG (0.5 mM), X-gal (40

μg/ml). The growth of colonies indicated positive selection of co-transformants. White coloured colonies/spots meant no interaction between the investigated proteins, while blue coloured colonies/spots meant that an interaction had occurred.

2.6.1 Preparation of chemically-competent cells of *E. coli BTH101*

E. coli BTH101 was grown in 5ml LB overnight and used to inoculate 50 ml of fresh LB. The volume of the overnight culture for inoculation was calculated using formula: (0.05/OD600) x 50 ml. The culture was incubated to an optical density of 0.4 at 600 nm. Then, the culture was centrifuged at 3,373 *g* and resuspanded in 5 ml of the ice-cold 0.1 M $CaCl_2$. The resuspanded culture was incubated for an hour on ice, then it was centrifuged at 3,373 *g* and resuspanded in 250 μl 0.1 M $CaCl_2$ and incubated for 30 minutes on ice. To store the competent cells, a drop of 80% glycerol was added and the cells were snap-freezed in the liquid nitrogen. The cells were stored at -80C^{o}. 250 μl of competent cells was enough for 16 co-transformations.

2.6.2 Co-transformation of *E. coli BTH101*

Competent *E. coli BTH101* cells were thawed on ice. 15 μl of the cells were transferred to 1.5 ml Eppendorf tubes pre-cooled on ice. 0.5-1 μl of each appropriate plasmid was added: pUT18 or pUT18C recombinant plasmid with pKT25 or pKT25N recombinant plasmid. pKT25 ZIP and pUT18C ZIP were used positive control. Co-transformation of the empty pUT18 or pUT18C and pKT25 or pKT25N was used as negative control. The co-transformation mix was incubated for 20 minutes on ice followed by 2 minutes at 42^{o}C and then back on ice for 5 minutes. Next 80 μl of SOC broth was added to each reaction and the mixture incubated for 2 hours at 30^{o}C with shaking. The transformants were then plated on the LB agar containing ampicillin, kanamycin, IPTG, X-gal for the selection and identification of co-transformants.

2.7 Transformation of *Bacillus spp.*

2.7.1 *B. subtilis* transformation

Bacillus subtilis was cultured overnight in the MM competence medium (**Appendix A**). 10 ml of the fresh MM competence medium was inoculated with 0.6 ml of overnight culture and incubated for 3 hours at 37^{o}C. This was followed by addition of 10 ml of starvation medium (**Appendix A**) to the culture and the incubation was continued for 2 hours to make cells competent. 500 ng of DNA was mixed with 0.4 ml of competent cells and incubated for 1 hour, followed by plating on a selective medium and overnight incubation.

2.7.2 *B. anthracis* transformation

The transformation of *B. anthracis* was carried out by electroporation, as described by Koehler et al. (1994). In the case of the construction of delition mutants, electrotransformation was followed by growing the transformed strains first in BHI (**Appendix A**) medium with kanamycin for two days and then in BHI medium without the antibiotic. Cultures were screened for kanamycin-resistant, erythromycin-sensitive clones.

2.8 RNA purification and analysis

2.8.1 Total RNA purification from *Bacillus spp.*

RNA was purified using the acid phenol method. Strains of *B. anthracis* were grown overnight in 5 ml LB, and used to inoculate 20 ml of fresh LB. The volume of overnight culture was used for inoculation was calculated using formula: $(0.05/OD_{600})$ x 20 ml. The culture was incubated to an optical density of 0.8 at 600 nm and then 10 ml of the culture was added to 5 ml of frozen killing buffer (-20^{o}C) mixing by invertion three times. The cells were harvested by centrifugation (10 minutes, 3,838 *g*, 4^{o}C). The supernatant was discarded and the cells were snap-freezed in the liquid nitrogen and stored at -20^{o}C. For RNA extraction the frozen pellets were thawed on ice and resuspanded in 1 ml Lysis solution I (25% sucrose, 50 mM Tris/Cl, pH 8.0, 0.25 mM EDTA). The cells were harvested by centrifugation (16,099 *g*, 5 minutes, 4^{o}C) followed by removal of the supernatant. The pellet was resuspanded by pipetting in 300 µl Lysis solution II (3 mM EDTA, 200 mM NaCl) and the suspension was transferred immediately to the 1 ml prewarmed mixture of 500 µl Lysis solution II and 200 µl 10% SDS prewarmed to 95^{o}C. The samples was mixed and incubated for 5 minutes at 95^{o}C in a heating block. Next, 1 ml acid phenol solution was added to the sample and mixed rapidly in the reaction tube shaker for 5 minutes at room temperature. Following centrifugation (13,684 *g*, room temperature), 850 µl of the upper (aqueous) layer was transferred into fresh an Eppendorf tube, avoiding carry-over of the DNA-containing interphase. 850 µl acid phenol solution was added to the sample and mixed using a reaction tube shaker at room temperature for 5 minutes. Followed the centrifugation (13,684 *g*, room temperature), 700 µl of the upper aqueous phase was transferred into a fresh Eppendorf tube. 700 µl chloroform/isoamylalcohol was added to the sample which was mixed and centrifuged (13,684 *g*, room temperature). The upper aqueous phase was transferred to a fresh Eppendorf tube with 70 µl 3 M sodium acetate, pH 5.2 and the sample was mixed, followed by addition of 1 ml isopropanol and mixing. The sample

was incubated at -20^{o}C overnight to precipitate RNA. Next the sample was centrifuged (21,918 *g*, 4^{o}C, 15 minutes), the supernatant removed and the pellet resuspended in 70% ethanol. The sample was centrifuged (21,918 *g*, 4^{o}C, 15 minutes), the supernatant was removed and the pellet was air dried. The RNA pellet was dissolved on ice in 50 µl dd$H_2$0 and the purity and quality determined with a Nanodrop ND-1000 spectrophotometer. The ratios of A_{230}, A_{260} and A_{280} reflect the degree of purity of DNA samples. The value of ratios of A_{260}/A_{280} between 1.8 and 2, and A_{260}/A_{230} between 2.0 and 2.2 is indication of good quality RNA; lower values indicate contamination. The RNA quality and integrity was additionally assessed by gel electrophoresis by inspection of the 16S and 23S rRNA bands visible on an agarose gel.

2.8.2 Northern blotting

2.8.2.1 RNA electrophoresis

RNA electrophoresis was done under denaturation conditions to disrupt secondary structures which can strongly impact on how RNA migrates through the gel. The 1.2% gel was prepared: 1.2 g agarose is dissolved in 10 ml 10 x MOPS (3-[N-morpholino] propanesulphonic acid) buffer (**Appendix A**) and 74 ml sterile dd$H_2$0 in the microwave, mixing every 10 seconds. The dissolved agarose was put to the 65^{o}C oven for 30 minutes and 18 ml of 37% (12.3 M) formaldehyde was added and incubated for another 30 minutes at 65^{o}C. The gel was poured and left to solidify for 60 minutes. RNA samples were prepared for loading: 5 µg RNA was added to a 1.5 ml Eppendorf tube and the sample was made up to 10 µl. Next, 10 µl loading dye was added and the sample was mixed and incubated at 65^{o}C for 10 minutes. In the case of the RNA size marker (Invitrogen), 3 µl of ladder were added 3 µl loading dye and mixed. The pre-electrophoresis of the empty gel was run for 10 minutes at 60 V in 1 x MOPS as the running buffer. The samples were loaded and the gel run at 52 V for 90 minutes. Next, the gel was turned around, the buffers mixed and two cables swapped to prevent buffer exhaustion. The gel was stained with ethidium bromide (5 µg/ml) for 2-5 minutes on the shaker and then washed 3 times 20 minutes on the shaker with sterile ddH_2O. The fourth wash was done overnight at 4^{o}C without shaking. The following day, the picture of the gel exposed to UV light and the quality and integrity of the purified RNA assessed by inspection of bands corresponding to the 16S and 23S RNA.

2.8.2.2 Immobilisation of RNA on membrane

The transfer of RNA from the gel into the membrane was performed using a vacuum blotter (model 785, BioRad). The blotting was performed according to the manufacturer's standard procedure with some modification. Denaturation solution (0.5 M NaOH, 1.5 M NaCl) was applied for 5 minutes, followed by neutralisation solution (0.5 M Tris-HCl, 3 M NaCl). Next, 20 x SSC solution (175.3 g/l NaCl, 88.2 g/l trisodium citrate, adjusted to pH 7.0 with NaOH) was applied onto the membrane for 5 hours. RNA was fixed to the nylon membrane by exposing it to UV light (60,000 J cm^{-2}, Stratalinker, Strategene). Membranes were immediately subjected to the subsequent hybridization step or stored at 4^{o}C.

2.8.2.3 Generation of the probe for the detection of target gene

The 5' end of target gene (400 – 500 bases) was amplified by PCR with forward primers of 18 – 25 bases. The reverse primer, in addition to 18 – 25 bases complementary to the target gene, contained a T7 promoter sequence (ctaatacgactcactatagggaga) at 5' end. The PCR products were checked by gel electrophoresis to verify the presence of the fragment of the expected size. Next, PCR products were purified using the QIAquick^{TM} PCR purification kit (Qiagen) according to the manufacturer's instructions. The DNA was used in an *in vitro* transcription reaction to create a DIG-labelled mRNA probe, using component and volumes shown in the Table 2.3.

Table 2.3: In vitro transcription reaction for the creation of the mRNA probe

Components	Volume (µl)	Final concentration
Purified PCR product	variable	600 ng
10 x Labelling mix (containing digoxigenin-11-UTP, Roche Diagnostics)	2	1 x
10 x Transcription buffer (Roche Diagnostics)	2	1 x
T7 RNA polymerase (400 U/µl) (Sigma)	2	20 U/ µl
RNasin (40 U/µl) (Promega)	2	2 U/ µl
ddH_2O	Fill up to 20 µl	

The mixture was incubated for 3 hours at 37^{o}C. Next, 2 µl of 0.2 M EDTA (pH 8.0) was added to stop the transcription reaction. The labelling efficiency was determined by preparing serial dilutions (10^{-1} – 10^{-3}) and applying 1 µl of each dilution as well as undiluted probe onto a strip of positively charged nylon membrane (Roche). The RNA probe was fixed to the nylon membrane by exposing the membranes to UV light (60, 000 J cm^{-2}, Stratalinker, Stratagene).

2.8.2.4 Hybridization

Nylon membranes were placed in pre-hybridization buffer (0.02% SDS, 0.1% N-laurylsarcosin, 2% blocking reagent, 5 x SSC buffer, 50% v/v foramide pre-warmed to 65°C) in hybridization tubes (20 ml per membrane). Pre-hybridization was performed in a rotating hybridization oven for 1 hour at 65°C. DIG-labelled RNA probes were denatured for 15 minutes at 90°C in a water bath and then placed on ice. Once the pre-hybridization was completed, the pre-hybridization buffer was discarded and the hybridization solution containing the probe was added (10 ml per membrane). The hybridization was performed at 65°C overnight in the hybridization oven.

2.8.2.5 Stringency washes

The hybridization buffer was removed and the membrane was washed with the Wash Buffer I (2 x SSC, 0.1% SDS) (2 x 5 min) followed by Wash Buffer II (0.1 x SSC, 0.1% SDS) (2 x 15 minutes) at 65°C in the hybridization oven.

2.8.2.6 Immunological detection

After the stringency washing step, the membrane was rinsed with Tween Wash Buffer (0.1 M Maleic acid, 0.15 M NaCl, 0.3% Tween 20; pH 7.5) for 5 minutes under high agitation on the table shaker. The membrane was incubated for 30 minutes in 30 ml of the Blocking Buffer (**Appendix A**). The Blocking buffer was discarded and 20 ml of the Blocking Buffer with 2 µl of anti-digoxigenin-AP antibody (Roche) was added to the container with the membrane and incubated for 30 minutes with gentle agitation. The membrane was washed twice with the Tween Washing Buffer (first washing for 30 minutes, second for 1 hour). The membrane was equilibrated using 30 ml of the Detection Buffer (0.1 M Tris-HCl, 0.1 M NaCl, pH 9.5) for 5 minutes. The membrane was transferred into the bottom sheet of plastic pocket and approximately 500 µl - 1000 µl Detection Reagent (CDP-Star, Roche), depending on the size of the membrane, was applied. The membrane was covered by the top sheet of the plastic pocket and Detection Reagent was spread evenly on the membrane, squeezing out any air bubbles. After 5 minute incubation in the dark, the membrane was exposed to an autoradiography film (Hyperfilm-ECL, Amersham Bioscience, France) in the autoradiography cassette (Genetic Research Instrumentation Ltd, UK). The exposure time was varied depending on the strength of the probe. The films were developed using a film processor (Konika). Alternatively, the membrane blots were exposed in ImageQuant LAS 4000 and ImageQuant LAS 4010 imager (GE Healthcare) and analysed by ImageQuant TL

software (GE Healthcare). The sizes of transcripts were determined in reference to RNA size marker (Invitrogen).

2.8.3 Analysis of gene expression by quantitative RT-PCR

RNA was purified as described in the **Section 2.8.1** and used to generate cDNA by reverse transcription reaction, using a Moloney Murine Leukemia Virus (MMLV)-RT Kit (Promega, Madison, USA). The components, volumes and final concentrations of components of the reaction mix are given in the Table 2.4.

Table 2.4: Reverse transcription reaction

Components	Volume (µl)	Final concentration
RNA (50 ng/µl)	4	200 ng
0.5 mg/ml Random Hexamers pd(N)6 (GE Healtcare)	1	25 µg/ml
ddH_2O	9	
5 x M-MLV RT reaction buffer	4	1 x
10mM dNTPs	1	20 U/ µl
RNasin Ribonuclease Inhibitors (20 U/µl) (Promega)	0.5	10 U
M-MLV RT (10 U/µl)	0.5	100 U

First, RNA was diluted in such a way to obtain the concentration of 50 ng/µl. 4 µl of RNA (200 ng in total) was mixed with random hexamers $pd(N)_6$ (GE Healtcare) and ddH_2O and incubated for 5 minutes at 65^{o}C. The remaining components were added and the mixture was incubated for 2 hours at 42^{o}C for primer extension followed by denaturation of the reverse transcriptase at 70^{o}C for 10 minutes. The RT products were subsequently diluted 1:200 and used immediately for the RT-PCR reaction or stored at -20^{o}C for the later use. The 1:200 diluted RT products were used to prepare RT-PCR reaction mix with the volumes and concentrations components shown in the Table 2.5. The primers for the reaction were designed in such a way to amplify 100 – 200 bases of the 5' end of the target gene. The RT-PCR reactions mixes were prepared by benchtop instrument (QIAgility, Qiagen). The RT-PCR was performed using Rotor-Gene™ Q (Qiagen).

Table 2.5: Relative quantitative Real-Time PCR reaction components

Components	Volume (µl)	Final concentration
PCR primers (10 µM)	4	0.5 µM
SYMBR Green Master Mix (2x concentrated)	10	1 x
RT product (1:200 diluted)	6	-

The temperature and time profile for the PCR cycle were as shown in the Table 2.6. The Real-time amplification of the target and the reference genes (*gyrB* and *gatB*) were performed. For the purpose of analysis, the threshold level was set arbitrarily and Ct

values (the cycle number at which the fluorescence crosses the threshold level) were recorded. As Ct values are inversely proportional to the amount of template – the more templates in a sample, lower the Ct values are. This served as the basis of gene expression quantification. In this study Ct values obtained for the mutants were compared to those of the wild type strain to evaluate change in the gene expression in the mutant strains. The reference/housekeeping genes (*gyrB* and *gatB*) were used to take account of variations in the cDNA input and the sample-to-sample differences. Melting curve analysis was also performed in parallel to the RT-PCR to confirm that only a single, specific product was amplified.

Table 2.6: The temperature and time profile for RT-PCR cycle

Parameter	Temperature (^{o}C)	Times (sec)
Denaturation	95	300
Amplification (35 cycles)	95 60	5 10
Melting curve	65-95^{o}C, increment of 1^{o}C	90s for first step, 5s for subsequent steps

2.9 Precipitation of proteins from culture supernatants

2.9.1 Basic protocol for precipitation of proteins from culture supernatant

Strains of *B. anthracis* were grown overnight in 5 ml LB broth and used to inoculate 60 ml of fresh LB broth without antibiotics. The volume of overnight culture for inoculation was calculated using formula: ($0.05/OD_{600}$) x 60 ml, and the culture incubated with shaking at 37°C until an OD_{600} of 0.8. The cells were harvested by centrifugation at 3,838 *g* for 30 minutes at 4°C and the supernatant transferred carefully in to a 100 ml glass bottle (making sure no cells were transferred). To the transferred 45-50 ml of supernatant, 16 ml of pre-cooled TCA was added and the mixture was mixed by shaking. The samples were incubated at 4°C overnight. The following day, the samples were centrifuged at 30,000 *g* at 4°C for 70 minutes and the majority of the supernatant decanted. 1-2 ml of the supernatant that was left, was used to, resuspend the pellet. The mixture was transferred into a 2 ml Eppendorf tube. Following, centrifugation at 20,000 *g* for 15 minutes at 4°C, the supernatant was decanted and the pellet washed with 100% ethanol 3 times, each time, with centrifugation at 20,000 *g* for 15 minutes at 4°C. Subsequently, the pellet was dried at 65°C in an oven with the tube lids open for approximately 20 minutes. 200 µl of Urea/Thiourea were added into the each tube, then tubes were vortexed to dissolve the pellet and centrifuged at 20,000 *g*

for 30 minutes at 4°C. The supernatant was transferred into a clean tube and protein concentration was determined.

2.9.2 Precipitation of inducible proteins from culture supernatant

When induction of proteins was required, the basic protocol for precipitation of proteins from culture supernatant (**Section 2.9.1**) was followed with some modifications. As previously, the overnight culture was used to inoculate 60 ml of fresh LB (in 500 ml flask) without antibiotics, and the bacterial culture was incubated with shaking at 37°C until an OD_{600} of 0.8. The culture was split into 2 flasks (250 ml flasks). Into one flask, the inducer: 20% xylose (final concentration is 1%) or 1 M IPTG (final concentration 10 mM), was added to induce expression. Both cultures (with and without inducer) were incubated with shaking at 37°C for 90 minutes. The cells were harvested by centrifugation at 3,838 *g* for 30 minutes at 4°C and the supernatant transferred carefully in to a 100 ml glass bottle (making sure no cells were transferred). To the transferred 20-25 ml supernatant, 8 ml of pre-cooled TCA was added and the mixture was mixed by shaking. Next, the basic protocol was followed (**Section 2.9.1**).

2.9.3 Extraction of EA1 protein

The protocol was followed as in the **Section 2.9.2** with some modifications. The cells were harvested by centrifugation at 3,838 *g* for 30 minutes at 4°C and the supernatant transferred carefully in to a 100 ml glass bottle (to make sure no cells were transferred). After centrifugation, the supernatant was kept on ice and the pellet was resuspended in 4 M LiCl, 200 µM PMSF, 50 mM Tris-Cl (pH7.5), next mixed for 1h at 4℃ on the rotating plate, following centrifugation (21,918 *g*, 10 minutes, 4℃). The supernatant was added into the tube with the supernatant obtained after spinning down the culture. The samples were added to 8 ml pre-cooled TCA and mixed by shaking. Next, the basic protocol for precipitation of proteins from culture supernatant was followed (**Section 2.9.1**).

2.10 Purification of SecA1, SecA2 and SecH proteins

SecA1, SecA2 and SecH were purified using *E. coli* BL21 as an expression host. SecA1 and SecA2 were expressed from pGEX 6p1 as GST-tagged proteins: GST-SecA1 and GST-SecA2, respectively, while SecH was produced from pET16b as a His-tagged protein. Cultures were grown in 250 ml LB medium in at 37°C. When the OD_{600} reached about ~ 0.6, expression was induced by the addition of IPTG to a final concentration of 0.05 mM, and the incubation continued overnight at room temperature.

Subsequently, the cells were harvested by centrifugation (15 minutes, 3,000 *g*, 4°C) and resuspended in 250 µl of 1 x PBS with protease inhibitor and lysozyme. The cell suspension was incubated on ice for 30 minutes, with mixing every 10 minutes. Afterwards, cells were sonicated for 5 x 10 seconds, amplitude 10%. 10 µl of the sonicate was withdrawn to be analysed by SDS-PAGE. The remaining sonicate was centrifuged (15,000 *g*, 15 minutes) and 5 µl of the supernatant was taken to run on the gel. To optimize the solubilisation of proteins, the following modifications were used: (1) sarcosyl was added (1% final concentration) to cell suspension, after incubation with lysozyme, and mixed by inversion; (2) Triton X-100 was added (1% final concentration) to the sonicate and mixed by inversion. Purification of GST-SecA1 and GST-SecA2 was continued using a column packed with Glutathione Sepharose 4 Fast Flow affinity chromatography medium (GE Healtcare), according to the manufacturer's instructions. The protein fractions were separated on a SDS-PAGE gels, which was then stained with Coomassie blue.

2.11 Determination of protein concentration

The protein concentration was determined using 2-D Quant Kit (GE Healthcare) according to the manufacturer's instructions.

2.12 The SDS-PAGE electrophoresis

The SDS-polyacrylamide gel electrophoresis (SDS-PAGE) was performed as described in Sambrook et al. (1989) using a 5% stacking gel and a 10% separating gel with the components listed in **Appendix A**. The thickness of gels was 1 mm. Alternatively, 10% NuSep protein gels (Generon) or Mini-PROTEAN TGX gels (Bio-Rad) were used. 20 µg of protein (in a total volume of 25 µl of the loading sample, including the bromophenol blue loading dye) was loaded per lane and the samples electrophoresed at 80 V and then the voltage was increased to 200 V, when the bromophenol blue dye had reached the separation gel. The electrophoresis was performed until the loading dye just ran off the bottom of the gel. The gel was stained with one of the following dyes: (i) Coomassie Blue (G-250) as described in Sambrook et al. (1989); (ii) silver stain using PageSilver™ Silver Staining Kit (Thermo Scientific) according to the manufacturer's instructions; (iii) SYPRO Ruby Protein Gel stain (Invitrogen) according to the manufacturer's instructions.

2.13 Pull-down experiment

The pull-down experiment was carried out using a Flag-tagged protein and ANTI-FLAG M2 affinity gel (Sigma-Aldrich). The culture of *B. anthracis* containing pKG400 plasmid encoding the gene of interest fused in frame to the sequence of the Flag-tag, was grown overnight and used to inoculate 500 ml of the LB broth. The new culture was then grown to an OD_{600}=0.8 and IPTG was added to a final concentration of 10 mM and incubated for a further 90 minutes. 250 ml culture was then withdrawn to a separate sterile flask, 7 ml 37 % formaldehyde was added (1 % w/v final concentration) and the culture was shaken gently at room temperature to facilitate protein cross-linking. 12.5 ml of glycine was added (final concentration 0.125 M) to quench the cross-linking reaction with the culture was shaken for further 5 minutes at room temperature. Both cultures (formaldehyde-treated and untreated) were harvested by centrifugation (15,000 *g*) and resuspended in TBE buffer (50 mM Tris HCl, 150 mM NaCl, pH 7.4). The cells were then disrupted with a dismembrator by shaking 1 ml resuspended cells with 300 µl glass beads at 2,600 rpm. The sample was centrifuged (21,918 *g*, 10 minutes, 4^{o}C) and the supernatant transferred into 2 ml Eppendorf tube. Its volume was topped up to 1.2 ml. The protein extracts were filtered with a 0.45 µm membrane filter to remove any remaining cells and particulates. ANTI-FLAG M2 affinity resin is supplied as a suspension in 50% glycerol. To remove the glycerol, the resin was resuspended in 1.5 ml TBS, incubated for 10 minutes with gentle mixing using rotating plate at 4^{o}C and then centrifuged at 1,000 *g* for 10 minutes. The washing step was done 6 times. ANTI-FLAG M2 affinity resin was resuspended in 25 µl TBE and protein extracts were added to the suspension. The samples were incubated for ~ 2 hour with gentle mixing to capture the FLAG fusion proteins. The resin was collected by centrifugation (1,000 *g* for 5 minutes) and resuspended in TBE with increased NaCl concentration to increase the stringency of washing (50 mM Tris HCl, 500 mM NaCl, pH 7.4). The resin was incubated for 10 minutes with gentle mixing at 4^{o}C and then centrifuged at 1,000 *g* for 10 minutes. The washing step was done 6 times. 5 µl 5 x sample buffer (without reducing agent) was added to 30 µl sample. The samples were boiled for 20 minutes to reverse crosslinking and then analysed by SDS-PAGE electrophoresis. The gels were stained with one of the following: (i) PageSilver™ Silver Staining Kit (Thermo Scientific) according to the manufacturer's instructions; (ii) SYPRO Ruby Protein Gel stain (Invitrogen) according to the manufacturer's instructions. The unique bands from the gel corresponding from the samples with Flag-tagged proteins were excised and sent for mass spectroscopy analysis.

2.14 Bocillin assay

Bocillin assay was used to measure activity of penicillin binding proteins (PBPs). Strains of *B. anthracis* were grown overnight in 5 ml LB broth and used to inoculate 10 ml of fresh LB broth. The volume of overnight culture for inoculation was calculated using formula: ($0.05/OD_{600}$) x 10 ml. The cultures were incubated to an OD_{600} of 0.8. The cultures were centrifuged (10 minutes, 3,838 *g*) cells were resuspended in the 330 µl Lysis buffer and 300 µl glass beads added. The cells were disrupted with a dismembrator by shaking at 2,600 rpm. The samples were centrifuged (21,918 *g*, 10 minutes, 4^oC) and 130 µl supernatant was transferred into 2 ml Eppendorf tube, Bocillin FL (final concentration 25 µM) was added into each sample and the samples were incubated for 20 minutes at room temperature. Next, 20 µl of each sample were mixed with 5 x loading buffer and incubated at 95^oC for 5 minutes. The samples were subjected to SDS-PAGE electrophoresis (80 V for 3 hours). To visualize the labelled PBPs, the gels were scanned with Typhoon Scanner (Typhoon Trio, GE Healthcare) (emission filter: 520 Cy2, ECL + Blue, sensitivity: medium, resolution: 100 µm).

2.15 Mass spectrometry

The mass spectrometry analysis was done by the Pinnacle Lab (Newcastle University, UK). The bands from the SDS-PAGE gels were subjected to trypsin digestion and then analysed using a Voyager DE-STR MALDI-TOF mass spectrometer (Applied Biosystems Inc., Framingham, MA, USA). The resulting peptide mass fingerprint data and the Mascot search engine program (Matrix Science Ltd, London) was used to identify respective proteins. Four samples were additionally subjected to HPLC/MS/MS analysis which generated significantly greater MASCOT confidence scores for the identified peptide fragments.

2.16 Microscopy

Cultures of the analyzed strains of *B. anthracis* were sampled during the exponential (OD_{600}=0.6-0.8) or transitional phases (OD_{600}=2.0-2.5). Aliquots of cultures treated with the FM5-95 membrane stain (final concentration 1µg/ml) and mounted onto a microscope slide coated with 1.2% agarose and immobilized using a glass cover slip. Images were acquired on an Axiovert M200 microscope (Zeiss Ltd., Oberkochen, Germany) with a 300 W lambda light source (Sutter Instrument Company, California, USA) and a Zeiss × 100 plan-neofluar oil immersion objective lens (A = 1.3). Images were captured on a 1395 × 1040 pixel CoolSNAP HQ camera (Photometrics,

Ottobrunn, Germany) controlled by Metamorph software version 6.1r3 (Universal Imaging Corporation Ltd., Marlow, UK). The lengths of cells were measured using ImageJ software (http://rsb.info.nih.gov/ij).

2.17 Computational methods

DNA sequence data for *B. subtilis 168* and *B. anthracis Ames* were obtained from the SubtiList-database (http://genolist.pasteur.fr/SubtiList/) and AnthraList database, respectively (http://bioinfo.hku.hk/GenoList/index.pl?database=anthralist). The primers were designed using Primer3 software (available on-line: http://frodo.wi.mit.edu/). DNA sequence alignments were done were carried out using the ClustalW2 multiple sequence alignment program available online from the European Institute of Bioinformatics (http://www.ebi.ac.uk/Tools/clustalw2/index.html). Homology searches were done by blast programmes (http://blast.ncbi.nlm.nih.gov/).

Chapter 3: Construction of null mutants of *B. anthracis*

This chapter contains description of the strategy of construction of mutants and how the constructed mutants were verified.

3.1 Strategy of mutant construction

The first mutants constructed for investigation of the secondary translocase of *B. anthracis*, prior to this thesis project, were Δ*secA2* and Δ*secY2*. Their analysis revealed that SecA2 but not SecY2 is necessary for secretion of two proteins: Sap and EA1 (Pohl *et al.*, unpublished). Additional mutants: Δ*secH*, Δ*secA2H*, Δ*prsAA*, Δ*prsAB*, Δ*prsAC*, Δ*sap-eag* were constructed as a part of this thesis and analysed together with Δ*secA2* and Δ*secY2*. Their construction was performed by deletion of the target gene using the selectable marker approach described below. Genes of selectable markers such as antibiotic resistance are commonly used to facilitate the introduction or deletion of genes in the genome. Such markers are therefore used for the selection of clones with gene deletions or additions. This was the approach used to construct mutants with deletion of genes encoding elements of the secondary translocation system of *B. anthracis*, as shown on the example of construction of Δ*secA2* (Figure 3.1). Plasmid pUTE583, encoding, chloramphenicol and erythromycin resistance and a multi-cloning site, was used for this purpose. The plasmid also contains two origins of replication – one functioning in *E. coli* and another one in members of *B. cereus* group. An integration fragment carrying a kanamycin resistance cassette (ΩKm) surrounded by 5' and 3' flanking sequences of the target gene – of *secA2* in this example - were cloned into the pUTE583 plasmid, giving rise to the integration vector pSA102. The construction of pSA102 was carried out using the *E. coli* XL-I blue strain as an intermediate host. Subsequently, pSA102 was passaged through a Dam and Dcm methylase-deficient strain of *E. coli* (GM48) as this process improves the efficiency of transformation into *B. anthracis* (Marrero and Welkos, 1995). Following transformation of the integration vector, a double crossover RecA-mediated integration (allelic replacement) event resulted in the target gene being replaced with integration fragment. As a result, the target gene was excised from the chromosome. The mutant strain carrying the targeted gene knock-out as well as the integration plasmid now containing the target gene was counter selected to lose the plasmid, so that the desired mutant genotype was achieved. The counter-selection involves passaging the mutant though numerous generations in liquid culture in the presence of kanamycin (to which resistance is encoded by ΩKm cassette of the integration fragment), but in the absence

of erythromycin (to which resistance gene is associated with the pUTE583 vector). Subcultures of the broth were plated onto agar and the resulting colonies subjected to the replica-plating onto plates with kanamycin and erythromycin. This procedure was continued until erythromycin-sensitive but kanamycin-resistant clones were identified, representing the required potential knockout strains. All other null mutants in this study were constructed in the similar way.

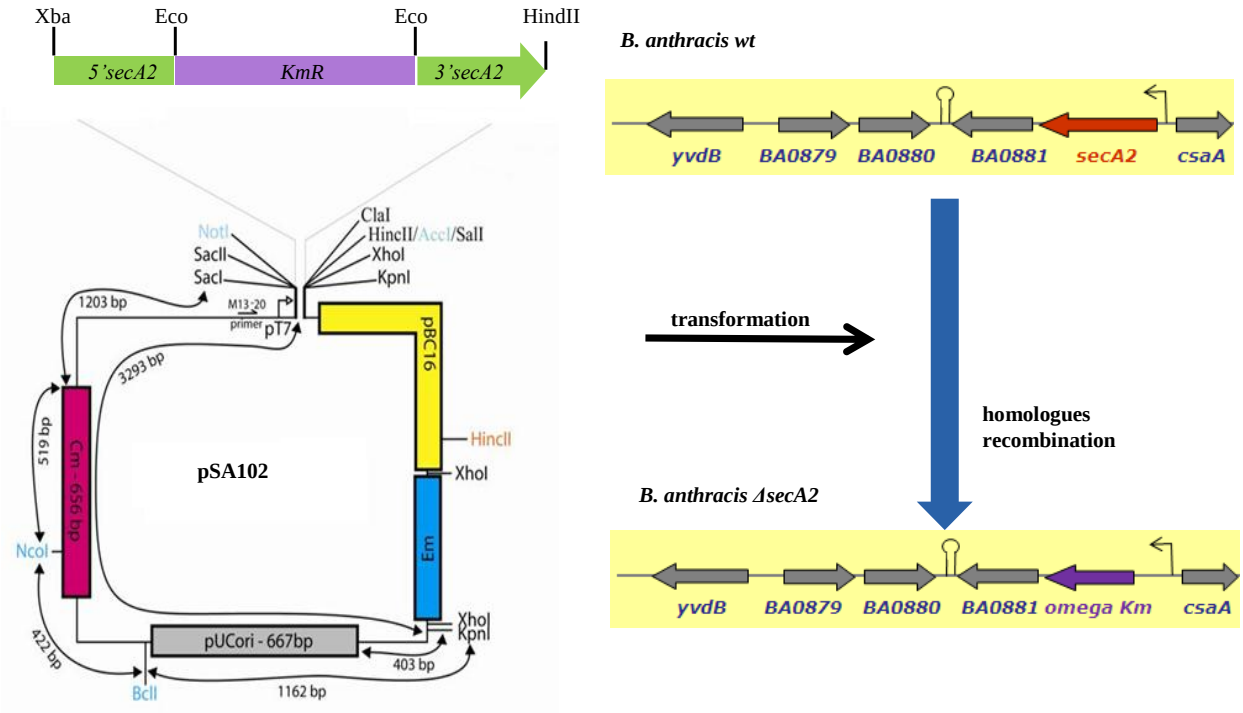

Figure 3.1: Construction of SA102 mutant. The mutant was constructed via the plasmid pSA102 carrying the integration fragment: 5' *secA2* flanking fragment (upstream) - omega Km cassette - 3' *secA2* flanking fragment (downstream). The plasmid was generated by cloning the integration fragment into XbaI/HindIII restriction sites of pUTE583 plasmid. Upon transformation, the homologues recombination replaced the secA2 gene with the integration, generating the SA102 mutant. pSA102 is pUTE583-based plasmid, which possesses chloramphenicol-resistance gene (Cm), erythromycin-resistance gene (Em), two origins of replication: (1) pUCori: functioning in *E. coli*; (2) pBC16: functioning in *B. anthracis*.

The deletion of the target genes was confirmed by diagnostic PCR and Northern blotting. Diagnostic PCR was done using following sets of primers: (i) forward upstream and reverse downstream primer; (ii) forward chromosomal and reverse primers binding within kanamycin cassette - schematic representation of the diagnostic PCR fragments and primers is shown on the Figure 3.2.

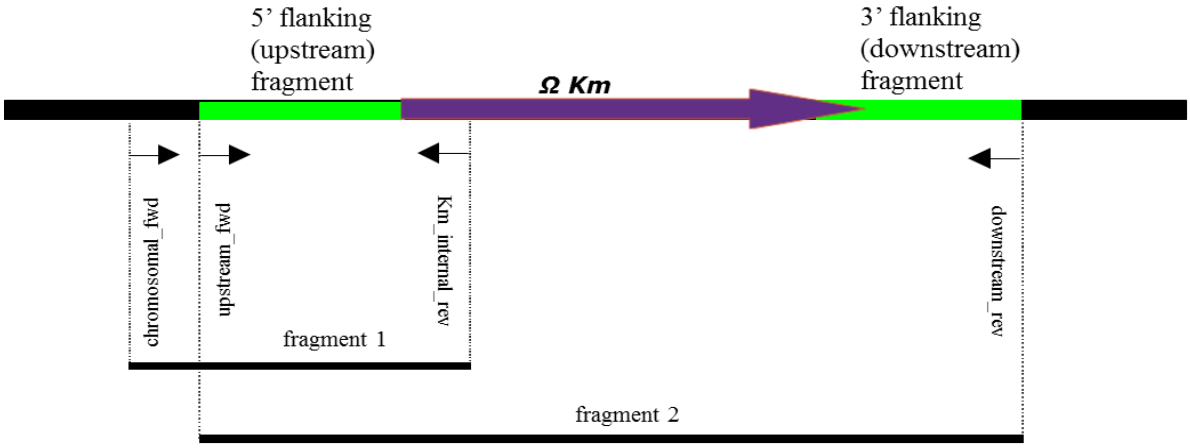

Figure 3.2: Diagnostic PCR to confirm the deletion of the target gene and correct integration of the integration fragment into the chromosome. Two sets of primers were used: **(1)** chromosomal_fwd, which binds to the chromosome upstream the integration fragment, and Km_internal_rev primer amplify fragment 1 which both confirms chromosomal integration of the ΩKm cassette and the deletion of the target gene; the control PCR reaction with chromosomal DNA of the wild type strain is not expected to yield any product.
(2) upstream_fwd and downstream_rev primers allow to verify that a complete fragment 2 is inserted, which corresponds to the combined size of: upstream fragment – kanamycin cassette (Ω Km) – downstream fragment; the control PCR reaction of the chromosomal DNA of the wild type strain will yield a fragment the size of: upstream fragment – target gene – downstream fragment.

3.2 Construction *B. anthracis* Δ*secH* mutant

Previous work has shown that SecA2 is required for the secretion of a subset of proteins, namely Sap and EA1 and possibly other unidentified substrates, even in the presence of SecA1. This observation implies the presence of a specificity factor that facilitates the interaction between SecA2 and its substrates and/or prevents the interaction of these substrates with SecA1. In an attempt to identify that specificity factor, the genomic context of *secA2* in the members of *Bacillus cereus* group was analysed (Figure 3.3). Whenever *secA2* is found in the genomes of members of this group, the same gene is located downstream. This gene, with the locus tag *BA0881* represented a target specificity gene and was therefore subjected to detailed analysis. For reasons that will become clear later in **Section 4**, *BA0881* was renamed *secH*. To evaluate the impact of SecH on secretion, a *B. anthracis* Δ*secH* mutant was constructed. Deletion of *secH* was confirmed by diagnostic PCR (Figure 3.4), according to the principle shown on the Figure 3.2.

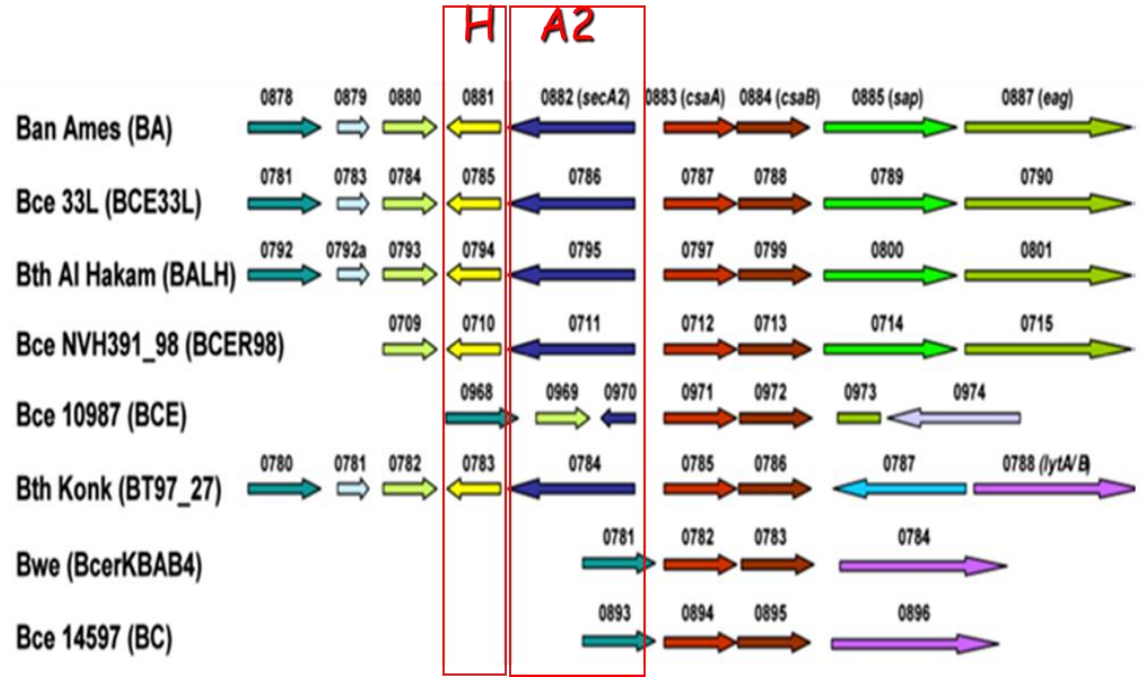

Figure 3.3: Alignment of chromosomal sequences in the gene neighbourhoods associated the *secA2* in members of *B. cereus* group. Homologous genes are shown in the same colours. Aligned *secA2* and *0881* (renamed *secH*) genes are shown in the red frames annotated as A2 and H, respectively. Ban, *Bacillus anthracis*; Bce, *Bacillus cereus;* Bth, *Bacillus thuringiensis;* Bwe, *Bacillus weihenstephanensis.*

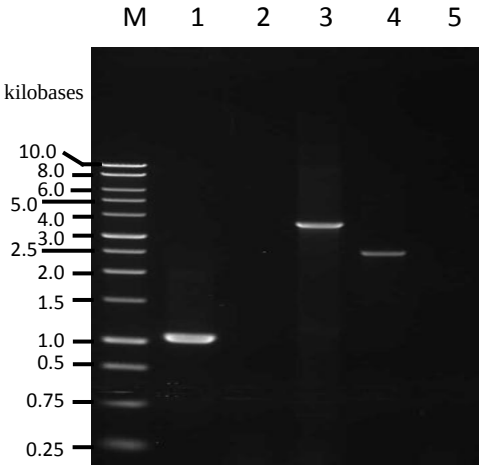

Figure 3.4: Confirmation of absence of *secH* in *B. anthracis* Δ*secH*. **Lane M**: 1 kb molecular ladder (Promega); **Lanes 1 and 2:** PCR product amplified with *secH*_chromosomal_fwd and Km_internal_rev with template of chromosomal DNA of *B. anthracis* Δ*secH* (expected product size 1052 bp) and *B. anthracis* wild type (no product expected - negative control), respectively. **Lanes 3,4,5:** PCR product amplified with *secH*_upstream_fwd and *secH*_downstream_rev with template of chromosomal DNA of *B. anthracis* Δ*secH* (expected product size 3087 bp), *B. anthracis* wild type (expected product size 2574 bp) and no DNA (no product expected), respectively.

3.3 Construction of *B. anthracis* Δ*secA2H*

The *secA2-secH*-null mutant of *B. anthracis* (Δ*secA2H*) was constructed for the purpose of complementation analysis to verify essentiality of SecA2 and SecH for secretion of Sap and EA1. The construction of Δ*secA2H* was confirmed by the diagnostic PCR (Figure 3.5).

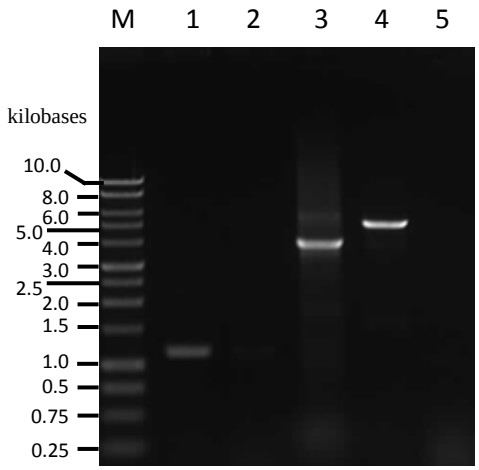

Figure 3.5: Confirmation of absence of *secA2* and *secH* in *B. anthracis* Δ*secA2H*. **Lane M:** 1 kb molecular ladder (Promega); **Lanes 1 and 2:** PCR product amplified with *secA2* chromosomal_fwd and Km_internal_rev with template of chromosomal DNA of Δ*secA2H* (expected product size 1128 bp) and *B. anthracis* wt (no product expected - negative control), respectively. **Lanes 3,4,5:** PCR product amplified with *secA2*_upstream_fwd and *secH*_downstream_rev with template of chromosomal DNA of Δ*secA2H* (expected product size 3870 bp), *B. anthracis* wt (expected product size 5021 bp) and no DNA (no product expected), respectively.

3.4 Construction of *ΔprsAA, ΔprsAB, ΔprsAC* mutants of *B.anthracis*.

B. anthracis has three PrsA-like proteins: PrsAA, PrsAB and PrsAC. The genes encoding those foldases: *prsAA*, *prsAB*, *prsAC* are predicted to be transcribed as monocistronic transcripts with their genomic contexts shown on the Figure 3.6.

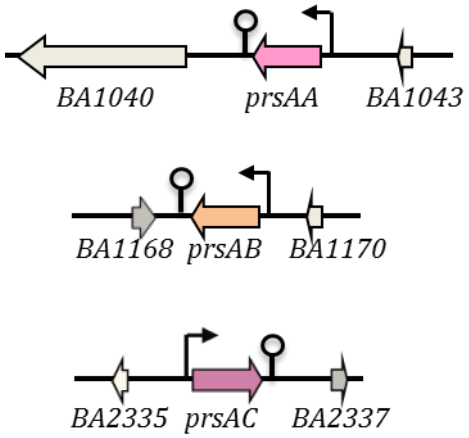

Figure 3.6: Genomic context of *prsAA*, *prsAB* and *prsAC*. Predicted promoters and terminators of *prsAA*, *prsAB*, *prsAC* are represented by angled arrows and omega-like symbols, respectively.

With the aim to identify substrates for the *B. anthracis* PrsA-like proteins, Δ*prsAA*, Δ*prsAB*, Δ*prsAC* mutants were constructed. Their construction was confirmed by diagnostic PCR (Figure 3.7), according to the principle depicted on the Figure 3.2. The absence of expression of *prsAA* and *prsAB* was confirmed by Northern blotting in Δ*prsAA* and Δ*prsAB*, respectively (Figure 3.8).

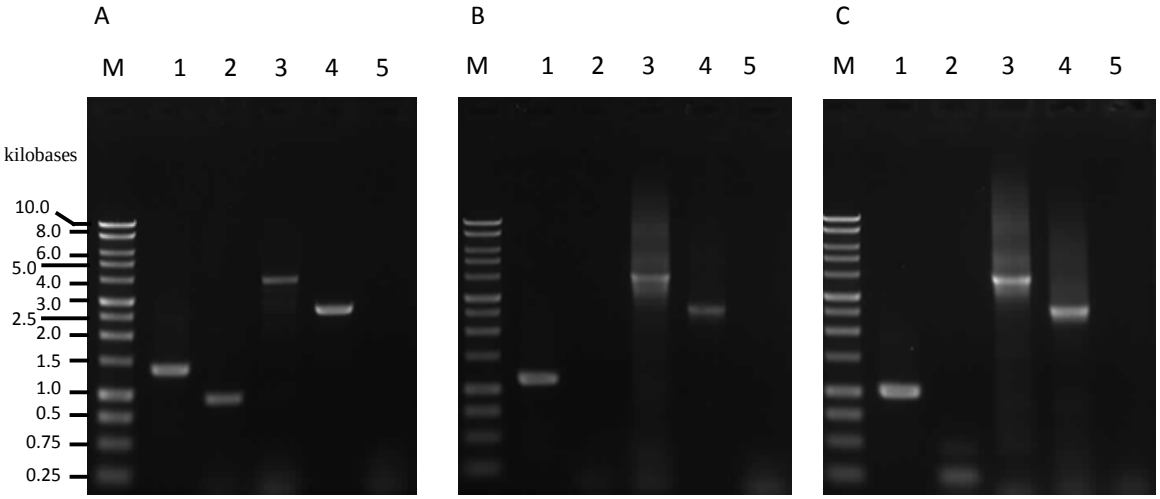

Figure 3.7: The confirmation of absence of the *prsA*-like genes of *B. anthracis* by diagnostic PCR.

A confirmation of absence of *prsAA* in *B. anthracis* Δ*prsAA*. Lanes 1 and 2 : PCR product amplified with *prsAA*_chromosomal_fwd and Km_internal_rev with template of chromosomal DNA of *B. anthracis* Δ*prsAA* (expected product size 1384 bp) and *B. anthracis* wt (no product expected - negative control, unspecific product of approx. 900 bp visible, lack of *prsAA* expression confirmed by the Northern blotting: Figure 3.8), respectively. **Lanes 3,4,5**: PCR product amplified with *prsAA*_upstream_fwd and *prsAA*_downstream_rev with template of chromosomal DNA of *B. anthracis* Δ*prsAA* (expected product size 4000 bp), *B. anthracis* wt (expected product size 2714 bp) and no DNA (no product expected), respectively.

B confirmation of absence of *prsAB* in *B. anthracis* Δ*prsAB*. Lanes 1 and 2 : PCR product amplified with *prsAB*_chromosomal_fwd and Km_internal_rev with template of chromosomal DNA of *B. anthracis* Δ*prsAB* (expected product size 1148 bp) and *B.anthracis* wt (no product expected - negative control), respectively. **Lanes 3,4,5**: PCR product amplified with *prsAB*_upstream_fwd and *prsAB*_downstream_rev with template of chromosomal DNA of *B. anthracis* Δ*prsAB* (expected product size 3831 bp), *B. anthracis* wt (expected product size 2591 bp) and no DNA (no product expected), respectively.

C confirmation of absence of *prsAC* in *B. anthracis* Δ*prsAC*. Lanes 1 and 2 : PCR product amplified with *prsAC*_chromosomal_fwd and Km_internal_rev with template of chromosomal DNA of *B. anthracis* Δ*prsAC* (expected product size 1027 bp) and *B.anthracis* wt (no product expected - negative control), respectively. **Lanes 3,4,5**: PCR product amplified with *prsAC*_upstream_fwd and *prsAC*_downstream_rev with template of chromosomal DNA of *B. anthracis* Δ*prsAC* (expected product size 3836 bp), *B. anthracis* wt (expected product size 2674 bp) and no DNA (no product expected), respectively.

Lane M: 1 kb molecular ladder (Promega)

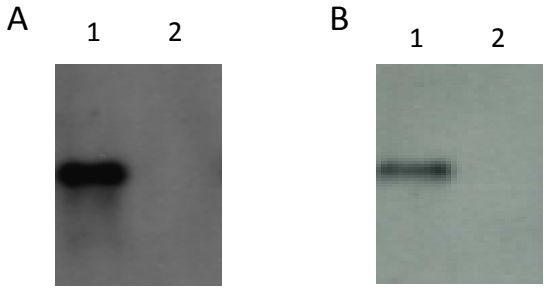

Figure 3.8: Northern blots confirming absence of expression of *prsAA* and *prsAB* in *B. anthracis* Δ*prsAA* and Δ*prsAB*, respectively. A: blot with *prsAA*-specific probe on RNA of: (1) *B. anthracis* wild type, (2) Δ*prsAA*; (B) blot with *prsAB*-specific probe on RNA of: (1) *B. anthracis* wild type, (2) *B. anthracis* Δ*prsAB.*

3.5 Construction of the *B. anthracis* Δ*sap-eag* mutant

B. anthracis Δ*sap-eag* mutant was constructed to serve as a negative control strain in the subsequent experiments. The construction of *B. anthracis* Δ*sap-eag* was confirmed by diagnostic PCR (Figure 3.9).

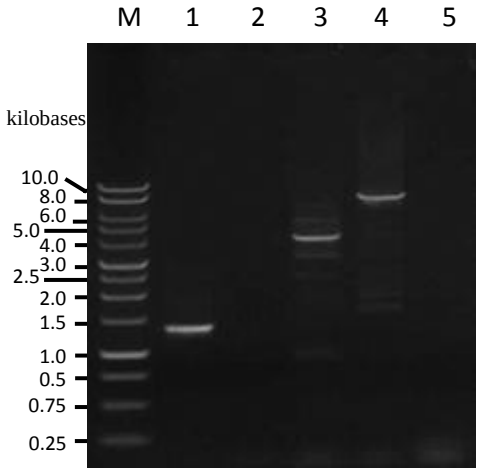

Figure 3.9: The confirmation of absence of *sap* and *eag* in *B. anthracis* Δ*sap-eag*. Lane M: 1 kb molecular ladder (Promega); **Lanes 1 and 2 :** PCR product amplified with *sap*_chromosomal_fwd and Km_internal_rev with template of chromosomal DNA of *B. anthracis* Δ*sap-eag* (expected product size 1382 bp) and *B. anthracis* wt (no product expected - negative control), respectively. **Lanes 3,4,5:** PCR product amplified with *sap*_upstream_fwd and *eag*_downstream_rev with template of chromosomal DNA of *B. anthracis* Δ*sap-eag* (expected product size 3980 bp), *B. anthracis* wt (expected product size 7619 bp) and no DNA (no product expected), respectively.

Summary

Prior to this thesis, it was found that *B. anthracis* might possess a secondary translocation system encompassing SecA2 and SecY2. SecA2 but not SecY2 turned out to be involved in the secretion of S-layer proteins: Sap and EA1 (*Pohl et al.*, unpublished). To learn more about SecA2-based secondary translocase, a range of null mutants: Δ*secH*, Δ*secA2H*, Δ*prsAA*, Δ*prsAB*, Δ*prsAC*, Δ*sap-eag* was generated for subsequent analysis to be performed together with previously constructed mutants Δ*secA2* and Δ*secY2*. Out of the deleted genes, the role of *BA0881* was not previously investigated. As this gene is located in the same operon as *secA2*, we thought that it might be implicated in the SecA2-mediated translocation, possibly conferring SecA2 specificity to its substrates. We re-named *BA0881* as '*secH*'.

Acknowledgement: Northern blotting experiments were done in collaboration with Dr. Susanne Pohl.

Chapter 4: Investigation of protein secretion in *B. anthracis* Δ*secH* and Δ*secA2H*

4.1 SecH enhances EA1 and Sap secretion

We found that *BA0881* gene (renamed as *secH*) is located downstream *secA2* in the same operon (**Section 3.2**) suggesting that BA0881 (SecH) could be implicated in SecA2-mediated secretion of Sap and EA1. To evaluate that, extracellular proteins were extracted (**Section 2.9.1**) from Δ*secH* and subjected to SDS-PAGE and 2D-PAGE. SDS-PAGE analysis showed that, as compared to the wild type strain, the Δ*secH* mutant has a reduced ability to secrete Sap and EA1. However, unlike the Δ*secA2* mutant, it was still capable of secreting significant amounts of the surface associated proteins (Figure 4.1). This data were confirmed by 2D-PAGE analysis, clearly showing a reduction is Sap and EA1 secretion compared with the wild type strain (Figure 4.2). Deletion of *secH* therefore decreases, but does not abolish Sap and EA1 secretion, indicating that SecH is required for the efficient secretion of these proteins. Thus, SecH seems to be a factor conferring partial specificity of SecA2 to its substrates; however, other specificity factor(s) remain to be identified. As *BA0881* was clearly shown to encode a protein involved in secretion, it justified renaming it as *secH*, as ''H'' was next free letter available in the nomenclature of the components of the Sec pathway.

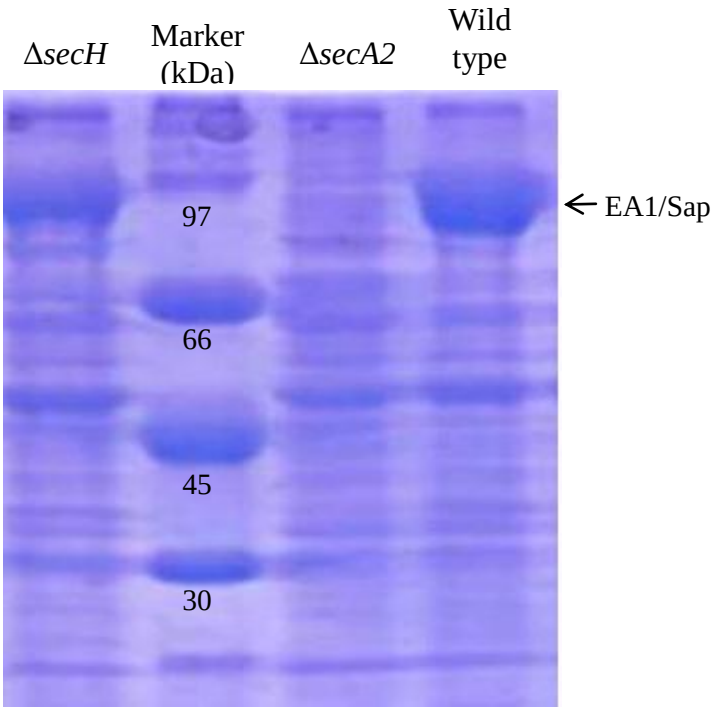

Figure 4.1: SDS-PAGE analysis of the extracellular proteins in the supernatant fraction of strains *B. anthracis* wild type, Δ*secA2*, Δ*secH*. As Sap and EA1 are similar in size, they are visible as single band – of approximately 90 kDa on the Tris-Glycin gel. LMW-SDS marker (GE Healthcare) was used.

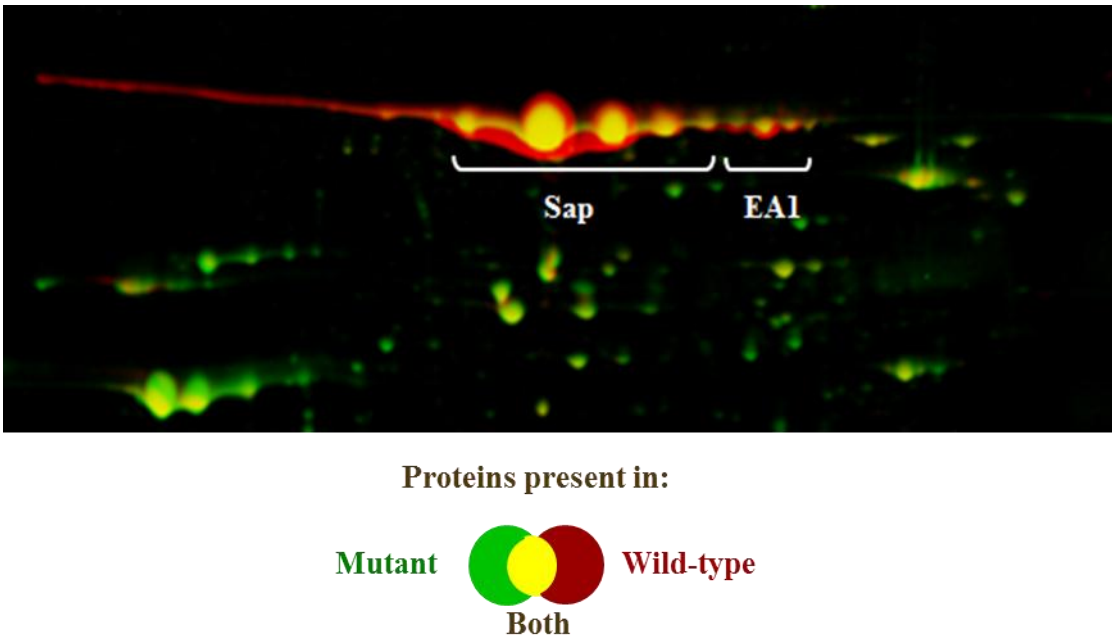

Figure 4.2: False-coloured 2D gel overlays of *B. anthracis* extracellular proteins isolated from the wild-type and the Δ*secH* mutant. The extracellular proteome of Δ*secH* showed a reduction but not the abolishment in the secretion of the major surface-associated antigens, Sap and EA1 (orange spots).

4.2 Complementation of *B. anthracis* Δ*secA2H* to confirm that SecA2, but not SecH, is essential for Sap and EA1 secretion

A complementation approach was used to confirm that SecA2 but not SecH is necessary for Sap and EA1 secretion. For that purpose we decided to clone *secA2* and *secH* gene individually and in combination, into an expression vector, so that those genes could be expressed in *B. anthracis* Δ*secA2H*, and so that the effect of that expression on Sap and EA1 secretion could be investigated. Since a suitable expression plasmid was not available, the first task was to construct such a plasmid that was able to replicate in *B. anthracis* and which would possess an inducible promoter from which the gene of interest could be expressed. Next, the constructed expression plasmid was transformed into *B. anthracis* to analyse the influence of various Sec pathway components on the secretion of Sap and EA1.

4.2.1 Construction of the complementation plasmid

In the first instance we attempted to use existing plasmids previously used for the expression of genes in the related *B. subtilis*, namely pLOSS and pHT01. We therefore attempted to transform *B. anthracis* with pLOSS and pHT01. However, no transformants were obtained after repeated attempts, presumably because origins of replication on those vectors are not functional in *B. anthracis*. Therefore, an expression

vector specific for *B. anthracis* was constructed based on pUTE583, used previously to construct null mutants (**Section 3.1**). A fragment from pHT01 encoding the IPTG-inducible P_{grac} promoter and *lacI* repressor gene was cloned into pUTE583 to obtain pKG400 (Figure 4.3).

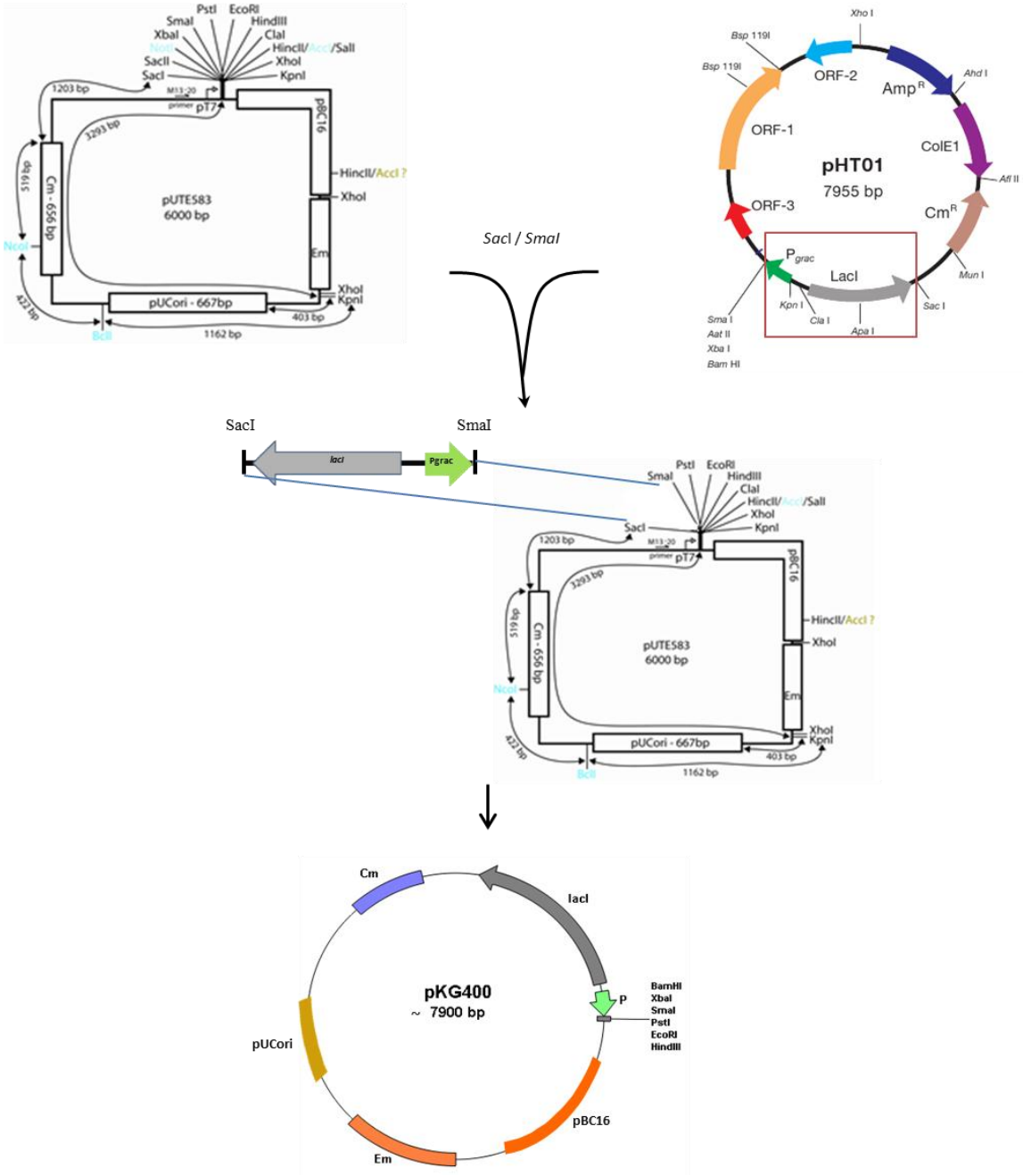

Figure 4.3: Construction of the *B. anthracis* expression vector pKG400. A fragment encoding the IPTG-inducible P_{grac} promoter and *lacI* repressor gene was excised from pHT01 following digestion with SacI and SmaI restriction enzymes. The resulting fragment was ligated into pUTE583 digested with the same enzymes to generate pKG400. Apart from P_{grac} promoter and *lacI* repressor gene, pKG400 also contains pUTE583-related sequences: chloramphenicol-resistance gene (Cm), erythromycin-resistance gene (Em), two origins of replication: one functioning in *E. coli* (pUCori) and another one in *B. anthracis* (pBC16).

4.2.2 Complementation of *B. anthracis* Δ*secA2H* to confirm that SecA2, but not SecH, is essential for Sap and EA1 secretion

Previously, we found that SecA2 is necessary for secretion of Sap and EA1, while SecH enhances secretion of these proteins, but is not essential for this process. To establish whether SecA2 alone, or a combination of SecA2 and SecH was responsible for the failure to secrete Sap and EA1, a Δ*secA2-secH* double null mutant (called Δ*secA2H*) was generated and complemented with: (i) *secA2*; (ii) *secH*; (iii) *secA2*, *secH*. Using pKG400 as the expression vector, the following complementation plasmids were constructed: pKG401 (pKG400-*secA2-secH*), pKG402 (pKG400-*secA2*), and pKG403 (pKG400-*secH*). The plasmids were transformed into *B. anthracis* Δ*secA2H* and expression of the genes of interest was induced at an OD_{600}=0.8 with 10 mM IPTG, followed by incubation for a further 90 minutes and extraction of proteins from the supernatant fraction (**Section 2.9.2**). The extracellular proteins of the complementation strains, with and without induction, were analysed by SDS-PAGE (Figure 4.4). The data showed that Sap and EA1 secretion was restored in the Δ*secA2H* mutant following complementation with *secA2-secH* (pKG401) and *secA2* (pKG402), but not with *secH* (pKG403). This confirmed previous data that SecA2 but not SecH was essential for Sap and EA1 secretion.

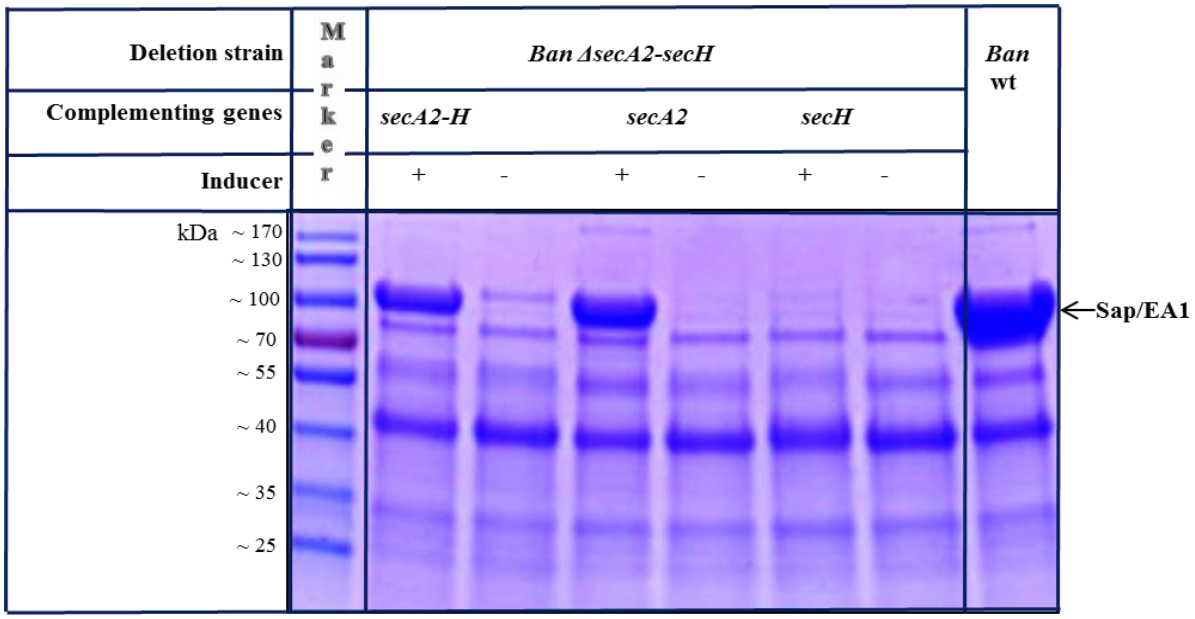

Figure 4.4: SDS-PAGE gel of the extracted proteins of supernatant fractions of the Δ*secA2H* (*B. anthracis* Δ*secA2-secH*) complemented with: (1) *secA2* and *secH*; (2) *secA2*; (3) *secH*. The expression of the target genes located on pKG400 was induced with 10 mM IPTG (+). The non-induced plasmid-containing strains were used as controls (-). The sample extracted from the culture media of *B. anthracis* wild type was used as a positive control for Sap and EA1 secretion. Marker = PageRuler™ Prestained Protein Ladder (Fermentas).

4.3 Discussion

The question that arises in relation to SecA2, and that was addressed in this thesis, is what confers SecA2 specificity to its substrates? Analysis of the signal peptides of Sap and EA1 revealed that they are almost identical, except for a single conservative amino acid substitution at position 23. Since signal peptides are known to be involved in targeting secretory preprotein substrates to the secretion apparatus, it is likely that they are at least partially involved in the determining substrate specificity. Additionally, the bioinformatic analysis of the genomic context of *secA2* revealed that whenever *secA2* is found in the genome of a member of the *B. cereus* group, including, *B. anthracis*, the same gene is located downstream and in the same operon. In *B. anthracis Ames* this gene is annotated as *BA0881*. As a result of the reduction in Sap and EA1 secretion in a *BA0881*-null mutant, as shown by SDS-PAGE and 2D-PAGE analyses, we have renamed this gene a *secH*. SecH enhances the secretion of Sap and EA1, but is not essential for this process. Complementation of the Δ*secA2H* mutant, both jointly and individually with *secA2* and *secH*, confirmed that SecA2 alone without the participation of SecH is able to drive the secretion of EA1 and Sap while SecH does not. This observation reinforces the view that SecH is an accessory component of the secondary translocation system that serves to enhance the efficiency of EA1 and Sap secretion. However, these results mean that there must exist another, yet not detected, factor which directs EA1 and Sap specifically to SecA2 instead of SecA1. It would be possible that the specificity factor would be preventing interaction of Sap and EA1 with SecA1 and facilitating the interaction with SecA2.

In relation to the observed SecA2 specificity towards Sap and EA1, it might be also possible that SecA2 is responsible not for the secretion of those of proteins, but it might be involved in the secretion of other proteins that are part of the secretion machinery. For example, SecA2 could be responsible for the secretion of a foldase involved in folding of Sap and EA1 on the cell surface. Lack of that foldase would lead to the degradation of S-layers proteins and consequently to their absence in the secretome. Similarly, lack of one or more of the seven Sip signal peptidases, could also lead to the absence of Sap and EA1 in the secretome. At the moment it is not known if Sip signal peptidases have any substrate specificity. It can not be excluded that Sap and EA1 are substrates for a specific Sip and that that Sip is a substrate for SecA2. Equally, it can not be excluded that Sap and EA1 are substrates for a foldase which is, in turn, a substrate for SecA2.

Chapter 5: Studies of the *B. anthracis* secondary translocase in *B. subtilis*

5.1 Complementation analysis of SecY of *B. subtilis* (*Bsu* SecY) by SecY2 of *B. anthracis* (*Ban* SecY2)

5.1.1 Introduction

It has been shown previously that *B. anthracis* SecA1 but not SecA2 can complement *B. subtilis* SecA. We now wished to determine whether *B. anthracis* SecY2 could complement *B. subtilis* SecY. SecY2 shows a high level of similarity to both *Bsu* SecY and *Ban* SecY1, and recent evidence has emerged that its role is to maintain secretion capacity during the stationary phase of the growth cycle (Pohl *et al.*, unpublished). This would require it to form an active translocase that interacts with both SecA1 and SecA2 rather than with SecA2 alone. To investigate this possibility we decided to check if *Ban* SecY2 can complement *Bsu* SecY. In *B. subtilis*, complementation can be carried out by locating the test gene on the chromosome at an ectopic location under the control of an inducible promoter. The target gene is then placed under the control of a different controllable promoter. This system allows both the target and the test gene to be expressed independently. In the present study the complementation system was established using integration vectors. First, the 5' end of the target gene was cloned into an integration vector in such a way that it placed its expression under the control of an IPTG inducible promoter. Upon transformation into *B. subtilis*, the vector was integrated into the chromosome via a single crossover recombination. The test gene was cloned intact under the control of a xylose-inducible promoter and introduced into the *amyE* locus via a double crossover recombination. Once the complementation strain was established, the addition of either IPTG or xylose to the growth medium should allow the growth and phenotype of the cells to be established when either the test or target protein is being synthesised. A main limitation of this approach is the polar effects of the integration event on genes downstream of the target gene. In the case of *secY*, two known essential genes, *adk* (adenylate kinase) and *map* (methionine aminopeptidase), are located downstream and in the same operon. This means that irrespective of the expression of *secY*, the lack of induction of *adk* and *map* would lead to cell death.

This SecY complementation study employed two types of integration vector: (i) pMUTIN4, a single crossover vector with an IPTG-inducible P_{spac} promoter and (ii) pJPRI, a double crossover replacement vector that is targeted to the *amyE* locus and

xylose-inducible promoter. In this study, the 5' end of *Bsu secY* gene, together with its ribosome binding site, was amplified and cloned into pMUTIN4 downstream of the P_{spac} promoter. Upon transformation into *B. subtilis* selecting for erythromycin resistance, a single crossover recombination leads the integration of the vector into the chromosome in such a way that *secY* is placed under control of P_{spac} promoter. Thus the target *secY* can be expressed only in the presence of IPTG. SecY is essential for viability, thus the growth of the mutant with *secY* under control of P_{spac} promoter should be dependent on the presence of IPTG.

The *secY2, adk, map* genes from *B. anthracis* were inserted into pJPRI. Upon transformation and selection for chloramphenicol resistance, a double crossover recombination at the *amyE* locus places the test gene under control of the xylose-dependent promoter. As integration takes place within the *amyE* gene, which encodes α-amylase AmyE, the ability of the mutant to hydrolyse starch becomes reduced: when grown on starch agar and stained with iodine, a reduced zone of starch hydrolysis is visible around individual colonies.

The *B. subtilis* strain used for the complementation test was constructed with both vectors integrated into the chromosome, placing *secY* under the control of the IPTG-inducible promoter and *secY2* under the control of the xylose-inducible promoter. If SecY2 can complement SecY, then the complementation strain should be able to grow in the presence of xylose and the absence of IPTG. For the reasons mentioned earlier in this section, the complementation strategy needed to be modified to include copies of *adk* and *map* downstream of the *B. anthracis secY2*. Induction with xylose would therefore lead to the production of SecY2, Adk and Map, compensating for the absence of the latter two enzymes in the absence of IPTG. The genomic map of *secY* and *secY2* loci of the mutant to be created is depicted graphically in the Figure 5.1.

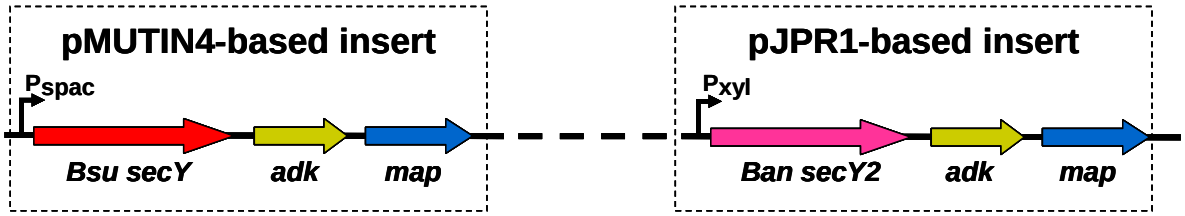

Figure 5.1: The genomic map of *secY* and *secY2* loci of the mutant strain for complementation analysis of *Bsu* SecY *by Ban* SecY2.

5.1.2 Construction of a *B. subtilis* 168 mutant for the complementation analysis using pMUTIN4 and pJPRI

In order to construct a strain of *B. subtilis* for the complementation analysis of *Bsu* SecY by *Ban* SecY2, the following recombinant plasmids were constructed: pMUTIN4-*secY5*' (pKG101) and pJPRI-*secY2-adk-map* (pKG203). In the case of the construction of the pMUTIN4-based mutant, the 5' end of *Bsu secY*, including its RBS (370bp) was amplified using primers *secY*_fwd and *secY*_rev. Next both, the amplified fragment and pMUTIN4 were subjected to the restriction digestion with BamHI and NotI and were ligated together. The ligation products were transformed into *E. coli TOP10* and the transformants were selected on LB agar containing ampicillin. Recombinant plasmid (pKG101) was recovered and subjected to a diagnostic PCR reaction (Figure 5.3), restriction digest and sequencing to confirm the presence of the required insert in the vector.

Construction of the recombinant pJPRI (pKG203) vector involved the amplification and subsequent cloning of three full-length genes into the vector: *B. anthracis secY2, B. subtilis adk* and *map*. *secY2* was amplified primers: *secY2*_fwd and *secY*_rev. *adk* and *map* were amplified with one set of primers: *adk*_fwd and *map*_rev. Next *secY2* and *adk-map* amplified fragments were subjected to the restriction digestion with restriction enzymes BamHI, SpeI, and SpeI, NotI, respectively. The *secY2* and *adk-map* fragments were ligated separately into pJPRI, to generate pJPRI-*secY2* (pKG201) and pJPRI-*adk-map* (pKG202), respectively. In the next stage, the *adk-map* fragment of pKG202 was cloned into pKG201 downstream of *secY2*, through ligation into SpeI and NotI restriction sites, resulting in plasmid pJPRI-*secY2-adk-map* (pKG203) (Figure 5.2). The presence of the required fragments was confirmed by PCR, restriction digest (Figure 5.4) and sequencing.

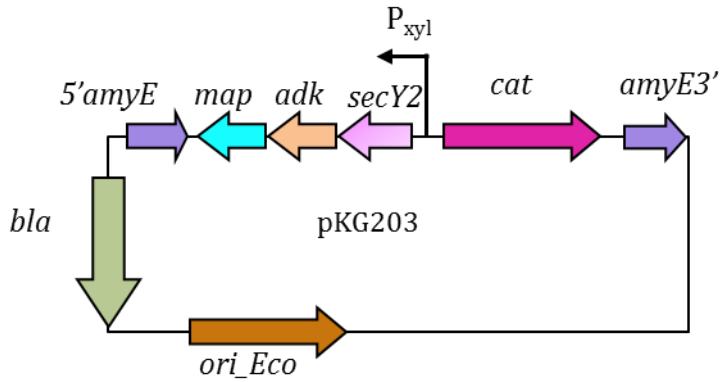

Figure 5.2: Genetic map of pKG203 with *secY2*, *adk*, *map* under control of xylose-dependent promoter. *5'amyE* and *amyE3'*: 5' and 3' terminus of *amyE* locus, respectively; *cat*: chloramphenicol resistance gene; *bla*: β-lactamase gene, ori_Eco: origin of replication.

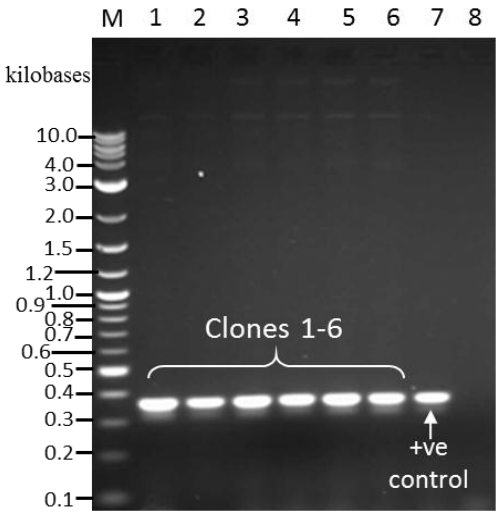

Figure 5.3: Confirmation of the presence of *secY* in pKG101 by PCR. **Lanes 1**: 2-log molecular marker (NEB). **Lanes 2-7**: PCR products (370 bp) of clones 1-6, respectively; **Lane 7**: positive control (chromosomal DNA of *B. subtilis* as a template); **Lane 8**: negative control (no DNA).

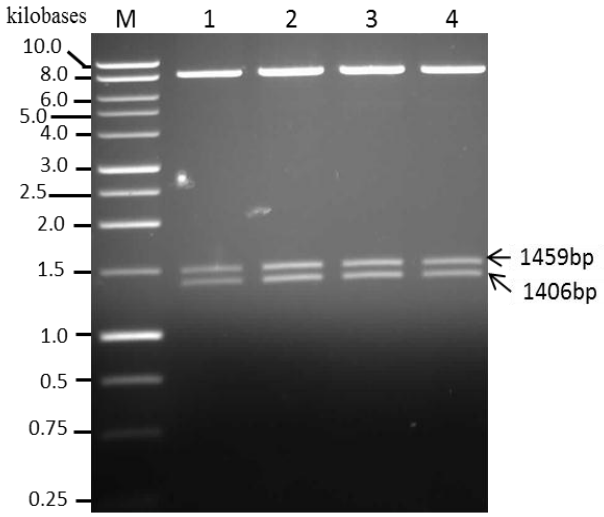

Figure 5.4: Confirmation of presence of *secY2*, *adk* and *map* in pKG203 by a restriction triple digest. **Lane 1**: 1 kb molecular marker (Promega). **Lanes 1-4**: pKG203 digested with enzymes: BamHI, SpeI, NotI, clones 1-4, respectively. Size of inserts: *secY2* (1406 bp); *adk-map* (1459 bp).

Attempts were made to transform plasmids pKG101 and pKG203 into *B. subtilis* 168. The repeated attempts made to transform pKG101 into *B. subtilis* to create *B. subtilis* s*ecY*::pMUT-*Bsu-secY*-F (KG101) were unsuccessful. In contrast, transformation of pKG203 into the *amyE* locus was successful, generating strain KG203 (*amyE*::P_{xyl} *Bsu secY2-adk-map*). The KG203 transformants were selected on LB plates containing chloramphenicol and xylose. The integration of pKG203 to the target *amyE* locus was initially confirmed by growing the transformants on the LB-starch agar to confirm that the transformants exhibited reduced zones of starch hydrolysis, indicating that the *amyE* gene had been inactivated. The authenticity of the insert was subsequently verified by diagnostic PCR using primers for: (1) the insert (*secY2*_fwd & *map*_rev), (2) the P_{xyl} promoter located upstream the insert (Pxyl_fwd) and (3) the sequence downstream the insert (*amyE*_rev) (Figure 5.5).

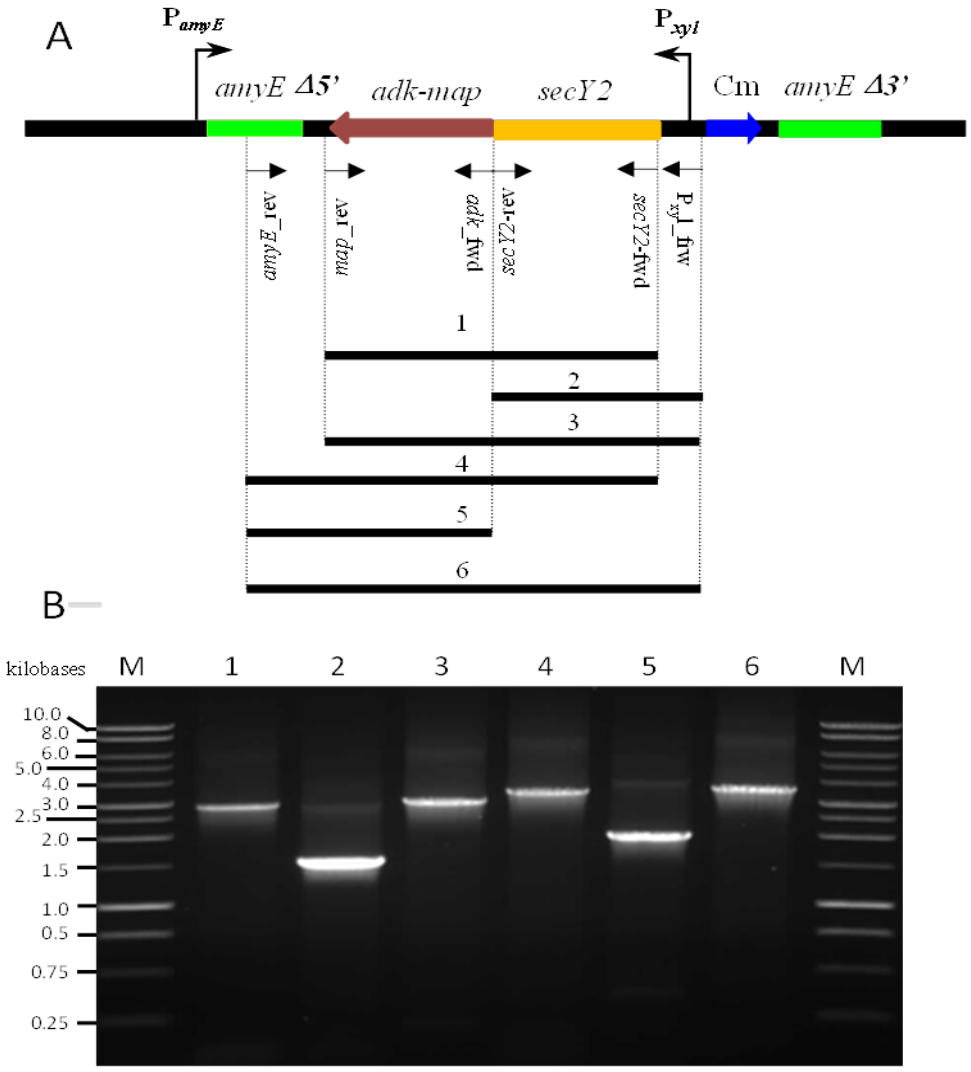

Figure 5.5: Diagnostic PCR to confirm the presence and orientation of *secY2-adk-map* fragment in strain KG203. (A) Schematic representation of *secY2-adk-map* region in KG203 after integration of pKG203. Filled thick arrows represent structural genes. The *amyE* integration site is represented by green boxes and the *amyE* promoter (P_{amyE}) and xylose-inducible promoter (P_{xyl}) represented by a thick, angled arrows. The arrows beneath the genes indicate the location and the orientation of the primers, while thick lines indicate their expected PCR products. (B) Gel separated PCR products of the diagnostic PCR verifying the correct construction of KG203. **Lane M**: 1 kb molecular ladder (Promega); **Lanes 1-6**: PCR products amplified with following sets of primers: (1) **Lane 1**: *secY2*_fwd & *map*_rev, expected product size 2871 bp (2) **Lane 2**: P_{xyl} _fwd and *secY2*_rev, expected product size 1515 bp; (3) **Lane 3**: P_{xyl} _fwd and *map*_rev, expected product size 2981 bp; (4) **Lane 4**: *secY2*_fwd & *amyE*_rev, expected product size 3337 bp; (5) **Lane 5**: *adk*_fwd & *amyE*_rev, expected product size 1934 bp; (6) **Lane 6**: P_{xyl} _fwd and *amyE*_rev, expected product size 3447 bp.

Strain KG203 was subsequently transformed with pMAP65 (generating strain KG204). pMAP65 encodes an additional copy of *lacI* repressor gene that reduces the non-induced level of expression of the pMUTIN4-derived P_{spac} promoter. KG204 was then transformed with pKG101, selecting 13 transformants of KG205 on LB agar supplemented with erythromycin, lincomycin, chloramphenicol with inducers IPTG and

xylose. Diagnostic PCR was used to determine whether pKG101 had integrated into the *secY* locus of KG205. However, this transformant failed to generate the PCR amplicons expected for the integrant (Figure 5.6). Specifically, a PCR product was generated with primers Pmut_fwd and Pmut_rev, which are located upstream and downstream of the cloned gene, respectively, in pMUTIN4. Following pMUTIN4 integration into the chromosome these primers should become oriented away from each other, so no PCR product should have been generated with this primer pair. These results suggested that the integration of pKG101 did not occur correctly and consequently that *secY* was not put under control of Pspac (IPTG-inducible) promoter in KG205.

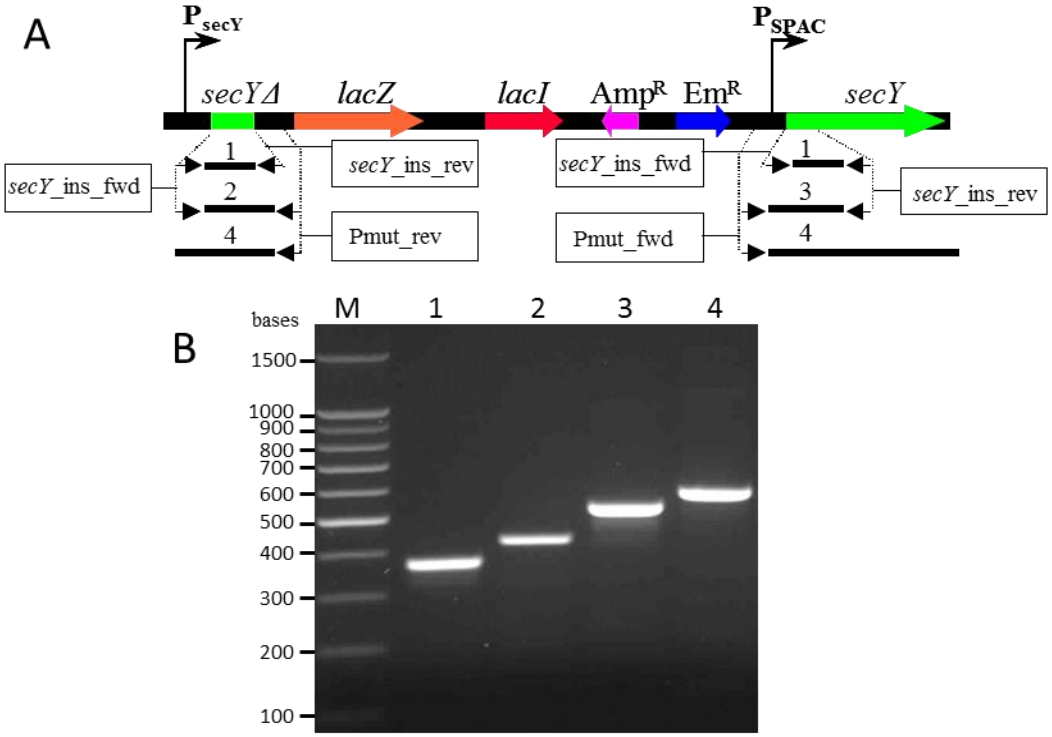

Figure 5.6: Diagnostic PCR to confirm the presence and orientation of *secY* in KG205. (A) Schematic representation *secY* region of KG205 after integration of pMUT- *secY*-F. Filled arrows represent structural genes: the *lacZ* reporter gene, *lacI*, *secY*, ampicillin (Amp^R), erythromycin (Em^R) resistance genes. *secYΔ* is 5'-end of *secY*. Promoters (P_{secY} and P_{SPAC}) are marked with a thick, angled arrow. The arrows below the genes indicate the location and orientation of the oligonucleotide primers, whilst the bold lines indicate their expected PCR products. The numbers above the bold lines correspond to the lanes of the agarose electrophoresis gels shown in panels B. (B) Gel separated PCR products of the diagnostic PCR verifying the correct construction of KG205. **Lanes M**: 100 bp molecular marker (Promega); **Lanes 1-4**: amplified with following sets of primers: **Lane 1**: *secY*_ins_fwd & *secY*_ins_rev, expected product size 370 bp; **Lane 2:** *secY*_ins_fwd and Pmut_rev, expected product size 430 bp; **Lane 3**: Pmut_fwd and *secY*_ins_rev, expected product size 514 bp; **Lane 4**: Pmut_fwd & Pmut_rev, no product expected in KG205.

In spite of the apparent failure to integrate pKG101 correctly into the chromosome, the dependency of KG205 strain on the inducers IPTG and xylose was tested. Two clones KG205-1 and KG205-12 were inoculated into LB broth (25 ml) containing erythromycin, lincomycin, chloramphenicol, kanamycin, IPTG and xylose and their cultures were incubated for five to six hours until it reached exponential phase. Following three washings with LB broth without any supplements, serial dilutions of the culture were plated on LB agar with erythromycin, lincomycin, kanamycin, chloramphenicol and (1) without inducers (IPTG or xylose), (2) with IPTG, (3) with xylose. Both clones were dependent on xylose, forming big colonies on the plates with xylose (colonies of KG205-1 are shown on Figure 5.7), but colony count from a xylose plate of the clone 1 was 10-fold higher on agar with xylose than on the agar with IPTG or without any inducer, while bacterial count of the clone 12 didn't exhibit a significant difference (Figure 5.8).

Figure 5.7: Growth of xylose-dependant clone KG205-1 on the LB agar with erythromycin and lincomycin and without inducers (10^{-4} dilution shown) or with inducers (xylose (10^{-6} dilution shown) or IPTG (10^{-4} dilution shown)).

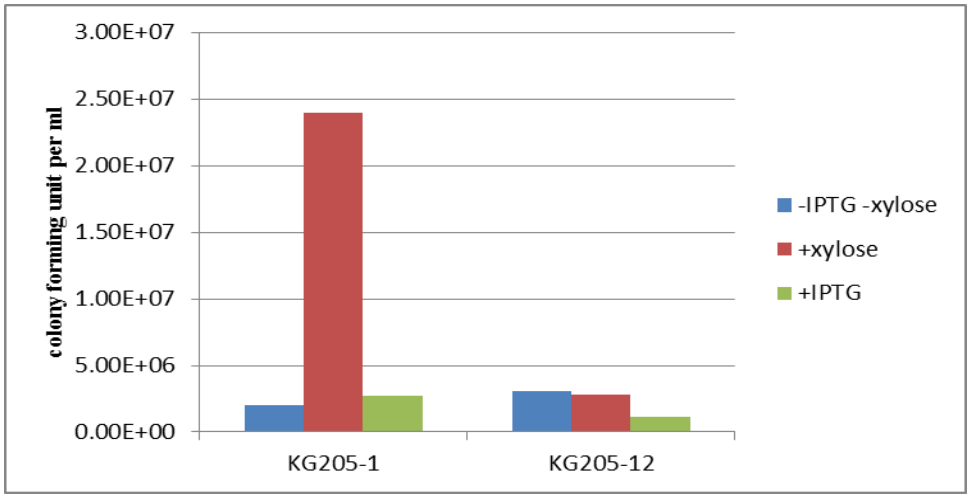

Figure 5.8: Determination of the dependency of KG205 on xylose. The strain was grown on LB agar supplemented with: (1) neither IPTG nor xylose, (2) 1 mM IPTG, (3) 1 % (w/v) xylose.

However, when colonies of clones 1 and 12 growing on a xylose plate were subsequently restreaked onto an LB agar plate with or without inducers, then both clones grew only in the presence of xylose (Figure 5.9).

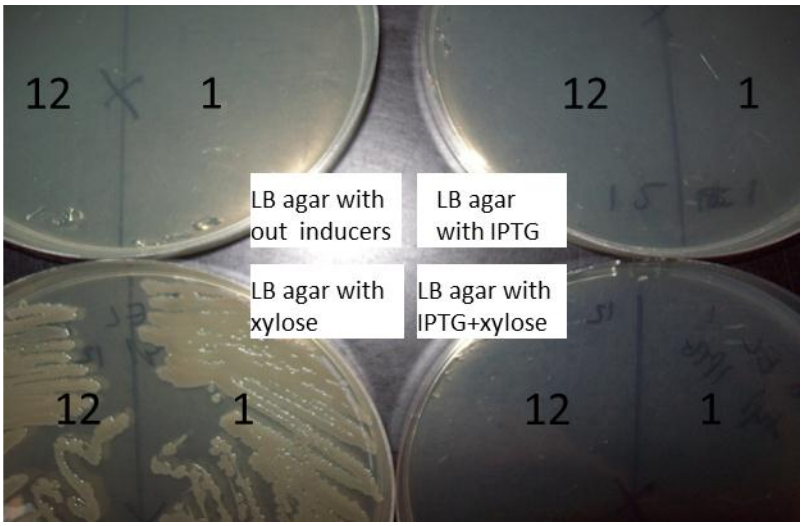

Figure 5.9: Growth of xylose-dependant KG205-1 and KG205-12 restreaked from dilution plate with xylose onto the LB agar with erythromycin and lincomycin and without or with inducers (xylose and/or IPTG).

This suggests that the original isolate was unstable and subject to a rearrangement potentially involving the inactivation of some or all of the native *secY/adk/map* genes, thus requiring these genes to be expressed from xylose-dependent promoter for its viability. However, KG205-1 and KG205-12, from the LB agar with xylose shown on the Figures 5.7 and 5.9 were not able to grow in LB broth with xylose, meaning that they lose their xylose-dependence in the liquid culture. Due to instability of KG205-1 and KG205-12, further analysis of the mutant was not possible and this part of the project was discontinued.

5.2 The specificity of Sap and EA1 secretion is lost in *B. subtilis*

B. anthracis encodes two homologues of *B. subtilis* SecA, namely SecA1 and SecA2. Analysis has shown that *B. anthracis* SecA1 but not SecA2 can functionally complement *B. subtilis* SecA. The deletion of *secA2* in *B. anthracis* does not affect bacterial growth, but has a severe negative impact on the secretion of the two surface-associated proteins, *i.e.* Sap and EA1. In the light of these findings, it was predicted that SecA2 functions to export a subset of proteins, namely Sap and EA1, which are either inefficiently exported *via* SecA1 or encode a specific SecA1 avoidance mechanism. Bioinformatic analysis revealed that the signal peptides of Sap and EA1 are almost identical, differing only by a single conservative substitution, suggesting that the signal peptides might be involved in conferring SecA2 specificity to its substrates (Pohl *et al.*, unpublished). Secondly, we found that SecH protein enhances SecA2-mediated secretion of Sap and EA1. To investigate if signal peptide conferred SecA2 specificity to its substrates and to get more information on participation of SecH in facilitating of secretion of those substrates, the *B. subtilis* genome was engineered to produce Sap and EA1 as well as other elements of *B. anthracis* translocation system. Firstly, the ability of *B. subtilis* SecA (*Bsu* SecA) and *B. anthracis* SecA1 (*Ban* SecA1) to complement *B. anthracis* SecA2 (*Ban* SecA2) was analysed. Then, it was investigated how secretion of Sap and EA1 is influenced, in SecA and SecA1 backgrounds, by the presence of SecA2 and SecH. The common problem in *B. subtilis* is degradation of secretory proteins by the quality control proteases, once they have been translocate (Wong S-L., 1995). That is why, *B. subtilis* WB600 (strain deficient in six quality control proteases) was used as a host for the production of Sap and EA1 to decrease the risk of them being degraded.

Analysis of complementation of *Ban* SecA2 by *Bsu* SecA

Previous studies had shown that PrsAB was essential for the secretion of both Sap and EA1 in *B. subtilis* (Pohl *et al.*, unpublished), and therefore two xylose-dependent operons (*prsAB*, *sap* and *prsAB*, *eag*) were selected for these studies. The operons were introduced into *B. subtilis* 168 via integration vector pJPRI, which is a double crossover replacement vector that is targeted to the *amyE* locus. Upon transformation and selection for chloramphenicol resistance, a double crossover recombination at the *amyE* locus placed the *prsAB-sap* and *prsAB-eag* under control of the xylose-dependent promoter, resulting in two strains AB06Jsap1 (*amyE*::*prsAB-sap*) (Figure 5.10A) and AB06Jeag1 (*amyE*::*prsAB-eag*) (Figure 5.10B).

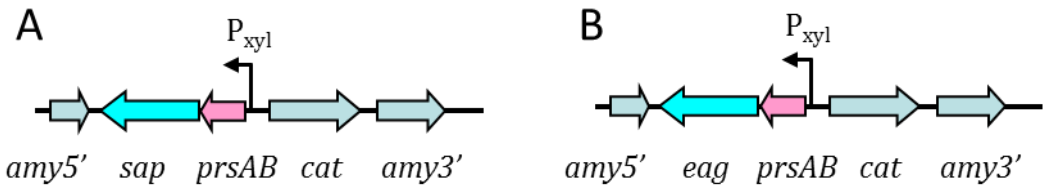

Figure 5.10: Genomic map of *amyE* locus of (A) AB06Jsap1 and (B) AB06Jeag1

SDS-PAGE analysis of proteins of the supernatant fraction showed, that when the expression of either *prsAB, eag* or *prsAB, sap* was induced in *B. subtilis* with xylose two additional bands were observed compared to the uninduced control (Figure 5.11). The bands had apparent molecular size of ~ 90 kDa and ~ 125 kDa. Since the estimated sizes of the mature Sap and EA1 proteins are 86.6 kDa and 91.4 kDa, respectively, the lower of the two bands (~ 90 kDa) was expected to represent the mature versions of these proteins. The question arises as to the nature of the bands at ~ 125 kDa. We considered the possibility that the lower (~ 90 kD) band corresponded to an unmodified version of Sap or EA1, but that the upper band was the result of translational read-through from the upstream PrsAB gene, resulting in a fusion protein of Sap or EA1 with PrsAB. Since PrsAB is 34 kDa in size, this would generate a fusion protein of approximately the right size, namely ~ 120-125 kDa. However, the sequencing analysis of both proteins showed that they are translated in different reading frames and there is a single STOP codon between the two - sequencing of *prsAB-eag* junction in AB06Jeag1 strain showed that the STOP codon of *prsAB* was intact (Figure 5.12).

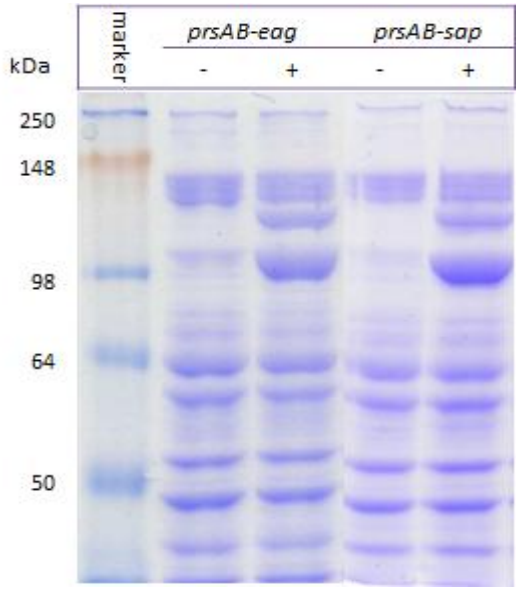

Figure 5.11: Secretion of EA1 and Sap by *Bsu* SecA in *B. subtilis*. '-' = no xylose; '+' = xylose addition (1% (w/v)). *prsAB-eag*: *prsAB* and *eag* genes; *prsAB-eag*: *prsAB* and *eag* genes. In the xylose induced samples, two additional bands of apparent molecular size of ~ 90 kDa and ~ 125 kDa are visible.

We therefore excised the representative ~ 125 kDa bands from the gel shown on the Figure 5.11 and subjected them to MALDI-TOF-MS analysis. In the case of the band corresponding to the strain expressing *eag*, the protein was identified as EA1 (Table 6.1), while the band corresponding to the strain expressing *sap*, the protein was identified as Sap (Table 5.2). We re-analysed the mass spectrometry data by removing the peaks associated with either Sap or EA1 and reanalysing the data using the MASCOT software. None of the remaining peptides matched peptides from PrsAB, indicating that that a PrsAB-Sap/EA1 fusion was unlikely to account for the less mobile version of these S-layer proteins. Following this analysis, the most likely explanation for the two Sap/EA1 band that occur exclusively in *B. subtilis* is that they are due to their folding into structures that run aberrantly in SDS-PAGE gels. If this structure retards their motility in SDS-PAGE, then the larger bands might represent full-length copies of the respective proteins, while the smaller bands may represent a degradation product. Therefore the analysis of proteins in the culture supernatant by 2D-PAGE was performed (by Dr. Susanne Pohl) (Figures 5.13 and 5.14).

```
prsAB-eag       TCTCCGCAAGGAAATTAAAAAAGCACAACCTTATTTTTTCAGATAAGGTTGTGCTTGGAT
300
sequenced       TCTCCGCAAGGAAATTAAAAAAGCACAACCTTATTTTTTCAGATAAGGTTGTGCTTGGAT
128
                ************************************************************

prsAB-eag       CCTAGCATATTCCTGAAGGAGGAAATTTATAAAATGGCAAAGACTAACTCTTACAAAAAA
360
sequenced       CCTAGCATATTCCTGAAGGAGGAAATTTATAAAATGGCAAAGACTAACTCTTACAAAAAA
188
                ************************************************************

prsAB-eag       GTAATCGCAGGTACAATGACAGCAGCAATGGTAGCAGGTATTGTATCTCCAGTAGCAGCA
420
sequenced       GTAATCGCAGGTACAATGACAGCAGCAATGGTAGCAGGTATTGTATCTCCAGTAGCAGCA
248
                ************************************************************

prsAB-eag       GCAGGTAAATCATTCCCAGACGTTCCAGCTGGACATTGGGCAGAAGGTTCTATTAATTAC
480
sequenced       GCAGGTAAATCATTCCCAGACGTTCCAGCTGGACATTGGGCAGAAGGTTCTATTAATTAC
308
                ************************************************************

prsAB-eag       TTAGTAGATAAAGGTGCAATTACAGGTAAGCCAGACGGTACATATGGTCCAACCGAATCA
540
sequenced       TTAGTAGATAAAGGTGCAATTACAGGTAAGCCAGACGGTACATATGGTCCAACCGAATCA
368
                ************************************************************
```

Figure 5.12: Alignment of sequences of the sequenced *prsAB-eag* junction in AB06Jeag1 with the template sequence. STOP codon of *prsAB* is highlighted in orange; START codon of *eag* is highlighted in green.

Table 5.1: Peptide mass fingerprinting data summary for EA1 taken from Mascot search results. Method of analysis: MALDI-TOF-MS.

Obs	Mr(expt)	Mr(calc)	ppm	Miss	Score	Expect	Peptide	Identification
1206.6589	1205.6516	1205.5677	69.6	0	144	2.4e-10	R.NGDAVFNAGDVK.L	**EA1**
1336.7700	1335.7627	1335.6783	63.2	1			K.SGAEQGKLYLDR.N	
1421.6996	1420.6923	1420.7198	19.35	1			K.LAVEKLTFDDDR.A	
1667.9330	1666.9257	1666.8315	56.5	1			K.LTFDDDRAGQAIAFK.L	
1766.0165	1765.0093	1764.9046	59.3	0			K.SVNFKPVQTENFVEK.K	
1771.9740	1770.9667	1770.8537	63.8	0			K.GNADVEYLNLANHDVK.F	
1857.9483	1856.9411	1856.8316	59.0	0			R.VYSDPENLEGYEVESK.N	
1867.0236	1866.0164	1865.9272	47.8	1			K.LYLDRNGDAVFNAGDVK.L	
1894.1252	1893.1179	1892.9996	62.5	1			K.SVNFKPVQTENFVEKK.I	
1919.1439	1918.1366	1918.0160	62.9	1			K.LSGKDFALNSQNLVVGEK.A	
1997.0877	1996.0804	1995.9902	45.2	1			K.NFELVSKVGQYGQSPDTK.L	
2063.1679	062.1607	2062.0430	57.0	0			K.TGVVAEGGLDVVTTDSGSIGTK.T	
2371.3056	2370.2983	2370.1451	64.6	1			K.LNDEKGNADVEYLNLANHDVK.F	
2480.2745	2479.2673	2479.1027	66.4	1			K.YTSDRVYSDPENLEGYEVESK.N	
2497.3497	2496.3424	2496.1769	66.3	0			K.FVANNLDGSPANIFEGGEATSTTGK.L	
2527.4577	2526.4504	2526.2643	73.7	0			K.TLPVTFVTTDQYGDPFGANTAAIK.E	
3093.8402	3092.8330	3092.6070	73.0	1			K.TLPVTFVTTDQYGDPFGANTAAIKEVLPK.T	

Table 5.2: Peptide mass fingerprinting data summary for Sap taken from Mascot search results. Method of analysis: MALDI-TOF-MS.

Obs	Mr(expt)	Mr(calc)	ppm	Miss	Score	Expect	Peptide	Identification
977.5432	976.5359	976.5342	1.79	1	194	2.7e-15	K.FEVRGLEK.E	**Sap**
990.5172	989.5099	989.5182	-8.33	0			K.APVLDQYGK.E	
991.5350	990.5277	990.5386	-10.98	0			K.EFTAPVTVK.V	
1135.5936	1134.5864	1134.5921	-5.04	0			K.TVEIEAFAQK.A	
1217.6684	1216.6611	1216.6816	-16.82	1			K.VKAPVLDQYGK.E	
1264.6309	1263.6236	1263.6281	-3.58	1			K.GMFEPGKELTR.A	
1280.6040	1279.5968	1279.6231	-20.55	1			K.GMFEPGKELTR.A + Oxidation (M)	
1350.6820	1349.6747	1349.6979	-17.22	1			K.FKDLETLNWGK.E	
1461.6916	1460.6844	1460.7008	-11.26	1			K.GTGNGFEPNGKIDR.V	
1495.7010	1494.6937	1494.7202	-17.72	1			K.ELDKYVTEENQK.N	
1516.8461	1515.8389	1515.8660	-17.94	1			K.ATLALELKAPGAFSK.F	
1545.7830	1544.7757	1544.7947	-12.31	1			K.AGVIKGTGNGFEPNGK.I	
1694.7897	1693.7824	1693.8410	-34.60	0			K.VEYESLNTEVAVVDK.A	
1783.9021	1782.8948	1782.9437	-27.42	1			R.VSMASLLVEAYKLDTK.V + Oxidation (M)	
1963.0166	1962.0093	1962.0462	-18.81	1			K.APVLDQYGKEFTAPVTVK.V	
2161.1017	2160.0945	2160.1426	-22.29	0			K.ELVLNAAGQEAGNYTVVLTAK.S	
2190.1572	2189.1499	2189.1579	-3.66	1			K.GLAVEFTSTSLKEVAPNADLK.A	
2407.2185	2406.2112	2406.1989	5.13	0			K.TIEMADQTVVADEPTALQFTVK.D	
2416.1287	2415.1214	2415.1747	-22.07	0			K.TFPDVPADHWGIDSINYLVEK.G	
2444.1758	2443.1685	2443.2191	-20.69	0			K.EVDATDAQVTVQNNSVITVGQGAK.A	
2479.1653	2478.1580	2478.2238	-26.56	0			K.ATVSNVEFVSADTNVVAENGTVGAK.G	
2556.2134	2555.2061	2555.2332	-10.63	0			K.DAKPSFADSQGQWYTPFIAAVEK.A	
2665.3592	2664.3519	2664.4122	-22.63	1			K.YVNKELVLNAAGQEAGNYTVVLTAK.S	
2688.3193	2687.3120	2687.3079	1.53	1			K.VYEGDNAYVQVELKDQFNAVTTGK.V	

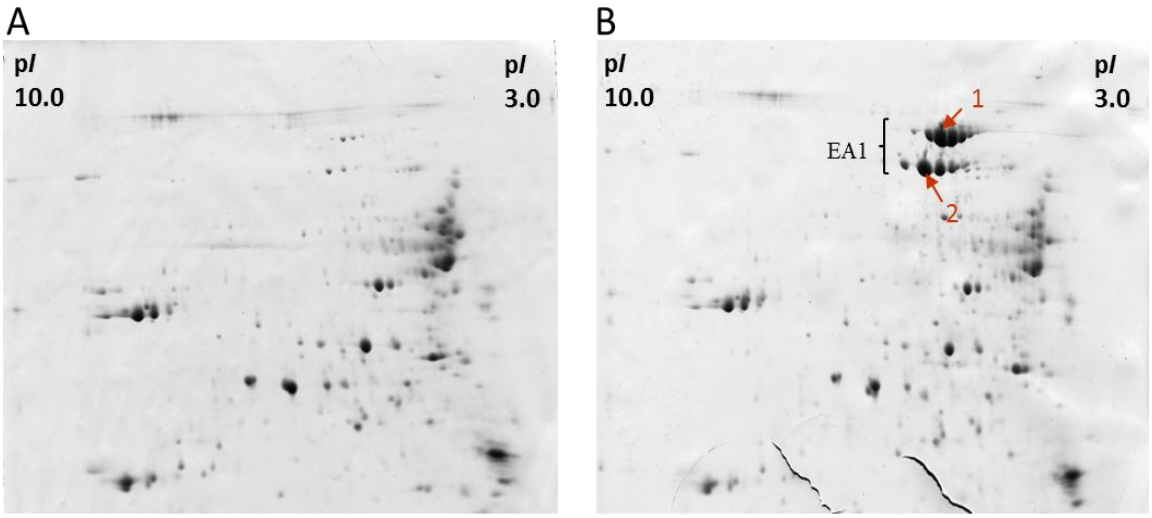

Figure 5.13: 2D PAGE analysis of the extracellular proteins of *B. subtilis amyE*:: *prsAB_eag* (AB06Jeag1) isolated from (A) non-induced sample and (B) induced sample (xylose 1% w/v). EA1 is visible as two bands of spot clusters. Spots 1 and 2 were excised from the gel and analysed by mass spectroscopy (MALDI-TOF-MS).

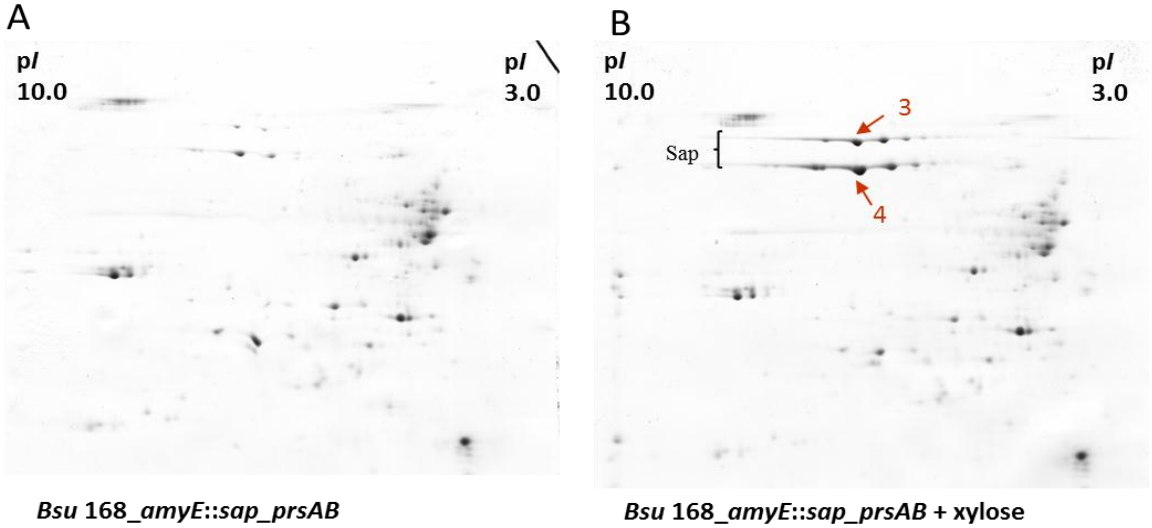

Figure 5.14: 2D PAGE analysis of the extracellular proteins of *B. subtilis 168 amyE*:: *prsAB_sap* (AB06Jsap1) isolated from (A) non-induced sample and(B) induces sample (xylose 1% w/v). Sap is visible as two bands of spot clusters. Spots 3 and 4 were excised from the gel and analysed by mass spectroscopy (MALDI-TOF-MS).

The induction of *sap* and *eag* expression together with *prsAB* results in the appearance of two bands consisting of clusters of spots. One spot of each band (upper and lower) was analysed by mass spectroscopy (MALDI-TOF-MS). Spot 1 of the upper band on the Figure 5.13B and spot 3 of the upper band on the Figure 5.14B were identified as full length, mature proteins of EA1 and Sap, respectively. The presence of the full length proteins was based on the detection by mass spectroscopy of peptides through the entire proteins, apart from the signal peptide (first thirty amino acids) (Figures 5.15 and 5.17), which is absent from the mature, secreted protein. Spot 2, the lower band on the

Figure 5.13B and spot 4 of the lower band on the Figure 5.14B were identified as truncated proteins of EA1 and Sap, respectively. The N-terminal region of EA1 and Sap appears to be missing as the mass spectra obtained from these proteins generally lacked peptides corresponding to the first 200 amino acids (Figures 5.16 and 5.18). In the case of the spot 2 of the lower band of Sap (spot 4) a single mass spectroscopic peak corresponds in size to a single peptide within the first 200 residues. Since this was the only peptide that was putatively identified within this region, it was not considered significant. Overall, the mass spectroscopic analysis indicated that the higher molecular mass (upper) bands of Sap and EA1 observed in the supernatant fraction of *B. subtilis* were likely to correspond to the mature protein, which migrate aberrantly in SDS-PAGE gels, possibly due to the fact that they are structural protein that are not able to form globular-like structures in the presence of SDS and mercaptoethanol. The lower molecular band appears to be consistent with degradation products of mature EA1 and Sap proteins that are missing approximately 200 residues of their N-termini. This is likely to be the result of a proteolytic cleavage of EA1 and Sap occurring in *B. subtilis* but not their native host, *B. anthracis*. This is consistent with the common observation that heterologous proteins are degraded by quality control proteases (Wong S-L., 1995). The strain WB600 used here is deficient in six quality control proteases (Wu *et al.*, 1991), but this strain still exhibits some proteoltyic activity. Previously, it was observed that when endo-beta-1,4-glucanase was produced in *B. subtilis* WB600, two its forms could be found: the intact one and the partially cleaved one. However, when endo-beta-1,4-glucanase was produced in *B. subtilis* WB700, which is deficient in seven proteases, then the enzyme was almost exclusively found in the intact form (Yang *et al.*, 2004).
So, the occurrence of truncated form of Sap and EA1 results from the proteolytic activity remaining in the WB600 strain.

In conclusion, *Bsu* SecA can replace *Ban* SecA2 in respect to secretion of Sap and EA1 meaning that SecA2-related specificity of secretion of those proteins is lost in *B. subtilis.*

```
  1 MAKTNSYKKV IAGTMTAAMV AGIVSPVAAA GKSFPDVPAG HWAEGSINYL
 51 VDKGAITGKP DGTYGPTESI DRASAAVIFT KILNLPVDEN AQPSFKDAKN
101 IWSSKYIAAV EKAGVVKGDG KENFYPEGKI DRASFASMLV SAYNLKDKVN
151 GELVTTFEDL LDHWGEEKAN ILINLGISVG TGGKWEPNKS VSRAEAAQFI
201 ALTDKKYGKK DNAQAYVTDV KVSEPTKLTL TGTGLDKLSA DDVTLEGDKA
251 VAIEASTDGT SAVVTLGGKV APNKDLTVKV KNQSFVTKFV YEVKKLAVEK
301 LTFDDDRAGQ AIAFKLNDEK GNADVEYLNL ANHDVKFVAN NLDGSPANIF
351 EGGEATSTTG KLAVGIKQGD YKVEVQVTKR GGLTVSNTGI ITVKNLDTPA
401 SAIKNVVFAL DADNDGVVNY GSKLSGKDFA LNSQNLVVGE KASLNKLVAT
451 IAGEDKVVDP GSISIKSSNH GIISVVNNYI TAEAAGEATL TIKVGDVTKD
501 VKFKVTTDSR KLVSVKANPD KLQVVQNKTL PVTFVTTDQY GDPFGANTAA
551 IKEVLPKTGV VAEGGLDVVT TDSGSIGTKT IGVTGNDVGE GTVHFQNGNG
601 ATLGSLYVNV TEGNVAFKNF ELVSKVGQYG QSPDTKLDLN VSTTVEYQLS
651 KYTSDRVYSD PENLEGYEVE SKNLAVADAK IVGNKVVVTG KTPGKVDIHL
701 TKNGATAGKA TVEIVQETIA IKSVNFKPVQ TENFVEKKIN IGTVLELEKS
751 NLDDIVKGIN LTKETQHKVR VVKSGAEQGK LYLDRNGDAV FNAGDVKLGD
801 VTVSQTSDSA LPNFKADLYD TLTTKYTDKG TLVFKVLKDK DVITSEIGSQ
851 AVHVNVLNNP NL
```

Figure 5.15: The sequence of EA1 (including signal peptide in bold), showing (red) the peptides identified in spot 1 (Figure 5.13B) by MALDI-TOF-MS.

```
  1 MAKTNSYKKV IAGTMTAAMV AGIVSPVAAA GKSFPDVPAG HWAEGSINYL
 51 VDKGAITGKP DGTYGPTESI DRASAAVIFT KILNLPVDEN AQPSFKDAKN
101 IWSSKYIAAV EKAGVVKGDG KENFYPEGKI DRASFASMLV SAYNLKDKVN
151 GELVTTFEDL LDHWGEEKAN ILINLGISVG TGGKWEPNKS VSRAEAAQFI
201 ALTDKKYGKK DNAQAYVTDV KVSEPTKLTL TGTGLDKLSA DDVTLEGDKA
251 VAIEASTDGT SAVVTLGGKV APNKDLTVKV KNQSFVTKFV YEVKKLAVEK
301 LTFDDDRAGQ AIAFKLNDEK GNADVEYLNL ANHDVKFVAN NLDGSPANIF
351 EGGEATSTTG KLAVGIKQGD YKVEVQVTKR GGLTVSNTGI ITVKNLDTPA
401 SAIKNVVFAL DADNDGVVNY GSKLSGKDFA LNSQNLVVGE KASLNKLVAT
451 IAGEDKVVDP GSISIKSSNH GIISVVNNYI TAEAAGEATL TIKVGDVTKD
501 VKFKVTTDSR KLVSVKANPD KLQVVQNKTL PVTFVTTDQY GDPFGANTAA
551 IKEVLPKTGV VAEGGLDVVT TDSGSIGTKT IGVTGNDVGE GTVHFQNGNG
601 ATLGSLYVNV TEGNVAFKNF ELVSKVGQYG QSPDTKLDLN VSTTVEYQLS
651 KYTSDRVYSD PENLEGYEVE SKNLAVADAK IVGNKVVVTG KTPGKVDIHL
701 TKNGATAGKA TVEIVQETIA IKSVNFKPVQ TENFVEKKIN IGTVLELEKS
751 NLDDIVKGIN LTKETQHKVR VVKSGAEQGK LYLDRNGDAV FNAGDVKLGD
801 VTVSQTSDSA LPNFKADLYD TLTTKYTDKG TLVFKVLKDK DVITSEIGSQ
851 AVHVNVLNNP NL
```

Figure 5.16: The sequence of EA1 (including signal peptide in bold), showing (red) the peptides identified in spot 2 (Figure 5.13B) by MALDI-TOF-MS.

```
  1 MAKTNSYKKV IAGTMTAAMV AGVVSPVAAA GKTFPDVPAD HWGIDSINYL
 51 VEKGAVKGND KGMFEPGKEL TRAEAATMMA QILNLPIDKD AKPSFADSQG
101 QWYTPFIAAV EKAGVIKGTG NGFEPNGKID RVSMASLLVE AYKLDTKVNG
151 TPATKFKDLE TLNWGKEKAN ILVELGISVG TGDQWEPKKT VTKAEAAQFI
201 AKTDKQFGTE AAKVESAKAV TTQKVEVKFS KAVEKLTKED IKVTNKANND
251 KVLVKEVTLS EDKKSATVEL YSNLAAKQTY TVDVNKVGKT EVAVGSLEAK
301 TIEMADQTVV ADEPTALQFT VKDENGTEVV SPEGIEFVTP AAEKINAKGE
351 ITLAKGTSTT VKAVYKKDGK VVAESKEVKV SAEGAAVASI SNWTVAEQNK
401 ADFTSKDFKQ NNKVYEGDNA YVQVELKDQF NAVTTGKVEY ESLNTEVAVV
451 DKATGKVTVL SAGKAPVKVT VKDSKGKELV SKTVEIEAFA QKAMKEIKLE
501 KTNVALSTKD VTDLKVKAPV LDQYGKEFTA PVTVKVLDKD GKELKEQKLE
551 AKYVNKELVL NAAGQEAGNY TVVLTAKSGE KEAKATLALE LKAPGAFSKF
601 EVRGLEKELD KYVTEENQKN AMTVSVLPVD ANGLVLKGAE AAELKVTTTN
651 KEGKEVDATD AQVTVQNNSV ITVGQGAKAG ETYKVTVVLD GKLITTHSFK
701 VVDTAPTAKG LAVEFTSTSL KEVAPNADLK AALLNILSVD GVPATTAKAT
751 VSNVEFVSAD TNVVAENGTV GAKGATSIYV KNLTVVKDGK EQKVEFDKAV
801 QVAVSIKEAK PATK
```

Figure 5.17: The sequence of Sap (including signal peptide in bold), showing (red) the peptides identified in spot 3 (Figure 5.14B) by MALDI-TOF-MS.

```
  1 MAKTNSYKKV IAGTMTAAMV AGVVSPVAAA GKTFPDVPAD HWGIDSINYL
 51 VEKGAVKGND KGMFEPGKEL TRAEAATMMA QILNLPIDKD AKPSFADSQG
101 QWYTPFIAAV EKAGVIKGTG NGFEPNGKID RVSMASLLVE AYKLDTKVNG
151 TPATKFKDLE TLNWGKEKAN ILVELGISVG TGDQWEPKKT VTKAEAAQFI
201 AKTDKQFGTE AAKVESAKAV TTQKVEVKFS KAVEKLTKED IKVTNKANND
251 KVLVKEVTLS EDKKSATVEL YSNLAAKQTY TVDVNKVGKT EVAVGSLEAK
301 TIEMADQTVV ADEPTALQFT VKDENGTEVV SPEGIEFVTP AAEKINAKGE
351 ITLAKGTSTT VKAVYKKDGK VVAESKEVKV SAEGAAVASI SNWTVAEQNK
401 ADFTSKDFKQ NNKVYEGDNA YVQVELKDQF NAVTTGKVEY ESLNTEVAVV
451 DKATGKVTVL SAGKAPVKVT VKDSKGKELV SKTVEIEAFA QKAMKEIKLE
501 KTNVALSTKD VTDLKVKAPV LDQYGKEFTA PVTVKVLDKD GKELKEQKLE
551 AKYVNKELVL NAAGQEAGNY TVVLTAKSGE KEAKATLALE LKAPGAFSKF
601 EVRGLEKELD KYVTEENQKN AMTVSVLPVD ANGLVLKGAE AAELKVTTTN
651 KEGKEVDATD AQVTVQNNSV ITVGQGAKAG ETYKVTVVLD GKLITTHSFK
701 VVDTAPTAKG LAVEFTSTSL KEVAPNADLK AALLNILSVD GVPATTAKAT
751 VSNVEFVSAD TNVVAENGTV GAKGATSIYV KNLTVVKDGK EQKVEFDKAV
801 QVAVSIKEAK PATK
```

Figure 5.18: The sequence of Sap (including signal peptide in bold), showing (red) the peptides identified in spot 4 (Figure 5.14B) by MALDI-TOF-MS.

Analysis of complementation of *Ban* SecA2 by *Ban* SecA1

To gain new insights about SecA2 substrate recognition, Sap and EA1 secretion by *Ban* SecA1 was also investigated in *B. subtilis*. The strain of *B. subtilis* 168 was constructed in which *Bsu secA* was replaced with *Ban secA1*. To replace *Bsu secA* with *Ban secA1*, a gene replacement approach was used. The kanamycin resistance gene was cloned together with *secA1* into vector pGEM in such a way that both the kanamycin resistance and *secA1* genes were placed between flanking regions containing upstream and downstream of *Bsu secA*. Introduction of the recombinant plasmid into strains AB06Jsap1 (*amyE*::*prsAB-sap*) and AB06Jeag1 (*amyE*::*prsAB-eag*), followed by selection with kanamycin, resulted in isolation of clones of GQ32 (*secA*::*secA1*, *amyE*::*prsAB-eag*) and GQ34 (*secA*::*secA1*, *amyE*::*prsAB-sap*) in which the native *Bsu secA* had been replaced by *Ban secA1*. This was confirmed by diagnostic PCR. Unexpectedly, SecA1 facilitated effective secretion of both S-layer proteins, as when *eag* and *sap* expression was induced in *B. subtilis* by the addition of xylose, two additional and very prominent bands were observed with estimated sizes of ~ 90 kDa and ~ 125 kDa (Figure 5.19).

In conclusion, *Ban* SecA1, like *Bsu* SecA, can replace *Ban* SecA2 in respect to secretion of Sap and EA1 meaning that SecA2-related specificity of secretion of those proteins is lost in *B. subtilis.*

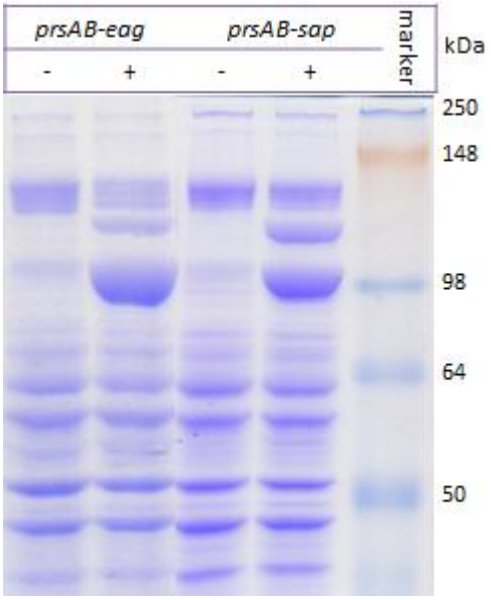

Figure 5.19: Secretion of EA1 and Sap by *Ban* SecA1 in GQ32 (*secA*::*secA1*, *amyE*::*prsAB-eag*) and GQ34 (*secA*::*secA1*, *amyE*::*prsAB-sap*) mutants of *B.subtilis*. '-' = no xylose; '+' = xylose addition (1% (w/v)). *prsAB-eag*: *prsAB* and *eag* genes; *prsAB-eag*: *prsAB* and *eag* genes. In the xylose induced samples, two additional bands of apparent molecular size of ~ 90 kDa and ~ 125 kDa are visible.

Analysis of Sap and EA1 secretion, in SecA and SecA1 backgrounds, in the presence of SecA2 and SecH

As SecH was shown to enhance the secretion of Sap and EA1 in *B. anthracis*, we considered the possibility that this protein was either involved in conferring SecA2 specificity to its substrates and/or preventing their secretion by SecA1. Consequently, *secH* and *secA2* was cloned into AB06Jeag1 (*amyE*::*prsAB-eag*) and GQ32 (*secA*::*secA1*, *amyE*::*prsAB-eag*) individually or in combination. The introduction of those genes was performed via integration of pAX01 which is double crossover replacement vector that is targeted to the *lacA* locus. Upon transformation and selection for erythromycin resistance, a double crossover recombination, at the *lacA* locus, placed the *secA2* and *secH* under control of the xylose-dependent promoter. As a result, the following strains were created: (1) GQ48 (*lacA*::*secA2*, *amyE*::*prsAB-eag*), (2) GQ72 (*lacA*::*secH*, *amyE*::*prsAB-eag*), (3) GQ69 (*lacA*::*secA2secH*, *amyE*::*prsAB-eag*), (4) GQ65 (*secA*::*secA1*, *lacA*::*secA2*, *amyE*::*prsAB-eag*), (5) GQ74 (*secA*::*secA1*, *lacA*::*secH*, *amyE*::*prsAB-eag*), (6) GQ75 (*secA*::*secA1*, *lacA*::*secA2-secH*, *amyE*::*prsAB-eag*) (Figure 5.20).

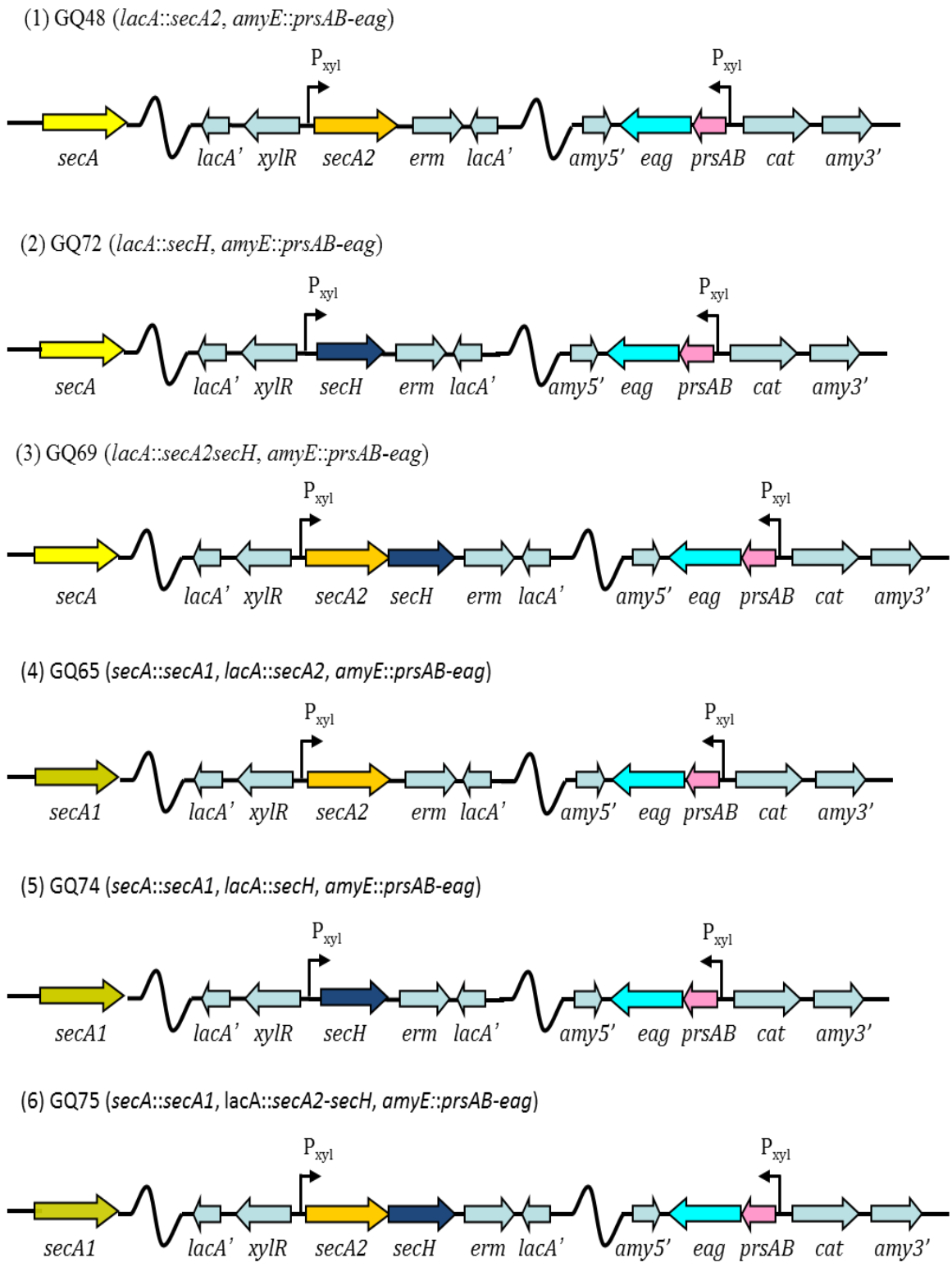

Figure 5.20: Genomic maps of *secA*/*secA1*, *amyE* and *lacA* loci of the constructed mutants: (1) GQ48, (2) GQ72, (3) GQ69, (4) GQ65, (5) GQ74 and (6) GQ75.

The strains: AB06Jeag1, GQ32, GQ48, GQ72, GQ69, GQ65, GQ74 and GQ75 were grown in nutrient medium and their extracellular protein profiles were compared to determine the influence of *Bsu* SecA, *Ban* SecA1, *Ban* SecA2 and SecH on EA1 secretion. The protein profiles of the *B. subtilis* mutants (Figures 5.21 and 5.22) indicate that:

(i) *Ban* SecA1 is more efficient at secreting EA1 than the native *Bsu* SecA.

(ii) SecA2 and SecH individually have a small inhibitory influence on the secretion of EA1 in strains encoding *Bsu* SecA, but together they increase the secretion of this protein.

(iii) When *Bsu* SecA is replaced with *Ban* SecA1, the presence of *either* SecA2 or SecH reduces the yield of EA1.

(iv) When *Bsu* SecA is replaced with *Ban* SecA1, the presence of *both* SecA2 and SecH restores the level of secretion of EA1 to that of SecA1 alone.

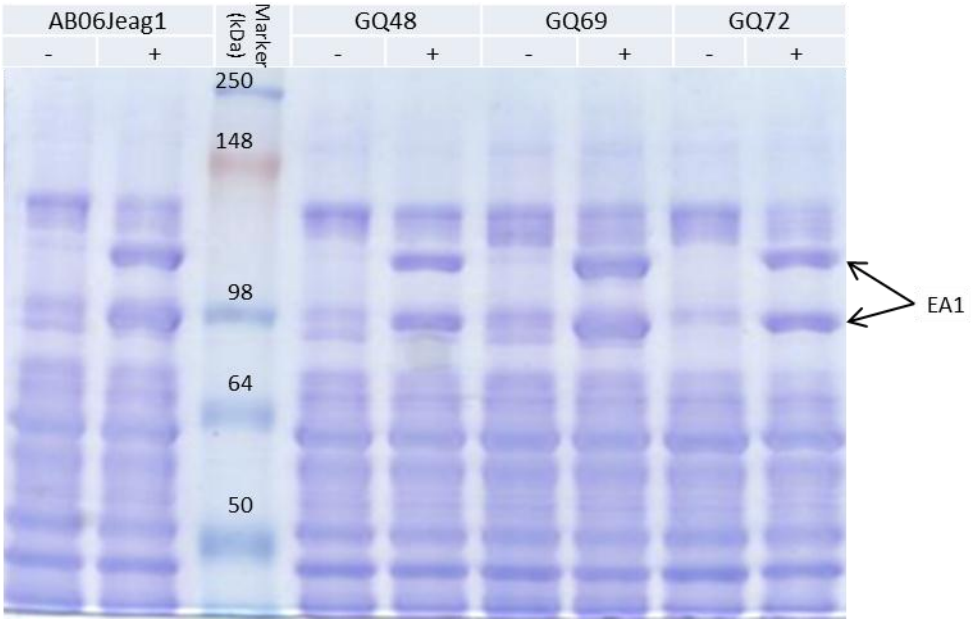

Figure 5.21: Secretion of EA1 with or without the presence of *Ban* SecA1, SecA2 and SecH in *B. subtilis* encoding its nature SecA. Four mutants (AB06Jeag1: *Bsu amyE*::*prsAB-eag*; GQ48: *lacA*::*secA2*, *amyE*::*prsAB-eag*; GQ69: *lacA*::*secA2secH*, *amyE*::*prsAB-eag*; GQ72: *lacA*::*secH*, *amyE*::*prsAB-eag*) have been tested. The presence of the various genes in the mutants is shown above the gel lanes. '-' = no xylose; '+' = xylose addition (1% (w/v)). In the induced samples (+), there are two additional bands of two sizes of approx. 90 kDa and 120-130 kDa visible corresponding to EA1. Marker: SeeBlue Plus Prestained Standard (Invitrogen).

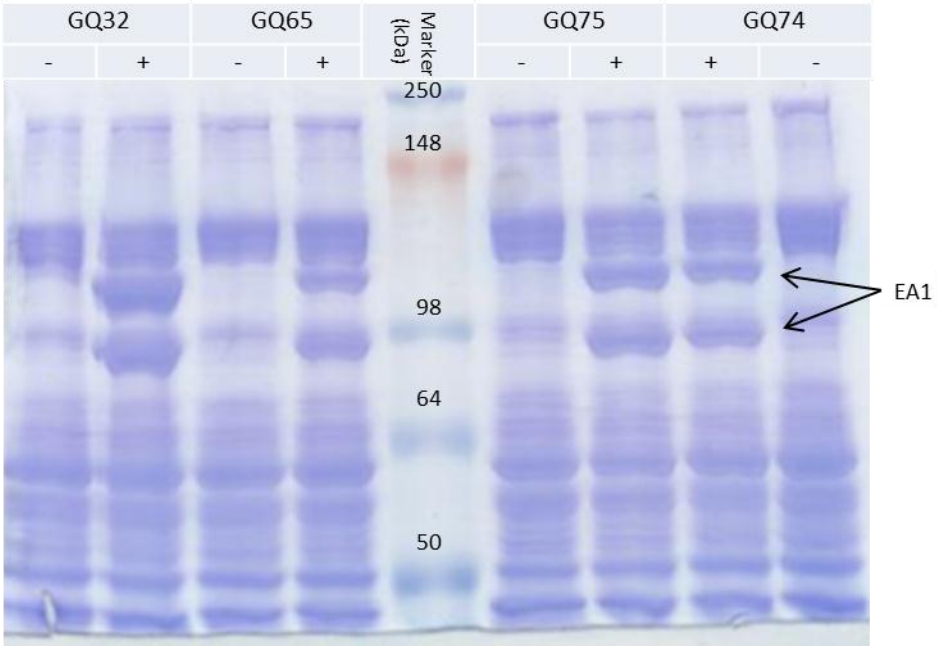

Figure 5.22: Secretion of EA1with participation of *Ban* SecA1, SecA2 and SecH in *B. subtilis secA::secA1*. Four mutants (GQ32: *Bsu secA*::*secA1*, amyE::*prsAB-eag*; GQ65: *Bsu secA*::*secA1*, *lacA*::*secA2*, amyE::*prsAB-eag*; GQ74: *Bsu secA*::*secA1*, *lacA*::*secH*, *amyE*::*prsAB-eag*; GQ75: *Bsu secA*::*secA1*, *lacA*::*secA2-secH*, *amyE*::*prsAB-eag*) have been tested. The presence of the various genes in the mutants is shown above the gel lanes. '-' = no xylose; '+' = xylose addition (1% (w/v)). In the induced samples (+), there are two additional bands of two sizes of approx. 90 kDa and 120-130 kDa visible corresponding to EA1. Marker: SeeBlue Plus Prestained Standard (Invitrogen).

Overall, the data in Figures 5.21 and 5.22 show that SecH moderately reduced the secretion of EA1 by Bsu SecA and Ban SecA1, and does not confer SecA2 the specificity to EA1 in *B. subtilis.* However, the results indicate that SecH and SecA2 interact in some way to influence the secretion of EA1 in *B. subtilis.*

5.3 Discussion

B. anthracis possesses two homologues of *B. subtilis* components of the secretory machine: (i) SecA (SecA1 and SecA2) and SecY (SecY1 and SecY2). The complementation analysis showed that *B. anthracis* SecA1, but not SecA2 can complement *B. subtilis* SecA (Pohl *et al.*, unpublished) Thus, *B. subtilis* SecA and *B. anthracis* SecA1 are functional homologues. *B. anthracis* SecA2 was shown to be involved in the secretion of S-layer proteins, Sap and EA1 (**Section 1.7**). This finding meant that there must be a factor or factors conferring the specificity of SecA2 for its substrates. Two possible specificity factors were identified: (1) the signal peptides of EA1 and Sap which are almost identical and (2) SecH protein which enhances the secretion of Sap and EA1 in *B. anthracis*.

When Sap and EA1 are expressed in *B. subtilis* strains 168, both are secreted at a significant concentrations provided PrsAB is present. This implies that *B. subtilis* SecA is able to facilitate this secretion. This prompted consider whether Ban SecA1 has a Sap and EA1 avoidance mechanism – that there is a factor preventing the interaction between Sap, EA1 and SecA1. Consequently, *B. subtilis* SecA was replaced with *B. anthracis* SecA1. Not only was Sap and EA1 secreted by these strains of *B. subtilis*, but secretion was enhanced. These results mean that SecA2-related specificity of Sap and EA1 secretion is lost in *B. subtilis*. Thus, this indicates that the signal peptide is not the factor responsible for conferring SecA2 specificity to its substrates in *B.anthracis*. However, we can not exclude that it contributes to that task by cooperating with some yet unknown factors.

Next, we looked at the effects of SecA2 and SecH, on Sap and EA1 secretion, in the *Bsu* SecA and *Ban* SecA1 backgrounds. When SecH was present in those backgrounds, the secretion of the S-layer proteins decreased. When both SecA2 and SecH were present, the secretion of Sap and EA1 was restored to the level observed in the mutant expressing *secA* or *secA1*, but not *secA2* and *secH*. These observations may suggest that SecH has a role in preventing the interaction between SecA1 and S-layer proteins and enhancing the interaction between SecA2 and those proteins. However, there must be an additional factor that is present in *B. anthracis* but not *B. subtilis*, which ensures that the secretion of Sap and EA1 is dependent on SecA2 but not on SecA1.

This project attempted also to determine whether *B. anthracis* SecY2 could complement SecY of *B. subtilis*. SecY2 is not essential for viability in *B. anthracis* and it may function cooperatively with SecY1 to assure high-level of secretion of the S-

layer proteins throughout the bacterial growth cycle as SecY1 is highly expressed during exponential phase while SecY2 is highly expressed during stationary phase. A *B. subtilis* strain containing the *secY2, adk* and *map* genes under the control of xylose promoter was successfully constructed (strain KG204). However, the construction of a strain with an IPTG-dependent *secY* encountered problems. When pKG101, containing *secY* under control of IPTG-inducible promoter, was transformed into KG204. The resulting transformants did not have a correctly integrated copy of pKG101 in its chromosome. However, when two of these transformants were passaged through the LB broth with erythromycin, lincomycin, chloramphenicol, kanamycin, IPTG and xylose, xylose-dependent variants were selected on LB+xylose plates, suggesting these clones must be relying on *B. anthracis* SecY2 rather than *Bsu* SecY for growth. However, further analysis of the xylose-dependent mutants was not possible as they were unstable, and failed to grow in the LB broth with either xylose or IPTG. As result this part of the project was discontinued. The failure to generate a strain for complementation analysis might have been due to toxicity associated with increased amounts of SecY, a membrane pore-forming protein, as shown by Kihara et al. (1995). In their study, the relationship between FtsH and SecY expression was investigated. FtsH is a cellular protease that degrades SecY uncoupled to SecE. When SecY was overexpressed in an *E. coli ftsH* mutant, a deleterious impact on the bacterial growth and protein export was observed. It is also possible that overexpression of *adk* and *map* from the inducible promoter leads to high levels of Adk and Map, which has toxic effect of cells. The alternative way to check if SecY2 can complement Bsu SecY would be to delete *Bsu secY* in KG204 (*amyE::*P_{xyl} *Bsu secY2-adk-map*), while expressing secY2. If *secY2* can complement *Bsu secY*, then *secY2*-positive, *Bsu secY*-negative strain should be viable.

Acknowledgement: Experimental work presented in this Section was done in collaboration with Dr. Susanne Pohl and Dr. Guoqing Wang.

Chapter 6: Identification of factor(s) conferring SecA2 substrate specificity using the pull-down technique

Previously, we showed that SecA2 mediates specifically secretion of Sap and EA1 proteins. To identify a factor or factors which coffer SecA2 specificity to its substrates, we analysed the genomic context of *secA2* gene in *B. anthracis* and found *secA2* is located within an operon containing also a downstream gene that was re-named *secH*. When *secH* was deleted from the genome of *B. anthracis* Sap and EA1 secretion was reduced but not abolished. This result suggests that SecH participates in the secretion of Sap and EA1, but there must be an additional specificity factor/s (which might cooperate with SecH) responsible for S-layer proteins being secreted by SecA2 but not by SecA1. To identify that/those specificity factor/s, the pull-down technique was attempted.

6.1. The principle of the pull-down technique

The so-called pull-down technique is an approach to identify putative protein:protein interactions *in vivo,* using a 'bait' and 'pray' approach. The 'bait' is a target protein that can be immobilised on an affinity column by virtue of it encoding an affinity tag. The "prey" protein is any protein that interacts with the immobilised 'bait' after the cells have been lysed and soluble fraction applied to the affinity column. The putative interacting proteins are stabilised *in vivo* by reversibly cross-linking with formaldehyde, so that captured 'pray' will not dissociate during the subsequent cell lysis and processing events. Once the sample has been applied to the affinity column, the resin is washed extensively to eliminate non-specific protein binding to the matrix. After washing, the complex is eluted from the resin and the cross-linking between proteins reversed by boiling in the sample buffer. Finally, the proteins are separated by SDS-PAGE and the individual protein identified immunologically or by mass-spectroscopy. In this study, the pull-down assay was done in the batch format. The analysed proteins were fused to the FLAG-tag and produced in the host strain from an expression vector. The steps of the pull-down assay used in this study are shown on the Figure 6.1.

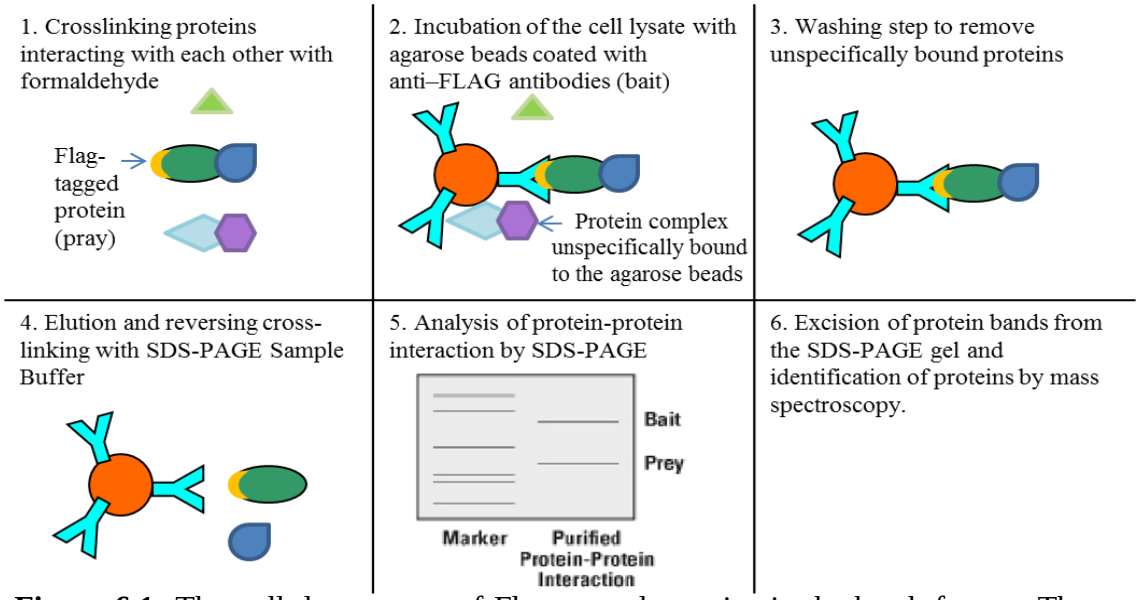

Figure 6.1: The pull-down assay of Flag-tagged proteins in the batch format. The assay was done in the following steps: (1) Interacting proteins were cross-linked with formaldehyde; (2) Cell lysate, containing FLAG-tagged protein (pray) was mixed with agarose beads coated with anti–FLAG antibodies (bait); (3) Unspecifically bound proteins were washed away in the washing step; (4) Flag-tagged protein were eluted and cross-linking reversed by boiling samples in the sample buffer; (5) Proteins were analysed by SDS-PAGE; (6) Protein bands were excised and identified by mass spectroscopy.

6.2. An attempt to identify proteins interacting with SecA2, SecH and Sap

In order to identify factor(s) potentially conferring substrate specificity to SecA2, a pull-down experiment was performed with a Flag tag-labelled version of SecA2, SecH and Sap. The Flag-tagged SecA2, SecH, Sap bait proteins were expressed from vectors pKG400-FLAG-*secA2*, pKG400-FLAG-*secH*, pKG400-FLAG-*sap*, respectively. The vectors were constructed by amplifying the *secA2*, *secH* and *sap* genes with the Flag-tag sequence (GAT TAC AAG GAT GAC GAC GAT AAG) incorporated in-frame into the forward primer. The amplified fragments were then cloned into the pKG400 expression plasmid. Subsequently pKG400-FLAG-*secA2*, pKG400-FLAG-*secH*, pKG400-FLAG-*sap* plasmids, as well as empty vector, were transformed into *B. anthracis* Δ*secA2*, *B. anthracis* Δ*secH*, *B. anthracis* Δ*sap-eag*, respectively. Cultures of the transformed strains were grown LB broth and induced with 10 mM IPTG and grown for a further 90 minutes. The procedure for cross-linking and the extraction of proteins is described in the **Section 2.13**. The proteins obtained in the pull-down experiment were separated by SDS-PAGE and stained with either SyproRuby Protein Gel Stain (Invitrogen) or PageSilver Staining Kit (Fermentas). The unique bands were selected for the samples with tagged proteins with and without cross-linking with formaldehyde. The negative controls were samples obtained for the strains with the empty plasmid (pKG400), with

and without formaldehyde treatment. The gels using SecA2 and Sap, were identical irrespective of the presence of the their respective expression plasmids, and only the pull-down experiment with SecH showed some unique bands (Figure 6.2), which were subsequently extracted and identified by mass spectroscopy.

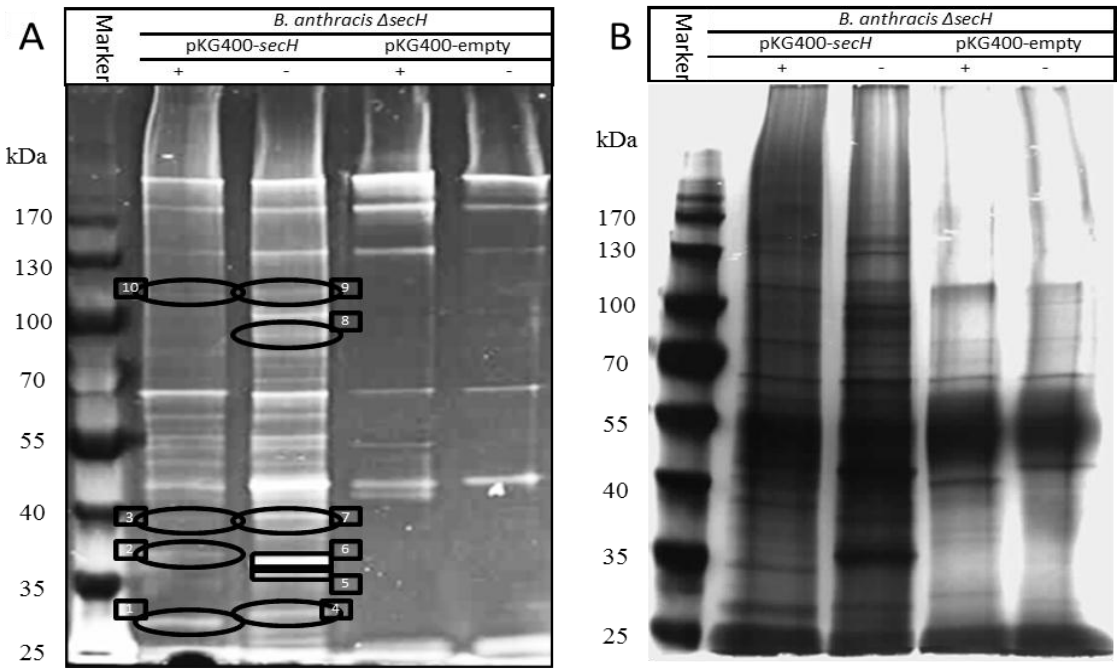

Figure 6.2: SDS-PAGE analysis of proteins, recovered from the pull-down experiments, stained with: (A) SyproRuby Protein Gel Stain; (B) PageSilver Staining Kit. The bait and prey proteins were obtained from *B. anthracis* Δ*secH* transformed with pKG400-FLAG-*secH* with (+) and without (-) formaldehyde treatment. *B. anthracis* Δ*secH* transformed with an empty pKG400 vector (pKG400) was used as a negative control. The unique bands (circled) for the samples with Flag-tagged SecH, with and without formaldehyde treatment were selected by comparison with the negative control.

The extracted bands were analysed by MALDI-TOF, however, the samples contained insufficient protein to provide positive identifications. The low yield of proteins was found to be due to the inefficiency of extraction of intracellular proteins from *B. anthracis*. The preferred method to break open cells of *B. anthracis*, which was used in this instance, is to subject cells to shearing by vigorously shaking cell pellets with glass beads at high-speed cell dismembrator. The limitation of this method is that only small volume of culture can be processed. In this pull-down experiment, intracellular proteins were extracted from cell pellets obtained from 250 ml of culture. Although the concentrations of proteins remaining after washing were relatively low, sufficient material was obtained for mass spectroscopy. The four samples, which gave the clearest spectra by MALDI-TOF-MS were further subjected to liquid chromatography-mass spectrometry (LC/MS/MS) analysis. The fingerprint data for the protein identified by LC/MS/MS are shown in the Table 6.1.

Table 6.1: Peptide mass fingerprinting data summary for the protein identified in this study by LC/MS/MS.

Sample	Obs	Mr(expt)	Mr(calc)	ppm	Miss	Score	Expect	Unique	Peptide	Identification
1	875.4694	1748.9243	1748.9197	2.65	0	40	0.039	U	K.VDVFATGEIVDVTGISK.G	50S ribosomal protein L3
2	664.8818	1327.7491	1327.7459	2.40	0	89	4.4e-007		K.LVANLLETAGATR.V	ribose-phosphate pyrophosphokinase
	664.8819	1327.7492	1327.7459	2.49	0	(82)	2e-006		K.LVANLLETAGATR.V	
	664.8819	1327.7492	1327.7459	2.49	0	(79)	3.8e-006		K.LVANLLETAGATR.V	
	785.4418	1568.8690	1568.8661	1.83	0	(52)	0.0013	U	K.ELVVTNSIVLPEEK.K	
	785.4422	1568.8698	1568.8661	2.37	0	(58)	0.00041	U	K.ELVVTNSIVLPEEK.K	
	785.4427	1568.8709	1568.8661	3.08	0	63	0.00014	U	K.ELVVTNSIVLPEEK.K	
				Overall		152				
6	642.3481	641.3408	641.3384	3.69	0	22	0.46	U	K.ALVPQD	hypothetical protein BA_0881 (SecH)
	601.8438	1201.6731	1201.6707	2.01	0	38	0.047		K.GAFTLPNLEIK.A	
	634.8189	1267.6233	1267.6197	2.81	0	(71)	2.3e-005	U	R.DNGYDVAVFIR.S	
	634.8192	1267.6238	1267.6197	3.19	0	(73)	1.5e-005	U	R.DNGYDVAVFIR.S	
	634.8193	1267.6240	1267.6197	3.38	0	74	1.2e-005	U	R.DNGYDVAVFIR.S	
	875.9617	1749.9089	1749.9036	3.04	0	95	1.1e-007	U	R.LEEYQISLSGIEIEK.R	
	875.9617	1749.9089	1749.9036	3.04	0	(84)	1.5e-006	U	R.LEEYQISLSGIEIEK.R	
	875.9617	1749.9089	1749.9036	3.04	0	(52)	0.0022	U	R.LEEYQISLSGIEIEK.R	
	875.9620	1749.9095	1749.9036	3.39	0	(70)	3.9e-005	U	R.LEEYQISLSGIEIEK.R	
	1121.5071	2240.9996	2241.0033	-1.65	0	(72)	4.7e-006	U	K.DTTVSSNQLFGQEETNTENK.T	
	1121.5087	2241.0028	2241.0033	-0.24	0	(85)	2.9e-007	U	K.DTTVSSNQLFGQEETNTENK.T	
	1121.5096	2241.0047	2241.0033	0.63	0	(62)	5.4e-005	U	K.DTTVSSNQLFGQEETNTENK.T	
	1121.5096	2241.0047	2241.0033	0.63	0	85	3.1e-007	U	K.DTTVSSNQLFGQEETNTENK.T	
	1121.5104	2241.0062	2241.0033	1.29	0	34	0.033	U	K.DTTVSSNQLFGQEETNTENK.T	
	1121.5107	2241.0069	2241.0033	1.62	0	(77)	1.7e-006	U	K.DTTVSSNQLFGQEETNTENK.T	
	1258.1335	2514.2525	2514.2503	0.89	0	64	0.00011	U	R.NFVDNLTPPNDGEINFLGLQAAR.K	
	1258.1339	2514.2533	2514.2503	1.19	0	(58)	0.00054	U	R.NFVDNLTPPNDGEINFLGLQAAR.K	
	1258.1359	2514.2572	2514.2503	2.74	0	(55)	0.001	U	R.NFVDNLTPPNDGEINFLGLQAAR.K	
				Overall		**378**				
8	672.4052	671.3979	671.3966	1.95	0	(19)	6.5	U	K.TVSIPR.D	membrane-bound transcriptional regulator LytR
	672.4066	671.3993	671.3966	4.05	0	(11)	47	U	K.TVSIPR.D	
	672.4072	671.4000	671.3966	4.96	0	28	0.87	U	K.TVSIPR.D	
				Overall		28				

Band 1 was matched with a significant score to a single peptide, namely ribosomal protein L3. Bands 2 and 6 were both matched to proteins with a significant score, ribose-phosphate pyrophosphokinase and SecH (BA_0881) itself, respectively. Band 8 was also matched to a protein, namely the membrane-bound transcriptional regulator LytR, but the match was not significant. However, the expected and observed species identified by LC/MS/MS are about the same, making this protein a candidate worth further investigation. The possibility that SecH interacts with 50S protein L3 might indicate that SecH forms a complex with ribosome. As SecH was shown by bacterial-two hybrid assay, to interact with SecA2 and its substrate, this observation might indicate that SecH, SecA2, and its substrate may form a complex with the ribosome. The other protein identified in the pull-down experiment, ribose-phosphate pyrophosphokinase is an intracellular enzyme catalysing the formation of D-ribose 5-phosphate, but what would be the reason for its interacting with SecH is unclear.

6.3 Discussion

In the search for factors conferring substrate specificity on SecA2, a pull-down assay was employed. However, since we did not have time to optimise the methods for *B. anthracis* the results were ambiguous. Nevertheless, one protein identified in this analysis, LytR, is worth further investigation. LytR belongs to the LytR-CpsA-Psr family of cell envelope-associated transcription attenuators. Members of LytR family are also essential for optimal cell division in *S. aureus* (Over *et al.*, 2011). LytR is a putative transmembrane protein, harbouring a predicted extracytoplasmic LytR-CpsA-Psr domain. First described in *B. subtilis*, LytR was shown to act as an attenuator of the *lytABC* operon and of its own expression. The *lytABC* operon encodes a putative lipoprotein (LytA), an *N*-acetylmuramoyl-L-alanine amidase (LytC) and its modifier LytB (Lazarevic *et al.*, 1992). In *Streptococcus pneumoniae* LytR is essential for cell division (Johnsborg and Håvarstein, 2009) and its deletion affects septum formation. Consequently, cells of a *lytR*-null mutant are highly variable in both size and shape with some cells 2-3 times larger than the wild type. The mutant also forms irregularly shaped mini cells. LytR could be implicated as a sensor of cell wall stress or as an additional substrate for SecA2. The failure to transport it to the membrane is likely to lead to changes in the cell morphology observed in the *secA2*-null mutant (**Section 12.1**). The possible interaction between SecH and the L3 protein of the 50S ribosomal protein could indicate that SecH interacts with ribosomes.

Chapter 7: Substrate specificity of PrsA-like proteins in *B. anthracis*

7.1 Introduction

B. anthracis possesses three homologues of the *B. subtilis* PrsA-like foldase: PrsAA, PrsAB, PrsAC. All three homologues complement *B. subtilis* PrsA with respect to the secretion of *B. anthracis* recombinant protective antigen and the *B. licheniformis* α-*amylase*, AmyL (Williams *et al.*, 2003). However, the complementation with PrsAC led to an altered colony morphology, implying that PrsA-like proteins exhibit some substrate specificity. It was also shown that, in *B. subtilis*, Sap and EA1 proteins of *B. anthracis* can only be found to be secreted in the presence of PrsAB (Pohl *et al.*, unpublished). In an attempt to identify substrates for the *B. anthracis* PrsA-like proteins, we generated null mutations in the genes encoding these foldases: *prsAA, prsAB* and *prsAC* yielding Δ*prsAA*, Δ*prsAB* and Δ*prsAC* mutants, respectively (**Section 3.4**).

7.2 Analysis of the extracellular proteins of *B. anthracis* Δ*prsAA*, Δ*prsAB* and Δ*prsAC*

SDS-PAGE and 2D-PAGE was used to analyse the pattern of extracellular proteins produced by these mutants in comparison with the wild type (Figures 7.1 and 7.2). The resulting gels showed that the secretion of Sap and EA1 was abolished in Δ*prsAB*, indicating that the PrsA-like proteins of *B. anthracis* exhibit substrate specificity and that PrsAB, but not PrsAA or PrsAC is required for the secretion of these S-layer proteins.

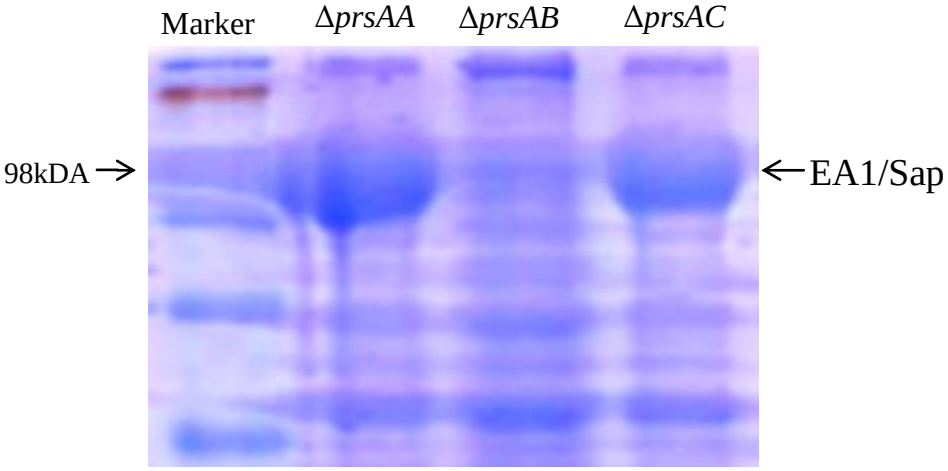

Figure 7.1: SDS-PAGE analysis of the extracellular proteins in the supernatant fractions of *B. anthracis* null mutants: Δ*prsAA*, Δ*prsAB* and Δ*prsAC*. The secretion of EA1 and Sap, which co-migrate as a single ~ 90 kDa band, is abolished in the Δ*prsAB* mutant. Marker: SeeBlue Plus Prestained Standard (Invitrogen).

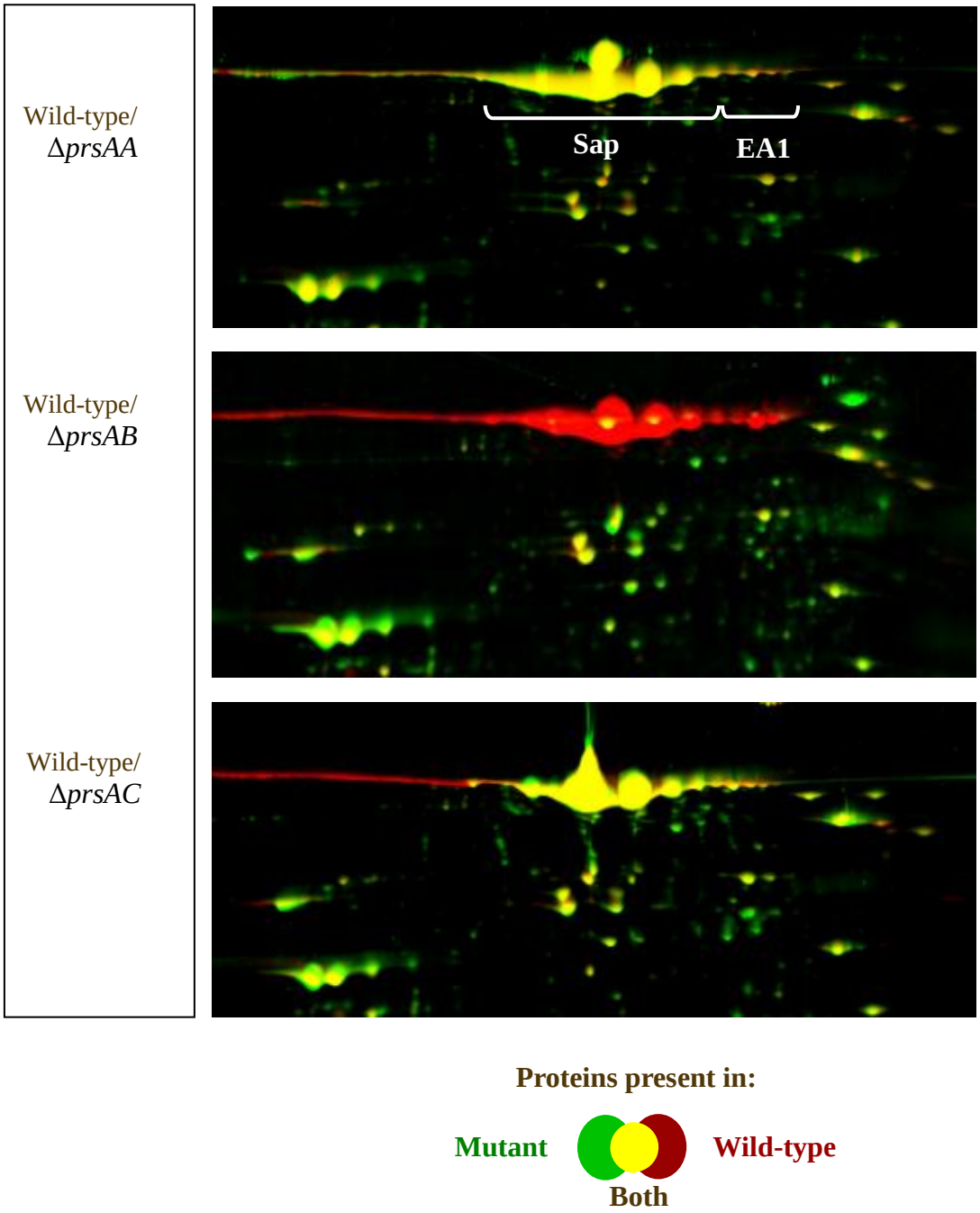

Figure 7.2: False-coloured 2D gel overlays of *B. anthracis* extracellular proteins isolated from the wild-type and Δ*prsAA*, Δ*prsAB* and Δ*prsAC* mutants. The extracellular proteome of Δ*prsAB* showed a dramatic reduction in the secretion of two of the major surface-associated antigens, Sap and EA1, resulting in them generating red spots. In contrast, the extracellular proteomes of the Δ*prsAA* and Δ*prsAC* gave identical profiles to that of the wild-type (yellow spots).

7.3 Discussion

Interestingly, apart from SecA2, PrsAB foldase was also found to be involved in the secretion of both: Sap and EA1. Why have *B. anthracis* evolved to have specific components of the translocation system involved specifically in secretion of S-layer proteins? It could indicate importance of the S-layer. However, as it was mentioned in the **Section 1.8**, the role of S-layer in *B. anthracis* is not clear. *In vivo*, the EA1 S-layer predominates when the toxins and capsule are produced, while the Sap S-layer predominates in non-capsulated bacteria (Mignot *et al.*, 2004). This may indicate that Sap and EA1 play distinct roles *in vivo*. Sap, as the outermost layer, may participate in interaction with the environment, while EA1 might play role inside the host.

The only other substrate-specificity for PrsA-like foldase was demonstrated in *Listeria monocytogenes*. This bacterium, encodes two PrsA-like proteins, PrsA1 and PrsA2. PrsA2 was shown to be essential for the virulence of *L. monocytogenes* in mice (Alonzo *et al.*, 2009; Zemansky *et al.*, 2009), and in its absence, cell-to-cell spreading and flagellar motility are impaired, while activities of virulence factors such as listeriolysin-O and the broad-range phosphatidyl-choline phospholipase are reduced (Alonzo *et al.*, 2009; Zemansky *et al.*, 2009). The secretion of several other proteins were also abolished in the absence of PrsA2 (Alonzo and Freitag, 2010). It can not be excluded that PrsAB, like *Listeria monocytogenes*, possesses specificity also to other substrates then Sap and EA1.

There is also a possibility that PrsAB might be a substrate for SecA2 and that the lack of Sap and EA1 in the secretome of *B. anthracis* Δ*secA2*, results from the absence of PrsAB on cell surface in that mutant. PrsAB is a foldase, a membrane-anchored protein, and the secretion of that group of proteins was not investigated in this thesis and it can not be excluded that PrsAB is a substrate for SecA2. It is also possible that PrsAB is responsible for folding a specific Sip signal peptidase that, in turn, might be responsible for processing of Sap and EA1. The lack of that signal peptidase might be the direct reason for the lack of Sap and EA1 in the secretome of *B. anthracis* Δ*secA2* and/or *B. anthracis* Δ*prsAB*.

Chapter 8: Dealing with the issue of polar effects of gene expression in *secA2*-null mutant of *B. anthracis*

The deletion and/or insertion of genes in the genome has the potential to exert polar effects on neighbouring genes by causing changes in their expression. In this study the selectable marker approach was used to delete target genes; the target gene being replaced by the gene of the selectable marker *i.e.* kanamycin resistance gene. This manipulation of the genome could potentially affect gene expression of the surrounding genes. Therfore we analysed the expression of genes in the proximity the gene deletions in the strains investigated in this study.

8.1 Analysis of *secA2* and *secH* expression in *B. anthracis* null mutants

Since *secA2* and *secH* are adjacent on the chromosome, we used Northern blot analysis to determine whether they were co-expressed from the same promoter. Total RNA was extracted from the wild type strain and a series of mutants. Following agarose electrophoresis and blotting, the RNA was hybridised with labelled *secA2*- and *secH*-specific probes. In the case of the wild type strain and *B. anthracis* Δ*secY2*, both probes hybridised to a single transcript of ~ 3200 bases, the expected size of a bicistronic transcript. In the case of the Δ*secH* mutant, two bands of the approximate size of 2350 bases and 5200 bases were detected with the *secA2*-specific probe. 2350 bases band corresponds in size to the transcript of *secA2* while 5200 bases band indicates the incomplete transcriptional termination within the downstream ΩKm cassette. As expected, no *secH* specific transcript was detected in the Δ*secH* mutant. When the Δ*secA2H* mutant was analysed, neither *secA2* nor *secH* transcripts were detected. Finally, Northern blot analysis revealed that *secH* was not expressed in the Δ*secA2* mutant, indicating that phenotypically it behaved similarly to the Δ*secA2H* mutant (Figure 8.1).

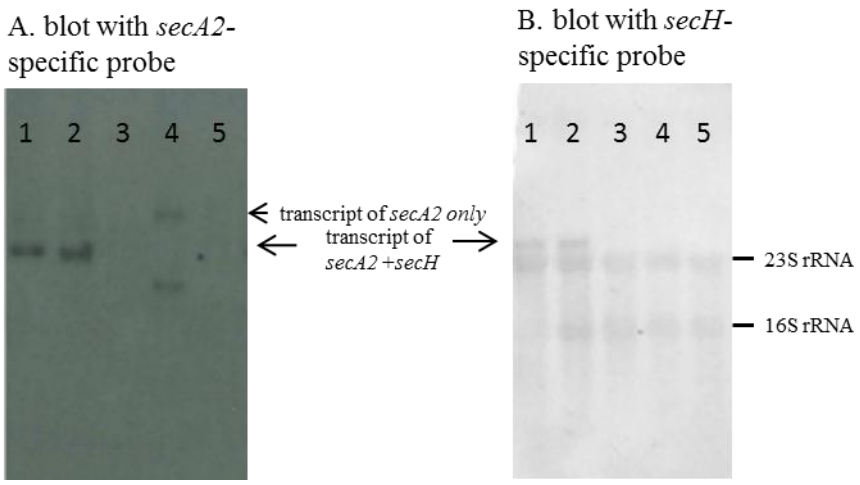

Figure 8.1: Northern blots of RNA from various *B. anthracis* strains: (1) wild type, (2) Δ*secY2*, (3) Δ*secA2*, (4) Δ*secH*, (5) Δ*secA2H*, with *secA2*- and *secH*-specific probes (Figure A and B, respectively). As *secA2* and *secH* are located in the same operon, they also are located on the same transcript, corresponding approximately to their combined size (3250 bases). RNA of Δ*secH* gives a positive signal with *secA2*-specific probe – two bands are visible: lower band corresponding to the transcript of *secA2* only i.e. 2350 bases and unidentified upper band (approx. 5200 bases). On the Figure B, 16S rRNA (approx. 3000 bases) and 23S rRNA (approx. 1500 bases) are visible.

8.2 Construction of *secA2*-null mutant expressing *secH*

The lack of expression of *secH* in the *B. anthracis* Δ*secA2* mutant was likely to be due to the polar effect of kanamycin cassette used as a marker to construct that mutant, resulting in transcription termination. It was therefore necessary to construct a Δ*secA2* mutant in which the expression of *secH* was not affected. In the first place we attempted to develop a 'clean' deletion approach exploiting the endogenous Dif/Xer recombination system. This type of system was employed successfully in *B. subtilis* (Bloor and Cranenburgh, 2006). The Dif/Xer recombination systems can be used for creating 'clean' deletions or gene replacements without the need to maintain a selective gene. The Dif/Xer recombination systems involve two Xer-like recombinases, e.g. RipX and CodV in *B. subtilis* or XerC and XerD in *E. coli*. These recognise 28-nucleotide *dif* motifs that are normally located at or near the chromosome replication terminus (Leslie and Sherratt, 1995; Sciochetti *et al.*, 2001). *dif* motifs consist of two inverted sequences separated by a hexanucleotide. The action of the recombinases on *dif* sites allows resolution of dimeric chromosomes that can be generated during DNA replication. Dif/Xer recombination systems are found in most bacterial species containing circular genomes (Carnoy and Roten, 2009). The Dif/Xer system can be employed to eliminate the selectable marker introduced into the bacterial chromosome as a part of the insertion cassette, with the aim of target gene knock-out or replacement. The concept of the gene

deletion using Dif/Xer system is depicted on the Figure 8.2 (Bloor and Cranenburgh, 2006).

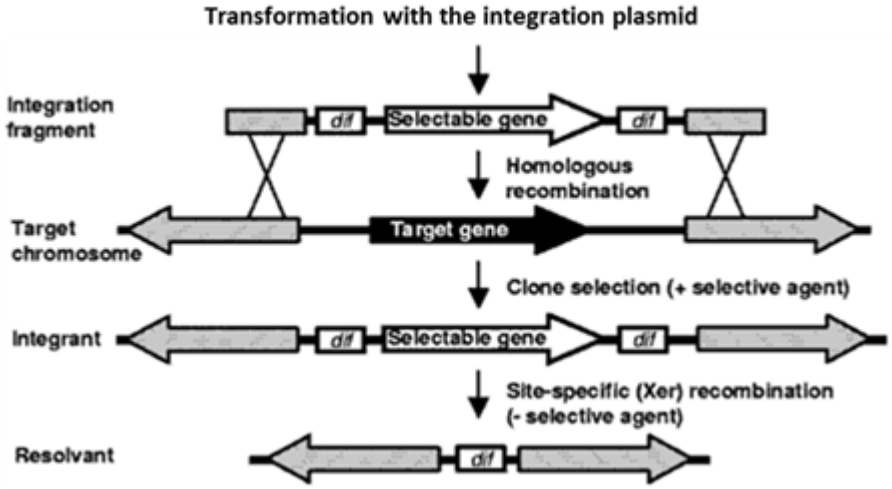

Figure 8.2: Deletion of a target chromosomal gene and subsequent removal of the selectable marker (e.g., antibiotic resistance) gene by Xer recombination at flanking *dif* sites (Xer-cise). Shaded regions represent homology between the integration cassette and genes flanking the target gene (Bloor and Cranenburgh, 2006).

The construction of mutants using Dif/Xer system is similar to the selectable marker approach employed to construct mutants in this study. The difference is that the selectable marker gene is flanked by *dif* sites (Figure 8.3). Target gene on the chromosome is replaced with the integration fragment and the clones carrying the integrants are selected by a selective agent to which they are resistant, due to presence of the gene encoding the selectable marker. When the clones with deletion of the target gene are grown without selection pressure, then the action of native Xer recombinases, excises the gene resistance marker located between them. To identify *dif* sites in bacterial genomes, Le Bourgeois et al. (2007) used homology searches with *B. subtilis dif* sites as query against complete genomes taking into account such parameters as: (1) occurrence only once per genome, and (2) localisation in the replication terminus (terC). The result of the query for some bacteria is summarised in the Table 8.1.

Table 8.1: Localisation of *dif* sites in some bacteria. Variable nucleotides are underlined. The sequence recognised by CodV/XerC, by RipX/XerD and the core of the dif sequence are shown (Le Bourgeois *et al.*, 2007).

Bacterial Species	Sequence		
	CodV (XerC) Arm	Core	RipX (XerD) Arm
B. *subtilis* 168	acttcctagaa	tatata	ttatgtaaact
B. *anthracis* Ames	actgcctataa	tatata	ttatgttaact
B. *anthracis* Ames ancestor	actgcctataa	tatata	ttatgttaact
B. *anthracis* A2012	actgcctataa	tatata	ttatgttaact
B. *anthracis* Sterne	actgcctataa	tatata	ttatgttaact
B. *cereus* ATCC 10987	actgcctataa	tatata	ttatgttaact
B. *cereus* ATCC 14579	actacctataa	tatata	ttatgttaact
B. *halodurans* C-125	ggttcctataa	tatata	ttatgtaaact
B. *thuringiensis* 97–27	actgcctataa	tatata	ttatgttaact
E. *faecalis* V583	actttgtataa	tgtata	ttatgttaact
L. *innocua* Clip11262	acttcctataa	tatata	ttatgtaaact
L. *monocytogenes* EGD-e	acttcctataa	tatata	ttatgtaaact
L. *monocytogenes* 4b F2365	acttcctataa	tatata	ttatgtaaact
Lb. *johnsonii* NCC533	aattcgtataa	tatata	ttatgtaaagt
Lb. *plantarum* WCFS1	actttgtataa	tatata	ttatgtaaact
Oceanobacillus iheyensis HTE831	acttcctataa	taaata	ttatgtctact
S. *aureus* MW2	acttcctataa	tatata	ttatgtaaact
S. *aureus* N315	acttcctataa	tatata	ttatgtaaact
S. *aureus* Mu50	acttcctataa	tatata	ttatgtaaact
S. *aureus* MRSA252	acttcctataa	tatata	ttatgtaaact
S. *aureus* MSSA476	acttcctataa	tatata	ttatgtaaact
S. *epidermitis* ATCC 12228	acttcctataa	tatata	ttatgtaaact
L. *lactis* IL1403	No homology		
Streptococcus (nine species)	No homology		

The *dif* sequence of *B. anthracis* (ACTGCCTATAA**TATATA**TTATGTTAACT) was used to generate the integration vector for *secA2* deletion. The plasmid pKG307 was constructed consisting of pUTE583 containing an integration fragment consisting of the kanamycin cassette flanked by 29 bp *dif* sites and then by 5' and 3' sequences flanking the *secA2* gene (Figure 8.3).

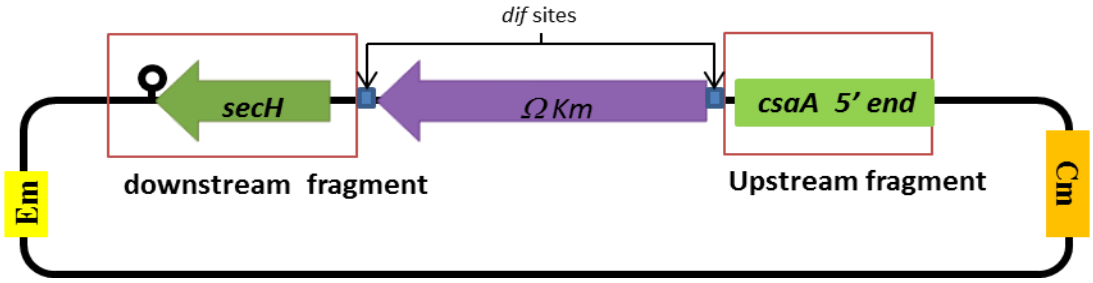

Figure 8.3: pKG307 plasmid for the 'clean' deletion of *secA2*. Upstream (5' sequence flanking *secA2*) and downstream fragments (3'sequence flanking *secA2*) are separated by the kanamycin resistance gene (Ω Km) which is flanked by *dif* sites. Erythromycin (Em) and chloramphenicol (Cm) resistance genes are shown.

The *dif* sites were introduced on the either side of the kanamycin cassette to provide targets for its removal via the CodV/RipX recombinases, leaving a single 29 bp scar. The *dif*-Ωkm-*dif* fragment was amplified with primers DifKmF and DifKmRev (**Appendix B**) and the resulting 2200 bp amplicon cloned into the SmaI restriction site of pUTE583 containing upstream and downstream flanking fragments of *secA2*, generating pKG307. The construction of pKG307 was carried out using the *E. coli* XL-I blue strain as an intermediate host. Subsequently, pKG307 was passaged through a Dam and Dcm methylase-deficient strain of *E. coli* (GM48) and the following transformation of the integration vector, a double crossover RecA-mediated integration (allelic replacement) event resulted in the target gene being replaced with the integration fragment. As a result, the entire target gene was excised from the chromosome. The mutant strain carrying the targeted gene knock-out, as well as the integration plasmid now containing the target gene was counter selected for loss of the plasmid, so that the desired mutant genotype could be isolated. The counter-selection involved passaging the mutant through numerous generations in liquid culture. Selection was made for ΩKm cassette, but not the erythromycin resistance gene associated with the pUTE583 vector. Subcultures of the broth were plated onto agar and the resulting colonies replica plated onto LB agar containing kanamycin or erythromycin. The expected result was the isolation of clones that were kanamycin-resistant and erythromycin-sensitive. This would indicate the removal of *secA2* from the chromosome by allelic exchange and the loss of the pUTE583 plasmid. Despite testing approximately 1500 colonies, no erythromycin sensitive clones were found. Instead, we frequently identified clones that were erythromycin resistant and kanamycin-sensitive, suggesting that there was high frequency deletion of the kanamycin cassette from the plasmid before allelic exchange event could take place, presumably mediated by the Xer recombinase. It therefore appears that the excision of the kanamycin cassette by Dif/Xer recombination system was too efficient with respect to the frequency of the chromosome integration event for this system to be used in *B. anthracis*. As the Dif/Xer recombination system was not successful in obtaining a clean deletion of *secA2*, an alternative approach was used in which a copy of the native *secA2H* promoter (P_{secA2H}) was used to drive *secH* expression. To achieve this, a *ΔsecA2* mutant was generated using pUTE583, as described in **Section 3.1**. However, the technique was modified so that the integration fragment contained an upstream *secA2* fragment lacking P_{secA2H} while the downstream

fragment had the P_{secA2H} cloned at its 5'end to drive *secH* expression (Figure 8.4).

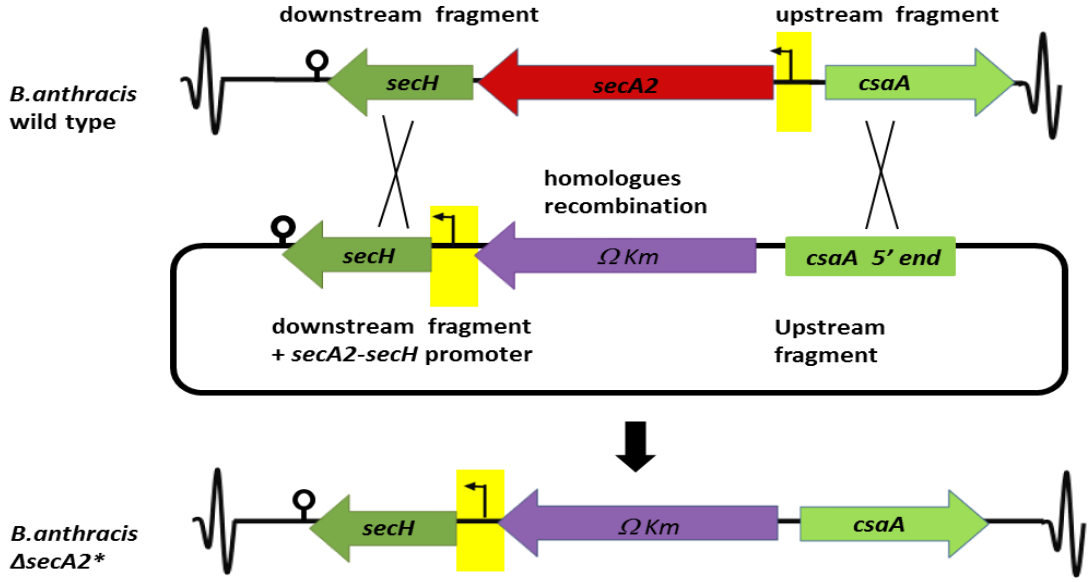

Figure 8.4: Construction of a *B. anthracis* Δ*secA2*-null mutant expressing *secH* (Δ*secA2**). The pUTE583-based plasmid encodes an integration fragment in which the site of P_{secA2H} (left-pointed arrow in the yellow box) has been repositioned to facilitate the expression of *secH* following integration. Two crossed lines represent double crossing over occurring between the target region and the integration fragment.

Following the selection of integrants and the confirmation of their structure by diagnostic PCR, the expression of *secA2* and *secH* by the newly generated Δ*secA2* mutant (annotated as Δ*secA2**) was analysed by Northern blotting (Figure 8.5). Genomic maps, of the wild type and the mutants analysed, are shown on the Figure 8.6.

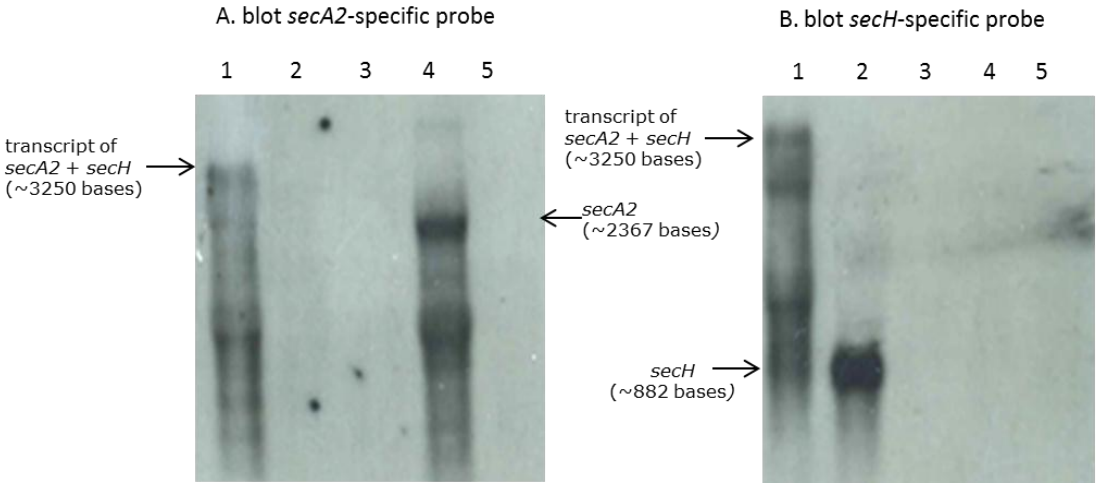

Figure 8.5: Northern blot analysis with *secA2*-specific probe (A) and *secH*-specific probe (B) for the following strains: (1) *B. anthracis* wild type, (2) Δ*secA2**, (3) Δ*secA2H*, (4) Δ*secH*, (5) Δ*secA2*. For the genomic maps of the mutants see Figure 8.6.

Northern blot analysis of the wild type detected the presence of a 3250 bases transcript by both the *secA2*- and *secH*-specific probes, confirming that these genes are co-transcribed (Figure 8.5, lane 1). In *B. anthracis* Δ*secA2** (*A2*$^{-}$*H*$^{+}$), there was a complete lack of signal from the *secA2*-specific probe, while a ~ 0.9 kb transcript, consistent with the size of the *secH* gene, was detected with the *secH*-specific probe (Figure 8.5, lane 2). Transcripts were not detected with either of these probes in the double deletion mutant *B. anthracis* Δ*secA2H* or the *B. anthracis* Δ*secA2* (*A2*$^{-}$*H*$^{-}$) mutant in which P_{secA2H} was not relocated (Figure 8.5, lanes 3 and 5). Finally, a ~ 2.4 kb transcript was detected by the *secA2*-specific probe in the Δ*secH* mutant, consistent with the size of *secA2*, but as expected, there was no *secH* transcript (Figure 8.5, lane 4).

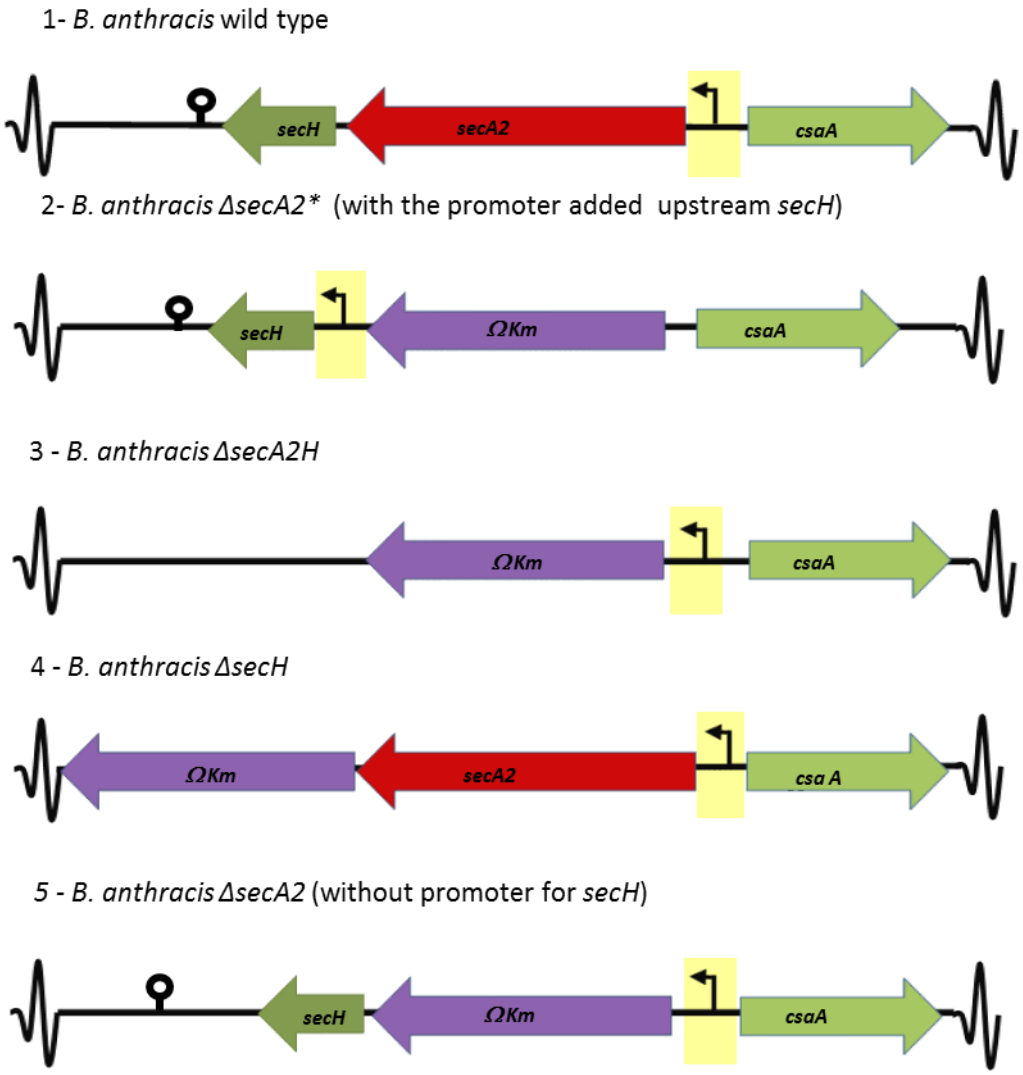

Figure 8.6: Genomic maps of *secA2-secH* locus of the *B. anthracis* strains: (1) wild type, (2) Δ*secA2**, (3) Δ*secA2H*, (4) Δ*secH*, (5) Δ*secA2*.

8.3 Polar effects on the expression of *csaA* and *csaB* in Δ*secA2**

We have already demonstrated that inactivation of the *secA2* in the *B. anthracis* Δ*secA2* mutant led to the down-regulation of *secH*, located immediately downstream and in the same operon as *secA2*. We now consider potential polar affects on *csaAB* operon. These genes, described in more detail in the **Section 1.8.2**, are located between the *secA2–secH* operon and *sap*. Deletion of the genes upstream or downstream of *csaAB*, by allelic replacement with the kanamycin resistance cassette, could potentially affect the expression of *csaAB*. To check the expression of *csaA-csaB* operon, total RNA was extracted from the cultures of mutants *B. anthracis* Δ*secA2**, *B. anthracis* Δ*secA2*, *B. anthracis* Δ*secH*, *B. anthracis* Δ*secA2H*, *B. anthracis* Δ*sap-eag*, *B. anthracis* Δ*prsAB*, and wild type strains, grown to OD_{600}=0.8. The extracted RNA was subjected to Northern blotting with *csaA*- and *csaB*-specific probes (Figure 8.7). The results confirm that *csaAB* are transcribed from a single transcript of ~ 2.8 kb that runs with a similar mobility to that of the 23S rRNA. There are two additional bands visible in the lower section of blots, with one corresponding presumably to 16S and the other one might be constituted by some RNA processing product. The data also indicate that in *B. anthracis* Δ*secA2** the expression of *csaA* and *csaB* has been down-regulated. However, the expression of these genes in each of the other constructed mutants was not affected.

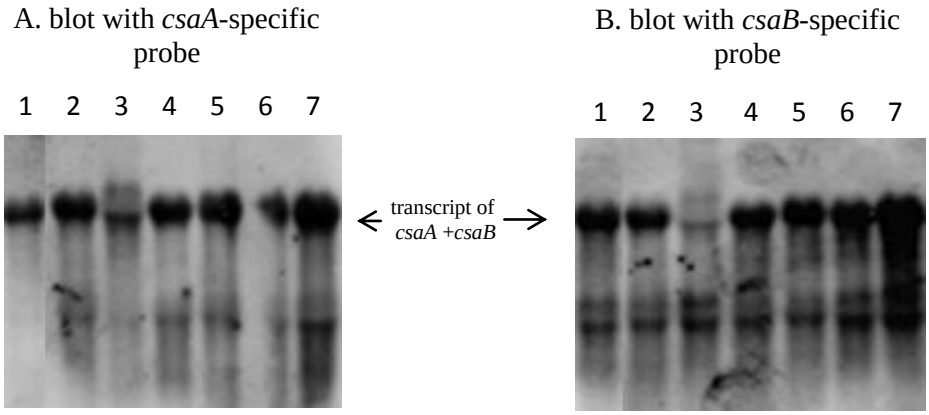

Figure 8.7: Northern blots of RNA from *B. anthracis* strains: (1) Δ*secA2*, (2) wild type, (3) Δ*secA2**, (4)) Δ*secA2H*, (5) Δ*secH*, (6)) Δ*prsAB*, (7) Δ*sap-eag* with (A) *csaA*- specific and (B) *csaB*-specific probes.

8.4 Secretion of Sap and EA1 is abolished in Δ*secA2**

It was shown that in *B. anthracis* Δ*secA2* the secretion of Sap and EA1 becomes abolished (**Section 1.8.1**). However, the Northern blot analysis showed the expression of *secH* is down-regulated in Δ*secA2* (**Section 8.1**). Thus, the *secA2*-null mutant with unaffected *secH* expression was constructed (Δ*secA2**). The extracellular proteins of the Δ*secA2** mutant were analysed by SDS-PAGE, following growth to OD 0.8 in LB medium at 37°C (Figure 8.8). This showed that SecA2 alone, rather than SecA2 and SecH, was absolutely necessary for the secretion of Sap and EA1, and that SecH simply improves the efficiency of their secretion (**Section 4**).

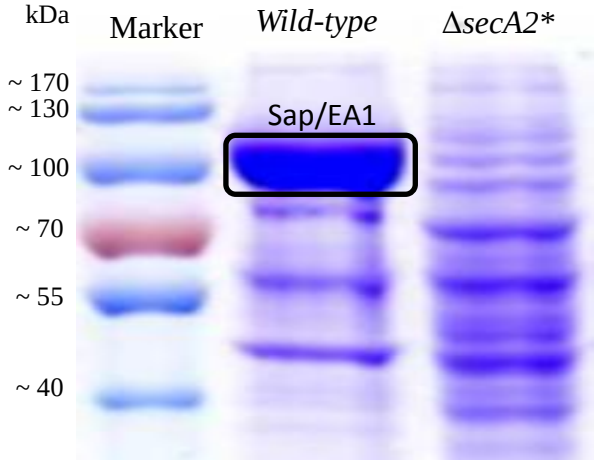

Figure 8.8: Secretion of Sap and EA1 by the Δ*secA2** mutant. The protein corresponding to Sap and EA1 (~90 kDa, circled) is visible in the wild type strain but not the Δ*secA2** mutant. Marker = PageRuler™ Prestained Protein Ladder

Acknowledgement: Northern blotting experiments were done in collaboration with Dr. Susanne Pohl.

8.5 Discussion

Prior to this thesis, it was found that SecA2 of *B. anthracis* is involved in the secretion of S-layer proteins: Sap and EA1 (*Pohl et al.*, unpublished). In this study, we also investigated the role of the gene *BA0881*, which function was not previously identified. As this gene is located in the same operon as *secA2*, we thought that it might be implicated in the SecA2-mediated translocation, possibly conferring SecA2 specificity to its substrates. We re-named *BA0881* as '*secH*'. Selectable marker approach was used to delete target genes, the target gene being replaced by the gene of the selectable marker *i.e.* kanamycin resistance gene. However, gene deletions generated using this approach may result in polar effects, if neighbouring genes are located in the same operon or in close proximity. Indeed, Northern blot analysis showed that the Δ*secA2* does not express *secH* and consequently behaves phenotypically like Δ*secA2H*. Attempts were made to construct a Δ*secA2* mutant expressing *secH*. In the first place the Dif/Xer system was used in an attempt to create a markerless *secA2* mutation, but this was unsuccessful because, possibly, the kanamycin resistance cassette was excised from the plasmid too efficiently and before the double crossing-over event had an opportunity to take place. The modified selectable marker approach employed to construct other mutants in this study was successful in generating a Δ*secA2* mutant expressing *secH* (Δ*secA2**). The construct was made in such a way that *secH* was expressed from the P_{secA2H} promoter. The absence of Sap and EA1 secretion was confirmed in Δ*secA2** by SDS-PAGE analysis, thus confirming the absolute requirement of SecA2 but not SecH for the secretion of S-layer proteins. Analysis of this mutant, however, showed that expression of *csaA* and *csaB* genes, located in close proximity to *secA2-secH* operon, is affected. As *csaA* and *csaB* encode products which are responsible for the attachment of all SLH domain-containing proteins to the peptidoglycan, including Sap and EA1 (Mesnage *et al.*, 2000; Kern *et al.*, 2010), then Δ*secA2** could have the display of SLH-containing proteins, other than Sap and EA1, reduced or abolished.

Chapter 9: Growth analysis of created null mutants

The growth analysis was done to determine if the mutants being analysed have the similar pattern of growth and to determine what OD600 values correspond to exponential, transitional and stationary phases. The growth of the *B. anthracis* wild type in LB broth was compared with that of several mutants, namely: Δ*secA2*, Δ*secA2**, Δ*secH*, Δ*secA2H*, Δ*prsAA*, Δ*prsAB*, Δ*prsAC*, Δ*sap-eag*. LB broth cultures were inoculated with overnight cultures and incubated at 37^{o}C with shaking (180 rpm). Samples were taken every 60 minutes to measure OD_{600} of each culture. The OD_{600} values were plotted against time and resulting growth curves are shown on the Figures 9.1 and 9.2.

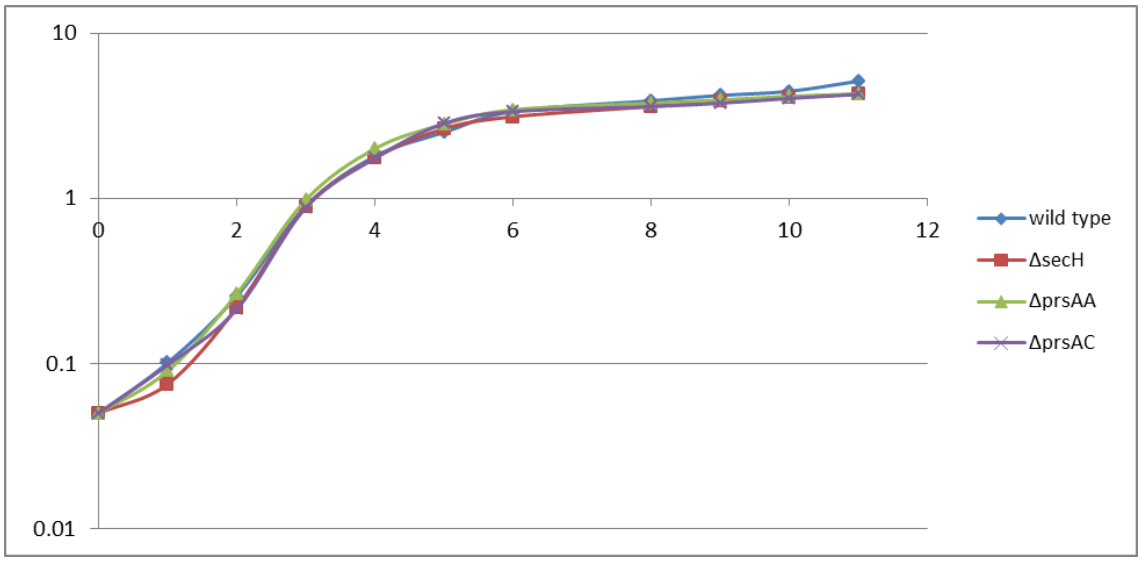

Figure 9.1: Growth curves of *B. anthracis* UM23C1-2 (wild type), Δ*secH*, Δ*prsAA*, Δ*prsAC*. Bacterial cultures were grown with shaking (180 rpm). Samples were taken every 60 minutes to measure OD_{600}. The OD_{600} values were plotted against time.

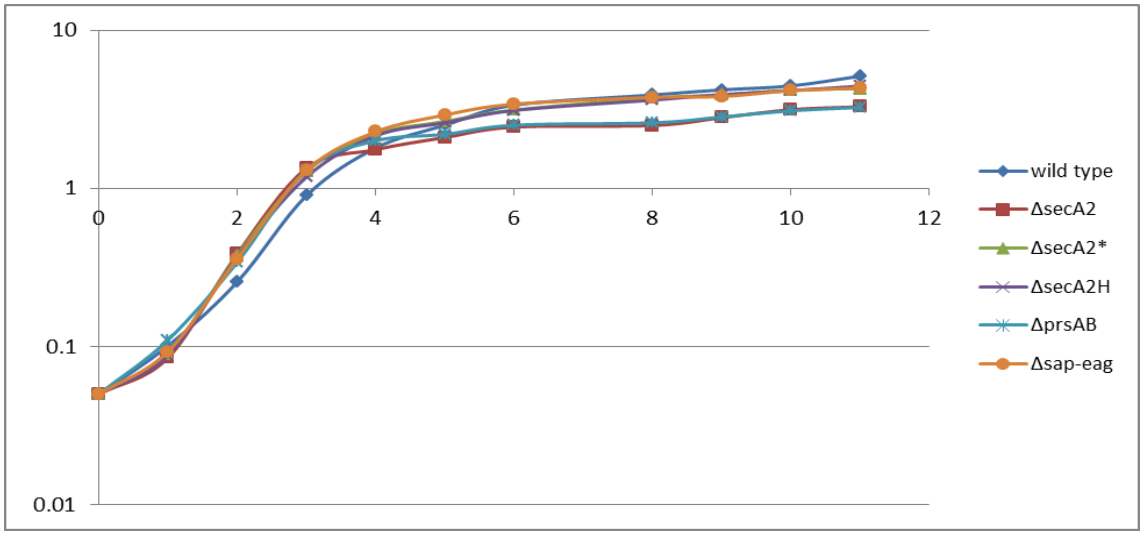

Figure 9.2: Growth curves of *B. anthracis* UM23C1-2 (wild type), Δ*secA2*, Δ*secA2**, Δ*secA2H*, Δ*prsAB* and Δ*sap-eag*. Bacterial cultures were grown with shaking (180 rpm). Samples were taken every 60 minutes to measure OD_{600}. The OD_{600} values were plotted against time.

The analysis of the strains of *B. anthracis* (Figures 9.1 and 9.2) shows that they all enter the exponential phase around OD_{600} of 0.1; the transitional phase starts around OD_{600} of 1.3 and the stationary phase around OD_{600} of 3.0. Knowing what values of OD_{600} correspond to which growth phase it was subsequently possible to design experiments investigating changes in the gene expression and in the cell morphology in the specific growth phases.

Chapter 10: Analysis of gene expression of *sap* and *eag* in *B. anthracis* mutants

Since, the deletion of the *B. anthracis secA2* gene abolishes the secretion of Sap and EA1, it was assumed that these proteins would accumulate in the cytoplasm. However, analysis of the intracellular fraction of *B. anthracis* Δ*secA2* mutant failed to detect any significant accumulation of EA1 and Sap in the cytoplasm (Figure 10.2). This observation suggests that SecA2 acts not only as a molecular motor for the secretion of EA1 and Sap, but also plays a chaperone-like role. Hence, in the absence of SecA2, its substrates are prone to degradation. However, the absence of EA1 and Sap from the cytoplasm, might also have been due to the down-regulation of their gene expression. This possibility was investigated initially by Northern blot, followed by qPCR analysis.

10.1 Investigation of *sap* and *eag* expression by Northern blotting and qPCR

Total RNA was isolated from cultures of wild type *B. anthracis* as well as Δ*secA2* (*secA2*-null mutant which encodes *secH*, but fails to expresses it), Δ*secH*, Δ*secA2H*, Δ*prsAA*, Δ*prsAB*, Δ*prsAC*, Δ*secY2*. The extracted RNA (2 µg) was subjected to Northern blotting against *sap*- and *eag*-specific probes. The analysis of the blots shows that expression of both *eag* and *sap* is down-regulated in the Δ*secA2* and Δ*prsAB* mutants (Figure 10.1).

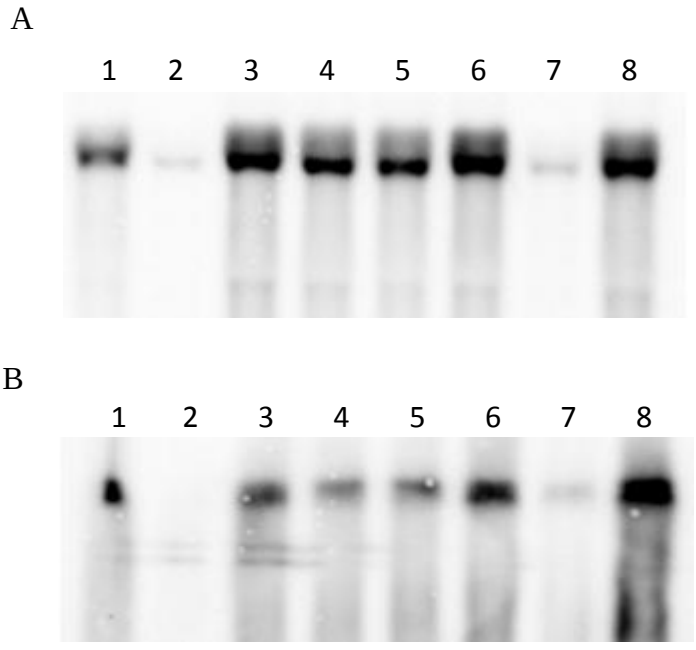

Figure 10.1: Northern blot analysis of: (1) *B. anthracis* wild type, (2) Δ*secA2*, (3) Δ*secY2*, (4) Δ*secH*, (5) Δ*secA2H*, (6) Δ*prsAA*, (7) Δ*prsAB*, (8) Δ*prsAC* with A, *eag*-specific probe; B, *sap*-specific probe. RNA was extracted from LB broth culture at an OD_{600} of ~ 0.8.

The down-regulation of *sap* and *eag* in the Δ*secA2* and Δ*prsAB* mutants was unexpected, particularly since SecA2 and PrsAB have different cellular locations: SecA2 being cytoplasmic and PrsAB tethered to the outer leaf of the cytoplasmic membrane. Since the absence of either SecA2 or PrsAB results in decreased *sap* and *eag* expression, it is likely that their influence on *sap* and *eag* expression is indirect. One possibility that we consider is that the absence of this protein might trigger cell wall stress. However, it is important to recognise that the stress might not be the absence of either Sap or EA1, but to an as yet unidentified substrate of SecA2 and PrsAB. The altered cell morphology of cells of the Δ*secA2* and Δ*prsAB* mutants (Figures 12.1 and 12.2, **Section 12.1**) tends to support this hypothesis.

The influence of SecA2 and PrsAB on the expression of *sap* and *eag* was further investigated by relative quantitative PCR. In addition to the mutants analysed by Northern blotting (Figure 10.1), Δ*secA2** (*secA2*-null mutant expressing *secH*) was analysed to distinguish between the effects of Δ*secA2* and Δ*secH*. RNA was isolated from cultures harvested in the exponential (OD_{600} ~ 0.8), transitional (OD_{600} ~ 2.2) and stationary (OD_{600} ~ 4.5) phases and qPCR was performed as described in the **Section 2.8.3**.

Ct values obtained for the analysed strains were used to calculate the fold change of expression *eag* and *sap* in the analysed mutants. Firstly, the change of expression of those genes during bacterial growth cycle was analysed. The fold change of expression of *eag* and *sap* was calculated for the transitional and stationary phases in reference to the exponential phase (Table 10.1, first two columns). In the case of the wild type, *eag* expression decreased in the transitional phase, and peaked in the stationary phase, while *sap* expression did not change much in the transitional phase, but exhibited strong down-regulation of *sap* in the stationary phase. This observation is consistent with the growth phase-dependent manner of Sap and EA1 production, where Sap is produced predominantly in the exponential phase and EA1 in the stationary phase with *sap* expression peaking at the exponential phase and that of *eag* at the stationary phase (Mignot *et al.*, 2002). In the case of *eag*, in the analysed mutants, the pattern of change in the gene expression was also similar to the wild type, although the increase in *eag* expression in the stationary phase was not so big, apart from the Δ*prsAC* mutant. In case of *sap*, in Δ*secH*, Δ*secA2H*, Δ*prsAA*, Δ*prsAC*, Δ*secY2* as in the wild type, the gene expression did not change much in the transitional phase, and down-regulation of *sap* was observed in the stationary phase. However, apart from the Δ*prsAC* mutant, the decrease in *eag* expression in the stationary phase in those strains was not so big as in

the wild type. In Δ*secA2* and Δ*prsAB*, *sap* was down-regulated in the transitional phase but its expression in the stationary phase increased towards the level observed in exponential phase. Δ*secA2** showed no much difference in *sap* expression in both transitional and stationary phases.

Table 10.1: The fold change of expression *eag* and *sap* in the analysed mutants by qPCR. The first two columns show the fold change of expression of those genes during bacterial growth cycle (in the transitional and stationary phase in reference to the expression in exponential phase). The three last three columns show the fold change in expression of *eag* and *sap* in reference to the wild type strain; Δ*sap-eag* was used as a negative control strain.

		Fold change with respect to the exponential phase		Fold change with respect to the wild-type		
	Strain	transitional phase	stationary phase	exponential phase	transitional phase	stationary phase
eag	Wild type	-4.8	12.9	-	-	-
	Δ*secA2*	-1.3	1.6	-9.6	-2.6	-72.5
	Δ*secA2**	-5.3	3.3	1.2	1.2	-3.0
	Δ*secH*	-20.1	1.8	3.5	-1.2	-2.0
	Δ*secA2H*	-14.4	2.3	3.0	1.0	-1.8
	Δ*secY2*	-24.5	1.7	7.8	1.6	1.1
	Δ*sap-eag*	-	-	-1484.7	-331.3	-1329.2
	Δ*prsAA*	-17.1	1.6	5.7	1.6	-1.4
	Δ*prsAB*	-2.2	3.1	-8.5	-3.8	-35.2
	Δ*secAC*	-8.7	11.9	-1.1	-2.0	-1.2
sap	Wild type	-1.8	-48.5	-	-	-
	Δ*secA2*	-5.8	-1.8	-3.8	-12.3	7.1
	Δ*secA2**	-0.8	-1.5	-4.1	-1.9	8.1
	Δ*secH*	-0.2	-5.6	-13.3	-1.5	-1.5
	Δ*secA2H*	-0.3	-11.7	-6.9	-1.3	-1.6
	Δ*secY2*	-0.4	-9.9	-4.7	1.0	1.0
	Δ*sap-eag*	-	-	-15329.3	-7650.7	-166.3
	Δ*prsAA*	-0.2	-5.5	-9.3	-1.3	-1.0
	Δ*prsAB*	-3.1	-1.4	-3.9	-6.8	9.0
	Δ*secAC*	-0.6	-25.1	-1.4	2.0	1.4

Secondly, the Ct values obtained for the wild type strain were used as reference points to calculate the fold change in expression of *eag* and *sap* in the analysed mutants in reference to the wild type (Table 10.1, last three columns; Figure 10.2). The down-regulation of *eag* and *sap*, observed in the Northern blotting experiment, was confirmed in both exponential and transitional phase in the Δ*secA2* and Δ*prsAB* mutants. In stationary phase, *eag* was down-regulated while *sap* was up-regulated. Unexpectedly, Δ*secA2H,* although phenotypically similar to Δ*secA2*, since neither expresses *secH*, did

not show the same pattern of changes in *eag* and *sap* expression. In Δ*secA2H*, *eag* was overexpressed, while *sap* was down-regulated in the exponential phase; little or no variation was observed in transitional and stationary phase. Δ*secA2** showed a similar pattern of gene expression to Δ*secA2* and Δ*prsAB* in the stationary phase (down-regulation of *eag*, up-regulation of *sap*); However, in the transitional phase *sap* and *eag* Δ*secA2** showed no significant change in expression, while in the exponential phase there was no change in expression of *eag*, but down-regulation of *sap*. It is noteworthy that four mutants: Δ*secH*, Δ*secA2H*, Δ*prsAA*, Δ*secY2*, exhibited the same pattern of expression in the exponential phase: up-regulation of *eag* and down-regulation of *sap*. The analysis of *eag* and *sap* expression confirmed that the absence of SecA2 and PrsAB resulted in changes in the expression of *sap* and *eag*. It was interesting to note that the expression pattern of the three mutants with lesions at the *secA2*, *secH* locus, namely Δ*secA2**, Δ*secA2* and Δ*secA2H* differed significantly. The differences in expression in Δ*secA2** as compared to Δ*secA2* and Δ*secA2H* may be the result of the presence in the former of a functional *secH* gene. The reasons for differences in the expression pattern of Δ*secA2* and Δ*secA2H* are not clear, since phenotypically they are similar; neither is able to express *secA2* or *secH*. The deletion of other genes (*secY2*, *secH*, *prsAA*, *prsAC*) whose products are involved in secretion also caused changes in *sap* and *eag* expression. The expression of *eag* was up-regulated and of *sap* was down-regulated in the exponential phase in Δ*secY2*, Δ*secH* and Δ*prsAA*; while the expression of *eag* was down-regulated and of *sap* up-regulated in the transitional phase in Δ*prsAC*.

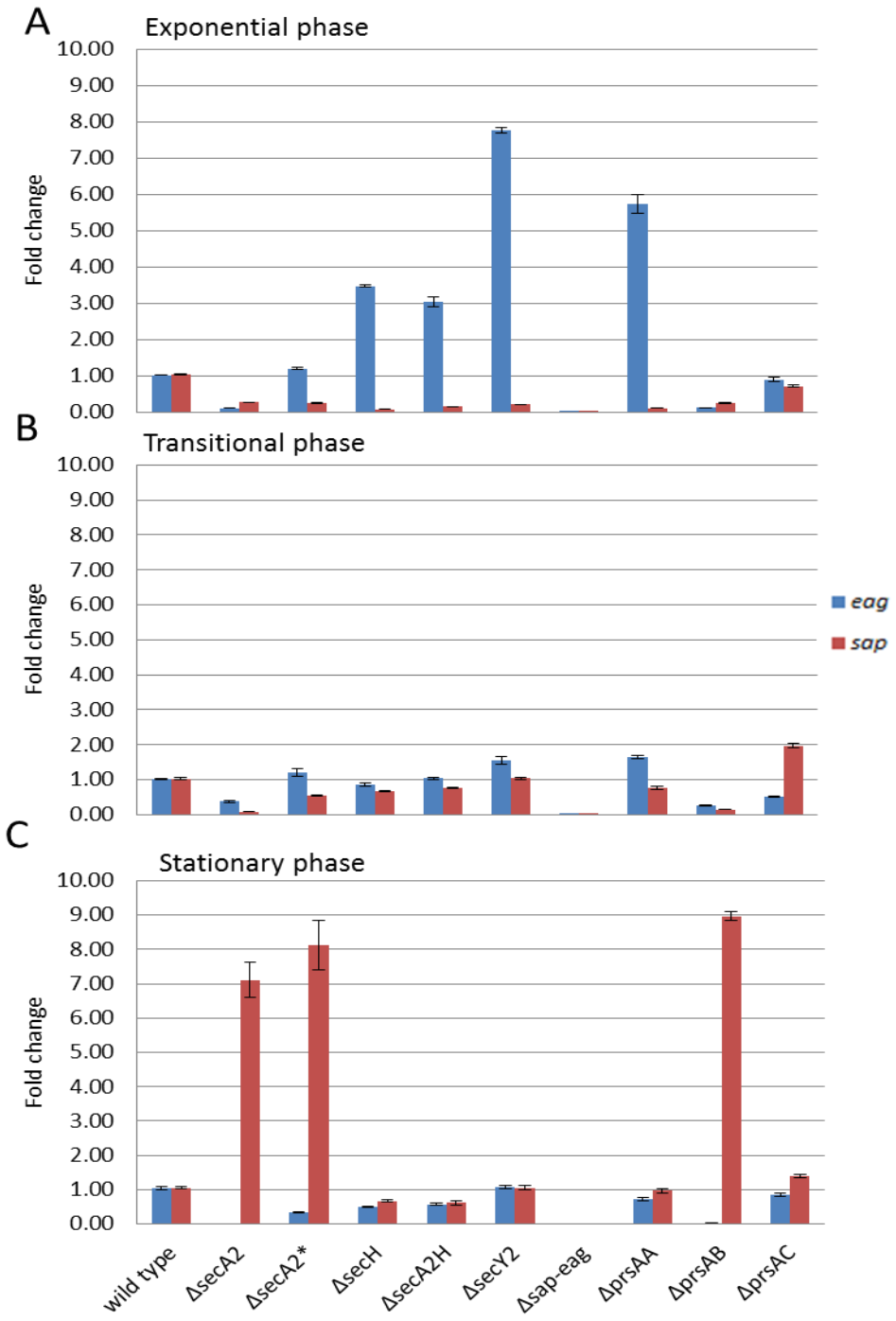

Figure 10.2: Changes in the expression of *eag* and *sap* in various secretion mutants of *B. anthracis* compared to the wild type. RNA was isolated from cultures in: **A**. exponential (OD ~ 0.8); **B**. transitional (OD ~ 2.2); **C**. stationary phase (OD ~ 4.5). The expression was determined by SYBR green real-time relative quantitative PCR (qRT-PCR), normalised against the reference gene *gyrB*. Error bars represent standard deviations

Acknowledgment: Northern blotting experiments and qPCR experiments were done in collaboration with Dr. Susanne Pohl.

10.2 Discussion

In the absence of SecA2 and PrsAB, no EA1 and Sap are detected either in the culture supernatant or in the cytoplasm. The latter observation suggests that SecA2 might have a chaperone function. We therefore decided to study the effect of various secretion mutants on *eag* and *sap* expression. The initial conclusions drawn from Northern blotting analysis indicated that a lack of SecA2 and PrsAB had a supressing effect on expression of *eag* and *sap*. These data were supported by subsequent qPCR experiments. Moreover, qPCR showed that this observation extends to other components of secretion machinery occurring both inside (SecY2, SecH) as well outside (PrsAA, PrsAC) the cell. Since SecA2 and PrsAB are active in different cellular compartments this suggests that the effect on *eag* and *sap* expression was indirect. Such one indirect effect might come from the putative cell wall stress caused by the lack or reduction in presence of S-layer proteins on the surface of the cell wall in Δ*secA2**, Δ*secA2*, Δ*secH*, Δ*secA2H*, Δ*prsAB* or due to the absence of an as yet unidentified component(s) of the cell envelope that is/are substrate(s) of PrsAA, PrsAC, PrsAB, SecA2, SecH, SecY2.

The cell wall stress, which could be induced by the lack or reduction of the cell surface components, could lead to the triggering of a two-component signal transduction system, such as WalRK, which has been shown previously to sense cell wall stress (Cao *et al.*, 2000, Dubrac *et al.*, 2007). WalRK is a typical two-component system consisting of a transmembrane sensor kinase, (WalK) and the response regulator (WalR). The sensor kinase WalK senses a signal that leads to its activation via autophosphorylation. WalK in turn phosphorylates its cognate transcriptional response regulator WalR, the activated form of which modulates its own gene expression and that of members of the WalRK regulon. Members of WalRK regulon encode proteins such as autolysins, that are involved in the cell wall metabolism (Dubrac *et al.*, 2008). It is possible that activation of the two-component system, like WalRK could lead to the modulation of *sap* and *eag* expression. Alternatively, the cell wall stress could be related to the transcriptional attenuator, LytR which was identified as potentially interacting with SecH in the pull-down experiment (**Section 6.2**). If LytR was also a substrate for SecA2 and possibly PrsAB, then the absence of SecA2 and PrsAB would lead to the decrease or absence of LytR in the cytoplasmic membrane. The function of LytR is attenuating the expression of genes encoding autolysins. Consequently, absence of LytR could lead to the derepression of those autolysins as observed in *B. subtilis and S. pneumoniae* (Lazarevic *et al.*, 1992; Johnsborg and Håvarstein, 2009). This would, in

turn, lead to cell wall perturbations. The resulting cell wall stress would then be detected by a two-component system, which might modulate *eag* and *sap* expression in analysed mutants.

It is also noteworthy that the results of the qPCR experiment of this study correlate the expression pattern of *sap* and *eag* and the phase-dependent production of Sap and EA1 previously observed by Mignon et al. (2002). They showed that when grown in rich media, *B. anthracis* exhibits growth-phase dependant manner of Sap and EA1 production, where Sap is produced predominantly in the exponential phase and EA1 in the stationary phase with *sap* expression peaking at the exponential phase and that of *eag* at the stationary phase. In this study, the similar pattern of expression was found to be present in the wild type strain: the decrease of *sap* expression and the increase of *eag* expression in the stationary phase, implying that the highest expression of *sap* takes place in the exponential phase while that of *eag* in the stationary phase. In the analysed mutants, overall, the expression of *eag* was also increased in the stationary phase, while the expression of *sap* was decreased in the stationary phase in Δ*secH*, Δ*secA2H*, Δ*prsAA*, Δ*prsAC*, Δ*secY2* mutants, while in Δ*secA2* and Δ*prsAB*, Δ*secA2** not much change was observed.

In many instances when *sap* was up-regulated, *eag* was down-regulated: this was observed in the transitional phase for Δ*prsAC*, and in the stationary phase for Δ*secA2*, Δ*secA2**, Δ*prsAB*. The opposite pattern of expression: *sap* down-regulation and *eag* up-regulation was observed commonly in the exponential phase in: Δ*secH*, Δ*secA2H*, Δ*prsAA*, Δ*secY2*. This observations correlate with findings by Mignon et al. (2002) that Sap binds to the promoter of *eag*, supressing its expression. Thus when *sap* was up-regulated, implying increased production of Sap, then *eag* expression was probably supressed due to the increased Sap levels binding to the *eag* promoter. Similarly, when *sap* was down-regulated, so less Sap was produced, then the level of *eag* expression increased, as the *eag* promoter was predicted not to be repressed by Sap.

The analysis of expression of *sap* and *eag* in Δ*secA2**, *Δ*secH*, Δ*secA2H*, Δ*prsAB*, Δ*secY2* is being continued by microarray analysis, to get more insights what is happening on the transcriptional level in those mutants. The microarray experiments have been already done, but the microarray data are awaiting analysis and they are not included in this thesis.

Chapter 11: Analysis of *B. anthracis* null mutants complemented with *sap* and *eag*

A complementation approach was used to confirm the roles of and to get new insights into various components of the alternative Sec pathways on the secretion of EA1 and Sap. To achieve that, genes of interest were cloned into an expression plasmid pKG400. The recombinant plasmids were then introduced into various *B. anthracis* null mutant strains. Next, the constructed expression plasmid was transformed into *B. anthracis* to analyse the influence of various Sec pathway components on the secretion of Sap and EA1.

11.1 Secretion of Sap and EA1 in *B. anthracis* null mutants complemented with *eag* and *sap*

In a set of reciprocal experiments, the *sap* and *eag* genes were cloned on the complementation plasmid pKG400 and transformed into *B. anthracis* wild type as well as into various mutant strains. The aim was to monitor Sap and EA1 secretion under conditions in which their expression could be controlled independently of their intrinsic promoters and associated regulatory sequences. Consequently, the entire coding sequences of *eag* and *sap* were cloned independently downstream of the P_{grac} promoter of pKG400, to generate pKG400-*sap* and pKG400-*eag*. By transforming these plasmids into strains lacking various components of the accessary Sec pathway, and analysing the resulting supernatant fractions by SDS-PAGE, it was possible to evaluate the effect of these components on the secretion of Sap and EA1 without the complication of any feedback regulation.

The *sap* and *eag* genes were cloned independently into the pKG400 expression vector and subsequently transformed into *B. anthracis* wild type and Δ*secA2**, Δ*secH*, Δ*secA2H*, Δ*prsAB* and Δ*sap-eag* mutants. The presence of the complementation plasmid and its authenticity in each strain was confirmed by restriction digest analysis of purified plasmids. The *B. anthracis* strains complemented with pKG400-*sap* and pKG400-*eag* were grown to an OD_{600} of 0.8 when *sap* or *eag* expression was induced with IPTG. The cultures were incubated by a further 90 minutes and then proteins extracted from the supernatant were analysed by SDS-PAGE. The procedures for extracting proteins for the strains complemented with *sap* and *eag* differed slightly due to their cell wall binding characteristics. The extraction of extracellular proteins from the strains complemented with *sap* was carried out according to the standard procedure (**Section 2.9.2**). As EA1 binds more strongly to the cell wall, the extraction of

extracellular proteins from the strains complemented with *eag* was carried using a modified protocol (**Section 2.9.3**). In this method, lithium chloride was used to break non-covalent interactions between the cell wall and EA1 with the effect of releasing more of this protein into the supernatant. The TCA-precipitated extracellular proteins were subsequently analysed by SDS-PAGE (Figures 11.1 and 11.2). *B. anthracis* wild type and the Δ*sap-eag* mutant served as positive and negative control strain, respectively. Interestingly and unexpectedly, the secretion of Sap was decreased in the wild type strain in the presence of the non-induced pKG400-*sap* complementation plasmid. Similarly, Δ*secH* complemented with the non-induced pKG400-*sap* plasmid showed negligible secretion of Sap compared with the induced sample, even though the previous experiments had clearly shown that Sap is secreted in the absence of *secH*. These results suggest that the additional copies of *sap* on the complementation plasmid lead to a down-regulation of *sap* expression. It raises the possibility of the existence of an antisense RNA species within *sap* with an inhibitory effect on *sap* expression. In contrast, similar levels of EA1 secretion were observed from the *B. anthracis* wild type complemented with pKG400-*eag* irrespective of whether the *eag* gene was induced, and for the wild type with the empty vector (pKG400-empty). In the case of the Δ*secH* mutant, EA1 was secreted irrespective of whether the inducer was added, although the level of secretion increased in the presence of IPTG.

Complementation of the Δ*prsAB* mutant with either *sap* or *eag* gave very different results. In the absence of induction, very little S-layer protein was observed in either case. However, when *sap* was induced, the concentration of Sap in the culture medium was similar to that of the wild type. In contrast, very little EA1 was observed in the culture medium when *eag* was induced. These results suggest that one or more of the following: (1) EA1 is more dependent on PrsAB than Sap, (2) that PrsAA and/or PrsAC can complement PrsAB with respect to Sap but not EA1 secretion (3), that Sap is more/equally dependent on PrsAB than EA1 and that the absence of EA1 is due to it interacting more strongly with the cell wall, meaning that less is secreted into the culture medium.

Finally, the complementation of the Δ*sap-eag* mutant with either Sap or EA1 also gave very contrasting results. While the secretion of Sap was restored by the induced pKG400-*sap* strain, very little EA1 was observed in the culture medium of the induced pKG400-*eag* strain. We concluded that this was likely to be due to the strong binding of EA1 to the cell wall due to the absence of Sap.

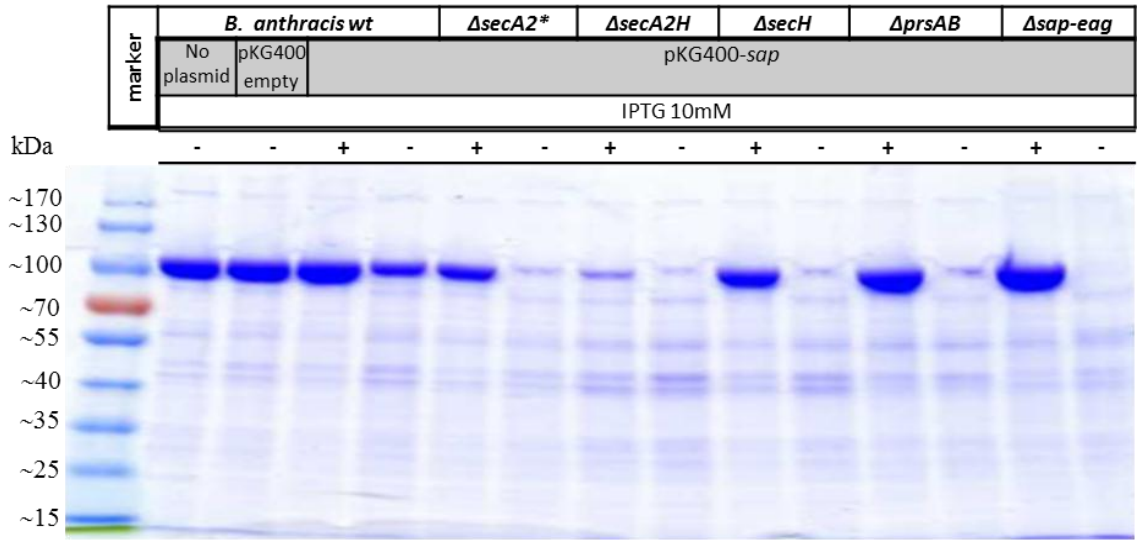

Figure 11.1: Complementation of *B. anthracis* wild type (wt) and Δ*secA2**, Δ*secH*, Δ*secA2H*, Δ*prsAB*, Δ*sap-eag* mutants with the pKG400-*sap* complementation plasmid. Expression of *sap* was induced with 10 mM IPTG (+). Non-induced cultures (-) served as negative controls of expression. The *B. anthracis* wild type and Δ*sap-eag* null mutant served as positive and negative control stain, respectively. Sap is visible as a band of ~ 90kDa.

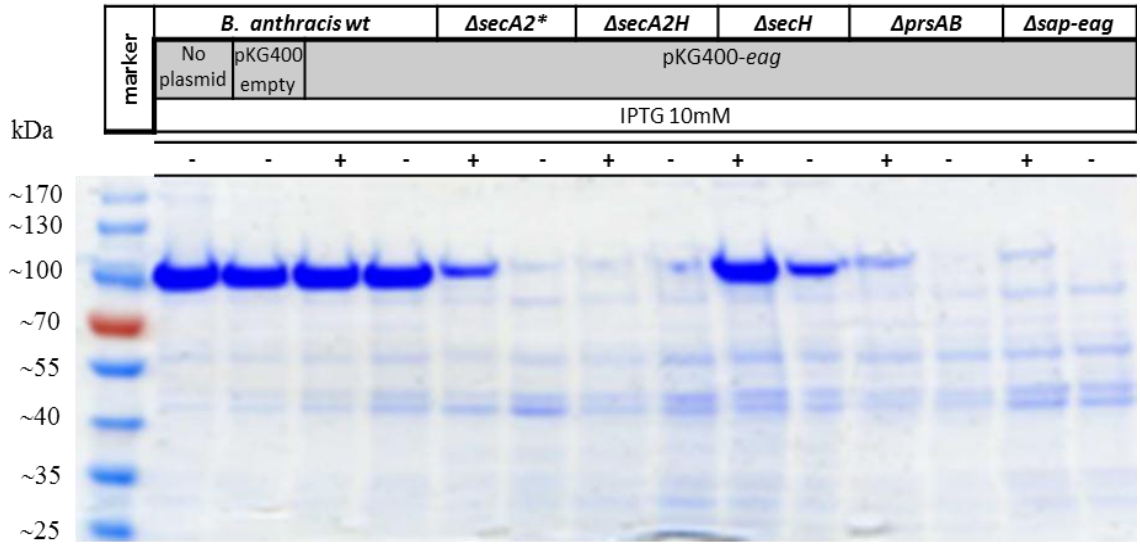

Figure 11.2: Complementation of *B. anthracis* wild type (wt) and Δ*secA2**, Δ*secH*, Δ*secA2H*, Δ*prsAB*, Δ*sap-eag* mutants with pKG400-*eag* complementation plasmid. The expression of *eag* was induced with 10 mM IPTG (+). Non-induced cultures (-) served as negative controls of expression. The *B. anthracis* wild type and Δ*sap-eag* null mutant served as positive and negative control stain, respectively. EA1 is visible as a band of ~ 90kDa.

B. anthracis Δ*secA2** complemented with *sap* or *eag* shows some degree of restoration of Sap and EA1 secretion although at a much lower than in the *B. anthracis* wild type or Δ*secH*, Δ*prsAB*, Δ*sap-eag* mutant strains complemented with *sap*. This confirms the importance in SecA2 in Sap secretion, but also indicates that SecA1 can complement SecA2. This observation is consistent with studies in *B. subtilis* (**Section 5**) showing that both *B. subtilis* SecA and *B. anthracis* SecA1 can mediate Sap and EA1secretion. In Δ*secA2H*, the ability to restore Sap and EA1 secretion is very low, confirming importance of SecH in the secretion of Sap and EA1 in participation with SecA2.

One possible explanation for some of the unexpected results obtained during the complementation studies was that some as yet unidentified factor interfered with the expression of the *sap* or *eag* genes that were not induced in some cases. We therefore carried out Northern blotting analyses on the complementation strains with or without induction (Figures 11.3 and 11.4). Upon induction, the expression of *sap* and *eag* increased in all the strains. It is noteworthy that the non-induced wild-type strain of *B. anthracis* encoding pKG400-*sap*, which shows reduced secretion of Sap, nevertheless shows a level of *sap* mRNA that is at least comparable to that of the wild type without the empty plasmid. This might indicate that putative inhibitory sRNA (small, regulatory) binds to the *sap* mRNA preventing or reducing its translation. The induced levels of *sap* and *eag* mRNA in the complemented Δ*secA2H*, Δ*prsAB*, Δ*sap-eag* (and Δ*secH* in the case of pKG400-*sap*) are much higher than that of the complemented wild type strain. The reason for this increased level of expression was not investigated. The minimal level of Sap in the supernatant of the Δ*secA2H* mutant complemented with *sap*, in spite of its very high expression, confirms again crucial importance of SecA2 for secretion. At the same time, the minimal level of Sap secretion in this complemented strain is again suggestive of the participation of SecA1.

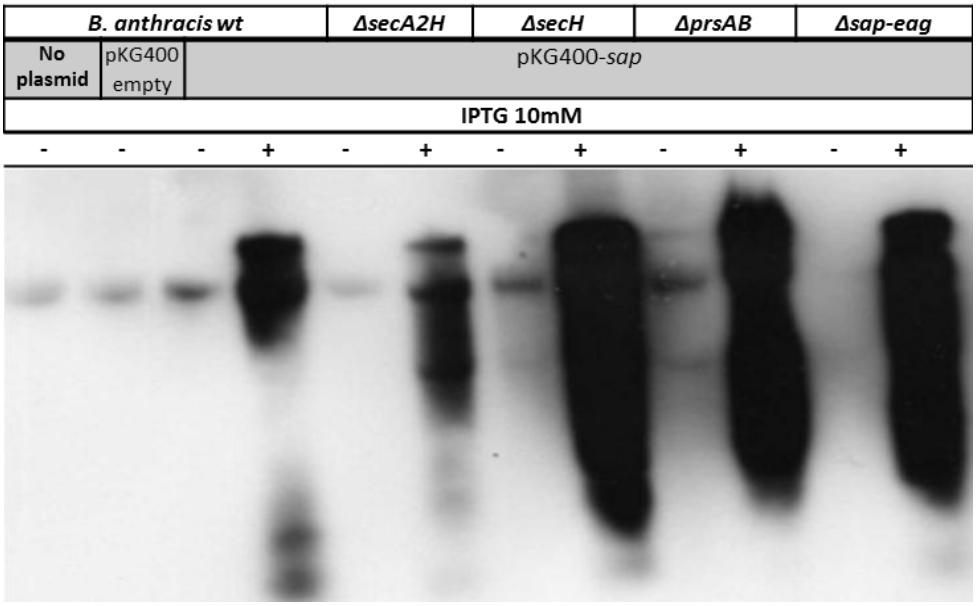

Figure 11.3: Northern blot analysis of the complementation of *B. anthracis* wild type (wt), Δ*secH*, Δ*secA2H*, Δ*prsAB*, Δ*sap-eag* strains with pKG400-*sap*. The expression of *sap* was induced with 10 mM IPTG (+). Non-induced cultures (-) served as negative controls.

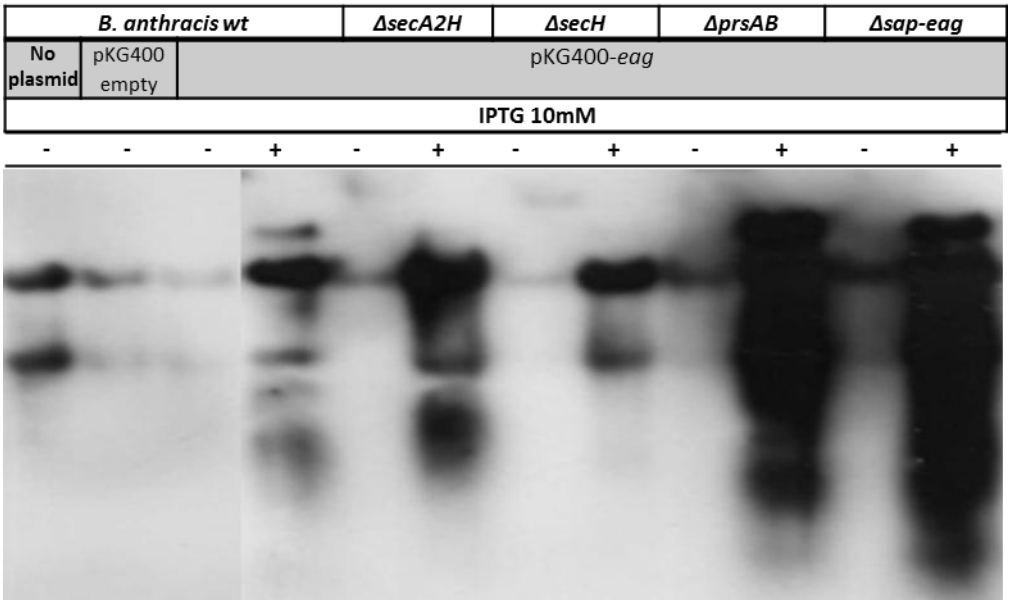

Figure 11.4: Northern blot analysis of the complementation of *B. anthracis* wild type (wt), Δ*secH*, Δ*secA2H*, Δ*prsAB*, Δ*sap-eag* with pKG400-*eag*. The expression of *eag* was induced with 10 mM IPTG (+). Non-induced cultures (-) served as negative controls.

11.2 Discussion

Complementation analysis allowed us to reinforce previous findings as well as get new insights about the secondary translocase of *B. anthracis*. Previous experiments showed the essential role of SecA2 for Sap and EA1 secretion. Similarly, studies in which the Δ*secA2** and Δ*secA2H* mutants were complemented with inducible *sap* and *eag* genes also confirmed the importance of SecA2 in Sap and EA1 secretion. However, these studies also show that SecA1 can mediate the secretion of these proteins in the absence of SecA2. This observation confirms data obtained from *B. subtilis* in which Sap and EA1 were secreted by cells in which either *B. subtilis* SecA or *B. anthracis* SecA1 were the only SecA-like proteins (**Section 5**). These observations support a model in which SecA1, SecA2 and SecH might form a complex with these substrates prior to their translocation through the SecYEG translocation channel.

As shown in **Section 7**, PrsAB is essential for the secretion of Sap and EA1 in *B. subtilis.* Moreover, the deletion of *prsAB*, but not *prsAA* or *prsAC* prevents Sap and EA1 secretion in *B. anthracis.* Because the expression of *eag* and *sap* is down-regulated in the Δ*prsAB* mutant, it was necessary to study the role of PrsAB in strains in which *sap* and *eag* expression was maintained. These showed contrasting results. EA1 appears to be significantly more dependent on PrsAB-mediated folding than Sap. This implies either that Sap is less PrsAB-dependent or that PrsAA and/or PrsAC may contribute to its folding. Thus, the lack of secretion of Sap and to some extent EA1 in the non-complemented Δ*prsAB* mutant might be due to the suppression of *sap* and *eag* expression from their native promoters. The putative cell wall stress mediated suppression in Δ*prsAB* could be triggered not only by absence of the S-layer proteins but also by an as yet unidentified PrsAB substrate(s) involved in cell wall metabolism.

In conclusion, these complementation studies add to the complexity of *eag* and *sap* regulation and the extent of their interaction with the cell wall. Complementation of *B. anthracis* wild type and *B. anthracis* Δ*secH* with *sap* suggest that there may also be inhibitory regulation of the *sap* expression by sRNA species encoded within *sap* gene. The inhibition might be achieved by preventing protein synthesis from *sap* mRNA.

Chapter 12: Analysis of cell morphology of *B. anthracis* mutants

12.1 Analysis of cell morphology by florescent microscopy

The deletion of genes encoding proteins involved in the secretion processes (SecA2, SecH, SecY2, PrsAA, PrsAB, PrsAC) and S-layer proteins (Sap and EA1), which were investigated in this study, could lead to changes in cell morphology. Firstly, absence or shortage of S-layer in Δ*secA2**, Δ*secH*, Δ*secA2H*, Δ*prsAB*, Δ*sap-eag* mutants could be causing some changes to the cell shape as S-layer is part of the cell envelope. If it is the case, it would indicate that the S-layer takes part in maintaining cell shape. If there was no change to the cell shape in Δ*sap-eag*, but it could be observed in Δ*secA2**, Δ*secH*, Δ*secA2H*, Δ*prsAB*, it would indicate that those mutants were defective in secretion of other substrate(s) than Sap and EA1 that are involved in the cell wall metabolism. Changes to the cell morphology of Δ*secY2* and Δ*prsAA* and Δ*prsAC* also would suggest their participation in secretion of substrates is important for maintaining the cell shape. To carry out evaluation of the cell morphology of the mutants being analysed, fluorescence microscopy was carried out. Cultures of *B. anthracis* wild type as well as Δ*secA2**, Δ*secH*, Δ*secA2H*, Δ*prsAA*, Δ*prsAB*, Δ*prsAC*, Δ*sap-eag* were sampled during the exponential (OD_{600}=0.6-0.8) and transitional (OD_{600}=2.0-2.5) phases. Aliquots of cultures were treated with the FM5-95 membrane stain (final concentration 1μg/ml) and mounted onto a microscope slide coated with 1.2% agarose and immobilized using a glass cover slip and images were acquired on an Axiovert M200 microscope (Zeiss Ltd., Oberkochen, Germany) (**Section 2.16**). The lengths of cells were measured using ImageJ software (http://rsb.info.nih.gov/ij) and the data are presented in the Table 12.1 together with the number of cells counted and variance values. The percentage of change of the cell length in relation to the wild type of *B. anthracis* is presented in the Table 12.2 (columns 1 and 2). Considerable differences were observed in shapes and/or sizes for cells of the *B. anthracis* Δ*secA2**, Δ*prsAA* and Δ*prsAB* mutants, both during the exponential and transitional phases (Figures 12.1 and 12.2, respectively). The significance of the change in their cell length in comparison with the wild type was confirmed statistically using the unpaired t-test, with p values below the significance level (0.05) for those strains (Table 12.2, columns 3 and 4). Cells of wild type *B. anthracis*, used as a control, were short and straight with average lengths of 4.01 μm and 3.97 μm in the exponential and transitional phase, respectively. Cells of Δ*secA2** were filamentous and some were twisted, with an average length of 7.95 μm in exponential phase and 8.56 μm in the transitional phase. Cells of Δ*prsAB* were also on

average longer and somewhat more twisted than the wild type with average lengths of 5.45 µm and 5.15 µm in the exponential and transitional phase, respectively. Cells of the Δ*prsAA* mutant were on average longer and somewhat twisted in comparison to the wild type, with average lengths of 4.95 µm and 4.76 µm in the exponential and transitional phase, respectively.

Histograms were used to illustrate the range of cell lengths of the wild type and mutants (Figures 12.3 and 12.4). The lengths of the wild type ranged from 2.0-7.0 µm in exponential phase and 2.0-9.0 µm in transitional phase. Overall, the range of cell length was related to the average length of cells in the analysed mutants. In all cases the range of lengths of the Δ*prsAA*, Δ*prsAB*, Δ*secA2** mutants was much larger; 2.0-45 µm and 2.0-30 µm in the case of the Δ*secA2** mutant in the exponential and transitional phase, respectively; 2.5-15.0 µm and 2.0-12.0 µm for the Δ*prsAB* mutant in the exponential and transitional phase, respectively, and 2.0-12.0 µm and 1.0-9.0 µm for the Δ*prsAA* mutant in the exponential and transitional phase, respectively. The shapes, average lengths and range of lengths of the other mutants (Δ*secH*, Δ*secA2H*, Δ*prsAC*, Δ*sap-eag* and Δ*secY2*) were not significantly different from those of the wild type (Table 12.1 and 12.2, Figures 12.1 and 12.2).

Table 12.1: The average lengths of cells during exponential and transitional phase of the analysed *B. anthracis* wild type and mutants. The range of lengths of *B. anthracis* wild type, Δ*secA2**, Δ*prsAA, and* Δ*prsAB* are shown on histograms (Figures 13.3 and 13.4). The number of cell counted is shown in columns 3 and 4. Variance is presented in columns 5 and 6.

	Growth phase					
	exponential	transitional	exponential	transitional	exponential	transitional
	average length (µm)		**Number of cells counted (n)**		**Variance**	
Wild type	4.01	3.97	100	121	0.88	0.86
Δ*secA2**	7.95	8.56	121	103	24.50	20.19
Δ*secH*	3.76	3.55	102	102	0.57	0.85
Δ*secA2H*	3.89	3.75	103	121	0.81	0.78
Δ*prsAA*	4.95	4.76	101	98	2.47	1.45
Δ*prsAB*	5.45	5.15	103	113	4.85	4.12
Δ*prsAC*	3.90	3.86	107	114	0.65	0.74
Δ*sap-eag*	3.42	3.56	102	105	0.60	0.81
Δ*secY2*	4.12	3.69	107	106	0.58	0.85

Table 12.2: The change in the cell length, in relation to the wild type in exponential and transitional phases, is presented in first two columns; two last columns show statistical significance of change of cell length of the null mutnt strains in comparison to the cell length of the *B. anthracis* wild type evaluated by unpaired t-test. The significance level = 0.05.

	Growth phase			
	exponential	transitional	exponential	transitional
	change in average length (%)		***p* values**	
Wild type				
Δ*secA2**	+98	+116	1.7E-35	6.0E-39
Δ*secH*	-6.0	-11	0.70	0.98
Δ*secA2H*	-3	-6	0.87	0.98
Δ*prsAA*	+23	+20	3.1E-19	7.4E-21
Δ*prsAB*	+36	+30	3.6E-29	6.6E-22
Δ*prsAC*	-3	-3	0.98	0.99
Δ*sap-eag*	-15	-10	0.93	1.00
Δ*secY2*	+3	-7	0.06	0.97

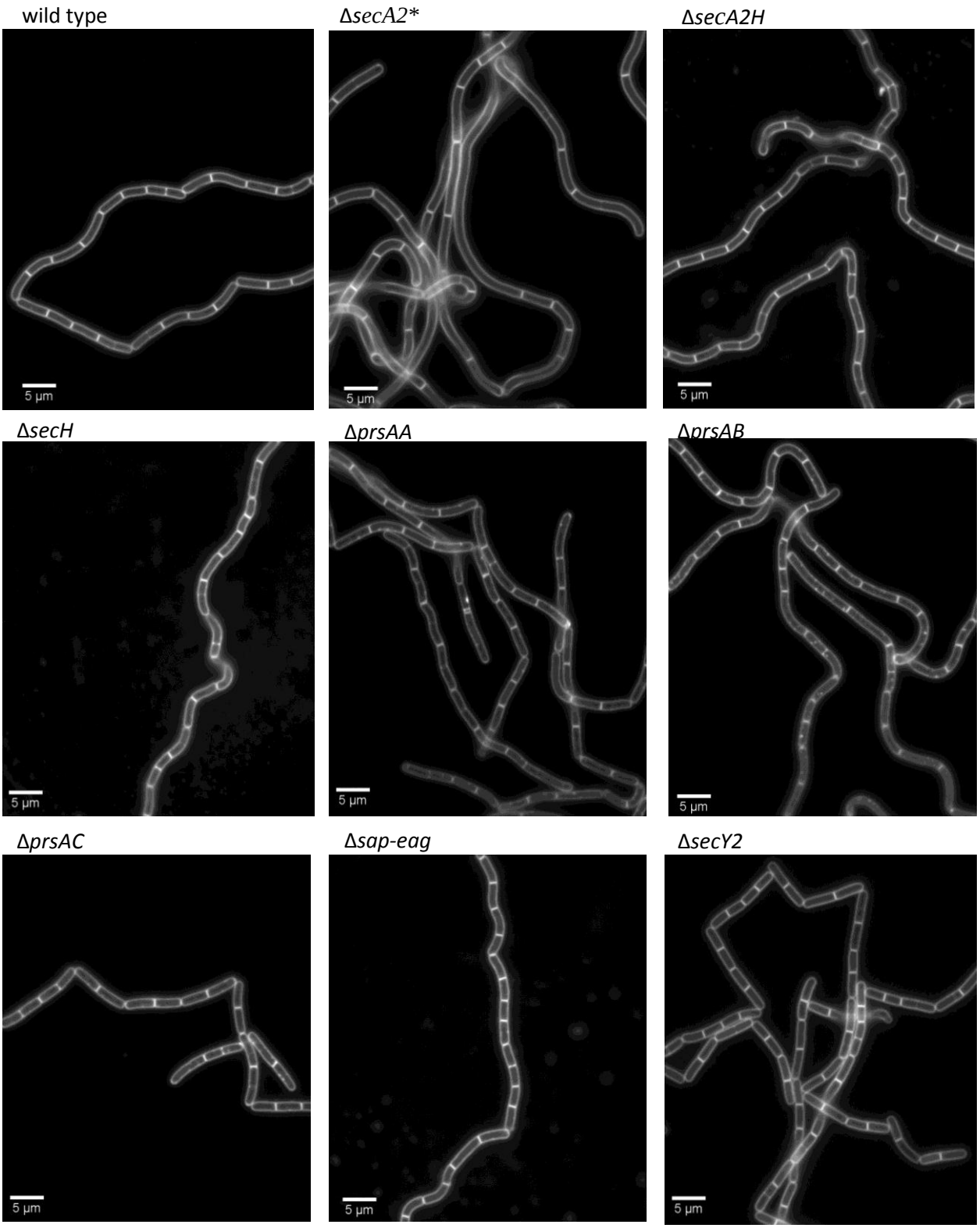

Figure 12.1: Micrographs of *B. anthracis* wild type and Δ*secA2**, Δ*secH* Δ*secA2H*, Δ*prsAA*, Δ*prsAB*, Δ*prsAC*, Δ*sap-eag* and Δ*secY2* mutants in exponential phase. Cells were stained with the membrane stain FM5-43FX.

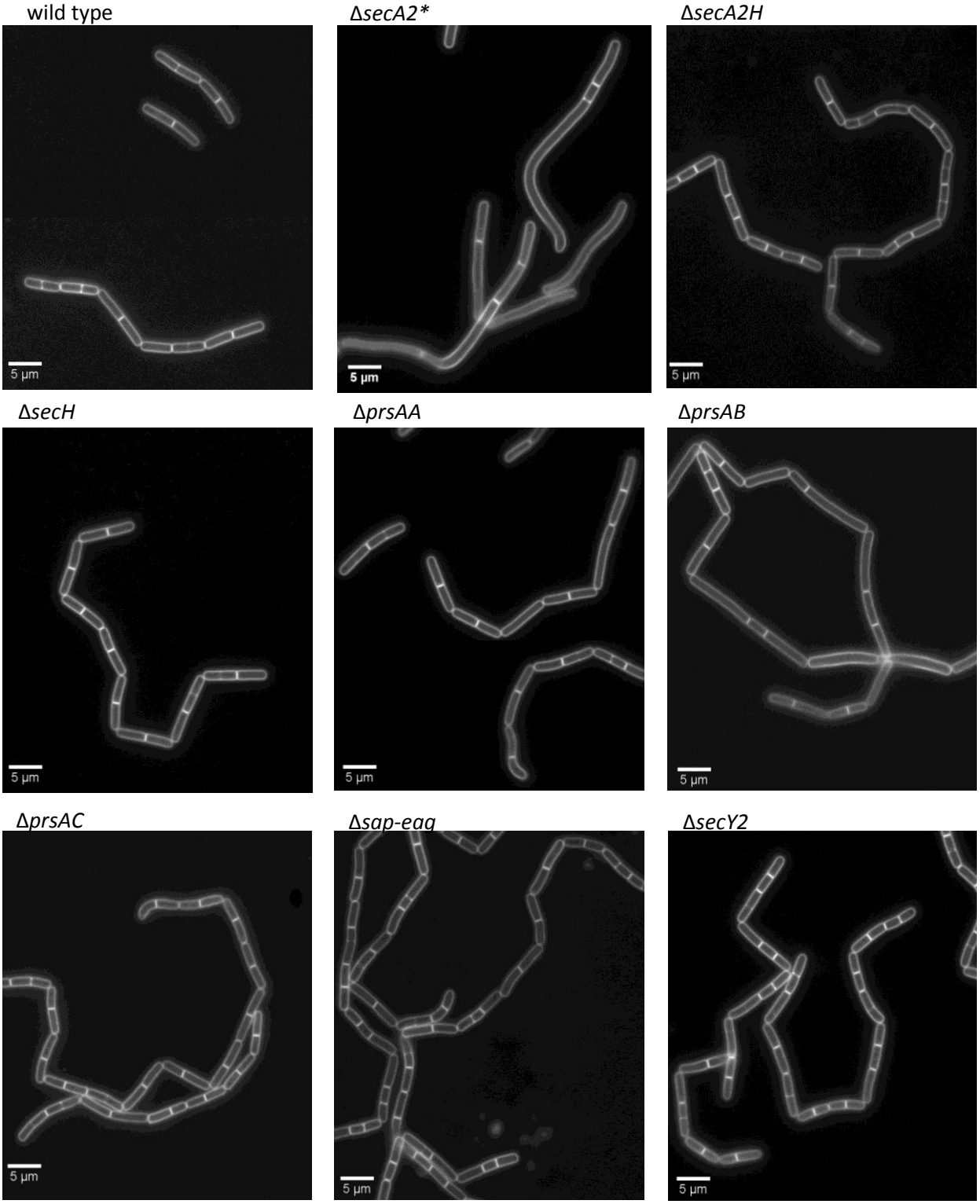

Figure 12.2: Micrographs of *B. anthracis* wild type and Δ*secA2**, Δ*secH* Δ*secA2H*, Δ*prsAA*, Δ*prsAB*, Δ*prsAC*, Δ*sap-eag* and Δ*secY2* mutants in transitional phase. Cells were stained with the membrane stain FM5-43FX.

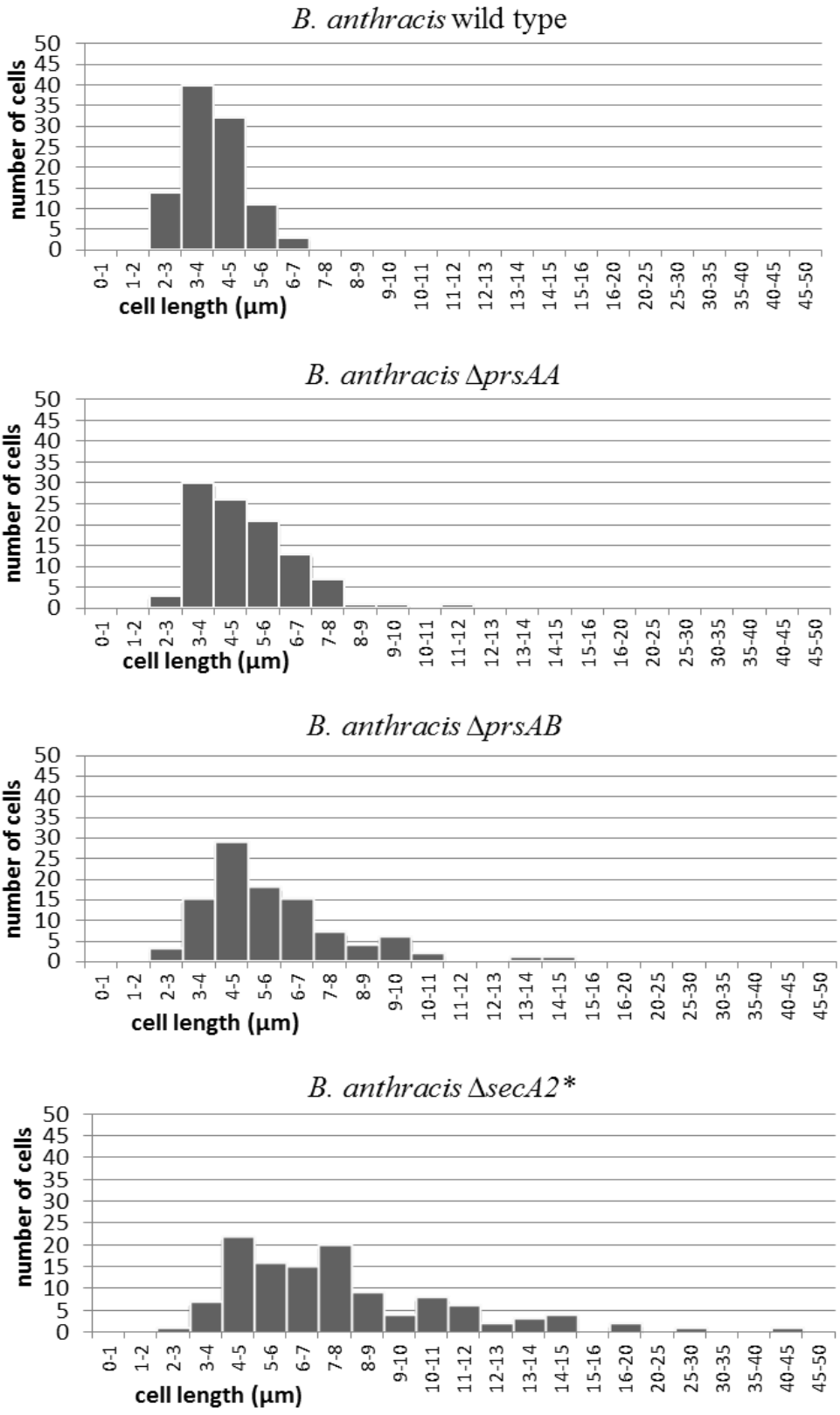

Figure 12.3: Histograms of the distributions of cell length during exponential phase of *B. anthracis* wild type and Δ*prsAA*, Δ*prsAB*, Δ*secA2** mutants.

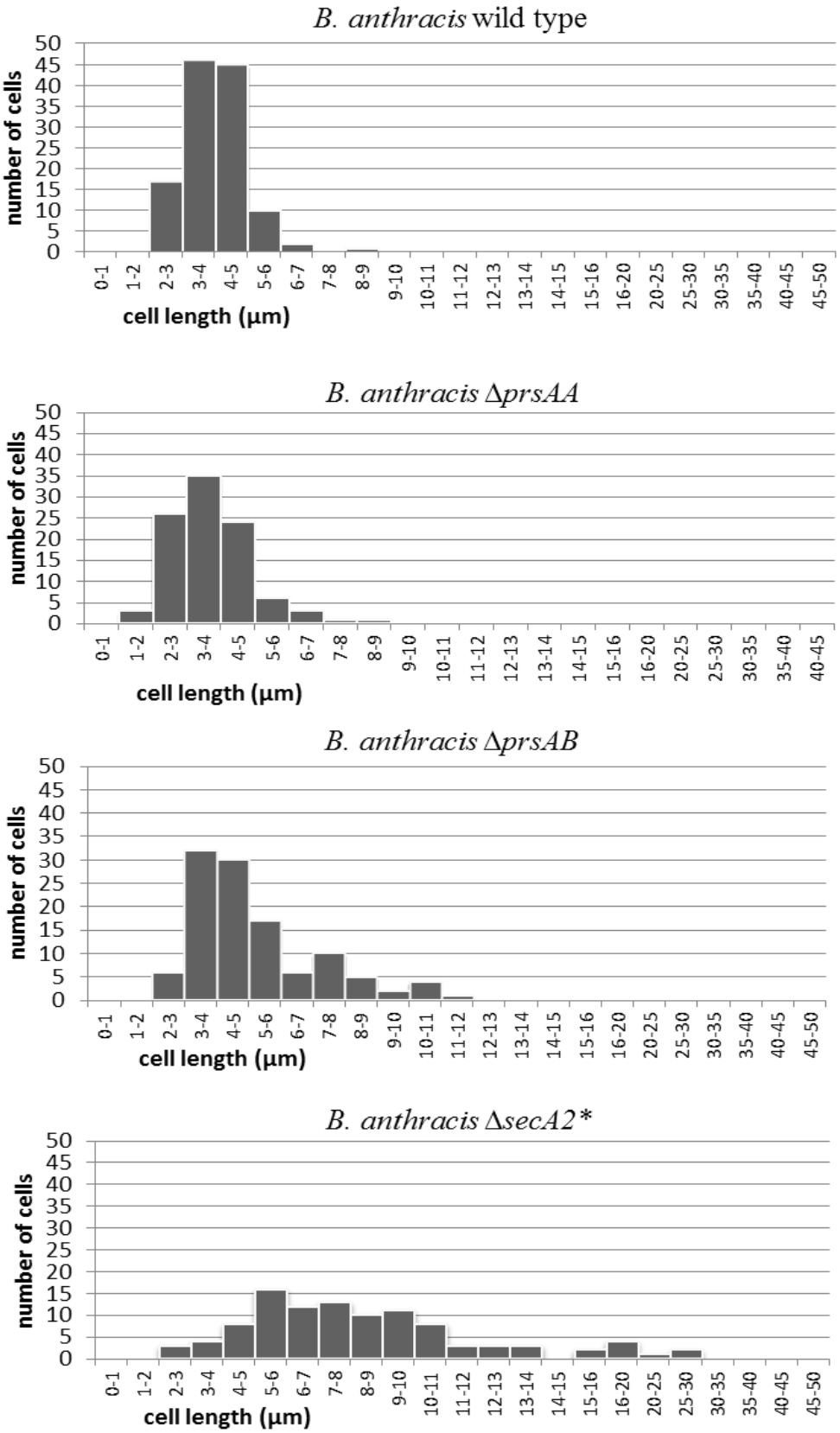

Figure 12.4: Histograms of the distributions of cell length during transitional phase of the *B. anthracis* wild type Δ*prsAA*, Δ*prsAB*, Δ*secA2** mutants.

Acknowledgement: Analysis of cell morphology by fluorescent microscopy was done in collaboration with Dr. Patricia Dominguez-Cuevas.

12.2 The secretion of penicillin binding proteins (PBPs)

The alternations of cell morphology in Δ*prsAA*, Δ*prsAB*, Δ*secA2** are possibly caused by reduction of secretion and activity of enzymes involved in cell wall metabolism. One group of those enzymes are penicillin-binding proteins. To evaluate if they contribute to the alterations in the cell shape of Δ*prsAA*, Δ*prsAB*, Δ*secA2** their activity was analysed. Penicillin-binding proteins are membrane-bound enzymes involved in the synthesis of the peptidoglycan (Macheboeuf *et al.*, 2006). There are three types of PBPs: (i) transpeptidases; (ii) transglycosylases; (iii) bifunctional transpeptidase-transglycosylases. Transglycosylase activity is responsible for polymerisation of the peptidoglycan, while transpeptidase activity is responsible for the cross-linking of peptidoglycan strands. PBPs bind penicillins because β-lactams are structural analogues of their natural substrates, the D-alanyl-D-alanine substituents of the crosslinking peptide of peptidoglycan. Deletion of PBPs leads to changes in cell morphology (length and shape). If secretion of one or more PBPs was to be altered in the Δ*prsAA*, Δ*prsAB*, Δ*secA2**, it might account for the observed changes in their cell morphology. We therefore used the Bocillin assay (**Section 2.14**) to determine the presence of PBPs in these mutants. There is no published detailed information on the PBPs of *B. anthracis* and therefore we annotated PBPs visualised in the Bocillin assay by reference to those of *B. subtilis* and *E. coli*. Six PBPs are detected in *E. coli* (PBP 1a, 1b, 2, 3, 4 and 5) (Zhao *et al.*, 1999), while seven are detected in *B. subtilis* (PBP 1a, 1b, 2a, 2b, 3, 4, and 5) (Hyyryläinen *et al.,* 2010). To confirm that annotation of gel-separated PBPs in *B. anthracis* is correct would require the generation of null mutants for each PBP identified in the *B. anthracis* genome, and comparing their profiles with that of the wild type. As this was beyond scope of this thesis, this has not been done. As the Bocillin assay for PBPs looked more like that of *E. coli*, its annotation was used for *B. anthracis*. Analysis of the PBPs visualised by the Bocillin assay indicated that the PBP profiles of each of the mutants was the same as the wild type excepting that of *prsAA* in which the presence of several bands, putatively named PBP1a/b, PBP2, PBP3 and PBP4 were reduced (Figure 12.5).

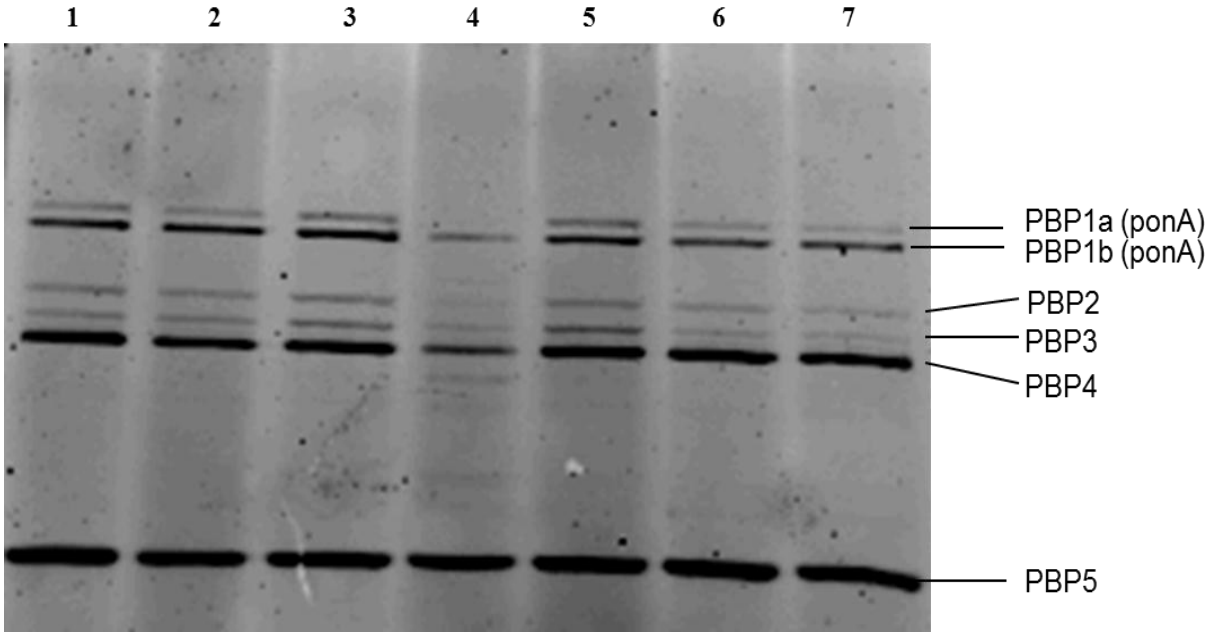

Figure 12.5: Bocillin assay of the PBPs of *B. anthracis* strains: (1) wild type, (2) Δ*secA2**, (3) Δ*secA2H*, (4) Δ*prsAA*, (5) Δ*prsAB*, (6) Δ*prsAC*, (7) Δ*sap-eag* visualised by Fluorography. The presence of PPB1a/b, PBP2, PBP3 and PBP4 is reduced in the Δ*prsAA* mutant but not in the other analysed mutants.

12.3 Discussion

The analysis of cell size data indicates that *B. anthracis* Δ*secA2**, Δ*prsAA* and Δ*prsAB* mutants show an increase in average cell length and range of cell length when compared with the wild type. The Δ*secA2** and Δ*prsAB* mutants also showed changes of cell morphology; the cells were longer and twisted in comparison with the short, straight cells of the wild type and other mutants. This suggests that SecA2 and PrsAB may have substrates other than that of Sap and EA1 that are involved in cell division, for example one or more autolysins, which are enzymes involved in cell wall metabolism. Currently, it is not clear whether these putative additional substrates are the same for SecA2 and PrsAB or distinct, since the cell morphologies of the Δ*secA2** and Δ*prsAB* are similar but not identical. However, PrsA-like proteins are known to have distinct but overlapping substrate specificities and that PrsAA and or AC may, to some extent, compensate for the lack of PrsAB. The analysis of the cell morphology also suggests that a substrate of PrsAA is also involved in the cell wall metabolism. This correlates with the results of the Bocillin assay, which showed a decrease in the activity of some of penicillin binding proteins (PBP1a and 1b, PBP2, PBP3, PBP4). The question arises as to why the cell morphology of the Δ*secA2** mutant is changed, while that of Δ*secA2H* is not. The genes of two proteins involved in the modification of *B. anthracis* cell wall, namely CsaA and CsaB, are located upstream of *secA2* and we used Northern blot analysis to analyse their expression in the Δ*secA2** and Δ*secA2H* mutants (**Section 8.3**).

The resulting data indicated that *csaA/B* were down-regulated in the Δ*secA2** mutant. As *csaA* and *csaB* encode products which are responsible for the attachment of all SLH domain-containing proteins to the peptidoglycan, including Sap and EA1 (Mesnage *et al.*, 2000; Kern *et al.*, 2010), then Δ*secA2** could have the display of SLH-containing proteins, other than Sap and EA1, reduced or abolished. This conclusion would be consistent with the observation that cells of *B. anthracis csaB*-null mutant, like that of the Δ*secA2** mutant, are filamentous and twisted (Mesnage *et al.*, 2000).

Chapter 13: Investigation of interactions between elements of translocation system

In biological systems, the complex processes that take place are often due to the specific interactions that occur between individual components or groups of components. In this study, the bacterial-two hybrid system was employed to investigate interactions between elements of the Sec translocation system and between those elements and their substrates. An attempt was also made to purify SecA1, SecA2 and SecH for analysis by isothermal calorimetry and resolution of their crystal structures.

13.1 Bacterial-two hybrid assay (B2H)

The bacterial-two hybrid technique facilitates the analysis of potential protein-protein interactions. Briefly, the two-hybrid system uses the *Bordetella pertussis* enzyme, adenylate cyclase, involved in the synthesis of cyclic AMP (cAMP). Cyclic AMP is the secondary messenger which, together with the catabolite activator protein (CAP), is responsible for the induction of catabolite repressed genes such as *lacZ.* In the bacterial two hybrid system, two fragments of the *cya* gene, T25 and T18, are cloned independently into "bait" and "prey" plasmids. The target interacting proteins are then cloned in-frame with the T25 or T18 fragments and transformed into the same strain of *E. coli,* which lacks adenylate cyclase activity (Δ*cya*). Interaction between the target proteins results in a functional complementation between the T25 and T18 fragments. The 'reconstituted' Cya leads to the synthesis of cyclic AMP which, in turn, interacts with CAP to induce the expression of the reporter gene, for example *lacZ*. Expression of *lacZ* can be readily detected on plates containing X-gal (Figure 13.1).

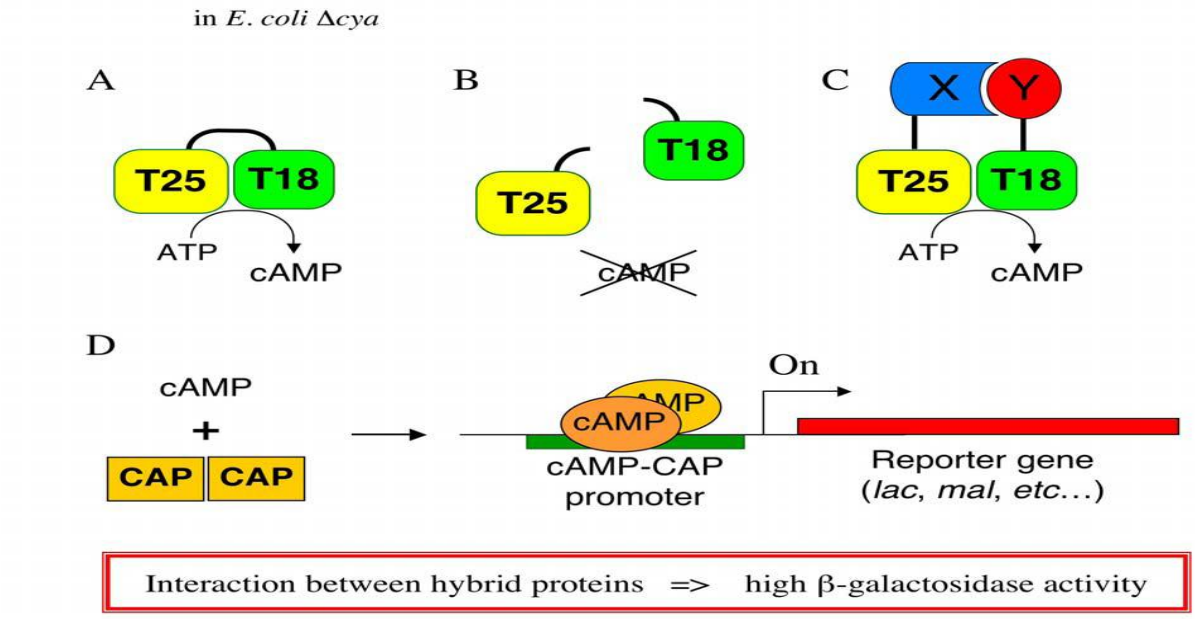

Figure 13.1: Detection of *in vivo* interactions between two proteins of interest with the bacterial two-hybrid system based on the reconstitution of adenylate cyclase activity (diagram from BACTH manual). T25 and T18 are fragments of the *Bordetella pertussis* adenylate cyclase. Both fragments, T18 and T25, form a catalytic domain which converts ATP into cAMP (A). When T25 and T18 are apart, then no cAMP is produced (B). In a bacterial two hybrid assay, two proteins of interest (X and Y) are fused to T18 and T25. If the proteins X and Y interact with each other, then T18 and T25 fragments are brought together to restore adenylate cyclase activity and be able to produce cAMP (C). cAMP interacts with CAP to induce expression of a number of operons such as the *lac* or *mal* operons (D). The consequence of induction of the *lac* operon is the production of β-galactosidase, the activity of which can be readily detected on the LB agar containing X-gal substrate, as X-gal cleaved by β-galactosidase, yields blue coloured colonies.

Analysis of the interaction between components of the Sec pathway and substrates Sap and EA1 by B2H

In this study the bacterial two-hybrid system was used to identify putative interactions between components of the SecA1 and SecA2 secretory machines and SecA2 substrates Sap and EA1. The mutual interactions of the following proteins were investigated: SecA1, SecA2, SecY1, SecY2, SecH, Sap, EA1 as well as SecA of *B. subtilis*. The coding regions of each of the above proteins were cloned in-frame into four vectors: (i) 5'-T25-target gene-3', (ii) 5'- target gene-T25-3', (iii) 5'-T18-target gene-3', (iv) 5'-target gene-T18-3'. Virtually all pairwise combinations of T25- and T18-based clones were tested by co-transforming them into *E. coli* Δ*cya*, selecting on LB agar plates

containing kanamycin, ampicillin, IPTG and X-gal. The presence of blue colonies indicated a putative positive interaction. To summarize the results visually, the matrix of interactions between analysed components of the Sec pathway was made (Figure 13.2). The table of all reciprocal interactions between T18- and T25-fusion proteins is presented in the Appendix D.

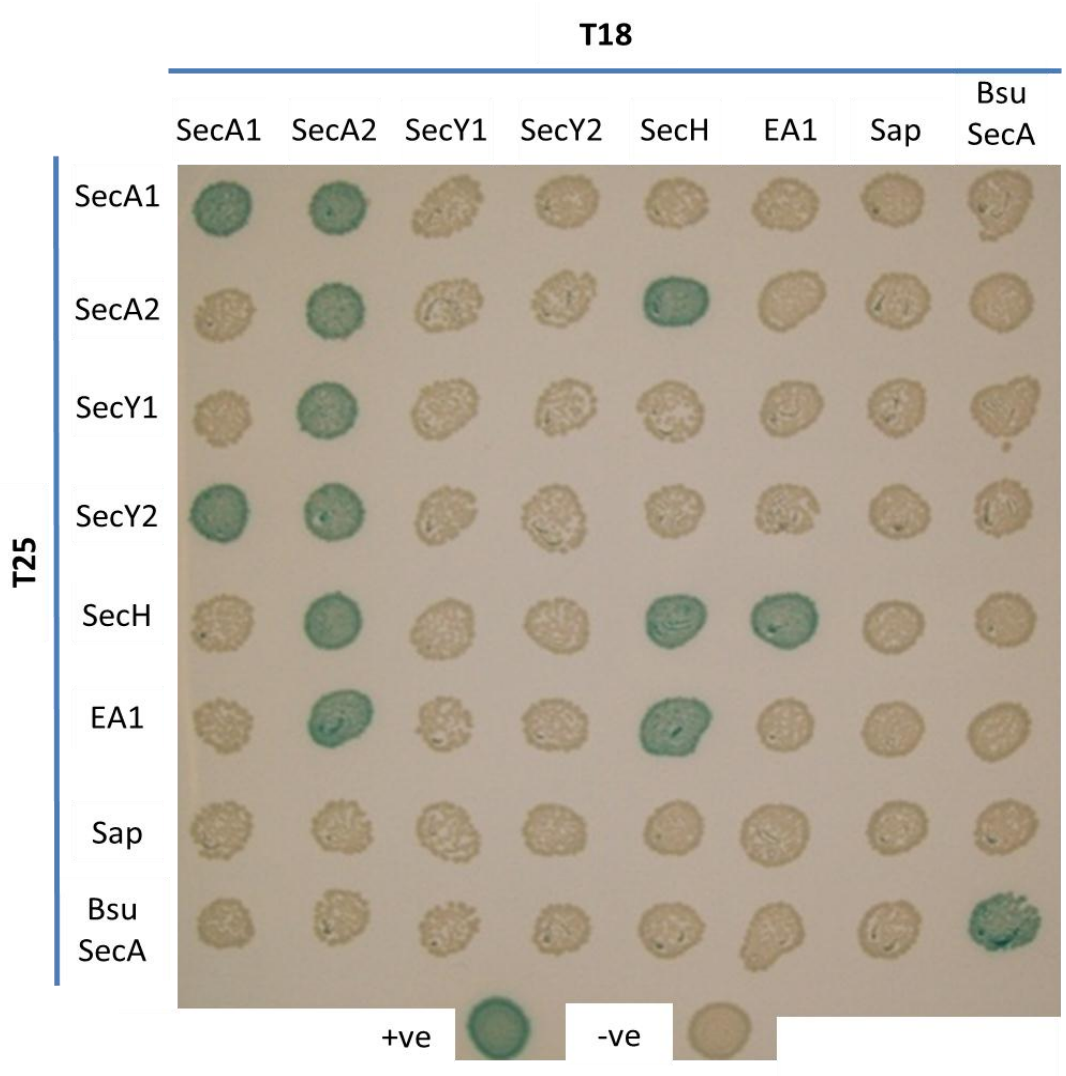

Figure 13.2: Results of bacterial-two hybrid (B2H) analysis of putative interactions between components of the Sec pathway of *B. anthracis*. The matrix shows the results of the B2H assay for putative interactions between components of the *B. anthracis* secondary Sec translocation systems and its putative substrates, as well as the SecA/A1 proteins of *B. subtilis* and *B. anthracis.* The proteins tested were *B. anthracis* SecA1, SecA2, SecY1, SecY2, SecH, EA1 and Sap, and *B. subtilis* SecA (Bsu SecA). The proteins were fused to T18 and T25 domains of the *Bordetella pertussis* adenylate cyclase. Positive results, showing putative *in vivo* interactions between target proteins are indicated by blue colonies/spots. Negative results are indicated by yellow colonies/spots. Abbrevations: + ve: positive control; -ve: negative control.

Consistent with the observation that SecA exists in monomer-dimer equilibrium, but with the balance shifted towards the dimeric form (Woodbury *et al.*, 2002; Vassylyev *et*

al., 2006; Papanikolau *et al.*, 2007), the SecA-like proteins, SecA (*B. subtilis*), SecA1 and SecA2 (*B. anthracis*) were shown to interact with themselves in the bacterial-two hybrid assay. Interestingly, SecA1 showed an interaction with SecA2, giving rise to the possibility that SecA1 and SecA2 interact *in vivo* to form a dimer. The only other interaction shown by SecA1 was with SecY2. SecA2 interactions were the most extensive and apart from the interaction with itself, SecA2 was shown to interact with SecY1, SecY2, SecH and EA1.

In the case of testing interaction between Sap and EA1 against components of the Sec pathway, only the N-terminus of the Sap and EA1 pre-proteins was used. To achieve that 5'ends of *sap* and *eag* were cloned in frame into T18 and T25 fragments of bacterial two hybrid vectors. The 5' ends of those genes encoded signal peptide and N-terminus of the mature protein (80 amino acids in case of EA1 and 67 amino acids in case of Sap). This approach was used as according the predominant concept the leader peptide, located on the N-terminus of secretory proteins is responsible for targeting them for secretion, with the signal peptide making initial interaction between a secretory protein and SecA (described in detail in the **Section 1.5.1**). Using the N-terminus of S-layer proteins was sufficient to show interaction between SecA2 and EA1, but not between SecA2 and Sap. As there was no interaction between SecA2 and the N-terminus of Sap, the whole gene was cloned, but still without positive interaction being observed (data not shown), although this interaction might have been expected since Sap is a putative SecA2 substrate (**Section 1.7 and 8.4**). The occurrence of interaction between SecA2 and N-terminal terminus of EA1 shown by bacterial two-hybrid assay indicates importance of N-terminus of EA1 for its interaction with SecA2 and we are currently unable to rule out interactions with the C-terminus of this protein. Moreover, it is noteworthy EA1 N-terminus interactions with both SecA2 and SecH were mediated by C-terminal fusions of T18 and T25 with EA1 N-terminus (Appendix D). This might suggest the importance of the signal peptide for those interactions.

SecH was shown to interact with both SecA2 and EA1, suggesting that SecH helps to facilitate interaction between SecA2 and its substrate. This is consistent with the data obtained with the *secH*-null mutant (**Section 4**). In this respect we considered the possibility that SecH might a functional homologue of SecB, which facilitates the interaction between SecA and its substrates in Gram-negative bacteria. In the bacterial two-hybrid assay, SecH interacts with itself, suggesting it functions as dimer or higher order multimer. For comparison, SecB is a tetramer, forming a dimer of dimers. There is no structure of SecH available, but it was possible to obtain a prediction of its

structure using I-Tasser structural prediction software available on-line at http://zhanglab.ccmb.med.umich.edu/I-TASSER/ (Figure 13.3A). The structure of SecB has been resolved (Dekker *at al.*, 2003) and it is shown on Figure 13.3B. SecB has extensive β-sheets which serve as the interaction interface with its substrate proteins. The cores of each monomer is formed by β-sheets linked by α-helices. Similarly, SecH is predicted to have extensive β-sheets joined by α-helices.

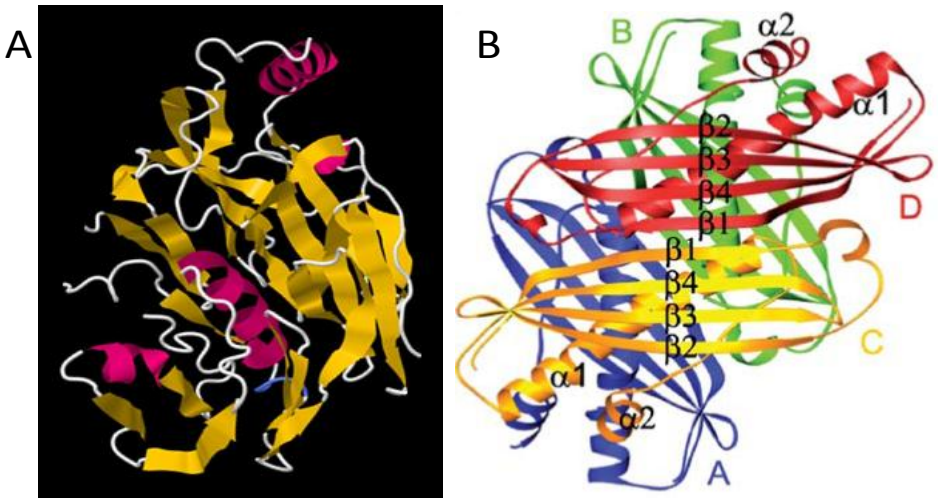

Figure 13.3: I-Tasser structure prediction of (A) SecH: β-sheets are shown in yellow, α-helices are shown in purple, loops are visible as white strands; (B) SecB: four subunits composed of β-sheets (β1-4) linked by α-helices and loops.

The predicted structural similarity of SecH as well as its interaction with both the SecA2 molecular motor and its substrate may support the hypothesis that SecB and SecH are potentially functional homologues.

13.2 Purification of SecA1, SecA2, SecH

Attempts were made to purify SecA1, SecA2 and SecH for *in vitro* interaction studies and for crystallisation and subsequent structural studies. GST tagged SecA1 and SecA2, and His-tagged SecH were expressed in *E. coli* BL21 and purified according to the protocol described in **Section 2.10**. To improve solubility of SecA1, SecA2 and SecH they were grown overnight at room temperature and induced with low concentration of the inducer IPTG (50 µM). The harvested culture was treated with 1% sarcosyl or 2% sodium deoxycholate for 30 minutes on ice prior to sonication. And then the sonicate as well as the supernatant fractions were analysed by SDS-PAGE. The procedure with treatment of the harvested culture with 1% sarkosyl gave considerable amount of soluble proteins: SecA1, SecA2, SecH (Figure 13.4 A and B).

Three attempts were made to purify the soluble fractions of sarcosyl-treated samples containing GST-SecA1 and GST-SecA2 using glutathione affinity columns.

However, the amount of the SecA1 and SecA2 proteins obtained in the eluates were insufficient: relatively small amount of GST-SecA1 were detected in the eluate fractions (1-4) (Figure 13.5) and no GST-SecA2 (Figure 13.6) was found in the elute. The proteins were found in the flow-through, indicating the lack of binding of the GST-tag to the glutathione. The lack of binding of GST-tagged SecA1 and SecA2 to the glutathione column could be due to GST-SecA1 and GST-SecA2 being folded in such a way that glutathione-binding domain of GST would be hidden within GST-protein complex, thus not available for interaction.

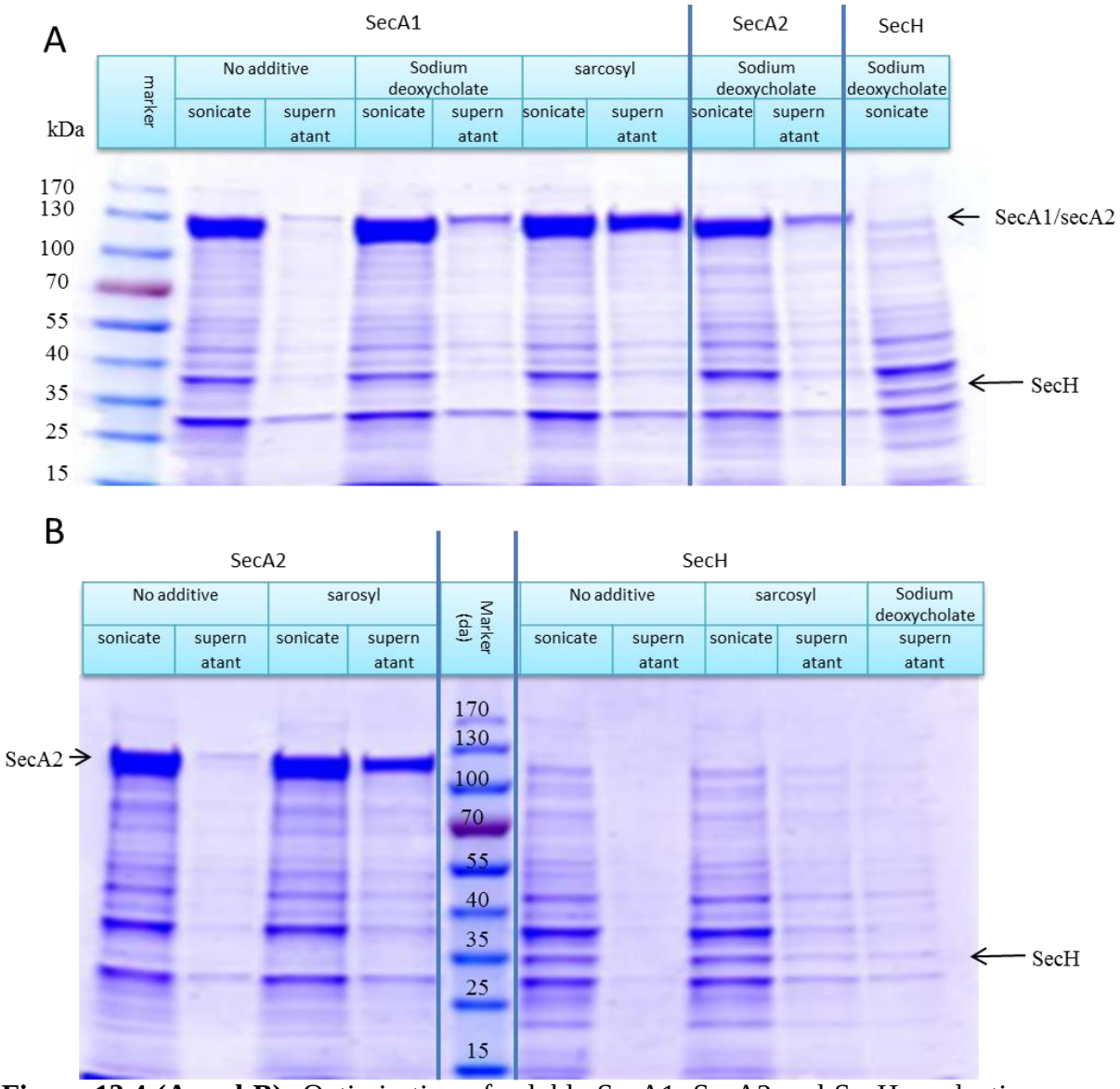

Figure 13.4 (A and B): Optimisation of soluble SecA1, SecA2 and SecH production. GST-SecA1, GST-SecA2 and His-SecH were expressed in *E. coli* BL21. Sonicated cell pellets were treated with either 1% sarcosyl or 2% sodium deoxycholate to solubilise released proteins and then analysed by SDS-PAGE. Proteins corresponding in size to GST-SecA1, GST-SecA2, His-SecH (125 kDa, 119, 34 kDa, respectively) are visible in the crude sonicate samples and in the supernatant samples. More soluble protein was observed after treatment 1% sarcosyl rather than 2% sodium deoxycholate.

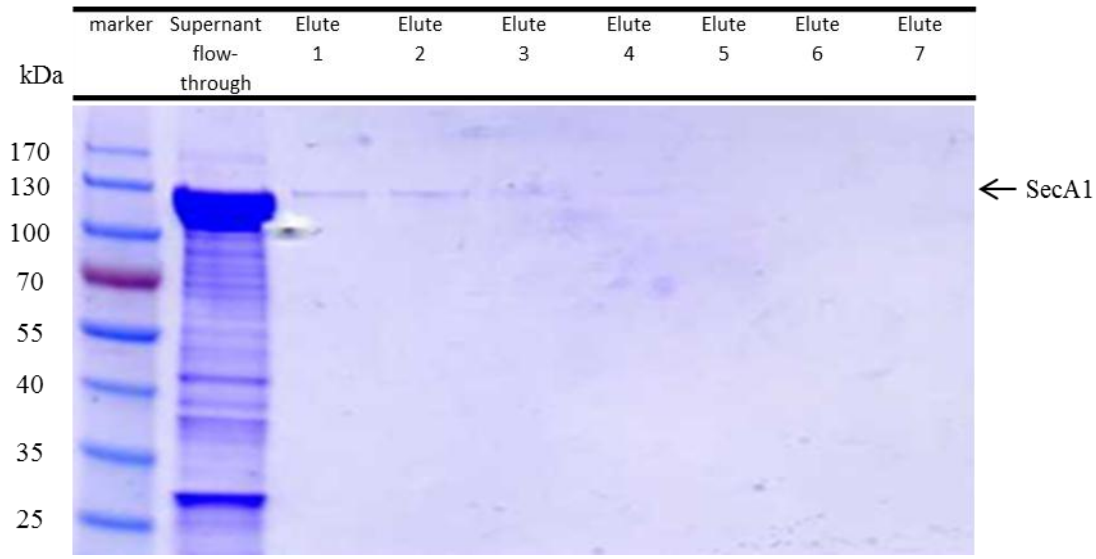

Figure 13.5: Purification of GST-SecA1 (~ 125 kDa) using a glutathione affinity column. The supernatant flow-through, elution fractions (1-7) were analysed by SDS-PAGE. Elution buffer used: 10 mM glutathione in 50 mM Tris-Cl.

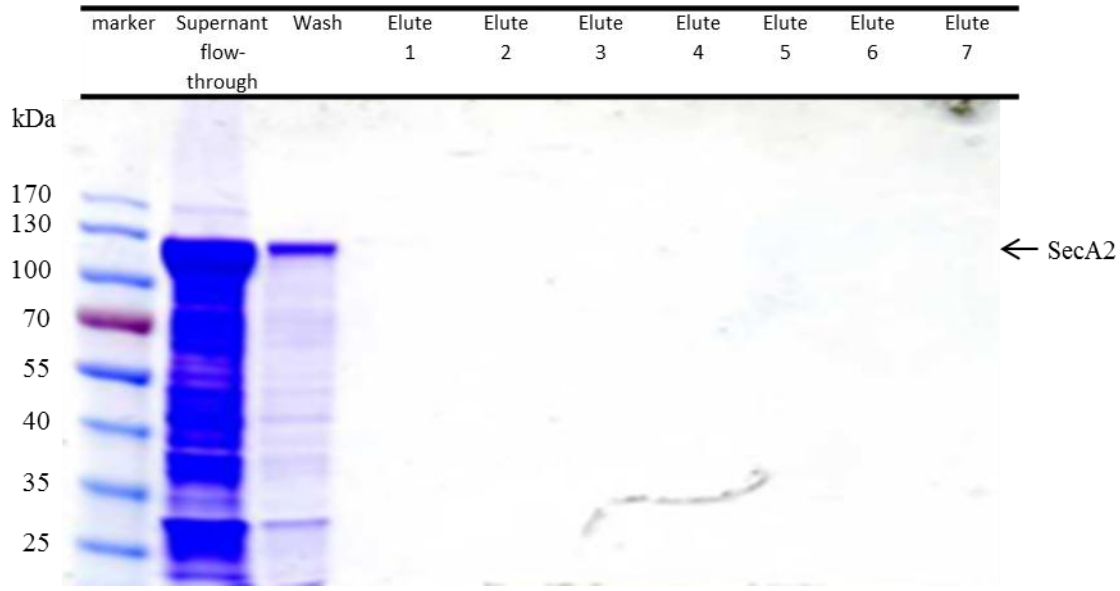

Figure 13.6: Purification of GST-SecA2 (~ 119 kDa) using a glutathione affinity column. The supernatant flow-through, wash and elution fractions (1-7) were analysed by SDS-PAGE. Elution buffer used: 10 mM glutathione in 50 mM Tris-Cl.

13.3 Discussion

Interactions between elements of the translocation system and EA1 and Sap were investigated in order to learn more about how the system functions. Previously, we found that SecA2 drives secretion of EA1 and Sap with SecH enhancing the process. More insights into interactions between SecA2, its substrates and SecH were provided by bacterial two-hybrid analysis. This analysis showed that both SecA2 and SecH were able to interact with each other as well as with EA1. As SecH enhances the secretion of EA1, this observation may suggest that all three proteins form a tertiary complex, with SecH possibly enhancing the interaction between SecA2 and its substrate. In this respect SecH would act as a functional homologue of SecB, which facilities the interaction between SecA and its cognate substrates in Gram-negative bacteria. However, while SecB is essential for that interaction, SecH is not, but serves to increase efficiency of the interaction. No interaction between SecH and Sap was observed, showing either the limitation of bacterial two-hybrid system or a genuine lack of interaction between these proteins. It might be that Sap is not a substrate for SecH, but its secretion might be mediated by SRP. However, the reduction in Sap secretion in the *secH*-null mutant is strongly suggestive of an involvement of SecH. SecH was also shown to interact with itself, and is likely to form at least as dimer. SecB, by comparison, forms a dimer of dimers (so effectively tetramer) (Dekker *et al.*, 2003). However, since SecB is approximately half the size of SecH, a SecH dimer would be similar in size to a SecB tetramer. The predicted structure of SecH, like that of SecB, has extensive β-sheets on one of its flattened surfaces and α-helices on the other. Consequently, the similarity of the SecB and SecH structures provides tentative support that they share similar functions.

Interestingly, our bacterial two-hybrid analysis also demonstrated potential interactions between SecA1 and SecA2, indicating possibility of forming a SecA1/SecA2 dimer. How might such a dimer be functional? In a *Mycobacterium smegmatis* strains engineered to deplete SecA1, the export of the SecA2-dependent substrate Msmeg1712 was severely impaired at low SecA1 concentrations, indicating SecA1 is required for SecA2-dependent export (Rigel *et al.*, 2009). A similar situation may also apply to *B. anthracis*, with a SecA2/SecA1 dimer required for the secretion of Sap and EA1. In addition, SecA2 was able to interact with both SecY1 and SecY2, supporting our model that both SecY1 and SecY2 can form components of a translocation channel that is common for all Sec-dependent substrates. We only detected

an interaction between SecY2 and SecA1. However, this is likely to be due to limitation of the two-hybrid system, since the *secY2*-null mutant did not affect the secretion of the extracellular proteins, indicating that SecY1 must also interact with SecA1.

To confirm interactions between SecH and other components of the SecA2 pathway and its substrates, biophysical studies such as isothermal calorimetry (ITC) or surface plasmon resonance (SPR) need to be performed. However, attempts to purify SecA1, SecA2 and SecH have been made but were unsuccessful. It was possible to solubilise SecH, but its purification was not followed due to time constraint.

Chapter 14: General discussion

In this thesis an investigation of the components of the secondary Sec translocase of *B. anthracis* was undertaken. Prior to this study, it was shown that *B. anthracis* encodes two homologues of SecA (SecA1/SecA2) and two homologues of secY (SecY1/SecY2). Based on the analysis the neighbourhoods of these genes, the effects of gene deletions and complementation studies, SecA1 and SecY1 were likely to be the direct functional homologues of *B. subtilis* SecA and SecY. SecA2 was shown to be required for the secretion of the two major S-layer proteins, namely Sap and EA1, while SecY2 did not show any substrate specificity. Instead, SecY2 appears to function to ensure high level of secretion of Sec-dependent substrates throughout the entire growth cycle (Pohl *et al.*, unpublished) since, in contrast to SecY1, it is up-regulated during stationary phase. More specifically, these studies have attempted to address the question as to how SecA2 recognises and distinguishes between its substrates rather than the other ~ 400 proteins with similar signal peptides.

A bioinformatic analysis of the *secA2* locus of other members of the *B. cereus* group indicated that whenever *secA2* was present in a genome, immediately downstream and in the same operon was a second gene that we named *secH*. The product of *secH* was subsequently found to be unique to members of the *B. cereus* group, and was not found in other bacterial species that encoded SecA2 homologues. In its absence, the lack of SecH was shown not to be essential for Sap and EA1 secretion, but did reduce its efficiency.

The bacterial two-hybrid assay was used to explore potential interactions between components of the *B. anthracis* Sec pathways. These experiments provided insights into how SecH might function. SecH was shown to interact with itself, SecA2 and EA1, but interestingly, not SecA1. This suggested that a multimeric SecH forms part of a tripartite complex with SecA2 and one or both of its substrates. Interestingly, SecA1 and SecA2 also appear to interact, thus raising the possibility that the functional unit for secretion of Sap and EA1 could be a SecA1/SecA2 dimer. The support for this observation comes from a complementation analysis in which *sap* and *eag* were over-expressed from a non-native, inducible promoter in the Δ*secA2** mutant, in which a detectable level of Sap and EA1 secretion was observed. This suggests that SecA1/SecA2 substrate specificity might not be as stringent as originally thought and these proteins may exhibit some overlapping specificity. This observation correlates well with observations from similar studies in *Mycobacterium smegmatis*. In strains of

M. smegmatis engineered to deplete SecA1, the export of the SecA2-dependent substrate Msmeg1712 was severely impaired at low SecA1 concentrations, indicating SecA1 is required for SecA2-dependent export (Rigel *et al.*, 2009).

Another candidate factor for conferring SecA2 specificity for Sap and EA1 is their signal peptides which, excepting for a single conservative amino acid substitution, are almost identical. However, studies in *B. subtilis* revealed that both its native SecA, as well as *B. anthracis* SecA1 can facilitate Sap and EA1 secretion. This indicates that, in *B. subtilis* at least, the signal peptide does not provide specificity for SecA2-mediated secretion. During the course of this work we identified SecH as a novel component of the Sap/EA1 secretion pathway. However, expressing SecH in *B. subtilis* in the presence *B. anthracis* SecA1 had an inhibitory effect on secretion of EA1, while the co-expression of SecA1, SecA2 and SecH restored Sap and EA1 secretion to the level observed in the mutant expressing SecA1. These observations suggest that SecH has a role in preventing the interaction between SecA1 and S-layer proteins and enhancing the interaction between SecA2 and these proteins. However, there appear to be additional, as yet unknown factor(s) that determine the strict requirement of SecA2 for Sap and EA1 secretion of in *B. anthracis*.

B. anthracis encodes three functional homologues of the *B. subtilis* PrsA lipoprotein (Williams *et al.*, 2003). Only PrsAB was shown to be involved in the secretion of Sap and EA1 in both *B. subtilis* and *B. anthracis.* PrsAB was previously shown to increase the secretion of *B. anthracis* protective antigen from *B. subtilis* (William *et al.*, 2003), and we cannot rule out the possibility that it has other substrates. We also attempted to identify specific substrates for PrsAA and PrsAC by 2D PAGE analysis, but were not successful. However, since the lethal phenotype of *B. subtilis* PrsA is due to its requirement for folding penicillin-binding proteins (PBPs), we carried out cell morphology analyses by fluorescent microscopy and a Bocillin assay. We observed distinct cell morphology changes for PrsAA and PrsAB mutants, suggesting that they may also have additional specific substrates involved in the cell wall metabolism. This was confirmed in the case of PrsAA since the Bocillin showed defects in a number of the PBPs, indicating that, as is the case of *B. subtilis*, PrsAA is required for their folding. However, unlike *prsA* of *B. subtilis*, *prsAA* is not an essential gene, presumably because of a degree of overlapping substrate specificity between the PrsA-like protein in *B. anthracis*, as first proposed by Williams and colleagues (2003). No specific substrate was identified for PrsAC. The Δ*secA2** mutant was also subject to fluorescence microscopy analysis and shown to have altered cell morphology. However,

the generation of this mutant resulted in the down-regulation of *csaB*, located immediately upstream of *sceA2*, but encoded on the opposite strand. We therefore cannot rule out at this stage that the resulting change in morphology is due to a reduction in cell wall pyruvylation.

The absence of SecA2, SecH, PrsAA, PrsAB and PrsAC resulted in alterations in the expression of *eag* and *sap* at some point of the growth cycle. This was most noticeable in the case of SecA2 and PrsAB. As SecA2 and SecH are intracellular proteins and PrsAA, PrsAB, PrsAC extracellular, it is likely that changes in *sap* and *eag* expression are indirect, possibly mediated by a cell wall stress response. We have not investigated this possibility further, although this clearly needs to be done.

In the respect of the future research on the SecA2-mediated transport of substrates of the Sec pathway a number of potential priorities have been identified. The purification of Sec pathway components such as *B. subtilis* SecA and *B. anthracis* SecA1, SecA2, SecH, EA1 and Sap would facilitate a series of *in vitro* protein interaction studies (*e.g.* surface plasmon resonance, isothermal calorimetry) to confirm the *in vivo* interactions observed in this study. Additionally, the purified proteins could potentially be used to determine the structures of SecA1, SecA2 and SecH. A second priority would be to attempt to identify additional substrates of SecA2, PrsAA and PrsAB. This could be achieved by comparing the protein profiles of cell wall and membrane fractions isolated from the wild type and Δ*secA2*, Δ*prsAA*, Δ*prsAB* mutants. The pull-down technique, attempted in this study, needs to be optimised for *B. anthracis* and would provide an ideal starting point for such studies.

The role of Sap and EA1 signal peptide in the secretion of these proteins by SecA2 should be investigated further. The expression plasmid pKG400, created as part of this project, could be used for this purpose. This would require cloning of a gene encoding the mature portion of secretory protein that was not a substrate for SecA2, in-frame with the *sap* or *eag* signal sequence. The reciprocal experiment should also be carried out in which the mature regions of *sap* or *eag* are cloned in-frame with a signal sequence from a SecA1-depenent substrate. The secretion of the resulting proteins would then be analysed by PAGE. If the secretion of Sap/EA1 with an alternative signal peptide were observed in the *secA2*-null mutant, this would provide good evidence for the role of the signal peptide in targeting protein substrates to SecA2 in *B. anthracis*. The same conclusion would be obtained if the secretion of a SecA1-dependent protein with the Sap/EA1 signal peptide, produced from the expression plasmid, were not increased in the *secA2*-null mutant, but if it were increased in the wild type strain.

Finally, the patterns of gene expression of the null mutants of Δ*secA2**, Δ*secA2H*, Δ*secH,* Δ*prsAB* is being subjected to a transcriptome analysis using microarrays, to gain insights into the regulation of *sap* and *eag* expression. The RNA from those strains (harvested in the exponential and stationary phases) was isolated and sent for the microarray analysis. However as the data were obtained just before finishing writing this thesis they have still to be analysed.

References

Agaisse, H., Gominet, M., Økstad, O.A., Kolstø, A.B., Lereclus, D., (1999). PlcR is a pleiotropic regulator of extracellular virulence factor gene expression in *Bacillus thuringiensis*. *Molecular Microbiology*, **32:** 1043–53.

Ahn, J.S., Chandramohan, L., Liou, L.E., Bayles, K.W., (2006). Characterization of CidR-mediated regulation in Bacillus anthracis reveals a previously undetected role of S-layer proteins as murein hydrolases. *Molecular Microbiology*, **62:** 1158–1169.

Akimaru, J., Matsuyama, S.I., Tokuda, H., Mizushima, S., (1991). Reconstitution of a protein translocation system containing purified SecY, SecE, and SecA from *Escherichia coli*. *Proceedings of the National Academy of Sciences of the United States of America*, **88:** 6545–49.

Akiyama, Y. and Ito, K., (1987). Topology analysis of the SecY protein, an integral membrane protein involved in protein export in *Escherichia coli*. *EMBO Journal*, **6:** 3465–3470.

Alileche, A., Serfass, E. R., Muehlbauer, S. M., Porcelli, S. A., Brojatsch, J., (2005). Anthrax lethal toxin-mediated killing of human and murine dendritic cells impairs the adaptive immune response. *PLoS Pathogens*, **1:** e19.

Alonzo III, F., Port, G.C., Cao, M., Freitag, N.E., (2009). The posttranslocation chaperone PrsA2 contributes to multiple facets of *Listeria monocytogenes* pathogenesis. *Infection & Immunity*, **77:** 2612–2623.

Alonzo, F., III and Freitag, N.E., (2010). *Listeria monocytogenes* PrsA2 is required for virulence factor secretion and bacterial viability within the host cell cytosol. *Infection & Immunity*, **78:** 4944–4957.

Anagnostopoulos, C. and Spizizen, J., (1961). Requirements for transformation in Bacillus subtilis. *Journal of Bacteriology*, **81:** 741-746.

Antelmann, H., Darmon, E., Noone, D., Veening, J.W., Westers, H., Bron, S., Kuipers, O.P., Devine, K.M., Hecker, M., van Dijl, J.M., (2003). The extracellular proteome of *Bacillus subtilis* under secretion stress conditions. *Molecular Microbiology*, **49:** 143–156.

Archambaud, C., Nahori, M.A., Pizarro-Cerda, J., Cossart, P., and Dussurget, O., (2006). Control of *Listeria* superoxide dismutase by phosphorylation. *Journal of Biological Chemistry*, **281:** 31812–31822.

Ash, C., Farrow, J.A.E., Wallbanks, S., Collins, M.D., (1991). Phylogenetic heterogeneity of the genus *Bacillus* revealed by comparative analysis of small-subunit-ribosomal RNA sequences. *Letters in Applied Microbiology*, **13:** 202-206.

Antikainen, J., Anton, L., Sillanpää, J., Korhonen, T.K. (2002). Domains in the S-layer protein CbsA of *Lactobacillus crispatus* involved in adherence to collagens, laminin and lipoteichoic acids and in self-assembly. *Molecular Microbiology*, **46:** 381–394.

Avall-Jaaskelainen, S., Kylä-Nikkilä, K., Kahala M., Miikkulainen-Lahti, T., Palva, A., (2002). Surface display of foreign epitopes on the *Lactobacillus brevis* S-layer. *Applied and Environmental Microbiology*, **68:** 5943–5951.

Baars, L., Ytterberg, A.J., Drew, D., Wagner, S., Thilo, C., van Wijk, K.J., and J. de Gier, W., (2006). Defining the role of the *Escherichia coli* chaperone SecB using comparative proteomics. *Journal of Biological Chemistry*, **281:** 10024–34.

Bahl, H., Scholz, H., Bayan, N., Chami, M., Leblon, G., Gulik-Krzywicki, T., Shechter, E., Fouet, A., Mesnage, S., Tosi-Couture, E., Gounon, P., Mock, M., Conway de Macario, E., Macario, A.J., Fernandez-Herrero, L.A., Olabarria, G., Berenguer, J., Blaser, M.J., Kuen, B., Lubitz, W., Sara, M., Pouwels, P.H., Kolen, C.P., Boot, H.J., Resch, S., (1997). Molecular biology of S-layers. *FEMS Microbiology Reviews*, **20:** 47–98.

Baud, C., Karamanou, S., Sianidis, G., Vrontou, E., Politou, A.S., Economou, A., (2002). Allosteric communication between signal peptides and the SecA protein DEAD motor ATPase domain. *Journal of Biological Chemistry*, **277:** 13724–13731.

Baumeister, W. and Lembcke, G., (1992). Structural features of archaebacterial cell envelopes. *Journal of Bioenergetics and Biomembranes*, **24:** 567–575.

Bavykin, S. G., Lysov, Y. P., Zakhariev, V., Kelly, J. J., Jackman, J., Stahl, D. A., Cherni, A., (2004). Use of 16S rRNA, 23S rRNA, and *gyrB* gene sequence analysis to determine phylogenetic relationships of *Bacillus cereus* group microorganisms. *Journal of Clinical Microbiology*, **42:** 3711-3730.

Bechtluft, P., Kedrov, A., Slotboom, D.-J., Nouwen, N., Tans, S.J.,, Driessen, A. J. M., (2010). Tight hydrophobic contacts with the SecB chaperone prevent folding of substrate proteins. *Biochemistry*, **49:** 2380–2388.

Beckmann, R., Bubeck, D., Grassucci, R., Penczek, P., Verschoor, A., Blobel, G., Frank, J., (1997). Alignment of conduits for the nascent polypeptide chain in the ribosome-Sec61 complex. *Science*, **278:** 2123–2126.

Beckmann, R., Spahn, C.M., Eswar, N., Helmers, J., Penczek, P.A., Sali, A., Frank, J., Blobel G., (2001). Architecture of the protein-conducting channel associated with the translating 80S ribosome. *Cell*, **107:** 361–372.

Bendtsen, J.D., Binnewies, T.T., Hallin, P.F., Sicheritz-Ponten, T., Ussery, D.W., (2005). Genome update: prediction of secreted proteins in 225 bacterial proteomes. *Microbiology*, **151:** 1725–1727.

Bensing, B.A. and Sullam, P.M., (2002). An accessory sec locus of *Streptococcus gordonii* is required for export of the surface protein GspB and for normal levels of binding to human platelets. *Molecular Microbiology*, **44:** 1081–1094.

Bensing, B.A., Takamatsu, D., Sullam, P.M., (2005). Determinants of the streptococcal surface glycoprotein GspB that facilitate export by the accessory Sec system. *Molecular Microbiology*, **58:**1468-81.

Van den Berg, B., Clemons Jr, W.M., Collinson, I., Modis, Y., Hartmann, E., Harrison S.C., Rapoport, T.A., (2004). X-ray structure of a protein-conducting channel. *Nature*, **427:** 36-44.

Beveridge, T.J. and Murray, R.G.E., (1976). Reassembly *in vitro* of the superficial cell wall components of *Spirillum putridiconchylium. Journal of Ultrastructure Research*, **55:** 105 -118.

Beveridge, T.J., (1994). Bacterial s-layers. *Current Opinion in Structural Biology*. **4:** 204 - 212.

Bhatnagar, R. and Batra, S., (2001). Anthrax toxin. *Critical Reviews in Microbiology*. **27:** 167–200.

Blaser, M.J., Smith, P.F., Repine, J.E., Joiner, K.A., (1988). Pathogenesis of **Campylobacter fetus** infections. Failure of encapsulated *Campylobacter fetus* to bind C3b explains serum and phagocytosis resistance. *Journal of Clinical Investigation*, **81:** 1434–1444.

Bloor, A.E. and Cranenburgh, R.M., (2006). An efficient method of selectable marker gene excision by Xer recombination for gene replacement in bacterial chromosomes. *Applied and Environmental Microbiology*, **72:** 2520–2525.

Bohle, B., Breitwieser, A., Zwölfer, B., Jahn-Schmid, B., S´ara, M., Sleytr, U.B., Ebner, C., (2004). A novel approach to specific allergy treatment: the recombinant fusion protein of a bacterial cell surface (S-layer) protein and the major birch pollen allergen Bet v 1 (rSbsC-Bet v 1) combines reduced allergenicity with immunomodulating capacity. *Journal of Immunology*, **172:** 6642–6648.

Bohr, M.T., (2002). Nanotechnology goals and challenges for electronic application. *IEEE Transactions on Nanotechnology*, **1:** 56–62.

Bolhuis, A., Sorokin, A., Azevedo, V., Ehrlich, S.D., Braun, P.G., de Jong, A., Venema, G., Bron, S., van Dijl, J.M., (1996). *Bacillus subtilis* can modulate its capacity and specificity for protein secretion through temporally controlled expression of the *sipS* gene for signal peptidase I. *Molecular Microbiology*, **22:** 605–618.

Bolhuis, A., Broekhuizen, C.P., Sorokin, A., van Roosmalen, M.L., Venema, G., Bron, S., Quax, W.J., and van Dijl, J.M., (1998). SecDF of *Bacillus subtilis*, a molecular Siamese twin required for the efficient secretion of proteins. *Journal of Biological Chemistry*, **273:** 21217-21224.

Bolhuis, A., Venema, G., Quax, W.J., Bron, S., van Dijl, J.M., (1999). Functional analysis of paralogous thiol-disulfide oxidoreductases in *Bacillus subtilis*. *Journal of Biological Chemistry*, **274:** 24531– 24538.

Bolotin, A., Mauger, S., Malarme, K., Ehrlich, S.D., Sorokin, A., (1999). Low-redundancy sequencing of the entire *Lactococcus lactis* IL1403 genome. *Antonie van Leeuwenhoek*, **76:** 27-76.

Braunstein, M., Espinosa, B.J., Chan, J., Belisle, J.T., Jacobs, Jr. ,W.R., (2003). SecA2 functions in the secretion of superoxide dismutase A and in the virulence of *Mycobacterium tuberculosis*. *Molecular Microbiology*, **48:** 453-64.

Breitwieser, A., Egelseer, E. M., Moll, D., Ilk, N., Hotzy, C., Bohle, B., Ebner, C., Sleytr, U. B., Sára, M., (2002). A recombinant bacterial cell surface (S-layer)-major birch pollen allergenfusion protein (rSbsC/Bet v1) maintains the ability to selfassemble into regularly structured monomolecular lattices and the functionality of the allergen. *Protein engineering*, **15:** 243–249.

Bruch, M.D., McKnight, C.J., Gierasch, L.M., (1989). Helix formation and stability in a signal sequence. *Biochemistry*, **28:** 8554–8561.

Brundage, L., Hendrick, J.P., Schiebel, E., Driessen, A.J.M., Wickner, W., (1990). The purified *E. coli* integral membrane protein SecY/E is sufficient for reconstitution of SecA-dependent precursor protein translocation. *Cell*, **62:** 649–57.

Bourgogne, A., Drysdale, M., Hilsenbeck, S.G., Peterson, S.N., Koehler, T.M., (2003). Global effects of virulence gene regulators in a *Bacillus anthracis* strain with both virulence plasmids. *Infection & Immunity*, **71:** 2736-2743.

Cao, M. and Helmann, J.D., (2004). The *Bacillus subtilis* extracytoplasmic-function sigmaX factor regulates modification of the cell envelope and resistance to cationic antimicrobial peptides. *Journal of Bacteriology*, **186:** 1136–1146.

Carnoy, C. and Roten, C.A., (2009). The dif/Xer recombination systems in proteobacteria. *PLoS*, **4:** e6531.

Cerretti, D.P., Dean, D., Davis, G.R., Bedwell, D.M., Nomura, M., (1983). The *spc* ribosomal protein operon of *Escherichia coli*: sequence and cotranscription of the ribosomal protein genes and a protein export gene, *Nucleic Acids Research*, **11:** 2599–2616.

Carucci, J.A., McGovern, T.W., Norton, S.A., Daniel, C.R., Elewski, B.E., Fallon-Friedlander, S., Lushniak, B.D., Taylor, J.S., Warschaw, K., Wheeland, R.G., (2002). Cutaneous anthrax management algorithm. *Journal of the American Academy of Dermatology*, **47:** 766–769.

Chauvaux, S., Matuschek, M., Beguin, P., (1999). Distinct affinity of binding sites for S-layer homologous domains in *Clostridium thermocellum* and *Bacillus anthracis* cell envelopes. *Journal of Bacteriology*, **181:** 2455–2458.

Chen, Q., Wu, H., Fives-Taylor, P.M., (2004). Investigating the role of secA2 in secretion and glycosylation of a fimbrial adhesin in *Streptococcus parasanguis* FW213. *Molecular Microbiology*, **53:** 843–856.

Claessen, D., Emmins, R., Hamoen, L.W, Daniel, R.A., Errington, J., Edwards, D.H., (2008). Control of the cell elongation-division cycle by shuttling of PBP1 protein in *Bacillus subtilis*. *Molecular Microbiology*, **68:** 1029-1046.

Comer, J. E., Chopra, A. K., Peterson, J. W. and Konig, R., (2005). Direct inhibition of T-lymphocyte activation by anthrax toxins *in vivo*. *Infection & Immunity*, **73:** 8275–8281.

Cristóbal, S., De Gier, J.W., Nielsen, H., Von Heijne, G. (1999). Competition between Sec- and Tat-dependent protein translocation in *Escherichia coli*. *EMBO Journal*, **18:** 2982–2990.

Crowley, P.J., Svensater, G., Snoep, J.L., Bleiweis, A.S., Brady, L.J., (2004). An ffh mutant of *Streptococcus mutans* is viable and able to physiologically adapt to low pH in continuous culture. *FEMS Microbiology Letters*, **234:** 315–24

Dalbey, R.E., Lively, M.O., Bron, S., van Dijl, J.M., (1997). The chemistry and enzymology of the type I signal peptidases. *Protein Science*, **6:** 1129–1138.

Dervyn, E. and Ehrlich, S.D., (2001). Analysis of essential genes. *In Functional analsysis of bacterial genes.*, 25-32. Edited by Schumann, W., Ehrlich, S. D. and Ogasawara, N. Chichester, U.K.: John Wiley & Sons, Ltd.

Dixon, T. C., Meselson, M., Guillemin, J., Hanna, P. C., (1999). Anthrax. *New England Journal of Medicine*, **341:** 815-826.

Doig, P., Emödy, L., Trust, T.J. (1992). Binding of laminin and fibronectin by the trypsin-resistant major structural domain of the crystalline virulence surface array protein of *Aeromonas salmonicida*. *Journal of Biological Chemistry*, **267**: 43–49.

Dong, Y., Palmer, S. R., Hasona, A., Nagamori, S., Kaback, H. R., Dalbey R. E., Brady, L. J., (2008). Functional overlap but lack of complete cross-comple-mentation of *Streptococcus mutans* and *Escherichia coli* YidC orthologs. *Journal of Bacteriology*, **190:** 2458-2469.

Douville, K., Leonard, M., Brundage, L.A., Nishiyama, K., Tokuda, H., Mizushima, S., Wickner, W., (1994). Band 1 subunit of *Escherichia coli* preprotein translocase and integral membrane export factor P12 are the same protein. *Journal of Biological Chemistry*, **269:** 18705-18707.

Driessen, A.J., (1992). Precursor protein translocation by the *Escherichia coli* translocase is directed by the protonmotive force. *EMBO Journal*, **11:** 847–853.

Drysdale, M., Bourgogne, A., Hilsenbeck, S.G., Koehler, T.M., (2004). *atxA* controls *Bacillus anthracis* capsule synthesis via *acpA* and a newly discovered regulator, *acpB*. *Journal of Bacteriology*, **186**: 307–315.

Dubrac, S., Boneca, I.G., Poupel, O., Msadek, T., (2007). New insights into the WalK/WalR (YycG/YycF) essential signal transduction pathway reveal a major role in

controlling cell wall metabolism and biofilm formation in *Staphylococcus aureus.* *Journal of Bacteriology*, **189:** 8257–8269.

Dubrac, S., Bisicchia, P., Devine, K.M., Msadek, T., (2008). A matter of life and death: cell wall homeostasis and the WalKR (YycGF) essential signal transduction pathway. *Molecular Microbiology*, **70:** 1307–1322.

Duesbery, N.S., Webb, C.P., Leppla, S.H., Gordon, V.M., Klimpel, K.R., Copeland, T.D., Ahn, N.G., Oskarsson, M.K., Fukasawa, K., Paull, K.D., Vande-Woude, G. F., (1998). Proteolytic inactivation of MAP-kinase-kinase by anthrax lethal factor. *Science*, **280:** 734-737.

Dubrac, S., Bisicchia, P., Devine, K.M., Msadek, T., (2008). A matter of life and death: cell wall homeostasis and the WalKR (YycGF) essential signal transduction pathway. *Molecular Microbiology*, **70:** 1307–1322.

Duong F., (2003). Binding, activation and dissociation of the dimeric SecA ATPase at the dimeric SecYEG translocase. *EMBO Journal*, **22:** 4375–4384.

During, R. L., W. Li, B. Hao, J. M. Koenig, D. S. Stephens, C. P. Quinn, Southwick, F. S., (2005). Anthrax lethal toxin paralyzes neutrophil actin-based motility. *Journal of Infectious Diseases*, **192:** 837-845.

Economou, A., and Wickner, W., (1994). SecA promotes preprotein translocation by undergoing ATP-driven cycles of membrane insertion and deinsertion. *Cell*, **78:** 835–843.

Egelseer, E.M., Schocher, I., Sára, M., Sleytr, U.B., (1995). The S-layer fom *Bacillus stearothermophilus* DSM 2358 functions as an adhesion site for a high-molecular-weight amylase. *Journal of Bacteriology*, **177:**1444–1451.

Erwin, J.L., DaSilva, LM, Bavari, S., Little, S.F., Friedlander, A.M., Chanh, T.C., (2001). Macrophage-derived cell lines do not express proinflammatory cytokines after exposure to *Bacillus anthracis* lethal toxin. *Infection and Immunity*, **69:** 1175-1177.

Fekkes, P., van der Does, C., Driessen, A.J., (1997). The molecular chaperone SecB is released from the carboxy-terminus of SecA during initiation of precursor protein translocation. *EMBO Journal*, **16:** 6105–13.

Fekkes, P. and Driessen, A.J., (1999). Protein targeting to the bacterial cytoplasmic membrane. *Microbiology and Molecular Biology Reviews*, **63:** 161–73.

Fekkes, P., de Wit, J.G., J. van der Wolk, P., Kimsey, H.H., Kumamoto, C.A., Driessen, A J., (1998). Preprotein transfer to the *Escherichia coli* translocase requires the co-operative binding of SecB and the signal sequence to SecA. *Molecular Microbiology*, **29:** 1179–90.

During, R. L., W. Li, B. Hao, J. M. Koenig, D. S. Stephens, C. P. Quinn, Southwick, F. S., (2005). Anthrax lethal toxin paralyzes neutrophil actin-based motility. *Journal of Infectious Diseases*, **192:** 837-845.

Fischetti, V.A., Pancholi, V., Schneewind O., (1990). Conservation of a hexapeptide sequence in the anchor region of surface proteins from gram-positive cocci. *Molecular Microbiology*, **4:** 1603–5.

Flower, A.M., Hines, L.L., Pfennig, P.L., (2000). SecG is an auxiliary component of the protein export apparatus of *Escherichia coli*. *Molecular and General Genetics*, **263:** 131–136.

Fouet, A., (2009). The surface of *Bacillus anthracis*. *Molecular Aspects of Medicine*, **30:** 374–385.

Fouet, A., Mesnage, S., Tosi-Couture, E., Gounon, P., Mock, M., (1999). *Bacillus anthracis* surface: capsule and S-layer. *Journal of Applied Microbiology*, **87:** 251-255.

Fritze, D., (2004). Taxonomy of the genus Bacillus and related genera: the aerobic endospore-forming bacteria. *Phytopahthology*, **94:** 2004.

Gallagher, T., Gilliland, G., Wang, L., Bryan P., (1995). The prosegment-subtilisin BPN' complex: crystal structure of a specific 'foldase'. *Structure*, **3:** 907–914.

Gannon, P.M. and Kumamoto, C.A., (1993). Mutations of the molecular chaperone protein SecB which alter the interaction between SecB and maltose-binding protein. *Journal of Biological Chemistry*, **268:** 1590–5.

Garcia MM, Lutze-Wallace CL, Denes AS, Eaglesome MD, Hoist E, Blaser MJ., (1995). Protein shift and antigenic variation in the S-layer of *Campylobacter fetus subsp. venerealis* during bovine infection accompanied by genomic rearrangement of sapA homologs. *Journal of Bacteriology*, **177:** 1976–1980.

Garduño, R.A. and Kay, W.W., (1992). Interaction of the fish pathogen *Aeromonas salmonicida* with rainbow trout macrophages. *Infection & Immunity*, **60**: 4612–4620.

Garduño, R.A., and Kay, W.W. (1993)., Capsulated cells of *Aeromonas salmonicida* grown in vitro have different functional properties than capsulated cells grown in vivo. *Canadian Journal of Microbiology*, **41**: 941–945.

Garduño, R.A., Lee, E.J.Y., Kay, W.W., (1992). S-layermediated association of *Aeromonas salmonicida* with murine macrophages. *Infection & Immunity*, **60**: 4373–4382.

Gerhardt, P., (1967). Cytology of *Bacillus anthracis*. *Federation Proceedings*, **26**: 1504-1517.

González Jr, J.M. and Carlton, B.C., (1984). A large transmissible plasmid is required for crystal toxin production in *Bacillus thuringiensis* variety *israelensis. Plasmid*, **11:** 28–38.

Gothel, S.F. and Marahiel, M.A., (1999). Peptidyl-prolyl cis-trans isomerases, a superfamily of ubiquitous folding catalysts. *Cellular and Molecular Life Sciences*, **55:** 423–436.

Graham, S., Jeffries, A.H., Secombes, C.J. (1988). A novel assay to detect macrophage bactericidal activity in fish: Factors influencing the killing of *Aeromonas salmonicida*. *Journal of Fish Diseases*, **11**: 389–396.

Grogono-Thomas, R., Dworkin, J., Blaser, M.J., (1997). The role of S-layer proteins in ovine *Campylobacter* abortion. *FEMS Microbiology Rev*iews, **20:** 133–135.

Grogono-Thomas, R., Dworkin, J., Blaser, M.J., Newell, D.G., (2000). Roles of the surface layer proteins of *Campylobacter fetus subsp. fetus* in bovine abortion. *Infection & Immunity*, **68:** 1687–1691.

Hanna, P.C. Kochi, S., Collier, R.J., (1992). Biochemical and physiological changes induced by anthrax lethal toxin in J774 macrophage-like cells. *Molecular Biology of the Cell*, **3:** 1269–1277.

Hanna, P.C., Acosta, D., Collier, R,J., (1993). On the role of macrophages in anthrax. *Proceedings of the National Academy of Sciences of the United States of America*, **90:** 10198-10201.

Hanna, P.C., Kruskal, B.A., Ezekowitz, R.A.B., Bloom, B.R., Collier, R.J., (1994). Role of macrophage oxidative burst in the action of anthrax lethal toxin. *Molecular Medicine*, **1:**7–18.

Hardy, S.J. and Randall, L.L., (1991). A kinetic partitioning model of selective binding of nonnative proteins by the bacterial chaperone SecB. *Science*, **251:** 439–43.

Harris, C.R., Silhavy, T.J., (1999). Mapping an interface of SecY (PrlA) and SecE (PrlG) by using synthetic phenotypes and in vivo cross-linking. *Journal of Bacteriology*, **181:** 3438–44.

Hartl, F.U., Lecker, S., Schiebel, E., Hendrick, J.P., Wickner, W., (1990). The binding cascade of SecB to SecA to SecY/E mediates preprotein targeting to the *E. coli* plasma membrane. *Cell*, **63:** 269–79.

Health Protection Agency. (2010) Health Protection Agency Interim Guidelines for Action in the Event of a Deliberate Release of Anthrax, version 6.2.

Helgason, E., Tourasse, N.J., Meisal, R., Caugant, D.A, Kolstø, A.B., (2004). Multilocus sequence typing scheme for bacteria of the *Bacillus cereus* group. *Applied and Environmental Microbiology*, **70:** 191–201.

Helgason, E., Økstad, O.A., Caugant, D.A., Johansen, H.A., Fouet, A., Mock, M, Hegna, I., Kolstø, A.B., (2000). *Bacillus anthracis*, *Bacillus cereus*, and *Bacillus thuringiensis* - one species on the basis of genetic evidence. *Applied and Environmental Microbiology*, **66:** 2627–30.

Hoffmaster, A.R. and Koehler, T.M., (1997). The anthrax toxin activator gene atxA is associated with CO2-enhanced non-toxin gene expression in *Bacillus anthracis*. *Infection & Immunity*, **65:** 3091–3099.

Hoffmaster, A.R. and Koehler, T.M., (1999). Autogenous regulation of the *Bacillus anthracis* pag operon. *Journal of Bacteriology*, **181:** 4485 – 4492.

Holt, S., C. and Leadbetter, E., R., (1969). Comparative ultrastructure of selected aerobic spore-forming bacteria: a freeze-etching study. *Bacteriological Reviews*, **33**: 346-378.

Hovmöller, S., Sjögren, A., Wang, D.N., (1988). The structure of crystalline bacterial surface layers. *Progress in Biophysics and Molecular Biology*, **51:**131–163.

Huber, C., Egelseer, E.M., Ilk, N., Sleytr, U.B., Sára, M. (2006a). S-layerstreptavidin fusion proteins and S-layer-specific heteropolysaccharides as part of a biomolecular construction kit for application in nanobiotechnology. *Microelectronic Engineering*, **83:** 1589–1593.

Huber, C., Liu, J., Egelseer, E.M., Moll, D., Knoll, W., Sleytr, U.B. & Sára, M., (2006b). Heterotetramers formed by an S-layer-streptavidin fusion protein and core-streptavidin as nanoarrayed template for biochip development. *Small: nano micro,* **2:** 142–150.

Hunt, J.F., Weinkauf, S., Henry, L., Fak, J.J., McNicholas, P., Olivier, D.B., Deisenhofer, J., (2002). Nucleotide control of interdomain interactions in the conformational reaction cycle of SecA. *Science*, **297:** 2018–2026.

Hynönen, U., Westerlund-Wikström, B., Palva, A., Korhonen, T.K. *(*2002*).* Identification by flagellum display of an epithelial cell- and fibronectin-binding function in the SlpA surface protein of *Lactobacillus brevis.* Journal of Bacteriology, **184:** 3360–3367.

Ilk, N., Völlenkle, C., Edelseer, E.M., Breitwieser, A., Uwe, B., Sleytr, U.B., Sára, M., (2002). Molecular characterization of the S-layer gene, sbpA, of *Bacillus sphaericus* CCM2177 and production of functional S-layer fusion protein with ability to recrystallize in a definite orientation while presented the fused allergen. *Applied and Environmental Microbiology*, **68:** 3251–3260.

Inoue H., Nojima H., Okayama H., (1990). High efficiency transformation of *Escherichia coli with plasmids*. *Gene,* **96:** 23-28.

Ito, K., Cerretti, D.P., Nashimoto, H., Nomura, M., (1984). Characterization of an amber mutation in the structural gene for ribosomal protein L15, which impairs expression of the protein export gene, secy, in *Escherichia coli*. *EMBO Journal,* **3**: 2319–2324.

Jernigan, D.B., Raghunathan, P.L., Bell, B.P., Brechner, R., Bresnitz, E.A., Butler, J.C., Cetron, M., Cohen, M., Doyle, T., Fischer M., *et al.*, (2002). Investigation of bioterrorism-related anthrax, United States, 2001: Epidemiologic findings. *Emerging Infectious Diseases,* **8:** 1019–1028.

Joly, J.C. and Wickner, W., (1993). The SecA and SecY subunits of translocase are the nearest neighbors of the translocating preprotein, shielding it from phospholipids. *EMBO Journal*, **12:** 255–263.

Johnsborg, O. and Havarstein, L.S., (2009). Pneumococcal LytR, a protein from the LytR-CpsA-Psr family, is essential for normal septum formation in *Streptococcus pneumoniae*. *Journal of Bacteriology*, **191:** 5859-5864.

Joung, J.K., Ramm, E.R., Pabo, C.O., (2000). A bacterial two-hybrid selection system for studying protein−DNA and protein−protein interactions. *Proceedings of the National Academy of Sciences of the United States of America*, **97:** 7382−7387.

Karamanou, S., Vrontou, E., Sianidis, G., Baud, C., Roos, T., Kuhn, A, Politou, A.S., Economou, A., (1999). A molecular switch in SecA protein couples ATP hydrolysis to protein translocation. *Molecular Microbiology*, **34:** 1133-1145.

Kassam, A., Der, S.D., Mogridge, J. (2005). Differentiation of human monocytic cell lines confers susceptibility to *Bacillus anthracis* lethal toxin. *Cellular Microbiology*, **7:** 281-292.

Kawaguchi, S., Müller, J., Linde, D., Kuramitsu, S., Shibata, T., Inoue, Y., Vassylyev, D.G., Yokoyama, S., (2001). The crystal structure of the ttCsaA protein: an export-related chaperone from *Thermus thermophilus*. *EMBO Journal*, **20:** 562–569.

Keenan, R.J., Freymann, D. M., Stroud, R. M., Walter, P., (2001). The signal recognition particle. *Annual Review of Biochemistry*, **70:** 755–75.

Kern, J., Ryan, C., Faull, K., Schneewind, O., (2010). *Bacillus anthracis* surface-layer proteins assemble by binding to the secondary cell wall polysaccharide in a manner that requires *csaB* and *tagO*. *Journal of Molecular Biology*, **401:** 757–775.

Kihara, A., Akiyama, Y., Ito, K. (1995). FtsH is required for proteolytic elimination of uncomplexed forms of SecY, and essential protein translocase subunit. *Proceedings of the National Academy of Sciences of the United States of America*, **92**: 4532–4536.

Kimura, E., Akita, M., Matsuyama, S.-I., Mizushima, S., (1991). Determination of a region in SecA that interacts with presecretory proteins in *Escherichia coli*, *Journal of Biological Chemistry*, **206:** 6600– 6606.

Kist, M. and Murray, R.G.E., (1984). Components of the regular surface array of *Aquaspirillum serpens* MW5 and their assembly in vitro. *Journal of Bacteriology*, **157:** 599–606.

Ko, K. S., Kim, J.-W., Kim, J.-M., Kim, W., Chung, S.-i., Kim, I. J., Kook Y.-H., (2004). Population Structure of the *Bacillus cereus* Group as Determined by Sequence Analysis of Six Housekeeping Genes and the plcR Gene. *Infection & Immunity*, **72:** 5253-5261.

Kobayashi, K., Ehrlich, S.D., Albertini, A., Amati, G., Andersen, K.K., Arnaud, M., Asai, K., Ashikaga, S., Aymerich, S., Bessieres, P., *et al.*, (2003). Essential

Bacillus subtilis genes. *Proceedings of the National Academy of Sciences of the United States of America*, **100:** 4678–4683.

Koehler, T.M., Dai, Z., Kaufman-Yarbray, M., (1994). Regulation of the *Bacillus anthracis* protective antigen gene: CO2 and a trans-acting element activate transcription from one of two promoters. *Journal of Bacteriology*, **176:** 586-595.

Kontinen, V.P., Saris, P., Sarvas, M., (1991). A gene (*prsA*) of *Bacillus subtilis* involved in a novel, late stage of protein export. *Molecular Microbiology*, **5:** 1273-1283.

Kontinen, V.P. and Sarvas, M., (1993). The PrsA lipoprotein is essential for protein secretion in *Bacillus subtilis* and sets a limit for high-level secretion. *Molecular Microbiology*, **8:** 727-737.

Kontinen, V.P., Yamanaka, M., Nishiyama, K., Tokuda, H., (1996). Roles of the conserved cytoplasmic region and non-conserved carboxy-terminal region of SecE in *Escherichia coli* protein translocase. *Journal of Biochemistry*, **119:** 1124–1130.

Kotiranta, A., Haapasalo, M., Kari, K., Kerosuo, E., Olsen, I., Sorsa, T., Meurman, J. H., Lounatmaa, K., (1998). Surface structure, hydrophobicity, phagocytosis, and adherence to matrix proteins of *Bacillus cereus* cells with and without the crystalline surface protein layer. *Infection & Immunity*, **66:** 4895-4902.

Koval, S.F. and Murray, R.G.E., (1984). The isolation of surface array proteins from bacteria. *Canadian Journal of Biochemistry and Cell Biology*, **62:** 1181 - 1189.

Koval, S. F., (1997). The effect of S-layers and cell surface hydrophobicity on prey selection by bacterivorous protozoa. *FEMS Microbiology* Reviews, **20:** 138–142.

Kronstad, J.W., Schnepf, H.E., Whiteley, H.R., (1983). Diversity of location for *Bacillus thuringiensis* crystal protein genes. *Journal of Bacteriology*, **154:** 419–428.

Kumamoto, C. A. and Beckwith, J., (1983). Mutations in a new gene, SecB, cause defective protein localization in *Escherichia coli*. *Journal of Bacteriology*, **154:** 253–60.

Küpcü, S., Mader, C., Sara, M., (1995). The crystalline cell surface layer from *Thermoanaerobacter thermohydrosulfuricum* LIII–69 as an immobilization matrix: Influenceof the morphological properties and the pore size of the matrix on loss of activity of covalently bound enzymes. *Biotechnology and Applied Biochemistry*, **21:** 275–286.

Laaberki, M.H., Pfeffer, J., Clarke, A.J., Dworkin, J., (2010). O-Acetylation of peptidoglycan is required for proper cell separation and S-layer anchoring in *Bacillus. Journal of Biological Chemistry*, **286:** 5278-88.

Lazarevic, V., Margot, P., Soldo, B., Karamata, D., (1992). Sequencing and analysis of the *Bacillus subtilis lytRABC* divergon: a regulatory unit encompassing the structural genes of the *N*-acetylmuramoyl-L-alanine amidase and its modifier. *Journal of General Microbiology*, **138:** 1949-1961.

Le Bourgeois, P., Bugarel, M., Campo, N., Daveran-Mingot, M-L., Labonté, J., Lanfranchi, D., Lautier, T., Pagès, C., Ritzenthaler, P., (2007). The unconventional Xer recombination machinery of streptococci/lactococci. *PLoS Genet*, **3:** e17.

Lenz, L.L. and Portnoy, D.A., (2002). Identification of a second *Listeria secA* gene associated with protein secretion and the rough phenotype. *Molecular Microbiology*, **45:** 1043-56.

Lenz, L.L., Mohammadi, S., Geissler, A., Portnoy, D.A., (2003). SecA2-dependent secretion of autolytic enzymes promotes *Listeria monocytogenes* pathogenesis. *Proceedings of the National Academy of Sciences of the United States of America*, **100:** 12432–12437.

Leppla, S.H., (1982). Anthrax Toxin Edema Factor: A Bacterial Adenylate Cyclase That Increases Cyclic AMP Concentrations in Eukaryotic Cells. *Proceedings of the National Academy of Sciences of the United States of America*, **79:** 3162-3166.

Leslie, N.R. and Sherratt, D.J., (1995). Site-specific recombination in the replication terminus region of *Escherichia coli*: functional replacement of dif. *EMBO Journal*, **14:** 1561–1570.

Li, P., Beckwith, J., Inouye, H., (1988). Alteration of the amino terminus of the mature sequence of a periplasmic protein can severely affect protein export in *Escherichia coli*. *Proceedings of the National Academy of Sciences of the United States of America*, **85:** 7685–7689.

Liu, J. and Rost, B., (2001). Comparing function and structure between entire proteomes. *Protein Science*, **10:** 1970–1979.

Luirink, J., Hagen-Jongman, C.M., van der Weijden, C.C., Oudega, B., High, S., Dobberstein, B., Kusters, R., (1994). An alternative protein targeting pathway in *Escherichia coli*: studies on the role of FtsY. *EMBO Journal*, **13:** 2289–2296.

Luirink, J. and Sinning, I., (2004). SRP-mediated protein targeting: structure and function revisited. *Biochimica et Biophysica Acta*, **1694:**17–35.

Machata, S., Hain, T., Rohde, M., Chakraborty, T., (2005). Simultaneous deficiency of both MurA and p60 proteins generates a rough phenotype in *Listeria monocytogenes*. *Journal of Bacteriology*, **187:** 8385–8394.

Macheboeuf, P., Contreras-Martel, C., Job, V., Dideberg, O., Dessen, A., (2006). Penicillin binding proteins: key players in bacterial cell cycle and drug resistance processes. *FEMS Microbiology Reviews*, **30:** 673–691.

Mader, C., Kupcu, S., Sara, M., Sleytr, U.B., (1999). Stabilizing effect of an S-layer on liposomes towards thermal or mechanical stress. *Biochimica et Biophysica Acta*, **1418:** 106–116.

Mader, C., Küpcü, S., Sleytr, U.B., Sára M (2000). S-layer-coated liposomes as a versatile system for entrapping and binding target molecules. *Biochimica et Biophysica Acta*, **1463:** 142–150.

Makins, S-I., Ucluda, I., Terakado, N., Sasakawa, C., Yoshikawa, M., (1989). Molecular characterisation and protein analysis of the cap region, which is essential for encapsulation in *Bacillus anthracis*. *Journal of Bacteriology*, **171:** 722–30.

Marrero, R. and Welkos, S.L., (1995). The transformation frequency of plasmids into *Bacillus anthracis* is affected by adenine methylation. *Gene*, **152:** 75–78.

Matuschek, M., Sahm, K., Zibat, H., Bahl, H., (1996). Characterization of genes from *Thermoanaerobacterium thermosulfurigenes* EM1 that encode two glycosyl hydrolases with conserved S-layer-like domain. *Molecular and General Genetics*, **252:** 493–496.

Mazmanian, S.K., G. Liu, H. Ton-That, Schneewind, O., (1999). *Staphylococcus aureus* sortase, an enzyme that anchors surface proteins to the cell wall. *Science*, **285:** 760-763.

Meade, J., (2004). Images in emergency medicine. Cutaneous anthrax. *Annals of Emergency Medicine*, **43:** 664-673.

Meima, R., Eschevins, C., Fillinger, S., Bolhuis, A., Hamoen, L.W., Dorenbos, R., Quax, W.J., van Dijl, J.M., Provvedi, R., Chen, I., Dubnau, D., Bron, S., (2001). The bdbDC operon of *Bacillus subtilis* encodes thiol disulfide oxidoreductases required for competence development. *Journal of Biological Chemistry*, **277:** 6994–7001.

Menetret, J.F., Hegde, R.S., Heinrich, S.U., Chandramouli, P., Ludtke, S.J., Rapoport, T.A., Akey, C.W., (2005). Architecture of the ribosome-channel complex derived from native membranes. *Journal of Molecular Biology*, **348:** 445–457.

Mescher, M.F. and Strominger, J.L. (1976). Structural (shapemaintaining) role of the cell surface glycoprotein of *Halobacterium salinarium*. *Proceedings of the National Academy of Sciences of the United States of America*, **73:** 2687-2691.

Mesnage, S., Tosi-Couture, E., Mock, M., Gounon, P., Fouet, A., (1997). Molecular characterization of the *Bacillus anthracis* main S-layer component: evidence that it is the major cell-associated antigen. *Molecular Microbiology*, **23:** 1147-1155.

Mesnage, S., Tosi-Couture, E., Gounon, P., Mock, M., Fouet, A. (1998). The capsule and S-layer, two independent and yet compatible macromolecular structures in *Bacillus anthracis*. *Journal of Bacteriology*, **180:** 52 - 58.

Mesnage, S., Tosi-Couture, E., Fouet, A., (1999). Production and cell surface anchoring of functional fusions between the SLH motifs of the *Bacillus anthracis* S-layer proteins and the *Bacillus subtilis* levansucrase. *Molecular Microbiology*, **31:** 927–936.

Mesnage, S., Fontaine, T., Mignot, T., Delepierre, M., Mock, M., Fouet, A., (2000). Bacterial SLH domain proteins are non-covalently anchored to the cell surface via a conserved mechanism involving wall polysaccharide pyruvylation. *EMBO Journal*, **19:** 4473–4484.

Mesnage, S., Tosi-Couture, E., Gounon, P., Mock, M., Fouet, A., (1998). The capsule and S-layer: two independent and yet compatible macromolecular structures in *Bacillus anthracis. Journal of Bacteriology*, **180:** 52–58.

Mignot, T., Mesnage, S., Couture-Tosi, E., Mock, M., Fouet, A., (2002). Developmental switch of S-layer protein synthesis in *Bacillus anthracis*. *Molecular Microbiology*, **43:** 1615– 1627.

Mignot, T., Mock, M., Fouet, A., (2003). A plasmid-encoded regulator couples the synthesis of toxins and surface structures in *Bacillus anthracis*. *Molecular Microbiology*, **47:** 917-927.

Mignot, T., Couture-Tosi, E., Mesnage, S., Mock, M., Fouet, A., (2004). In vivo *Bacillus anthracis* gene expression requires PagR as an intermediate effector of the

AtxA signalling cascade. *International Journal of Medical Microbiology*, **293:** 619–624.

Miot, M. and Betton, J.-M., (2004). Protein quality control in the bacterial periplasm. *Microbial Cell Factories*, **3**: 4.

Mitra, K., Schaffitzel, C., Saikh, T., Tama, F., Jenni, S., Brooks III, C.L., Ban, N., Frank, J., (2005). Structure of the *E. coli* protein-conducting channel bound to a translating ribosome. *Nature*, **438:** 318–324.

Moayeri, M., Haines, D., Young, H.A., Leppla, S.H., (2003). *Bacillus anthracis* lethal toxin induces TNF-α independent hypoxia-mediated toxicity in mice. *Journal of Clinical Investigation*, **112:** 670-682.

Mogk, A., Schlieker, C., Friedrich, K. L., Schonfeld, H. J., Vierling, E., Bukau, B., (2003). *Journal of Biological Chemistry*, **278:** 31033-31042.

Moll, D., Huber, C., Schlegel, B., Pum, D., Sleytr, U.B., Sleytr, U.B., (2001). S-layer streptavidin fusion proteins as template for nanopatterned molecular arrays. *Proceedings of the National Academy of Sciences of the United States of America*, **99:** 14646–14651.

Müller, J.P., Bron, S., Venema, G., van Dijl, J.M., (2000). Chaperone-like activities of the CsaA protein of *Bacillus subtilis*. *Microbiology*, **146:** 77–88.

Munn, C. B., Ishiguro, E. E., Kay, W. W., Trust, T. J., (1982). Role of surface components in serum resistance of virulent *Aeromonas salmonicida*. *Infection & Immunity*, **36:** 1069-1075.

Muren, E.M., Suciu, D., Topping, T.B., Kumamoto, C. A., Randall, L.L., (1999). Mutational alterations in the homotetrameric chaperone SecB that implicate the structure as dimer of dimers. *Journal of Biological Chemistry*, **274:** 19397–402.

Murphy, C.K. and Beckwith, J., (1994). Residues essential for the function of SecE, a membrane component of the *Escherichia coli* secretion apparatus, are located in a conserved cytoplasmic region. *Proceedings of the National Academy of Sciences of the United States of America*, **91:** 2557–2561.

Musial-Siwek, M., Rusch, S.L., Kendall, D.A., (2007). Selective photoaffinity labeling identifies the signal peptide binding domain on SecA. *Journal of Molecular Biology*, **365:** 637-648.

Nakamura, K., Yahagi, S., Yamazaki, R., Yamane, K., (1999). *Bacillus subtilis* histone-like protein, HBsu, is an integral component of a SRP-like particle that can bind the Alu domain of small cytoplasmic RNA. *Journal of Biological Chemistry*, **274:** 13569-13576.

Natale, P., Bruser, T., Driessen, A.J., (2008). Sec- and Tat-mediated protein secretion across the bacterial cytoplasmic membrane—distinct translocases and mechanisms. *Biochimica et Biophysica Acta*, **1778:** 1735-1756.

Navarre, W.W. and Schneewind, O., (1999). Surface proteins of gram-positive bacteria and mechanisms of their targeting to the cell wall envelope. *Microbiology and Molecular Biology Reviews*, **63:** 174–229.

Nielsen, P., Rainey, F., Outtrup, H., Priest, F.G., (1994). Comparative 16S rDNA sequence analysis of some alkaliphilic bacilli and the establishment of a sixth rRNA group within the genus *Bacillus. FEMS Microbiology Letters*, **117:** 61-66.

Nishiyama, K., Mizushima, S., Tokuda, H., (1992). The carboxyl-terminal region of SecE interacts with SecY and is functional in the reconstitution of protein translocation activity in *Escherichia coli*. *Journal of Biological Chemistry*, **267:** 7170– 7176.

Nishiyama, K., Mizushima, S., Tokuda, H., (1993). A novel membrane protein involved in protein translocation across the cytoplasmic membrane of *Escherichia coli*. *EMBO Journal*, **12:** 3409–3415

O'Brien, J., Friedlander, A., Dreier, T., Ezzell, J., Leppla, S., (1985). Effects of anthrax toxin components on human neutrophils. *Infection & Immunity*, **47:** 306–310.

Okuda, K., Kigure, T., Yamada, S., Kaneko, T., Ishihara, K., Miura, T., Kato, T., Takazoe, I., (1997). Role for the S-layer of *Campylobacter rectus* ATCC33238 in complement mediated killing and phagocytic killing by leukocytes from guinea pig and human peripheral blood. *Oral Diseases*, **3:** 113–120.

Olivier, G., Eaton, C.A., and Campbell, N. (1986). Interaction between *Aeromonas salmonicida* and peritoneal macrophages of brook trout (*Salvelinus fontinalis*). *Veterinary Immunology and Immunopathology*, **12**: 223–234.

Osborne, A.R., Clemons, Jr. W.M., Rapoport, T.A., (2004). A large conformational change of the translocation ATPase SecA, *Proceedings of the National Academy of Sciences of the United States of America*, **101:** 10937-10942.

Over, B., Heusser, R., McCallum, N., Schulthess, B., Kupferschmied, P., Gaiani, J.M., Sifri, C.D., Berger-Bächi, B., Stutzmann Meier, P., (2011). LytR-CpsA-Psr proteins in *Staphylococcus aureus* display partial functional redundancy and the deletion of all three severely impairs septum placement and cell separation. *FEMS Microbiology Letters*, **320:** 142-151.

Paccani, S. R., F. Tonello, R., Ghittoni, M., Natale, L., Muraro, M. M., D'Elios, W. J., Tang, C., Montecucco, Baldari, C. T., (2005). Anthrax toxins suppress T lymphocyte activation by disrupting antigen receptor signalling. *Journal of Experimental Medicine*, **201:**325–331.

Papanikou, E., Karamanou, S., Baud, C., Frank, M., Sianidis, G., Keramisanou, D., Kolodimos, C.G., Kuhn, A., Economou, A., (2005). Identification of the preprotein binding domain of SecA. *Journal of Biological Chemistry*, **280:** 43209–43217.

Papanikolau, Y., Papadovasilaki, M., Ravelli, R.B., McCarthy, A.A., Cusack, S., Economou, A., Petratos, K., (2007). Structure of dimeric SecA, the *Escherichia coli* preprotein translocase motor. *Journal of Molecular Biology*, **366:** 1545–1557.

Pei, Z. and Blaser, M.J., (1990). Pathogenesis of *Campylobacter fetus* infections. Role of surface array proteins in virulence in a mouse model. *Journal of Clinical Investigation*, **85:** 1036-1043.

Peltier, J.B., Emanuelsson, O., Kalume, D.E., Ytterberg, J., Friso, G., Rudella, A., Liberles, D.A., Soderberg, L., Roepstorff, P., von Heijne, G., van Wijk, K.J., (2002). Central functions of the lumen and peripheral thylakoid proteome of *Arabidopsis* determined by experimentation and genome-wide prediction. *Plant Cell*, **14:** 211-236.

Peters, J., Nitsch, M., Kühlmorgen, B., Golbik, R., Lupas, A., Kellermann, J., Engelhardt H., Pfander, J.P., Müller, S., Goldie, K., Engel, A., Stetter, K.O., Baumeister, W., (1995). Tetrabrachion: a filamentous archaebacterial surface protein assembly of unusual structure and extreme stability. *Journal of Molecular Biology*, **245:** 385–401.

Pflughoeft, K.J., Sumby, P., Koehler, T.M., (2011). *Bacillus anthracis sin* Locus and Regulation of Secreted Proteases. *Journal of Bacteriology*, **193:** 631–639.

Phillips, G.J. and Silhavy, T.J., (1992). The *E. coli* ffh gene is necessary for viability and efficient protein export. *Nature*, **359:** 744– 746.

Plath, K., Mothes,W., Wilkinson, B.M., Stirling, C.J., Rapoport, T.A., (1998). Signal sequence recognition in posttranslational protein transport across the yeast ER membrane. *Cell*, **94:** 795–807.

Pleschberger, M., Neubauer, A., Egelseer, E. M., Weigert, S., Lindner, B., Sleytr, U. B., Muyldermans, S., Sára, M., (2003). Generation of a functional monomolecular protein lattice consisting of an S-layer fusion protein comprising the variable domain of a camel heavy chain antibody. *Bioconjugate Chemistry*, **14:** 440–448.

Pleschberger, M., Saerens, D.,Weigert, S., Sleytr, U.B., Muyldermans, S., Sára, M., Egelseer, E.M., (2004). An S-layer heavy chain camel antibody fusion protein for generation of a nanopatterned sensing layer to detect the prostate-specific antigen by surface plasmon resonance technology. *Bioconjugate Chemistry*, **15:** 664–671.

Pomerantsev, A.P., Sitaraman, R., Galloway, C.R., Kivovich, V., Leppla, S.H. (2006). Genome engineering in *Bacillus anthracis* using Cre recombinase. *Infection & Immunity*, **74:** 682–693.

Pum, D. and Sleytr, U.B., (1999). The application of bacterial S-layers in molecular nanotechnology. *Trends in Biotechnology*, **17:** 8–12.

Rahfeld, J.U., Rucknagel, K.P., Schelbert, B., Ludwig, B., Hacker, J., et al., (1994). Confirmation of the existence of a third family among peptidyl-prolyl cistrans isomerases. Amino acid sequence and recombinant production of parvulin. *FEBS Letters*, **352:** 180–84.

Randall, L.L. and Hardy, S.J., (2002). SecB, one small chaperone in the complex milieu of the cell. *Cellular and Molecular Life Sciences*, **59:** 1617-1623.

Rasko, D.A., Altherr, M.R., Han, C.S., Ravel, J. (2005). Genomics of the *Bacillus cereus* group of organisms. *FEMS Microbiology Reviews*, **29:** 303–329.

Ray, K.C., Mesnage, S., Washburn, R., Mock, M., Fouet, A., Blaser, M., (1998). Complement binding to *Bacillus anthracis* mutants lacking surface structures. Abstracts Book Poster 98th, General Meeting. American Society for Microbiology Atlanta, Georgia, USA, pp. B-418.

Read, T.D., Peterson, S.N., Tourasse, N., Baillie, L.W., Paulsen, I.T., Nelson, K.E., Tettelin, H., Fouts, D.E., Eisen, J.A., Gill, S.R., Holtzapple, E.K., Okstad, O.A.,

Helgason, E., (2003). The genome sequence of *Bacillus anthracis* Ames and comparison to closely related bacteria. *Nature*, **423:** 81-6.

Rigel, N.W., Gibbons, H.S., McCann, J.R., McDonough, J. ., Kurtz, S., Braunstein, M., (2009). The accessory SecA2 system of mycobacteria requires ATP binding and the canonical SecA1. *Journal of Biological Chemistry*, **284:** 9927–9946.

Sabet, M., Lee, S. W., Nauman, R. K., Sims, T., Um, H. S., (2003). The surface (S-) layer is a virulence factor of *Bacteroides forsythus*. *Microbiology*, **149:** 3617-3627.

Saller, M.J., Fusetti F., Driessen, A. J. M., (2009). *Bacillus subtilis* SpoIIIJ and YqjG Function in Membrane Protein Biogenesis, *Journal of Bacteriology*, **21:** 6749-6757.

Sambrook, J., Fritsch, E.F., Maniatis, T., (1989). Molecular cloning: a laboratory manual, 2nd ed. Cold Spring Harbor Laboratory Press, Cold Spring Harbor, N.Y.

Sanderson-Smith, M.L., Dinkla, K., Cole, J.N., Cork, A.J., Maamary P.G., McArthur, J.D., Chhatwal, G.S., Walker, M.J., (2008). M protein-mediated plasminogen binding is essential for the virulence of an invasive *Streptococcus pyogenes* isolate. *Faseb Journal*, **22:** 2715–2722.

Sára, M. and Sleytr, U.B., (1987). Molecular sieving through S layers of *Bacillus stearothermophilus* strains. *Journal of Bacteriology*, **169:** 4092-4098.

Sára, M., Pum, D., Sleytr, U.B., (1992). Permeability and chargedependent adsorption properties of the S-layer lattice from *Bacillus coagulans* E38-66. *Journal of Bacteriology*, **174:** 3487-3493.

Sára, M., Pum, D., Schuster, B., Sleytr, U.B., (2005). S-layers as patterning elements for application in nanobiotechnology. *Journal for Nanoscience and* ***Nanotechnology*** , **5:** 1939–1953.

Schatz, P.J., Bieker, K.L., Ottemann, K.M., Silhavy, T.J., Beckwith, J., (1991). One of three transmembrane stretches is sufficient for the functioning of the SecE protein, a membrane component of the *E. coli* secretion machinery. *EMBO Journal*, **10:** 1749–1757.

Schultze-Lam, S., Haranz, G., Beveridge, T.J., (1992). Participation of a cyanobacterial S-layer in fine-grain mineral formation. *Journal of Bacteriology*, **74:** 7971–7981.

Scheuring, J., Braun, N., Nothdurft, L., Stumpf, M., Veenendaal, A.K., Kol, S., van der Does, C., Driessen, A.J.M., Weinkauf, S., (2005). The oligomeric distribution of

SecYEG is altered by SecA and translocation ligands. *Journal of Molecular Biology*, **354:** 258–271.

Schiebel E., Driessen A.J.M., Hartl F.U., Wickner W., (1991). DAH + and ATP function at different steps of the catalytic cycle of preprotein translocase. *Cell*, **64:** 927–939.

Schnepf, E., Crickmore, N., Van Rie, J., Lereclus, D., Baum, J., Feitelson, J., Zeigler, D. R., Dean, D. H., (1998). *Bacillus thuringiensis* and its pesticidal crystal proteins. Microbiology and Molecular Biology Reviews, **62:** 775–806.

Schultze-Lam, S. and Beveridge, T. J., (1994). Nucleation of Celestite and Strontianite on a Cyanobacterial S-Layer. *Applied and Environmental Microbiology,* **60:** 447 – 453.

Sciochetti, S.A., Piggot, P.J., Blakely, G.W., (2001). Identification and characterisation of the *dif* site from *Bacillus subtilis*. *Journal of Bacteriology*, **183:** 1058–1068.

Shan, S.O. and Walter, P., (2005). Co-translational protein targeting by the signal recognition particle. *FEBS Letters*, **579:** 921–926

Sharma, V., Arockiasamy A., Ronning, D.R., Savva, C.G., Holzenburg, A., Braunstein, M., Jacobs, J., Sacchettini, J.C., (2003). Crystal structure of Mycobacterium tuberculosis SecA, a preprotein translocating ATPase. *Proceedings of the National Academy of Sciences of the United States of America*, **100:** 2243–2248.

Shafazand, S., Doyle, R., Ruoss, S., Weinacker, A., Raffin, T. A., (1999). Inhalation anthrax: epidemiology, diagnosis and management. *Chest*, **116:** 1369-1376.

Shimohata, N., Nagamori, S., Akiyama, Y., Kaback, H. R., Ito, K., (2007). SecY alterations that impair membrane protein folding and generate a membrane stress. *Journal of Cell Biology*, **176:** 307-317.

Shmid, F.X., (2001). Prolyl isomerases. *Advances in Protein Chemistry*, **59:** 243-282.

Sianidis, G., Karamanou, S., Vrontou, E., Boulias, K., Repanas, K., Kyrpides, N., Politou, A.S., Economou, A., (2001). Cross-talk between catalytic and regulatory elements in a DEAD motor domain is essential for SecA function. *EMBO Journal*, **20:** 961-970.

Siegel, V. and Walter, P., (1988). Each of the activities of signal recognition particle (SRP) is contained within a distinct domain: analysis of biochemical mutants of SRP. *Cell*, **52:** 39– 49.

Sillanpää, J., Martínez, B., Antikainen, J., Toba, T., Kalkkinen, N., Tankka, S., Lounatmaa, K., Keranen, J., Hook, M., Westerlund-Wikstrom, B., Pouwels, P. H., Korhonen, T. K., (2000). Characterization of the collagen-binding S-layer protein CbsA of *Lactobacillus crispatus. Journal of Bacteriology*, **182:** 6440–6450.

Sirisanthanta T., Brown, A.E., (2002). Anthrax of the gastrointestinal tract. *Emerging Infectious Diseases*, **8:** 649-651.

Sleytr, U. B., and Messner, P., (1983). Crystalline surface layers on bacteria. *Annual Review of Microbiology*, **37:** 311–339.

Sleytr, U.B., Sára, M., Küpcü, Z., Messner, P., (1986). Structural and chemical characterization of S-layers of selected strains of *Bacillus stearothermophilus* and *Desulfotomaculum nigrificans. Archives in Microbiology*, **146:** 19–24.

Sleytr, U.B., Messner, P., Pum, D., Sára, M. (Eds.: U.B.), (1988). Crystalline Bacterial Cell Surface Layers, Springer, Berlin, p. 193.

van der Sluis, E.O., Nouwen, N., Driessen, A.J.M., (2002). SecY–SecYand SecY–SecG contacts revealed by site-specific crosslinking. *FEBS Letters*, **527:** 159–165.

Smith, R.H., Messner, P., Lamontagne, L.R., Sleytr, U.B. and Unger, F.M., (1993). Induction of T-cell immunity to oligosaccharide antigens immobilized on crystalline bacterial surface layers (S-layers). *Vaccine*, **11:** 919–924.

Smith, H. and Stoner, H.B., (1967). Anthrax toxic complex. *Federation proceedings*, **26:** 1554-1557.

Soberón, M., Pardo-López, L., López, I., Gómez, I., Tabashnik, B.E., Bravo, A., (2007). Engineering modified Bt toxins to counter insect resistance. *Science*, **318:** 1640–42.

Song, C., Kumar, A., Saleh, M., (2009). Bioinformatic comparison of bacterial secretomes. *Genomics Proteomics, Bioinformatics*, **7:** 37–46.

Spencer, R.C., (2003). *Bacillus anthracis*. *Journal of Clinical Pathology*, **56:** 182-187.

Takamatsu, D., Bensing, B. A., Sullam, P. M., (2004). Genes in the accessory *sec* locus of *Streptococcus gordonii* have three functionally distinct effects on the expression of the platelet-binding protein GspB. *Molecular Microbiology*, **52:** 189–203.

Takamatsu, D., Bensing, B.A., Sullam, P.M., (2005). Two additional components of the accessory Sec system mediating export of the *Streptococcus gordonii* platelet-binding protein GspB. *Journal of Bacteriology*, **187:** 3878–3883.

Takami, H., Nakasone, K., Takaki, Y., Maeno, G., Sasaki, R., Masui, N., Fuji, F., Hirama, C., Nakamura, Y., Ogasawara, N., Kuhara, S., Horikoshi, K., (2000). Complete genome sequence of the alkaliphilic bacterium *Bacillus halodurans* and genomic sequence comparison with Bacillus subtilis. *Nucleic Acids Research*, **28:** 4317-4331.

Takeoka, A., Takumi, K., Kawata, T., (1991). Purification and characterization of S-layer proteins from *Clostridium difficile* GAI 0714. *Journal of General Microbiology*, **137:** 261–267.

Tjalsma, H., Noback, M.A., Bron, S., Venema, G., Yamane, K., van Dijl, J.M., (1997). *Bacillus subtilis* contains four closely related type I signal peptidases with overlapping substrate specificities: Constitutive and temporally controlled expression of different *sip* genes. *Journal of Biological Chemistry*, **272:** 25983–25992.

Tjalsma, H., Bolhuis, A., van Roosmalen, M L., Wiegert, T., Schumann, W., Broekhuizen, C.P., Quax, W., Venema, G., Bron, S., van Dijl, J.M., (1998). Functional analysis of the secretory precursor processing machinery of *Bacillus subtilis*: identification of a eubacterial homolog of archaeal and eukaryotic signal peptidases. *Genes & Development*, **12:** 2318–2331.

Tjalsma, H., Stover, A.G., Driks, A., Venema, G., Bron, S., van Dijl, J.M., (2000). Conserved serine and histidine residues are critical for activity of the ER-type signal peptidase SipW of *Bacillus subtilis*. *Journal of Biological Chemistry*, **275:** 25102-25108.

Tjalsma, H., Zanen, G., Bron, S., van Dijl, J.M., (2001). The eubacterial lipoprotein-specific (type II) signal peptidase. *Enzymes*, **22:** 3–23.

Tjalsma, H., Bron, S., van Dijl, J. M., (2003). Complementary impact of paralogous OxaI-like proteins of Bacillus subtilis on post-translocational stages in protein secretion. *Journal of Biological Chemistry*, **278:** 15622-15632.

Tjalsma, H., Antelmann, H., Jongbloed, J.D.H., Braun, P.G., Darmon, E., Dorenbos, R., Jean-Yves F. Dubois, J-Y.F, Westers, H., Zanen, G., Quax, W.J., *et al.*, (2004). Proteomics of protein secretion by *Bacillus subtilis*: separating the ‘‘secrets’’ of the secretome. *Microbiology and Molecular Biology Reviews*, **68:** 207–233.

Topping, T.B. and Randall L.L., (1997). Chaperone SecB from *Escherichia coli* mediates kinetic partitioning via a dynamic equilibrium with its ligand. *Journal of Biological Chemistry*, **272:**19314-19318.

Topping, T.B., Woodbury, R.L., Diamond, D.L., Hardy, S.J., Randall, L.L., (2001). Direct demonstration that homotetrameric chaperone SecB undergoes a dynamic dimer-tetramer equilibrium. *Journal of Biological Chemistry*, **276:** 7437–41.

Tournier, J. N., Quesnel-Hellmann, A., Mathieu, J., Montecucco, C., Tang, W. J., Mock, M., Vidal, D. R., Goossens, P. L., (2005). Anthrax edema toxin cooperates with lethal toxin to impair cytokine secretion during infection of dendritic cells. *Journal of Immunology*, **174:** 4934–4941.

Tournier, J.-N., Quesnel-Hellmann, A., Cleret, A., Vidal, D.R., **(2007).** Contribution of toxins to the pathogenesis of inhalational anthrax. *Cellular Microbiology*, **9:** 555–565.

Trust, T.J., Kostrzynska, M., Emödy, L., and Wadström, T. (1993). High-affinity binding of the basement membrane protein collagen type IV to the crystalline virulence surface protein array of *Aeromonas salmonicida*. *Molecular Microbiology*, **7:** 593–600.

Turnbull, P.C., Leppla, S.H., Broster, M.G., Quinn, C.P., Melling, J., (1988). Antibodies to anthrax toxin in humans and guinea pigs and their relevance to protective immunity. *Medical Microbiology and Immunology*, **177:** 293-303.

Turnbull, P.C.B., Boehm, R., Cosivi, O., Doganay, M., Hugh-Jones, M.E., Joshi, D. D., Lalitha, M.K., de Vos, V., (1998). Guidelines for the surveillance and control of anthrax in humans and animals. WHO/EMC/ZDI/98.6.

Tutrone, W.D., Scheinfeld, N.S., Weinberg, J.M., (2002). Cutaneous anthrax: a concise review. *Cutis*, **69:** 27–33.

Tziatzios, C., Schubert, D., Lotz, M., Gundogan, D., Betz, H., Schagger H., Haase, W., Duong, F., Collinson, I., (2004). The bacterial protein-translocation complex:

SecYEG dimers associate with one or two SecA molecules. *Journal of Molecular Biology*, **340:** 513–524.

Uchida, I., Hornung, J.M., Thorne, C.B., Klimpel, K.R., Leppla, S.H., (1993). Cloning and characterization of a gene whose product is a trans-activator of anthrax toxin synthesis. *Journal of Bacteriology*, **175:** 5329-5338.

Vagner, V., Dervyn, E., Ehrlich, S.D., (1998). A vector for systematic gene inactivation in *Bacillus subtilis*. *Microbiology*, **144:** 3097-3104.

Valent, Q.A., Scotti, P.A., High, S., De Gier, J.-W.L., Von Heijne, G., Lentzen, G., Wintermeyer, W., Oudega, B., Luirink, J., (1998). The *Escherichia coli* SRP and SecB targeting pathways converge at the translocon. *EMBO Journal*, **17:** 2504–2512.

Vassylyev, D.G., Mori, H., Vassylyeva, M.N., Tsukazaki, T., Kimura, Y., Tahirov, T. H., Ito, K., (2006). Crystal structure of the translocation ATPase SecA from Thermus thermophilus reveals a parallel, head-to-head dimer. *Journal of Molecular Biology*, **364:** 248–258.

Veenendaal, A.K., van der Does, C., Driessen, A.J.M., (2002). The core of the bacterial translocase harbors a tilted transmembrane segment 3 of SecE, *Journal of Biological Chemistry*, **277:** 36640–36645.

Vietri, N.J., Marrero, R., Hoover, T.A., Welkos, S.L., (1995). Identification and characterization of a trans-activator involved in the regulation of encapsulation by *Bacillus anthracis*. *Gene*, 152: 1-9.

Vitale, G.P., Recchi, C., Napolitani, G., Mock, M., Montecucco, C., (1998). Anthrax lethal factor cleaves N-terminus of MAPKK's and induces tyrosine/threonine phosphorylation of MAPK's in cultures macrophages. *Biochemical and Biophysical Research Communications*, **248:** 706-711.

Vitikainen, M., Pummi, T., Airaksinen, U., Wahlstrom, E., Wu, H., Sarvas, M., Kontinen, V.P., (2001). Quantitation of the capacity of thesecretion apparatus and requirement for PrsA in growth and secretionof alpha-amylase in *Bacillus subtilis*, *Journal of Bacteriology*, **183:** 1881– 1890.

Voth, D. E., Hamm, E. E., Nguyen, L. G., Tucker, A. E., Salles, I. I., Ortiz-Leduc, W., Ballard, J. D., (2005). *Bacillus anthracis* oedema toxin as a cause of tissue necrosis and cell typespecific cytotoxicity. *Cellular Microbiology*, **7:** 1139-1149.

Völlenkle, C., S. Weigert, N. Ilk, E. Egelseer, V. Weber, F. Loth, D. Falkenhagen, U. B. Sleytr, Sara, M., (2004). Construction of a functional S-layer fusion protein comprising an immunoglobulin G-binding domain for development of specific adsorbents for extracorporeal blood purification. *Applied and Environmental Microbiology*, **70:** 1514–1521.

Walter, P. and Blobel, G., (1981). Translocation of proteins across the endoplasmic reticulum III. Signal recognition protein (SRP) causes signal sequence-dependent and site-specific arrest of chain elongation that is released by microsomal membranes. *Journal of Cell Biology*, **91:** 557–561

Walz, A., Mujer, C.V., Connolly, J.P., Alefantis, T., Chafin, R., Dake, C., Whittington, J., Kumar, S.P., Khan, A.S., DelVecchio, V.G., (2007). Bacillus anthracissecretome time course under host-simulated conditions and identification of immunogenic proteins. *Proteome Science,* **5:** 11.

Wang, B., Kraig, E., Kolodrubetz, D., (2000). Use of defined mutants to assess the role of the **Campylobacter rectus** S-layer in bacterium-epithelial cell interactions. *Infection & Immunity*, **68:**1465–1473.

Wandersman, C., (1989). Secretion, processing and activation of bacterial extracellular proteases. *Molecular Microbiology*, **3:** 1825–1831.

Wang, L., Ruan, B., Ruvinov, S., Bryan, P.N., (1998). Engineering the independent folding of the subtilisin BPN' pro-domain: correlation of pro-domain stability with the rate of subtilisin folding. *Biochemistry*, **37:** 3165–3171.

van Wely, K. H. M., Swaving, J., Broekhuizen, C. P., Rose, M., Quax, W. J., Driessen, A. J. M. (1999). Functional identification of the product of the *Bacillus subtilis* yvaL gene as a SecG homologue. *Journal of Bacteriology*, **181:** 1786–1792.

Wildhaber, I. and Baumeister, W., (1987). The cell envelope of *Thermoproteus tenax*: three-dimensional structure of the surface layer and its role in shape maintenance. *EMBO Journal*, **6:** 1475-1480.

Williams, R.C., Rees, M.L., Jacobs, M.F., Pragai, Z., Thwaite, J.E., Baillie, L.W., Emmerson P.T., Harwood, C.R. (2003). Production of *Bacillus anthracis* protective antigen is dependent on the extracellular chaperone. PrsA. *Journal of Biological Chemistry*, **278:** 18056-18062.

van der Wolk, J.P., de Wit, J.G., Driessen, A.J., (1997). The catalytic cycle of the *Escherichia coli* SecA ATPase comprises two distinct preprotein translocation events. *EMBO Journal*, **16:** 7297– 7304.

Wong, S.L., (1995). Advances in the use of *Bacillus subtilis* for the expression and secretion of heterologous proteins. *Current Opinion Biotechnology*, **6:** 517-522.

Woodbury, R.L., Hardy, S.J.S., Randall, L.L., (2002). Complex behavior in solution of homodimeric SecA. *Protein Science*, **11:** 875-882.

Wu, X.C., Lee, W., Tran, L., Wong, S.L., (1991). Engineering a *Bacillus subtilis* expression–secretion system with a strain deficient in six extracellular proteases. *Journal of Bacteriology*, **173:** 4952–4958.

Yabuta, Y., Takagi, H., Inouye, M., Shinde, U., (2001). Folding pathway mediated by an intramolecular chaperone. Propeptide release modulates activation precision of pro-subtilisin. *Journal of Biological Chemistry*, **276:** 44427–44434.

Yamada, H., Tsukagoshi, N., Udaka, S., (1981). Morphological alterations of cell wall concomitant with protein release in a protein-producing bacterium *Bacillus brevis*. *Journal of Bacteriology*, **148:**322–332.

Yang, M. J., Jung, S. H., Shin, E. S., Kim, J., Yun, H. D., Wong, S. L., Kim, H. (2004). Expression of a *Bacillus subtilis* endoglucanase in protease-deficient *Bacillus subtilis* strains. *Journal of Microbiology and Biotechnology*, **14:** 430-434.

Young, J.A. and Collier, R., J., (2007). Anthrax Toxin: Receptor Binding, Internalization, Pore Formation, and Translocation. *Annual* Rev*iew Biochemistry*, **76:** 243–265.

Zemansky, J., Kline, B. C., Woodward, J. J, Leber, J. H., Marquis, H., Portnoy, D. A., (2009). Development of a mariner-based transposon and identification of *Listeria monocytogenes* determinants, including the peptidyl- prolyl isomerase PrsA2, that contribute to its hemolytic phenotype. *Journal of Bacteriology*, **191:**3950–3964.

Zhao, G., Meier, T.I., Kahl, S.,D., Gee, K.R., Blaszczak L.,C., (1999). BOCILLIN FL, a sensitive and commercially available reagent for detection of penicillin-binding proteins. *Antimicrobial Agents and Chemotherapy*. **43:** 1124–1128.

Zhou, J. and Xu, Z., (2005). The structural view of bacterial translocation-specific chaperone SecB: implications for function. *Molecular Microbiology*, **58:** 349–357.

Zimmer, J., Li, W., Rapoport, T., (2006). A novel dimer interface and conformational changes revealed by an X-ray structure of *B. subtilis* SecA. *Journal of Molecular Biology*, **364:** 259–265.

Zink, S.D. and Burns, D.L., (2005). Importance of *srtA* and *srtB* for growth of *Bacillus anthracis* in macrophages. *Infection & Immunity*, **73:**5222-5228.

Zuber, U. and Schumann, W., (1994). CIRCE, a novel heat shock element involved in regulation of heat shock operon dnaK of *Bacillus subtilis*. *Journal of Bacteriology*, **176:** 1359– 1363.

Appendix A: Growth media and solutions

General growth media

Luria-Bertani (LB) Growth Media (per litre) pH to 7.0	(Autoclave)
Bacto Tryptone	10 g
NaCl	10 g
Bacto Yeast Extract	5 g
(Agar; Mast Diagnostics; Merseyside, UK)	(15 g)

Modified LB media	Additive stock	Volume of stock added to 1000 ml LB medium
LB-Starch	Starch	10 g prior to autoclaving

***E.coli* transformation**

Basis of SOC and SOB broths (per litre)	Autoclave
Bacto Tryptone	20 g
Bacto Yeast Extract	5g
NaCl	0.58 g
KCl	0.189

2 M glucose	
glucose	34 g
Add distilled water to 100 ml and filter sterilize with 0.22 µM filter	

2 M Mg^{2+} stock	
$MgCl_2$	20.33 g
$MgSO_4$	24.65 g
Add distilled water to 100 ml and filter sterilize	

SOC and SOB broths
SOB broth: add 1 ml of 2M Mg^{2+} stock to 99 ml basis of SOB and SOC broth
SOC broth: add 1 ml of 2M glucose and 1 ml of 2M Mg^{2+} stock to 98 ml basis of SOB and SOC broth

TB (Inoue) buffer (per litre)	
$MnCl_2$	10.9 g
$CaCl_2$	2.2 g
KCl	18.7 g
10 mM PIPES (0.5M, pH 6.7)	20 ml
Add distilled water to 1 liter and filter sterilize with 0.45 µM filter	

Electrophoresis buffers

5x TBE	
Tris base	54 g
Boric acid	27.5g
EDTA	20ml of 0.5M (pH 8.0)

50 x TAE Running buffer (per liter)	
Tris base	48.4 g
Glacial acetic acid	11.4 ml
0.5M EDTA (pH 8.0)	20ml

Bacillus subtilis transformation media

Spizizen minimal medium (SMM) (per litre)	(Autoclave)
$(NH_4)_2SO_4$	2 g
K_2HPO_4	14 g
KH_2PO_4	6 g
$C_6H_5O_7Na_3 \cdot 2H_2O$	1 g
$MgSO_4.7H_2O$	0.2 g

MM competence medium (per transformation)	
SMM	10 ml
40% glucose	0.125 ml
Tryptophan solution (2 mg/ml)	0.1 ml
$MgSO_4$ (1M)	0.06 ml
Casamino acids (20%)	0.01 ml
$C_6H_8O_7$ $FeNH_4$	0.005 ml

MM starvation medium (per transformation)	
SMM	10 ml
40% glucose	0.125ml
$MgSO_4$ (1M)	0.06 ml

Koehler electrotransformation media for the transformation of *B. anthracis*

Growth Medium (per litre)	(Autoclave)
BHI medium (DIFCO)	37 g
Glycerol	5 g
(Agar; Mast Diagnostics, Merseyside, UK)	(10 g)

Electrotransformation buffer (per litre), pH to 7.0	(Autoclave)
HEPES-Na	1 mM
Glycerol	10 % (w /v)

Recovery Medium (per litre)	(Autoclave)
BHI medium (DIFCO)	37 g
Glycerol	100 *g*
Glucose (20 % (w/v) – filter sterilised, add to cooled sterilised medium	20 ml
$MgCl_2$ (0.5 M) – filter sterilised, add to cooled sterilised medium	20 ml

SDS-PAGE and protein purification

Acrylamide Gels for SDS-PAGE		
	Resolving Gel (10 %)	Stacking Gel (5 %)
dH_2O	5.0 ml	3.1 ml
40 % (w/v) Bis Acrylamide	2.5 ml	0.625 ml
1.5 M Tris pH 8.8	2.5 ml	-
1 M Tris pH 6.8	-	1.25 ml
10 % (w/v) APS	0.05 ml	0.03 ml
TEMED	0.001 ml	0.015 ml

2 x SDS-PAGE Loading Buffer	
TrisHCl (pH6.8)	100 mM
β-Mercaptoethanol	100 mM
SDS	4 % (w/v)
Bromophenol Blue	0.2 % (w/v)
Glycerol	20 % (w/v)

10 x SDS-PAGE Running Buffer (per litre)	
Tris Base	30.2 g
Glycine	150 g
SDS	10g

Coomassie Blue Stain (per litre)	
Coomassie Blue	0.25 g
Ethanol	500 ml
Glacial acetic acid	75 ml

SDS-PAGE Destain	
Ethanol	30 % (v/v)
Glacial Acetic Acid	10 % (v/v)

TCA solution	
TCA	80 g
dH_2O	200 ml

Urea/thiourea solution	
Urea	1.2 g
Add 1 ml dH_2O, vortex to dissolve add 0.38h thiourea and vortex to dissolve. Fill the volume up to 2.5ml.	

Lithium chloride solution (pH 7.5)	
LiCl	4 M
PMSF	200 µM
TrisCl	50 mM

Phosphate buffered saline (PBS) (pH 7.4)	
NaCl	136 mM
NaH_2PO_4	10 mM
KCl	2.5 mM
K_2HPO_4	1.8 mM

1x Tris buffered saline (TBS) (pH 7.4)	
NaCl	150mM or 500mM*
Tris-Cl	50 mM
*500 mM for high stringency washes	

Solutions for Northern blotting hybridization

Hybridization solution (10ml)	
20x SSC	2.5 ml
10% SDS	20 µl
10% N-laurylsarcosine	100 µl
10% blocking reagent	2 ml
Formamide	5 ml

Denaturation solution	
NaOH	0.5 M
NaCl	1.5 M

Neutralization solution	
Tris-HCl	0.5 M
1.5 NaCl	3 M

20x SSC (pH 7.0)	
NaCl	3 M
Sodium Citrate	0.3 M

10% Blocking reagent (pH 7.5)	
Blocking reagent (milk powder)	20 g
Maleic acid buffer	200 ml
Dissolve blocking reagent in maleic acid buffer in the microwave, stirring it from time to time. Adjust pH to 7.5 with NaOH, autoclave and store at 4^{o}C.	

10% Blocking buffer (pH 7.5) (per 50 ml)	
10% Blocking reagent	5 ml
Washing buffer I	5 ml
Fill up to 50ml litre with dH_2O and leave for about 30 min at 37^{o}C before use	

Maleic Acid Buffer (pH7.5)	
Maleic acid	0.1 M
NaCl	0.15 M

10x Washing Buffer I (pH 7.0)	
Maleic acid	116 g
NaCl	87.6 g
NaOH	72 g
Fill up to 1 litre with dH_2O	

Tween Washing buffer	
10% Washing buffer I	100 ml
Tween 80	3 ml
Fill up to 1 litre with dH_2O	

Washing Solution I (per 50 ml)	
20 x SSC	10 ml
10% SDS	1 ml
Fill up to 50ml litre with dH_2O	

Washing Solution I (per 150 ml)	
20 x SSC	0.75 ml
10% SDS	1.5 ml

Fill up to 150ml litre with dH_2O	

Buffer 3 (pH 9.0)	
diethanolamine	9.63 ml
Fill up to 1 litre with dH_2O	

Detection buffer (pH 9.5)	
Tris-HCl	0.1 M
NaCl	0.1 M
10x MOPS (pH 7.0)	
MOPS	0.2 M
NaCl	0.05 M
EDTA	0.02 M

Appendix B: Oligonucleotide primers used in the study

Primer	Sequence (restriction site inserted-red)	PCR amplification product (bp)/Comment
Complementation analysis of SecY of B. subtilis (Bsu SecY) by SecY2 of B. anthracis (Ban SecY2)		
secY_fwd	tttttt**gcggccgc**TGGCGGTACAGCTGAGG	*secY* (370)
secY_rev	cgc**ggatcc**ACGGCGGCCAACTTC	
secY2_fwd	tttttt**ggatcc**TGCGGAAGGAGGTTTGTG	*secY2* (1415)
secY2_rev	cgac**ggactagt**TTTTTACTTAATTCGCTTT	
adk_fwd	cgac**ggactagt**TTAATAAAGAGAGGACGGG	*adk-map* (1468)
Map_rev	ttt**gcggccgc**TCGGAATTATTTTCATCA	
Pmut_fwd	TCC TAA CAG CAC AAG AGC	Amplification over pMUTIN4 mcs
Pmut_rev	CCA CAG TAG TTC ACC ACC	
Pxyl_fwd	ATA AGT TAG TTT GTT TGG GC	Amplification over pJPR1 mcs
amyE_rev	GGA TAT ACA GCC ATT CAG AC	
Creation of deletion mutants of *B. anthracis*		
*prsAA*_upstream_fwd	ttttttcccgggGTAGTTATGTCCGATTC	*prsAA* upstream region (939)
*prsAA*_upstream_rev	ttttttcccgggTCGATAAACACTCCTAC	
*prsAA*_downstream_fwd	ttttttcccgggGTAGTTATGTCCGATTC	*prsAA* downstream region (885)
*prsAA*_downstream_rev	cgcgaattcGAACATAGAATCAATCTC	
*prsAB*_upstream_fwd	tttcgtgagctcACATAACCAGCGGCGATAATA	*prsAB* upstream region (906)
*prsAB*_upstream_rev	ttttttcccgggGCTAACACCTCATCCGAATATG	
*prsAB*_downstream_fwd	ttttttcccgggCCACTTCAATCAGCGCATC	*prsAB* downstream region (737)
*prsAB*_downstream_rev	tttcgcgaattcAGATGAGCATTTCCGTGCATT	
*prsAC*_upstream_fwd	ttttgtgagctcAAGGGCTGGTCGATTTACCT	*prsAC* upstream region (779)
*prsAC*_upstream_rev	ttttttcccgggTGAGTAAAATGACCCTTTACGT ATTC	
*prsAC*_downstream_fwd	ttttttcccgggAGGTTCCCTTTTCTAGTTAGTG	*prsAC* downstream region (849)
*prsAC*_downstream_rev	tttcgcgaattcAAATATAAAATCCCTGCCTAA ATTC	
*secH*_upstream_fwd	ttttgtgagctcAGCTAAAAGGTCGTGCTGGT	*secH* upstream region (828)
*secH*_upstream_rev	ttttttcccgggCACCTCGTTATTGTACGTTTTC A	
*secH*_downstream_fwd	ttttttcccgggCAAAAAGATGGTCATCACAC	*secH* downstream region (861)
*secH*_downstream_rev	ttttgtgaattcGCTTTTTTATTGTTATATTCAGT	
*secA2*_upstream_fwd	cacgagctcCTGCTACAACATCACTCTC	*secA2* upstream region (671)
*secA2*_upstream_rev	ccacccgggCTGACAATAGCTACAT	
*secA2*_downstream_fwd	ttttttcccgggCGAGGTGAAAGATTATG	*secA2* downstream region (909)
*secA2*_downstream_rev	cgcgaattcGTGGTACAAGTGCTTTC	
*secA2_promoter*_fwd	caacccgggACATCATAAAACGAGATAG	promoter region of

*secA2_promoter*_rev	ccactgcagACTGACAATAGCTAC	*secA2-secH* operon (241)
*sap*_upstream_fwd	caagagctcCTATGGTCGGTATTTCATATG	*sap* upstream region (671)
*sap*_upstream_rev	caacccgggCTCCTTAGGAATGTAATAC	
*eag*_downstream_fwd	caacccgggGTCGATTATAGATAAAGTG	*eag* downstream region (909)
*eag*_downstream_rev	ccactgcagTAAACGACTTATCTCAG	
DifKmF	ttttttcccgggACTGCCTATAATATATATTATG TTAACTGGTGATTGATTGAGCAAGCTTTA TGC	Primers to amplify kanamycin resistance cassette with *dif* sites (~2200)
DifKmR	ttttttcccgggAGTTAACATAATATATATTATA GG CAGTGGTGATTGATTGAGCAAGCTTTAT GC (66)	
*prsAA*_chromosomal_fwd	GAACTGATTGCTATCTTG	
*prsAB*_chromosomal_fwd	TACATGACGCGTATGAATCG	
*prsAC*_chromosomal_fwd	AATGATGCTAGAATGGATACACTA	
*secA2*_chromosomal_fwd	GCAATTGGAATCGAAACCTG	
*secH*_chromosomal_fwd	TGAGGGTGTTCACGAACTTG	
*sap*_chromosomal_fwd	GAACTGATTGCTATCTTG	
Km_internal_rev	TAGCGAGGGCTTTACTAAGC	
Complementation of *B.anthracis* null mutants		
*secA2*_compl_fwd	ttttttcccgggGAGGAGTGTTTACAACATGCTG	*secA2* (2414)
*secA2*_compl_rev	caactgcagTCACCTCGTTATTGTACG	
*secH*_compl_fwd	ttttttcccgggCGAGGTGAAAGATTATGTTATC ATTC	*secH* (998)
*secH*_compl_rev	caactgcagCCAAAGAGGTGTGATGACCA	
*secA2*_compl_fwd	ttttttcccgggGAGGAGTGTTTACAACATGCTG	*secA2-secH* (3416)
*secH*_compl_rev	caactgcagCCAAAGAGGTGTGATGACCA	
*sap*_compl_fwd	caaggatccATGGCAAAGACTAACTC	*sap* (2534)
*sap*_compl_rev	ccagaattcCCTATGATACTCATAGAC	
*eag*_compl_fwd	caaggatccATGGCAAAGACTAACTC	*eag* (2636)
*eag*_compl_rev	ccagaattcCACTTTATCTATAATCGAC	
Bacterial-Two-Hybrid (B2H) assay		
B2H_*secA1*_fwd	ttccgttctagaTAAAAAGAGGAGCGTATTTCC	*secA1* (2485)
B2H_*secA1*_rev	ttttttggtaccCATAAATCGTTGCGGCCGACTT GGTC	
B2H_*secA2*_fwd	ttttgttctagaTATTGTCAGTAAGAGGAGTGTT T	*secA2* (2375)
B2H_*secA2*_rev	ttttttggtaccGGAACACCTAAATGTCTTGC	
B2H_*secY1*_fwd	tttttttctagaAGGTGATCTAATGTTTCGTAC	*secY1* (1338)
B2H_*secY1*_rev	tttttggtaccTAATGGCGTTTTACCAGT	
B2H_*secY2*_fwd	tttttttctagaTGATAAAAATATAGGAGGCGAC A	*secY2* (1290)
B2H_*secY2*_rev	tttttggtaccATAAACCCTTTATAATGACGT	
B2H_*secH* _fwd	cgctctagaGATTATGTTATCATTCC	*secH* (900)
B2H_*secH*_rev	caaggtaccTCTTGTGGTACAAGTGC	
B2H_*eag*_fwd	gtacgctctagaTAGCATATTCCTGAAGGAGG	5'end *eag* (384)
B2H_*eag*_rev	ttctgtggtaccACTGCTGCAATATATTTTG	
B2H_*sap5*'_fwd	ttttttctagaTAAGGAGGAAATATATAAAATG GCA	5'end *sap* (333)
B2H_*sap5*'_rev	ttttttggtaccTCAGCGAAAGATGGTTTA	

B2H_*sap*_fwd	cacgtcgacAATGGCAAAGACTAACTC	*sap* (2441)
B2H_*sap*_rev	ttttttggtaccGTTGCAGGTTTTGCTTCT	
B2H_*eag/sap*_sig_fwd	cactctagaAATGGCAAAGACTAACTCTTAC	Signal sequence of
B2H_*eag/sap*_sig_rev	ttttttggtaccCCTGCTGCTGCTACTGGA	*sap* and *eag* (114)
B2H_*Bsu_ secA*_fwd	cgctctagaAATGCTTGGAATTTTAAAT	*secA* of *B. subtilis*
B2H_*Bsu_ secA*_rev	ttttttggtaccTCAGTACGGCCGCAGCA	(2541)

Sequencing primers for B2H

pUT18 for	GAGTTAGCTCACTCATTAGG
pUT18 rev	CCTAATGAGTGAGCTAACTC
pUT18C for	TCGACGATGGGCTGGGAGCC
pUT18C rev	AGCAGACAAGCCCGTCAGGGC
pKT25 for	GGCGGATATCGACATGT
pKT25 rev	ATCGGTGCGGGCCTCTTCGC
pKT25N for	GCTCACTCATTAGGCAC
pKT25 rev	GGCGGAACATCAATGTGGCG

Protein purification

pur_*secA1*_fwd	ttttttggatccATGATCGGTATTTTAAAAAAG	*secA1* (2535)
pur_*secA1*_rev	ttttttgtcgacTGATTACTTCCCGATACCACA	
pur_*secA2*_fwd	ttttttggatccATGCTGAATTCGGTAAAAAAG	*secA2* (2393)
pur_*secA2*_rev	ttttttgtcgacTGATTATTGTACGTTTTCAGG	
pur_*secH*_fwd	caacatatgAAAGATTATGTTATCATTCC	*secH* (893)
pur_*secH*_rev	ccaggatccTGATTAGTCTTGTGGTAC	

Northern blotting

*secA1*_probe_fwd	ATGATCGGTATTTTAAAAAAGG	5’ terminus of
*secA1*_probe_rev	ctaatacgactcactatagggagaAAGATAGAATCGACTTCATC	*secA1* (601)
*secA2*_probe_fwd	atgctgaattcggtaaaaaag	5’ terminus of
*secA2*_probe_rev	ctaatacgactcactatagggagaAAGCGGCCATATTATCACGT	*secA2* (664)
*secY1*_probe_fwd	ATGTTTCGTACAATCTCCAAC	5’ terminus of
*secY1*_probe_rev	ctaatacgactcactatagggagaCCTTTAGCTGTAATCTGTTC	*secY1* (545)
*secY2*_probe_fwd	ATGTTTCGTACGATTTCAAA	5’ terminus of
*secY2*_probe_rev	ctaatacgactcactatagggagaATTACCTACTCCATTAGCGG	*secY2* (555)
*secH*_probe_fwd	ATGTTATCATTCCTAAAAAAAGC	5’ terminus of
*secH*_probe_rev	ctaatacgactcactatagggagaTCTAGTGTATGCTTGCTTTC	*secH* (530)
*sap*_probe_fwd	ATGGCAAAGACTAACTCTTA	5’ terminus of
*sap*_probe_rev	ctaatacgactcactatagggagaATTCCTAATTCAACTAAGAT	*sap* (554)
*eag*_probe_fwd	ATGGCAAAGACTAACTCTTAC	5’ terminus of
*eag*_probe_rev	ctaatacgactcactatagggagaGATGTTTGCTTTCTCTTCAC	*eag* (492)
*prsAA*_probe_fwd	ATGAAGAAAGCTATGCTTGC	5’ terminus of
*prsAA*_probe_rev	ctaatacgactcactatagggagaATGATGTGGTAACCGAATTG	*prsAA* (671)
*prsAB*_probe_fwd	ATGAGAGGAAAACATATTTTC	5’ terminus of
*prsAB*_probe_rev	ctaatacgactcactatagggagaTCTTTTGATAGTAGGT	*secAB* (557)

	CTTG	
*prsAC*_probe_fwd	TTGTATAGTTATTCTTGTAT	5’ terminus of
*prsAC*_probe_rev	ctaatacgactcactatagggagaGTCTTTTCATCTTTTAC TAA	*secAC* (509)
*csaA*_probe_fwd	ATGTTTCGTACGATTTCAAA	5’ terminus of
*csaA*_probe_rev	ctaatacgactcactatagggagaTGCTACAACATCACTC TC	*csaA* (477)
*csaB*_probe_fwd	GTGCGGTTAGTTTTATCAG	5’ terminus of
*csaB*_probe_rev	ctaatacgactcactatagggagaCTGGATCTGGAACTAG TTC	*csaB* (511)
qPCR		
*eag*_qPCR_fwd	GTGCAATTACAGGTAAGCCAGAC	(125)
*eag*_qPCR_rev	AGCATCTTTGAAAGAAGGCTGAG	
*sap*_qPCR_fwd	CAGTTAAAGGTAACGACAAAGGAATG	(140)
*sap*_qPCR_rev	GAGTCAGCGAAAGATGGTTTAG	
*gyrB*_qPCR_fwd	ACCGTTCTTCATGCTGGTG	(170)
*gyrB*_qPCR_rev	GCAACCGGAATACCTCTTTC	
Pull-down experiment		
*secA2*_pull_fwd	caaggatccATG**GATTACAAGGATGACGACGA TAAG** AACATGCTGAATTCGGTA	*secA2* (2420)
*secA2*_pull_rev	cgctctagaTCACCTCGTTATTGTACG	
*secH*_pull_fwd	caaggatccATG**GATTACAAGGATGACGACGA TAAG** ATTATGTTATCATTCCTA	*secH* (934)
*secH*_pull_rev	cacctgcagCTCTATGATTAGTCTTGTG	
*sap*_pull_fwd	caaggatccATG**GATTACAAGGATGACGACGA TAAG** ATGGCAAAGACTAACTC	*sap* (2487)
*sap*_pull_rev	caagaattcTTATTTTGTTGCAGGTTTTG	

Appendix C: plasmids and strains used in the study

Table C.1. Strains used in the study

Strain	Characteristics	Source/ Reference
E.coli		
TOP10	F⁻ *mcrA* (*mrr-hsd*RMS-*mcr*BC) 80*lacZ* M15, *lac*X74, *deo*R, *rec*A1, *ara*D139 (*ara-leu*)7697, *gal*U, *gal*K, *rpsL*, (Str^R), *end*A1, *nup*G	Invitrogen Ltd, Paisley, UK.
XL1-Blue	*recA1 endA1 gyrA96 thi-1 hsdR17 supE44 relA1 lac* [F *proAB lacI* q. ZΔM15 Tn10 (Tet^r.)].	Stratagene
GM48	(JM110) dam^- dcm^-	Stratagene
BTH101	F-, *cya-99*, *araD139*, *galE15*, *galK16*, *rpsL1 (Str$_r$)*, *hsdR2*, *mcrA1*, *mcrB1*	Euromedex
B. subtilis 168	*trpC2*	Anagnostopoul -os, C and Spizizen, J.
KG101	*B. subtilis lacA*::pMut4*secY*-F; Em^r	This study
KG203	*B. subtilis amyE*::pJPR1-*Ban- prsAB- Ban secY2-Bsu adk-map*, Cm^r	This study
KG204	*B. subtilis amyE*::pJPR1-*Ban- secY2-Bsu adk-map*, Cm^r	This study
KG205	*B. subtilis amyE*::pJPR1-*Ban- prsAB- secY2-Bsu adk-map* with pMAP65, Cm^r Km^r	This study
KG206	*B. subtilis amyE*::pJPR1-*Ban- prsAB- secY2-Bsu adk-map; lacA*::pMut4*secY*-F with pMAP65, Cm^r Km^r Em^r	This study
GQ32	*secA*::*secA1*, amyE::*prsAB-eag*, Cm^r Km^r	Guoqing Wang
GQ48	*lacA*::*secA2*, *amyE*::*prsAB-eag*, Cm^r Em^r	Guoqing Wang
GQ69	*lacA*::*secA2secH*, *amyE*::*prsAB-eag*, Cm^r Em^r	Guoqing Wang
GQ72	*lacA*::*secH*, *amyE*::*prsAB-eag*, Cm^r Em^r	Guoqing Wang
GQ65	*secA*::*secA1*, *lacA*::*secA2*, *amyE*::*prsAB-eag*, Cm^r Km^r Em^r	Guoqing Wang
GQ74	*secA*::*secA1*, *lacA*::*secH*, *amyE*::*prsAB-eag*, Cm^r Km^r Em^r	Guoqing Wang
GQ75	*secA*::*secA1*, lacA::*secA2-secH*, amyE::*prsAB-eag*, Cm^r Km^r Em^r	Guoqing Wang
AB06Jeag1	*amyE*::*prsAB-eag*, Cm^r	Pijug Summpunn
AB06Jsap1	*amyE*::*prsAB-sap*, Cm^r	Pijug Summpunn
B. subtilis WB600	*trpC2*, Δ*nprE*, Δ*aprA*, Δ*epr*, Δ*bpf*, Δ *mpr*, Δ*nprB*	Wu et al., 1991

B. anthracis UMCI-2	pXO1$^-$ pXO2$^-$ derivative of UM23 , Ura-Rif^r	Hoffmaster *et* Koehler, 1997
Δ*secH*	UM23CI-2 *secH*:: Km^r *via* pKG3021	This study
Δ*secA2H*	UM23CI-2 *secA2-secH*::Km^r *via* pKG302	This study
Δ*prsAA*	UM23CI-2 *prsAA*::Km^r *via* pKG303	This study
Δ*prsAB*	UM23CI-2 *prsAB*::Km^r *via* pKG304	This study
Δ*prsAC*	UM23CI-2 *prsAC*::Km^r *via* pKG305	This study
Δ*sap-eag*	UM23CI-2 *sap-eag*:: Km^r *via* pKG306	This study
Δ*secA2**	UM23CI-2 *secA2*:: Km^r *via* pKG308	This study
Δ*secA2*	UM23C1-2 *secA2*:: Km^r *via* pSA102	Steven Addinal
KG400	UM23CI-2 with pKG400, Km^r Em^r	This study
KG401	Δ*secA2H* carrying pKG401, Km^r Em^r	This study
KG402	Δ*secA2H* carrying pKG402, Km^r Em^r	This study
KG403	Δ*secA2H* carrying pKG403, Km^r Em^r	This study
KG404-1	Δ*secA2** carrying pKG404, Km^r Em^r	This study
KG404-2	Δ*secA2H* carrying pKG404, Km^r Em^r	This study
KG404-3	Δ*secH* carrying pKG404, Km^r Em^r	This study
KG404-4	Δ*prsAB* carrying pKG404, Km^r Em^r	This study
KG404-5	Δ*sap-eag* carrying pKG404, Km^r Em^r	This study
KG405-1	Δ*secA2** carrying pKG405, Km^r Em^r	This study
KG405-2	Δ*secA2H* carrying pKG405, Km^r Em^r	This study
KG405-3	Δ*secH* carrying pKG405, Km^r Em^r	This study
KG405-5	Δ*prsAB* carrying pKG405, Km^r Em^r	This study
KG405-6	Δ*sap-eag* carrying pKG405, Km^r Em^r	This study
KG406	Δ*sap-eag* carrying pKG406, Km^r Em^r	This study
KG407	Δ*sap-eag* carrying pKG407, Km^r Em^r	This study
KG408	Δ*sap-eag* carrying pKG408, Km^r Em^r	This study

Table C.2. Plasmids used in the study

Plasmid	Characteristic	Reference/Source
Experiments in *B. subtilis*		
pJPR1	Integration vector, Amp^r Cm^r *5′amyE 3′amyE*, xylose-inducible P_{xyl}promoter	J. Errington (Newcastle University, UK)
pMUTIN4	Integration vector ,Ap^r Em^r Lm^r ,IPTG-inducible P_{spac} promoter	Vagner *et* al. 1998
pKG101	pMut4-P_{spac} -*secY*5’; *trpC2* Em^r	This study
pKG201	pJPR1-P_{xyl}-*Ban- secY2, trpC2* Cm^r	This study
pKG202	pJPR1-P_{xyl}-*Ban- adk-map, trpC2* Cm^r	This study
pKG203	pJPR1-P_{xyl}-*Ban- secY2-Bsu adk-map, trpC2* Cm^r	This study
pKG204	pJPR1-P_{xyl}-*Ban- secY2-Bsu adk-map trpC2* Cm^r	This study
pMAP65	pUB110 derivative carrying *lacI* under the PenP promoter. $Phleo^R$, Km^r	Dervyn & Ehrlich, 2001
Construction of *B. anthracis* deletion mutants		
pUTE583	*B.anthracis* gene knockout vector, Em^r Cm^r	Chen *et al.* 2004
pKG301	pUTE583 with 804bp 5’ and 837bp 3’ flanking fragments of *B. anthracis secH* separated by the ΩKm, Km^r Em^r Cm^r	This study
pKG302	pUTE583 with 826 bp 5’ *secA2* flanking fragment and 837 bp3’ *secH* flanking fragment of *B. anthracis* separated by the ΩKm, Km^r Em^r Cm^r	This study
pKG303	pUTE583 with 915 bp 5’ and 861 bp 3’ flanking fragments of *B. anthracis prsAA* separated by the ΩKm, Km^r Em^r Cm^r	This study
pKG304	pUTE583 with 882 bp 5’ and 713 bp 3’flanking fragments of *B. anthracis prsAB* separated by the ΩKm, Km^r Em^r Cm^r	This study
pKG305	pUTE583 with 755 bp 5’ and 825bp 3’ flanking fragments of *B. anthracis prsAC* separated by the ΩKm, Km^r Em^r Cm^r	This study
pKG306	pUTE583 with 826 bp 5’ *sap* flanking fragment and 837 bp3’ *eag* flanking fragments of *B. anthracis* separated by the ΩKm, Km^r Em^r Cm^r	This study
pKG307	pUTE583 with 946 bp 5’ and 816 bp 3’flanking fragments of *B. anthracis secA2* separated by the ΩKm, with dif sites between ΩKm and flanking fragments , Km^r Em^r Cm^r	
pKG308	pUTE583 with 553 bp 5’ *secA2* flanking sequence and 888 bp3’ *secH* flanking fragments of *B. anthracis* separated by the ΩKm, The promoter (223bp) of *secA2-secH* operon was introduced upstream of *secH* Km^r Em^r Cm^r	This study
pSA102	pUTE583 with 500bp 5’ and 3’ fragments of *B. anthracis secA2* separated by the ΩKm^r, Km^r Em^r Cm^r	Stephen Addinal
Complementation in *B.anthracis*		
pLOSS	*bla spc* P_{spac}*-mcs PdivIVA-lacZ lacI reppLS20*	Claessen *et al.*, 2008

pHT01	Amp^r, Cm^r, **P***grac* promoter (consisting of groEpromotor, the lacO operator and the gsiBSD sequence, ColE1 ori,, lacI repressor, *E. coli/B. subtilis* shuttle vector	MoBiTec
pKG400	Expression vector for *B.anthracis*. Derivative of pUTE583 containing P_{grac}, *lacI*, Em^r Cm^r	This study
pKG401	pKG400-P_{grac}-*secA2-secH*, Em^r Cm^r	This study
pKG402	pKG400-P_{grac}-*secA2*, Em^r Cm^r	This study
pKG403	pKG400-P_{grac}-*secH*, Em^r Cm^r	This study
pKG404	pKG400-P_{grac}-*sap*, Em^r Cm^r	This study
pKG405	pKG400-P_{grac}-*eag*, Em^r Cm^r	This study

Pull-down experiment

pKG406	pKG400-P_{grac}-FLAG-*secA2*, Em^r Cm^r	This study
pKG407	pKG400-P_{grac}-FLAG-*secH*, Em^r Cm^r	This study
pKG408	pKG400-P_{grac}-FLAG-*sap*, Em^r Cm^r	This study

Protein purification

pET16b	P_{T7lac}-*10his lacI*,Amp^r	Novagen
pKG500	pET16b- P*tac* –*secH*, Amp^r	This study
pGEX-6P-1	P*tac-gst-lacI*, Amp^r	GE Healthcare
pLH1	pGEX-6P-1- P*tac- secA1*, Amp^r	Lorraine Hewitt
pLH2	pGEX-6P-1- P*tac- secA2*, Amp^r	Lorraine Hewitt

Bacterial Two Hybrid assay

pUT18	*Plac-cya*$^{675-1197}$, *Amp*^{r} (for in-frame fusions at the N-terminal end of the T18 polypeptide)	Euromedex
pUT18C	*Plac-cya*$^{675-1197}$, *Amp*^{r} (for in-frame fusions at the C-terminal end of the T18 polypeptide)	Euromedex
pKT25	P_{lac}-*cya*$^{1-675}$ (for in-frame fusions at the C-terminal end of the T25 polypeptide)	Euromedex
pKT25N	P_{lac}-*cya*$^{1-675}$ for in-frame fusions at the N-terminal end of the T25 polypeptide)	Euromedex
pUT18C-zip	P_{lac}-*cya1-675-zip* (construct encoding leucine zipper from GCN4)	Euromedex
pKT25-zip	*Plac-cya675-1197-zip* (construct encoding leucine zipper from GCN4)	Euromedex
pUT18-SecA1	*pUT18 Plac-secA1::cyaAT18*, Amp^r	This study
pUT18C-SecA1	*pUT18C Plac- cyaAT18C ::secA1*, Amp^r	This study
pKT25-SecA1	*pKT25 Plac- cyaAT25 ::secA1*, Km^r	This study
pKT25N-SecA1	*pKT25N Plac-secA1::cyaAT25N*, Km^r	This study
pUT18-SecA2	*pUT18 Plac-secA2::cyaAT18*, Amp^r	This study
pUT18C-SecA2	*pUT18C Plac- cyaAT18C ::secA2*, Amp^r	This study
pKT25-SecA2	*pKT25 Plac- cyaAT25 ::secA2*, Km^r	This study
pKT25N-SecA2	*pKT25N Plac-secA2::cyaAT25N*, Km^r	This study
pUT18-SecH	*pUT18 Plac-secH::cyaAT18*, Amp^r	This study
pUT18C-SecH	*pUT18C Plac- cyaAT18C ::secH*, Amp^r	This study
pKT25-SecH	*pKT25 Plac- cyaAT25 ::secH*, Km^r	This study
pKT25N-SecH	*pKT25N Plac-secH::cyaAT25N*, Km^r	This study
pUT18-SecY1	*pUT18 Plac-secY1::cyaAT18*, Amp^r	This study

pUT18C-SecY1	*pUT18C Plac- cyaAT18C ::secY1*, Amp^r	This study
pKT25-SecY1	*pKT25 Plac- cyaAT25 ::secY1*Km^r	This study
pKT25N-SecY1	*pKT25N Plac-secY1::cyaAT25N*, Km^r	This study
pUT18-SecY2	*pUT18 Plac-secY2::cyaAT18*, Amp^r	This study
pUT18C-SecY2	*pUT18C Plac- cyaAT18C ::secY2*, Amp^r	This study
pKT25-SecY2	*pKT25 Plac- cyaAT25 ::secY2*, Km^r	This study
pKT25N-SecY2	*pKT25N Plac-secY2::cyaAT25N*, Km^r	This study
pUT18-Sap_ N-terminus	*pUT18 Plac-sap$_{1-290}$::cyaAT18*, Amp^R	This study
pUT18C-Sap_N-terminus	*pUT18C Plac- cyaAT18C :: sap$_{1-290}$*, Amp^r	This study
pKT25- Sap_N-terminus	*pKT25 Plac- cyaAT25 ::sap$_{1-290}$*, Km^r	This study
pKT25N- Sap_N-terminus	*pKT25N Plac- sap$_{1-290}$::cyaAT25N*, Km^r	This study
pUT18-EA1_ N-terminus	*pUT18 Plac-eag$_{1-329}$::cyaAT18*, Amp^r	This study
pUT18C-EA1_N-terminus	*pUT18C Plac- cyaAT18C ::eag$_{1-329}$*Amp^r	This study
pKT25- EA1_N-terminus	*pKT25 Plac- cyaAT25 :: eag$_{1-329}$*, Km^r	This study
pKT25N- EA1_N-terminus	*pKT25N Plac- eag$_{1-329}$::cyaAT25N*, Km^r	This study
pUT18-Sap	*pUT18 Plac-sap::cyaAT18*, Amp^r	This study
pUT18C-Sap	*pUT18C Plac- cyaAT18C ::sap*, Amp^r	This study
pKT25-Sap	*pKT25 Plac- cyaAT25 :: sap*, Km^r	This study
pKT25N-Sap	*pKT25N Plac- sap::cyaAT25N*,Km^r	This study
pUT18-Bsu_SecA	*pUT18 Plac-Bsu_secA::cyaAT18*,Amp^r	This study
pUT18C- Bsu_SecA	*pUT18C Plac- cyaAT18C ::Bsu_secA*, Amp^r	This study
pKT25- Bsu_SecA	*pKT25 Plac- cyaAT25::Bsu_secA*, Km^r	This study
pKT25N- Bsu_SecA	*pKT25N Plac- Bsu_secA::cyaAT25N*, Km^r	This study
pUT18-Sap_siganl peptide	*pUT18 Plac-sap$_{1-90}$::cyaAT18*, Amp^r	This study
pUT18C- Sap_siganl peptide	*pUT18C Plac- cyaAT18C :: sap$_{1-90}$*, Amp^r	This study
pKT25- Sap_siganl peptide	*pKT25 Plac- cyaAT25 ::sap$_{1-90}$*, Km^r	This study
pKT25N- Sap_siganl peptide	*pKT25N Plac- sap$_{1-90}$::cyaAT25N*,Km^r	This study
pUT18- EA1_siganl peptide	*pUT18 Plac-eag$_{1-90}$::cyaAT18*, Amp^r	This study
pUT18C- EA1_siganl peptide	*pUT18C Plac- cyaAT18C ::eag$_{1-90}$*, Amp^r	This study
pKT25- EA1_siganl peptide	*pKT25 Plac- cyaAT25 :: eag$_{1-90}$*, Km^r	This study
pKT25N- EA1_siganl peptide	*pKT25N Plac- eag$_{1-90}$::cyaAT25N*, Km^r	This study

Appendix D: Table of reciprocal interactions between T18- and T25- fused proteins of *B. anthracis* (SecA1, SecA2, SecY1, SecY2, SecH, EA1, Sap and *B. subtilis* (SecA: annotated as Bsu SecA). Abbreviations: **18**: protein fusion to the N-termimus of T18 subdomain; **18C**: protein fusion to the C-terminus of T18 subdomain; **25**: protein fusion to the C-terminus of T25 subdomain; **25N**: protein fusion to the N-terminus of T25 subdomain; '+' means occurence of of the interaction, '-' means no interaction observed.

		SecA1		**SecA2**		**SecY1**		**SecY2**		**SecH**		**EA1**		**Sap**		**Bsu SecA**	
		18	18C	18	18C	18	18C	18	18C	18	18C	18	18C	18	18C	18	18C
secA1	25	–	+	–	–	–	–	–	–	–	–	–	–	–	–	–	–
	25N	+	–	–	+	–	–	–	–	–	–	–	–	–	–	–	–
SecA2	25	–	–	–	+	–	–	–	–	–	+	–	–	–	–	–	–
	25N	–	–	+	+	–	–	–	–	+	+	–	–	–	–	–	–
SecY1	25	–	–	–	+	–	–	–	–	–	–	–	–	–	–	–	–
	25N	–	–	–	–	–	–	–	–	–	–	–	–	–	–	–	–
SecY2	25	–	–	–	+	–	–	–	–	–	–	–	–	–	–	–	–
	25N	–	–	–	+	–	–	–	–	–	–	–	–	–	–	–	–
SecH	25	–	–	–	–	–	–	–	–	–	–	–	+	–	–	–	–
	25N	–	–	+	+	–	–	–	–	–	–	–	+	–	–	–	–
EA1	25	–	–	+	–	–	–	–	–	–	–	–	–	–	–	–	–
	25N	–	–	–	–	–	–	–	–	–	–	–	–	–	–	–	–
Sap	25	–	–	–	–	–	–	–	–	–	–	–	–	–	–	–	–
	25N	–	–	–	–	–	–	–	–	–	–	–	–	–	–	–	–
Bsu SecA	25	–	–	–	–	–	–	–	–	–	–	–	–	–	–	+	+
	25N	–	–	–	–	–	–	–	–	–	–	–	–	–	–	–	–